



[Volume 3, Issue 2, March, 2013]

International Journal of Computational Engineering Research
(IJCER)

ISSN: 2250-3005

Ijcer Online



ijceronline@gmail.com

www.ijceronline.com



Editorial Board

Editor-In-Chief

Prof. Chetan Sharma

Specialization: Electronics Engineering, India
Qualification: Ph.d, Nanotechnology, IIT Delhi, India

Editorial Committees

DR.Qais Faryadi

Qualification: PhD Computer Science
Affiliation: USIM(Islamic Science University of Malaysia)

Dr. Lingyan Cao

Qualification: Ph.D. Applied Mathematics in Finance
Affiliation: University of Maryland College Park,MD, US

Dr. A.V.L.N.S.H. HARIHARAN

Qualification: Phd Chemistry
Affiliation: GITAM UNIVERSITY, VISAKHAPATNAM, India

DR. MD. MUSTAFIZUR RAHMAN

Qualification: Phd Mechanical and Materials Engineering
Affiliation: University Kebangsaan Malaysia (UKM)

Dr. S. Morteza Bayareh

Qualificatio: Phd Mechanical Engineering, IUT
Affiliation: Islamic Azad University, Lamerd Branch
Daneshjoo Square, Lamerd, Fars, Iran

Dr. Zahéra Mekkioui

Qualification: Phd Electronics
Affiliation: University of Tlemcen, Algeria

Dr. Yilun Shang

Qualification: Postdoctoral Fellow Computer Science
Affiliation: University of Texas at San Antonio, TX 78249

Lugen M.Zake Sheet

Qualification: Phd, Department of Mathematics
Affiliation: University of Mosul, Iraq

Mohamed Abdellatif

Qualification: PhD Intelligence Technology
Affiliation: Graduate School of Natural Science and Technology

Meisam Mahdavi

Qualification: Phd Electrical and Computer Engineering

Affiliation: University of Tehran, North Kargar st. (across the ninth lane), Tehran, Iran

Dr. Ahmed Nabih Zaki Rashed

Qualification: Ph. D Electronic Engineering

Affiliation: Menoufia University, Egypt

Dr. José M. Merigó Lindahl

Qualification: Phd Business Administration

Affiliation: Department of Business Administration, University of Barcelona, Spain

Dr. Mohamed Shokry Nayle

Qualification: Phd, Engineering

Affiliation: faculty of engineering Tanta University Egypt

CONTENTS :

S.No.	Title Name	Page No.
1.	Some Fixed Point Theorems for Expansion Mappings A.S.Saluja, Alkesh Kumar Dhakde ,Devkrishna Magarde	01-7
2.	Automatic Static Signature Verification Systems: A Review Vitthal K. Bhosale, Dr. Anil R. Karwankar	08-12
3.	Throughput of Wireless Multi-Mesh Networks: An Experimental Study P Ramachandran	13-22
4.	A Study on the Satisfaction with the Use of Leisure Food and Beverage Information System – Taking Traditional Farms for Example Hung-Teng Chang, Pin-Chang Chen, Han-Chen Huang, Hui-Min Huang	23-29
5.	On Presence of Interaction In An Unbalanced Two-Way Random Model F.C. Eze,P.E. Chigbu	30-35
6.	Wi-Max Physical Layer Simulator Using Different Modulation Schemes Vikas Kumar, Sukhjit Singh	36-42
7.	Reliability of Thermal Stresses in Bars When Stress Follows Half-Logistic Distribution P.Hari Prasad, T.S.Uma Maheswari	43-46
8.	A Multihop Dynamic Channel Assignment Scheme For Cellular Network Mr. Chetan D. Jadhav, Prof. A. S. Joshi	47-52
9.	Calculation of Stress And Deflection In Double Layer Microcantilever For Biosensor Application Lia Aprilia,Ratno Nuryadi,Djoko Hartanto	53-57
10.	Fatigue Failure Analysis of Small Wooden Wind Turbine Blade Maldhure S. S., Dr. kharde Y.R.	58-61
11.	Dependency Analysis of Other Service Sectors On Ict Narinder Singh Rana, Dr. S N Panda	62-66
12.	Computer-Aided Design of Concrete Mixes D.O. Onwuka, C.E. Okere, O.M. Ibearugbulem, S.U. Onwuka	67-81
13.	Determination through Use of ATND Method of Impact Strength of 359.0 Alloy Modified With Strontium Jacek Pezda	82-85
14.	BSMR: Byzantine-Resilient Secure Multicast Routing In Multi-Hop Wireless Networks Vijay Bahadur Singh, Ashok Prasad, Mukesh Chauhan	89-93

15.	Patient Monitoring By Using Wearable Wireless Sensor Networks with Zigbee Module A.Dasthagiraiah, N.Viswanadham, Y.P.Venkateswarlu, B.Balaobulesh, D.Murali Krishna	94-99
16.	Performance Analysis Of Multi Level Frequency Hopping For Cdma Systems M.Paul Vinod Kumar, C.Ravi Shankar Reddy	100-103
17.	Gravitational Energy and Its Field Harshit Binju,Debasish Talukdar, Sahil Mittal ,Abhishek	104-105
18.	An Ultra-Low Power Physical Layer Design For Wireless Body Area Network D.Venkadeshkumar , K.G.Parthiban	106-111
19.	An Elementary Review of Linkages & Gaps Among BPR, SOA & Software Reverse Engineering Prasenjit Kundu, Bikram Keshari Ratha, Debabrata Das	112-120
20.	An Appropriate F -Test for Two-Way Balanced Interactive Model F.C. Eze, F.O Adimonye, C.P. Nnanwa2 M.I. Ezeani	121-127
21.	Deploying Self-Organizing-Healing Techniques for Software Development of Iterative Linear Solver Okon S. C., Asagba P. O.	128-136
22.	Computation of Least Cost Pipe Network –An Alternate Method Briti Sundar Sil, Ajeet Kumar, Pallavi Saikia, P. Jarken Bui, Preetam Banerjee	137-142
23.	Design of Low Power Column bypass Multiplier using FPGA J.sudha rani, R.N.S.Kalpana	143-151

Some Fixed Point Theorems for Expansion Mappings

¹, A.S.Saluja, ², Alkesh Kumar Dhakde ³, Devkrishna Magarde

¹Department of Mathematics J.H.Govt.P.G.College Betul (M.P.)

²IES Group of institutions Bhopal (M.P.)

Abstract

In The Present Paper We Shall Establish Some Fixed Point Theorems For Expansion Mappings In Complete Metric Spaces. Our Results Are Generalization Of Some Well Known Results.

Keywords: Fixed Point, Complete Metric spaces, Expansion mappings.

1. Introduction & Preliminary:

This paper is divided into two parts

Section I: Some fixed point theorems for expansion mappings in complete metric spaces.

Section II: Some fixed point theorems for expansion mappings in complete 2-Metric spaces before starting main result some definitions.

Definition 2.1: (Metric spaces) A metric space is an ordered pair (X, d) where X is a set and d a function on $X \times X$ with the properties of a metric, namely:

1. $d(x, y) \geq 0$. (non-negative) ,
2. $d(x, y) = d(y, x)$ (symmetry),
3. $d(x, y) = 0$ if and only if $x = y$ (identity of indiscernible)
4. The triangle inequality holds:

$$d(x, y) \leq d(x, z) + d(z, y), \text{ for all } x, y, z \text{ in } X$$

Example 2.1: Let E_n (or R^n) = $\{x = (x_1, x_2, x_3, \dots, x_n), x_i \in R, R \text{ the set of real numbers}\}$ and let d be defined as follows:

$$\text{If } y = (y_1, y_2, y_3, \dots, y_n) \text{ then } d(x, y) = \left(\sum_1^n |x_i - y_i|^p \right)^{\frac{1}{p}} = d_p(x, y) \text{ where } p \text{ is a fixed number in } [0, \infty).$$

The fact that d is metric follows from the well-known Minkowski inequality. Also another metric on S considered above can be defined as follows

$$d(x, y) = \sup_i \{|x_i - y_i|\} = d_\infty(x, y)$$

Example 2.2: Let S be the set of all sequence of real numbers $x = (x_i)_1^\infty$ such that for some fixed

$p \in [0, \infty), \sum_1^\infty |x_i|^p < \infty$ In this case if $y = y_i$ is another point in S , we define

$$d(x, y) = \left(\sum |x_i - y_i|^p \right)^{\frac{1}{p}} = d_q(x, y), \text{ and from Minkowski inequality it follows that this is a metric space on } S.$$

Example 2.3: For $x, y \in R$, define $d(x, y) = |x - y|$. Then (R, d) is a metric space. In general, for $x = (x_1, x_2, x_3, \dots, x_n)$ and $y = (y_1, y_2, y_3, \dots, y_n) \in R^n$, define

$$d(x, y) = \sqrt{(x_1 - y_1)^2 + (x_2 - y_2)^2 + \dots + (x_n - y_n)^2}$$

Then (R^n, d) is a metric space. As this d is usually used, we called it the usual metric.

Definition 2.2: (Convergent sequence in metric space)

A sequence in metric space (X, d) is convergent to $x \in X$ if $\lim_{n \rightarrow \infty} d(x_n, x) \rightarrow 0$

Definition 2.3: (Cauchy sequence in Metric space) Let $M = (X, d)$ be a metric space, let $\{x_n\}$ be a sequence if and only if $\forall \varepsilon \in R : \varepsilon > 0 : \exists N : \forall m, n \in N : m, n \geq N : d(x_n, x_m) < \varepsilon$

Definition 2.4: (Complete Metric space) A metric space (X, d) is complete if every Cauchy sequence is convergent.

Definition 2.5: A 2-metric space is a space X in which for each triple of points x, y, z there exists a real function $d(x, y, z)$ such that:

$[M_1]$ To each pair of distinct points x, y, z $d(x, y, z) \neq 0$

$[M_2]$ $d(x, y, z) = 0$ When at least two of x, y, z are equal

$[M_3]$ $d(x, y, z) = d(y, z, x) = d(x, z, y)$

$[M_4]$ $d(x, y, z) \leq d(x, y, v) + d(x, v, z) + d(v, y, z)$ for all x, y, z, v in X .

Definition 2.6: A sequence $\{x_n\}$ in a 2-metric space (X, d) is said to be convergent at x if $\lim_{n \rightarrow \infty} d(x_n, x, z) = 0$ for all z in X .

Definition 2.7: A sequence $\{x_n\}$ in a 2-metric space (X, d) is said to be Cauchy sequence if $\lim_{m, n \rightarrow \infty} d(x_m, x_n, z) = 0$ for all z in X .

Definition 2.8: A 2-metric space (X, d) is said to be complete if every Cauchy sequence in X is convergent.

2. Basic Theorems

In 1975, Fisher [4], proved the following results:

Theorem (A): Let T be a self mapping of a metric spaces X such that,

$$d(Tx, Ty) \geq \frac{1}{2} [d(x, Tx) + d(y, Ty)] \forall x, y \in X, T \text{ is an identity mappings.}$$

Theorem (B): Let X be a compact metric space and $T : X \rightarrow X$ satisfies 4. (A) and $x \neq y$ and $x, y \in X$. Then T^r has a fixed point for some positive integer r , and T is invertible.

In 1984 the first known result for expansion mappings was proved by Wang, Li, Gao and Iseki [13].

Theorem (C): "Let T be a self map of complete metric space X into itself and if there is a constant $\alpha > 1$ such that, $d(Tx, Ty) \geq \alpha d(x, y)$ for all $x, y \in X$.

Then T has a unique fixed point in X .

Theorem (D): If there exist non negative real numbers $\alpha + \beta + \gamma > 1$ and $\alpha < 1$ such that

$$d(Tx, Ty) \geq \alpha \min \{d(x, Tx), d(y, Ty), d(x, y)\} \forall x, y \in X,$$

T is continuous on X onto itself, and then T has a fixed point.

Theorem (F): If there exist non negative real numbers $\alpha > 1$ such that $d(Tx, T^2x) \geq \alpha d(x, Tx) \forall x \in X$, T is onto and continuous then T has a fixed point.

In 1988, Park and Rhoades [8] shows that the above theorems are consequence of a theorem of Park [7]. In 1991, Rhoades [10] generalized the result of Iseki and others for pair of mappings.

Theorem (G): If there exist non negative real numbers $\alpha > 1$ and T, S be surjective self-map on a complete metric space (X, d) such that;

$$d(Tx, Sy) \geq \alpha d(x, y) \forall x \in X, \text{ Then } T \text{ and } S \text{ have a unique common fixed point.}$$

In 1989 Taniguchi [12] extended some results of Iseki .Later, the results of expansion mappings were extended to 2-metric spaces, introduced by Sharma, Sharma and Iseki [11] for contractive mappings. Many other Mathematicians worked on this way.

Rhoades [10] summarized contractive mapping of different types and discussed on their fixed point theorems. He considered many types of mappings and analyzed the relationship amongst them, where $d(Tx, Ty)$ is governed by,

$$d(x, y), d(x, Tx), d(y, Ty), d(x, Ty), d(y, Tx), d(x, y), d(x, Tx), d(y, Ty), d(x, Ty), d(y, Tx)$$

Many other mathematicians like Wang, Gao, Isekey [13], Popa [9], Jain and Jain [5], Jain and Yadav [6] worked on expansion mappings Recently, Agrawal and Chouhan [1,2], Bhardwaj, Rajput and Yadava [1] worked for common fixed point for expansion mapping.

Our object in this paper is, to obtain some result on fixed point theorems of expansion type's maps on complete metric space.

Now In Section I, We will find Some Fixed Point Theorems For Expansion Mappings In Complete Metric Spaces.

3. Main Results

Theorem (3.1): Let X denotes the complete metric space with metric d and f is a mapping of X into itself .If there exist non negative real's $\alpha, \beta, \gamma, \delta > 1$ with $\alpha + 2\beta + 2\gamma + \delta > 1$ such that

$$d(fx, fy) \geq \alpha \frac{[1 + d(y, fy)]d(x, fx)}{1 + d(x, y)} + \beta[d(x, fx) + d(y, fy)] + \gamma[d(x, fy) + d(y, fx)] + \delta d(x, y)$$

For each $x, y \in X$ with $x \neq y$ and f is onto then f has a fixed point.

Proof: Let $x_0 \in X$.since f is onto, there is an element x_1 satisfying $x_1 = f^{-1}(x_0)$.similarly we can write $x_n = f^{-1}(x_{n-1})$, ($n = 1, 2, 3, \dots$)

From the hypothesis

$$d(x_{n-1}, x_n) = d(fx_n, fx_{n+1})$$

$$\geq \alpha \frac{[1 + d(x_{n+1}, fx_{n+1})]d(x_n, fx_n)}{1 + d(x_n, x_{n+1})} + \beta[d(x_n, fx_n) + d(x_{n+1}, fx_{n+1})] + \gamma[d(x_n, fx_{n+1}) + d(x_{n+1}, fx_n)] + \delta d(x_n, x_{n+1})$$

$$\geq \alpha \frac{[1 + d(x_{n+1}, x_n)]d(x_n, x_{n-1})}{1 + d(x_n, x_{n+1})} + \beta[d(x_n, x_{n-1}) + d(x_{n+1}, x_n)] + \gamma[d(x_n, x_n) + d(x_{n+1}, x_{n-1})] + \delta d(x_n, x_{n+1})$$

$$(1 - \alpha - \beta - \gamma)d(x_n, x_{n-1}) \geq (\beta + \gamma + \delta)d(x_n, x_{n+1})$$

$$\Rightarrow d(x_n, x_{n+1}) \leq \left(\frac{1 - \alpha - \beta - \gamma}{\beta + \gamma + \delta} \right) d(x_n, x_{n-1})$$

Therefore $\{x_n\}$ converges to x in X . Let $y \in f^{-1}(x)$ for infinitely many n , $x_n \neq x$ for some n .

$$d(x_n, x) = d(fx_{n+1}, fy) = d(fy, fx_{n+1})$$

$$\geq \alpha \frac{[1 + d(y, fy)]d(x_{n+1}, fx_{n+1})}{1 + d(x_{n+1}, y)} + \beta[d(x_{n+1}, fx_{n+1}) + d(y, fy)] + \gamma[d(x_{n+1}, fy) + d(y, fx_{n+1})] + \delta d(x_{n+1}, y)$$

$$\geq \alpha \frac{[1 + d(y, x)]d(x_{n+1}, x_n)}{1 + d(x_{n+1}, y)} + \beta[d(x_{n+1}, x_n) + d(y, x)] + \gamma[d(x_{n+1}, x) + d(y, x_n)] + \delta d(x_{n+1}, y)$$

Since $d(x_n, x) \rightarrow 0$ as $n \rightarrow \infty$ we have $d(x_{n+1}, x_n) = d(x_{n+1}, x) = 0$

Therefore $d(x, y) = 0$ when $x = y$.

i.e $y = f(x) = x$

This completes the proof of the theorem.

Theorem (3.2): Let X denotes the complete metric space with metric d and S and T is a mapping of X into itself .If there exists non negative real's $\alpha, \beta, \gamma, \delta > 1$ with $\alpha + 2\beta + 2\gamma + \delta > 1$ such that

$$d(Sx, Ty) \geq \alpha \frac{[1 + d(y, Ty)]d(x, Sx)}{1 + d(x, y)} + \beta[d(x, Sx) + d(y, Ty)] + \gamma[d(x, Ty) + d(y, Sx)] + \delta d(x, y)$$

For each x, y in X with $x \neq y$ and S & T has a fixed point.

Proof: Let x_0 be an arbitrary point in X . Since S & T maps itself there exist points x_1, x_2 in X such that $x_1 = S^{-1}(x_0)$, $x_2 = T^{-1}(x_1)$

Continuing the process, we get a sequence $\{x_n\}$ in X such that

$$x_{2n+1} = S^{-1}(x_{2n}) \quad \& \quad T^{-1}(x_{2n+1}) = x_{2n+2}$$

We see that if $x_{2n} = x_{2n+1}$ for some n then x_{2n} is a common fixed point of S & T .

Therefore we suppose that $x_{2n} \neq x_{2n+1}$ for all $n \geq 0$

From the hypothesis

$$\begin{aligned} d(x_{2n}, x_{2n+1}) &= d(Sx_{2n+1}, Tx_{2n+2}) \\ &\geq \alpha \frac{[1 + d(x_{2n+2}, Tx_{2n+2})]d(x_{2n+1}, Sx_{2n+1})}{1 + d(x_{2n+1}, x_{2n+2})} + \beta[d(x_{2n+1}, Sx_{2n+1}) + d(x_{2n+2}, Tx_{2n+2})] \\ &\quad + \gamma[d(x_{2n+1}, Tx_{2n+2}) + d(x_{2n+2}, Sx_{2n+1})] + \delta d(x_{2n+1}, x_{2n+2}) \\ &\geq \alpha d(x_{2n+1}, x_{2n}) + \beta[d(x_{2n+1}, x_{2n}) + d(x_{2n+2}, x_{2n+1})] + \gamma[d(x_{2n+1}, x_{2n+1}) + d(x_{2n+2}, x_{2n})] + \delta d(x_{2n+1}, x_{2n+2}) \\ &\Rightarrow (1 - \alpha - \beta - \gamma)d(x_{2n}, x_{2n+1}) \geq (\beta + \gamma + \delta)d(x_{2n+1}, x_{2n+2}) \\ &\Rightarrow d(x_{2n+1}, x_{2n+2}) \leq \left(\frac{1 - \alpha - \beta - \gamma}{\beta + \gamma + \delta} \right) d(x_{2n}, x_{2n+1}) \end{aligned}$$

Where $k = \frac{1 - \alpha - \beta - \gamma}{\beta + \gamma + \delta} < 1$.similarly it can be shown that

$$d(x_{2n+1}, x_{2n+2}) \leq kd(x_{2n}, x_{2n+1})$$

Therefore, for all n ,

$$\begin{aligned} d(x_{n+1}, x_{n+2}) &\leq kd(x_n, x_{n+1}) \\ &\leq \dots \leq (k)^{n+1} d(x_0, x_1) \end{aligned}$$

Now, for any $m > n$,

$$\begin{aligned} d(x_n, x_m) &\leq d(x_n, x_{n+1}) + d(x_{n+1}, x_{n+2}) + \dots + d(x_{m-1}, x_m) \\ &\leq [(k)^n + (k)^{n+1} + \dots + (k)^{m-1}] d(x_1, x_0) \\ &\leq \frac{k^n}{1 - k} d(x_1, x_0) \end{aligned}$$

Which shows that $\{x_n\}$ is a Cauchy sequence in X and so it has a limit z .Since X is complete metric space, we have

$z \in X$, there exist $v, w \in X$ such that $S(v) = z, T(w) = z$

From the hypothesis we have

$$d(x_{2n}, z) = d(Sx_{2n+1}, Tw)$$

$$\begin{aligned} &\geq \alpha \frac{[1 + d(w, Tw)]d(x_{2n+1}, Sx_{2n+1})}{1 + d(x_{2n+1}, w)} + \beta[d(x_{2n+1}, Sx_{2n+1}) + d(w, Tw)] \\ &+ \gamma[d(x_{2n+1}, Tw) + d(w, Sx_{2n+1})] + \delta d(x_{2n+1}, w) \\ &\geq \alpha \frac{[1 + d(w, z)]d(x_{2n+1}, x_{2n})}{1 + d(x_{2n+1}, w)} + \beta[d(x_{2n+1}, x_{2n}) + d(w, Tw)] + \gamma[d(x_{2n+1}, Tw) + d(w, x_{2n})] + \delta d(x_{2n+1}, w) \end{aligned}$$

Since $d(x_n, z) \rightarrow \infty$ as $n \rightarrow \infty$ we have $d(x_{2n+1}, x_{2n}) = d(x_{2n+1}, z) = 0$

Therefore $w = z$ i.e $Sw = Tw = z$

This completes the proof of the theorem.

Section II: Some Fixed Point Theorems In 2-Metric Spaces For Expansion Mappings

Theorem 3.3: Let X denotes the complete 2-metric space with metric d and f is a mapping of X into itself. If there exist non negative real's $\alpha, \beta, \gamma, \delta > 1$ with $\alpha + 2\beta + 2\gamma + \delta > 1$ such that

$$\begin{aligned} d(fx, fy, a) &\geq \alpha \frac{[1 + d(y, fy, a)]d(x, fx, a)}{1 + d(x, y, a)} + \beta[d(x, fx, a) + d(y, fy, a)] + \gamma[d(x, fy, a) + d(y, fx, a)] \\ &+ \delta d(x, y, a) \end{aligned}$$

For each x, y in X with $x \neq y$ and f is onto then f has a fixed point.

Proof: Let $x_0 \in X$.since f is onto, there is an element $x_1 = f^{-1}(x_0)$.similarly we can write $x_n = f^{-1}(x_{n-1})$ $n = 1, 2, 3, \dots$

From the hypothesis

$$\begin{aligned} d(x_{n-1}, x_n, a) &= d(fx_n, fx_{n+1}, a) \\ &\geq \alpha \frac{[1 + d(x_{n+1}, fx_{n+1}, a)]d(x_n, fx_n, a)}{1 + d(x_n, x_{n+1}, a)} + \beta[d(x_n, fx_n, a) + d(x_{n+1}, fx_{n+1}, a)] + \gamma[d(x_n, fx_{n+1}, a) + d(x_{n+1}, fx_n, a)] \\ &+ \delta d(x_n, x_{n+1}, a) \\ &\geq \alpha \frac{[1 + d(x_{n+1}, x_n, a)]d(x_n, x_{n-1}, a)}{1 + d(x_n, x_{n+1}, a)} + \beta[d(x_n, x_{n-1}, a) + d(x_{n+1}, x_n, a)] + \gamma[d(x_n, x_n, a) + d(x_{n+1}, x_{n-1}, a)] \\ &+ \delta d(x_n, x_{n+1}, a) \\ &\geq \alpha d(x_n, x_{n-1}, a) + \beta[d(x_n, x_{n-1}, a) + d(x_{n+1}, x_n, a)] + \gamma[d(x_{n+1}, x_n, a) + d(x_n, x_{n-1}, a)] + \delta d(x_n, x_{n+1}, a) \\ &\Rightarrow (1 - \alpha - \beta - \gamma)d(x_n, x_{n-1}, a) \geq (\beta + \gamma + \delta)d(x_n, x_{n+1}, a) \\ &\Rightarrow d(x_n, x_{n+1}, a) \leq \frac{1 - \alpha - \beta - \gamma}{\beta + \gamma + \delta} d(x_n, x_{n-1}, a) \end{aligned}$$

Therefore $\{x_n\}$ converges to x in X .Let $y \in f^{-1}(x)$ for infinitely many $n, x_n \neq x$ for such n

$$\begin{aligned} d(x_n, x, a) &= d(fx_{n+1}, fy, a) = d(fy, fx_{n+1}, a) \\ &\geq \alpha \frac{[1 + d(y, fy, a)]d(x_{n+1}, fx_{n+1}, a)}{1 + d(x_{n+1}, y, a)} + \beta[d(x_{n+1}, fx_{n+1}, a) + d(y, fy, a)] + \gamma[d(x_{n+1}, fy, a) + d(y, fx_{n+1}, a)] \\ &+ \delta d(x_{n+1}, y, a) \\ &\geq \alpha \frac{[1 + d(y, x, a)]d(x_{n+1}, x_n, a)}{1 + d(x_{n+1}, y, a)} + \beta[d(x_{n+1}, x_n, a) + d(y, x, a)] + \gamma[d(x_{n+1}, x, a) + d(y, x_n, a)] + \delta d(x_{n+1}, y, a) \end{aligned}$$

Since $d(x_n, x, a) \rightarrow \infty$ as $n \rightarrow \infty$ we have $d(x_{n+1}, x_n, a) = d(x_{n+1}, x, a) = 0$

Therefore $d(x, y, a) = 0 \Rightarrow x = y$

i.e $y = f(x) = x$.

Theorem 3.4: Let X denotes the complete metric space with metric d and S & T is a mappings of X into itself .If there exists non negative real's $\alpha, \beta, \gamma, \delta > 1$ with $\alpha + 2\beta + 2\gamma + \delta > 1$ such that

$$d(Sx, Ty, a) \geq \alpha \frac{[1 + d(y, Ty, a)]d(x, Sx, a)}{1 + d(x, y, a)} + \beta[d(x, Sx, a) + d(y, Ty, a)] + \gamma[d(x, Ty, a) + d(y, Sx, a)] + \delta d(x, y, a)$$

For each x, y in X with $x \neq y$ and S & T has a fixed point.

Proof: Let x_0 be an arbitrary point in X . Since S & T maps into itself there exist points x_1, x_2 in X such that

$$x_1 = S^{-1}(x_0) \quad x_2 = T^{-1}(x_1)$$

Continuing the process, we get a sequence $\{x_n\}$ in C such that

$$x_{2n+1} = S^{-1}(x_{2n}) \quad \& \quad T^{-1}(x_{2n+1}) = x_{2n+2}$$

$$Sx_{2n+1} = x_{2n} \quad Tx_{2n+2} = x_{2n+1}$$

We see that if $x_{2n} = x_{2n+1}$ for some n then x_{2n} is a common fixed point of S & T .

Therefore we suppose that $x_{2n} \neq x_{2n+1}$ for all $n \geq 0$

From the hypothesis

$$d(x_{2n}, x_{2n+1}, a) = d(Sx_{2n+1}, Tx_{2n+2}, a)$$

$$\geq \alpha \frac{[1 + d(x_{2n+2}, Tx_{2n+2}, a)]d(x_{2n+1}, Sx_{2n+1}, a)}{1 + d(x_{2n+1}, x_{2n+2}, a)} + \beta[d(x_{2n+1}, Sx_{2n+1}, a) + d(x_{2n+2}, Tx_{2n+2}, a)]$$

$$+ \gamma[d(x_{2n+1}, Tx_{2n+2}, a) + d(x_{2n+2}, Sx_{2n+1}, a)] + \delta d(x_{2n+1}, x_{2n+2}, a)$$

$$\geq \alpha \frac{[1 + d(x_{2n+2}, x_{2n+1}, a)]d(x_{2n+1}, x_{2n}, a)}{1 + d(x_{2n+1}, x_{2n+2}, a)} + \beta[d(x_{2n+1}, x_{2n}, a) + d(x_{2n+2}, x_{2n+1}, a)]$$

$$+ \gamma[d(x_{2n+1}, x_{2n+1}, a) + d(x_{2n+2}, x_{2n}, a)] + \delta d(x_{2n+1}, x_{2n+2}, a)$$

$$\Rightarrow (1 - \alpha - \beta - \gamma)d(x_{2n}, x_{2n+1}, a) \geq (\beta + \gamma + \delta)d(x_{2n+1}, x_{2n+2}, a)$$

$$\Rightarrow d(x_{2n+1}, x_{2n+2}, a) \leq \frac{1 - \alpha - \beta - \gamma}{\beta + \gamma + \delta} d(x_{2n}, x_{2n+1}, a)$$

$$\text{where } k = \frac{1 - \alpha - \beta - \gamma}{\alpha + \beta + \gamma} < 1$$

$$d(x_{2n+1}, x_{2n+2}, a) \leq kd(x_{2n}, x_{2n+1}, a)$$

$$\text{Similarly } d(x_{2n+2}, x_{2n+3}, a) \leq kd(x_{2n+1}, x_{2n+2}, a)$$

$$\text{Therefore we obtain } d(x_{n+1}, x_{n+2}, a) \leq kd(x_n, x_{n+1}, a)$$

Which shows that $\{x_n\}$ is a Cauchy sequence in X and so it has a limit μ is complete metric space, we have $\mu \in X$,

there exists $v, w \in X$ such that $S(v) = \mu, T(w) = \mu$

From the hypothesis we have

$$d(x_{2n}, \mu, a) = d(Sx_{2n+1}, Tw, a)$$

$$\begin{aligned} &\geq \alpha \frac{[1 + d(w, Tw, a)]d(w, Sx_{2n+1}, a)}{1 + d(x_{2n+1}, w, a)} + \beta[d(x_{2n+1}, Sx_{2n+1}, a) + d(w, Tw, a)] \\ &+ \gamma[d(x_{2n+1}, Tw, a) + d(w, Sx_{2n+1}, a)] + \delta d(x_{2n+1}, w, a) \\ &\geq \alpha \frac{[1 + d(w, \mu, a)]d(w, x_{2n}, a)}{1 + d(x_{2n+1}, w, a)} + \beta[d(x_{2n+1}, x_{2n}, a) + d(w, Tw, a)] \\ &+ \gamma[d(x_{2n+1}, Tw, a) + d(w, x_{2n}, a)] + \delta d(x_{2n+1}, w, a) \end{aligned}$$

Since $d(x_{2n}, \mu, a) \rightarrow \infty$ as $n \rightarrow \infty$ we have $d(x_{2n+1}, x_{2n}, a) = d(x_{2n+1}, w, a) = 0$. Therefore $d(w, \mu, a) = 0$ implies $w = \mu$ i.e $Sw = Tw = \mu$

This completes the proof of the theorem.

References

- [1]. Agrawal, A.K. and Chouhan, P. "Some fixed point theorems for expansion mappings" Jnanabha 35 (2005) 197-199.
- [2]. Agrawal, A.K. and Chouhan, P. "Some fixed point theorems for expansion mappings" Jnanabha 36 (2006) 197-199.
- [3]. Bhardwaj, R.K. Rajput, S.S. and Yadava, R.N. "Some fixed point theorems in complete Metric spaces" International J.of Math.Sci. & Engg.Appls.2 (2007) 193-198.
- [4]. Fisher, B. "Mapping on a metric space" Bull. V.M.I. (4), 12(1975) 147-151.
- [5]. Jain, R.K. and Jain, R. "Some fixed point theorems on expansion mappings" Acta Ciencia Indica 20(1994) 217-220.
- [6]. Jain, R. and Yadav, V. "A common fixed point theorem for compatible mappings in metric spaces" The Mathematics Education (1994) 183-188.
- [7]. Park, S. "On extensions of the Caristi-Kirk fixed point theorem" J.Korean Math.Soc.19(1983) 223-228.
- [8]. Park, S. and Rhoades, B.E. "Some fixed point theorems for expansion mappings" Math.Japonica 33(1) (1988) 129-133.
- [9]. Popa, V. "Fixed point theorem for expansion mappings" Babes Bolyai University, Faculty of Mathematics and physics Research Seminar 3 (1987) 25-30.
- [10]. Rhoades B.E. "A comparison of various definitions of contractive mappings" Trans. Amer Math.Soc.226 (1976) 257-290.
- [11]. Sharma.P.L., Sharma.B.K. and Iseki, K. "Contractive type mappings on 2-metric spaces" Math.Japonica 21 (1976) 67-70.
- [12]. Taniguchi, T. "Common fixed point theorems on expansion type mappings on complete metric spaces" Math.Japonica 34(1989) 139-142.
- [13]. Wang, S.Z. Gao, Z.M. and Iseki, K. "Fixed point theorems on expansion mappings" Math.Japonica .29 (1984) 631-636.

Automatic Static Signature Verification Systems: A Review

Vitthal K. Bhosale¹ Dr. Anil R. Karwankar²

¹PG Student, Government College of Engineering, Aurangabad (M.S.),

²Assistant Professor, Dept. Of Electronics & Tele-Communication, Government College of Engineering, Aurangabad (M.S.), India

Abstract:

Handwritten signature is a distinguishing biometric feature which is the most widely employed form of secure personal authentication. Signature verification is used in a large number of fields starting from online banking, passport verification systems to even authenticating candidates in public examinations from their signatures. Even today thousands of financial and business transactions are being authorized via signatures. Therefore an automatic signature verification system is needed. This paper represents a brief review on various approaches used in Static signature verification systems.

Keywords: Biometrics, false acceptance rate, false rejection rate, forgeries, static signature, simple distance classifiers, support vector machines.

1. Introduction

Signature verification is a major area of research in the field of image processing and pattern recognition. It is widely used in the fields of finance, access control and security. Signature verification is the process which is carried out to determine whether a given signature is genuine or forged. Signature verification is different from character recognition thus consider signature as a complete image with some particular curves that represent a particular writing style of the person. Approaches to signature verification fall into two categories according to the acquisition of the data: On-line and Off-line. On-line signature verification focuses on capturing and analyzing the signature in real time, as the person is signing it. Off-line signature verification deals with analyzing images of a person's signature. In On-line signature verifications system stylus is used to obtain pen pressure, velocity, acceleration and location, as functions of time. In Off-line method an optical scanner is used to obtain handwriting data which deals with a 2-D image of the signature represented by a discrete 2D function i.e. $S(x, y)$ Where $x = 0, 1, 2, \dots, M$ and $y = 0, 1, 2, \dots, N$. (M, N) denote the spatial coordinates. The value of S in any (x, y) corresponds to the grey level at that point. This paper is organized as follows: Section 2 discusses various signature verification concepts, Section 3 introduces various steps in signature verification, Section 4 introduces different methods of signature verification, Section 5 introduces performance evaluation of different methods and Section 6 concludes the paper and shows scope of future work.

2. Signature Verification Concepts

Signature verification system involves some basic concepts that are forgeries, signature features and performance evaluation parameters i.e. error rates.

2.1. Types of Forgeries

There are mainly three types of forgeries:

- Random Forgery
- Simple Forgery
- Skilled Forgery

The random forgery is written by the person who doesn't know the shape of the original signature. Simple forgery is represented by the person who knows the shape of the original signature without much practice. While skilled forgery is produced by an individual who has appropriate knowledge about the original signature along with proper practice.

2.2. Types of Features

Features extracted for Static signature verification can be broadly divided into three main types:

- Global features
- Local features
- Geometric features

Global features which are extracted from the whole signature image. Global features can be easily extracted but depend upon the overall position alignment thus highly susceptible to distortion and style variations. Global features include – signature area, signature height to width ratio, centre of gravity etc. Local features are extracted from the small portion of signature image. These features are computationally expensive but are much more accurate than global features. Local features include – local pixel density, slant features, critical points etc. The geometric features represent the characteristic geometry of a

signature that keeps both their global as well as local feature properties. Geometrical features have the ability to tolerate with distortion, style variations, rotation variations and certain degree of translation.

2.3. Error Rate

- False Acceptance Rate
- False Rejection Rate

While dealing with any signature verification system, we consider False Rejection Rate and False Acceptance Rate as its performance evaluation parameters. The Efficiency of signature verification systems can be represented by these two types of error rates i.e. the percentage of genuine signatures rejected as forgery which is called False Rejection Rate (FRR) and the percentage of forgery signatures accepted as genuine which is called False Acceptance Rate (FAR). Generally signature verification system shall have an acceptable trade-off between a low FAR and a low FRR.

3. Processing Steps in Static Signature Verification

A signature verification (SV) system authenticates the identity of any person, based on an analysis of his/her signature through a set of processing steps. The major steps are as follows:

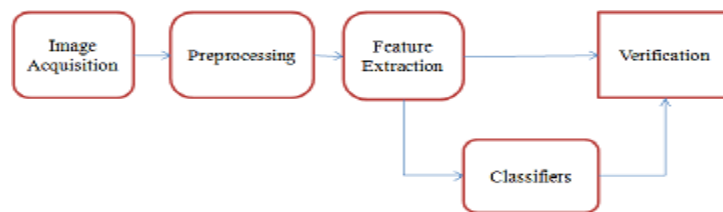


Figure 1. General overview of Static signature verification system

3.1. Image acquisition

The signatures to be processed by the system should be in the digital image format. The data for the offline signature verification system acquire from various ways like by optical pad, scanner etc. The signature samples are scanned and then scanned images are stored digitally for further processing.

3.2. Preprocessing

The purpose of Signature pre-processing step is to make signatures standard and ready for feature extraction. Preprocessing is a necessary step to improve the accuracy of Feature extraction and Verification. Before processing the image for feature extracting some pre-processing algorithm are applied on the scanned image like Binarization, Denoising, Skeltonization, Thinning, Calculating exact signature area etc.

3.3. Feature Extraction

The efficiency of a signature verification system mainly depends on Feature extraction stage. Feature extraction techniques should be fast and easy to compute so that system has low computational power. Selected features should discriminate between genuine and forgery signature. Features extracted for static signature verification can be divided as Global, Local and Geometric features.

3.4. Verification

Verification step compares test signature features with genuine signature features based on various pattern classification techniques and makes a final decision for verification as genuine or forged signature.

4. Methods for Static Signature Verification

Here we discuss some of the convenient existing signature verification systems. We categorise these systems according to the pattern recognition technique used. We discuss Template matching techniques, Simple Distance Classifiers (SDCs), Neural Networks (NNs), Structural techniques, Support Vector Machines (SVMs), Hidden Markov Models (HMMs) and Hybrid systems i.e. systems that use more than one pattern recognition technique.

4.1. Template Matching Techniques

Template matching is one of the earliest and simplest approaches to pattern recognition. A pattern class is represented by a template. Such a template pattern can either be a curve or an image. Dynamic Time Wrapping is the most popular template matching technique for Static signature verification. The Dynamic Time Warping (DTW) algorithm which is based on dynamic programming finds an optimal match between two sequences of feature vectors. The total dissimilarity between reference and test node is represented by $D(M, N)$.

$$D(m, n) = d(m, n) + \min [D(m-1, n), D(m-1, n-1), D(m, n-1)] \quad [1]$$

$$DTWdist = D(M, N)$$

The training of system using DTW is performed by equation (2) where G1 is the training score [6].

$$G1 = \frac{2}{d(d-1)} \sum_{i=1}^{d-1} \sum_{j=i+1}^d DTWdist(G_i, G_j) \quad \text{where } i, j \leq d \quad [2]$$

The verification of the system using DTW is performed by equation (3) where G2 is verification score [6].

$$G1 = \frac{1}{d} \sum_{i=1}^d DTWdist(G_t, G_i) \quad \text{where } i \leq d \quad [3]$$

The decision to accept or reject signature is based on the value of the threshold score given by equation [4]

$$\text{Score} = G1 / G2 \quad [4]$$

A. Piyush Shanker and A. N. Rajagopalan [1] proposed a signature verification system based on Modified Dynamic Time Warping (DTW). Authors made modifications to the basic DTW algorithm for stability of various components of a signature. This involves assigning weights to various components of a signature depending on their stability. These weights are then used to modify the cost function involved with the warping paths. Authors reported that the system based on the modified DTW algorithm performed significantly better than the basic DTW system. The method is computationally efficient and runs in real-time. Authors reported that with a threshold value of 1.5, the system has close to 0% acceptance rate for casual forgeries, 20% acceptance rate for skilled forgeries, and about 25% rejection rate for genuine signatures. Jayadevan R., Satish R. Kolhe and Pradeep M. Patil [7] developed static handwritten signature verification based on Dynamic Time Warping (DTW). The horizontal and vertical projection features of a signature are extracted using discrete Radon transform and the two vectors are combined to form a combined projection feature vector. The feature vectors of two signatures are matched using DTW algorithm. The closed area formed by the matching path around the diagonal of the DTW-grid is computed and is multiplied with the difference cost between the feature vectors. The test signature is compared with each genuine sample and a matching score is calculated. A decision to accept or reject is made on the average of such scores. Authors used a global signature database (GPDS-Signature Database) of 2106 signatures with 936 genuine signatures and 1170 skilled forgeries to evaluate the performance of system. Authors reported FAR of 26.06% and FRR of 17.94%.

4.2. Simple Distance Classifiers

A Simple Distance Classifiers represent each pattern class with a Gaussian probability distribution function, where each PDF is uniquely defined by the mean vector and covariance matrix of the feature vectors that belong to the particular class. Serestina Viriri and Bradley Schafer [13] presented an offline signature verification system based on global features and transition features. In this paper a database of 2106 signatures was used. To train the system, a subset of this database was taken comprising of 15 genuine samples taken from each of the 30 different individual's signatures. The features for all 15 signatures would then be averaged to form one centroid feature vector. When a claimed signature is entered into the system, it is compared against the centroid feature vectors for classification of genuine signature and forged signature. During the testing phase, two approaches were tested. During testing, a claimed signature is compared against template file using the Euclidean distance and if it is below a certain threshold value, then the signature is declared valid, otherwise it is a forgery. Using the global threshold, correct classification rate of 73% and a false acceptance rate of 18.5% were obtained. Using the calculation of the localized threshold, a correct classification rate of 84.1% and a false acceptance rate of 17.8% was obtained.

4.3. Neural Networks

An NN is a parallel computing system that consists of a large number of simple processors with many interconnections. Neural Network has the ability to learn complex non-linear input-output relationships, use sequential training procedures and adapt itself to the data. A Neural Network model uses organisational principles in a network of weighted directed graphs, in which the nodes are artificial neurons and the directed edges are connections between neuron outputs and neuron inputs. H. Baltzakisa, N. Papamarkos [15] developed a signature verification technique based on a two-stage neural network classifier. The proposed system was based on global, grid and texture features. For each one of these feature sets a special two stage Perceptron OCON (one-class-one-network) classification structure was implemented. In the first stage, the classifier combines the decision results of the neural networks and the Euclidean distance obtained using the three feature sets. The results of the first-stage classifier feed a second-stage radial base function (RBF) neural network structure, which makes the final decision. The performance of the system was checked by the use of the remaining subset (TS) of 500 signatures. A FAR of 9.81%, FRR of 3% and an overall efficiency of 90.09% was achieved. R.Abbas [4] developed the off-line signature recognition based on a back propagation neural network prototype. Authors used feed forward neural networks and three different training algorithms Vanila, Enhanced and batch were used. Author reported FAR between the ranges of 10.0 % for casual forgeries and FRR of 6.0%.

4.4. Hidden Markov models

Hidden Markov Models represent a signature as a sequence of states. According to the associated probability distribution, in each state an observation vector is generated. Transitions between the states are represented as a set of

transition probabilities. These probabilities of an HMM are trained using observation vector extracted from sample signature database. Justino, Bortolozzi and Sabourin [8] proposed an off-line signature verification system using Hidden Markov Models to detect random, casual, and skilled forgeries. Three features: a pixel density feature, a pixel distribution feature and an axial slant feature are extracted from a grid segmentation scheme. A False Acceptance rate of 2.83% is obtained and a False Rejection rate of 1.44%, 2.50%, and 22.67% are obtained for random, casual, and skilled forgeries, respectively.

4.5. Structural Techniques

In Structural pattern recognition techniques a pattern is viewed as being composed of simple sub-patterns which are built from further simpler sub-patterns. Abhay Bansal, Bharat Gupta, Gaurav Khandelwal, and Shampa Chakraverty [2] developed an Offline Signature Verification System based on Critical Region Matching. The system was designed to detect the skilled forgeries and was mainly dealt with the extraction of the critical regions and matched them following a modular graph matching approach. The method includes critical points extraction, critical region extraction, and formulation of signature verification problem as a graph matching problem. For semi-skilled forgeries accuracy of 95.69% and for skilled forgeries an accuracy of 89.09% was obtained. Majhi, Reddy and Prasanna [5] proposed a morphological parameter for signature recognition, authors proposed centre of mass of signature segments, and the signature was split again and again at its centre of mass to obtain a series of points in horizontal as well as vertical mode. The point sequence is then used as discriminating feature; the thresholds were selected separately for each person. They achieved FRR 14.58% and FAR 2.08%. Ismail et al. [10] proposed an off-line Arabic signature recognition and verification technique. Authors proposed a system of two separate phases for signature recognition and verification is developed. In the first phase some features based on Translation, circularity feature, image enhancement, partial histogram, centres of gravity, global baseline, thinning etc. are extracted. In the second phase some more features are also extracted such as Central line features, Corner line features Central circle features, Corner curve features and Critical point features. A set of signature data consisting of 220 genuine samples and 110 forged samples is used for experimentation. They obtained a 95.0% recognition rate and 98.0% verification.

4.6. Support Vector Machines

V.Vapnik et al. introduced this new learning method. SVMs are machine learning algorithms for binary classification based on recent advances in statistical learning theory. S. Audet, P. Bansal, and S. Baskaran [3], designed Off-Line Signature Verification and Recognition using Support Vector Machine. They used global, directional and grid features of signatures. Virtual Support Vector Machine (VSVM) was used to verify and classify the signatures and FAR of 16.0% and FRR of 13.0% was obtained. Ozgunduz et al. [12] proposed off-line signature verification system using Support vector machines. Author used Support Vector Machines in order to detect random and skilled forgeries. Author used extracted global geometric features, direction features and grid features for SVM classifier. In the experiments, a comparison between SVM and ANN is performed. Using a SVM with RBF kernel, an FRR of 0.02% and an FAR of 0.11% are obtained.

5. Performance Evaluation with Results

The performance of system is determined based on the accuracy of classification between the genuine and forged signature. Evaluation parameters for any signature verification system are FAR and FRR. The performances of different methods with results are shown in Table 1.

Table 1. Performance evaluation of different methods

Serial No.	Method	FAR (%)	FRR (%)
1.	Modified Dynamic Time Wrapping [1]	20.0	25.0
2.	Hidden Markov Model [8]	02.83	22.67
3.	Two Stage Neural Network classifier [15]	09.81	03.00
4.	Back-propagation Neural Network Prototype [4]	10.00	06.00
5.	Morphological Parameter based [5]	02.08	14.58
6.	Wavelet-based verification [9]	10.98	05.60
7.	Support Vector Machine [11]	04.83	05.30
8.	Virtual Support Vector Machine [3]	16.00	13.00
9.	Dynamic features based [16]	13.78	14.25

6. Conclusion

This review article presents a brief overview of the recent works on Static signature verification. Different existing approaches used for signature verification are discussed and compared along with their FAR and FRR. The results shows that the accuracy of existing available signature verification systems is not enough to implement in public use thus more research on Static Signature verification is required. There are still many challenges in this domain which includes the signatures from the same person are similar but not identical. In addition, a person's signature often changes during their life due to age, illness and up to some extent the emotional state of the person. Thus there is a need of research in feature extraction and classification techniques based on dynamic methods that extract dynamic information from static images. That would make it possible for researchers to achieve a better performance in this domain.

References

- [1] A. Piyush Shanker and A. N. Rajagopalan, Off-line signature verification using DTW, Pattern Recognition Letters, v.28 n.12, 2007 1407-1414.
- [2] Abhay Bansal, Bharat Gupta, Gaurav Khandelwal, and Shampa Chakraverty “Offline Signature Verification Using Critical Region Matching”, International Journal of Signal Processing, Image Processing and Pattern, 2009.
- [3] S. Audet, P. Bansal, and S. Baskaran ,“Off-line signature verification using virtual support vector machines”, ECSE 526 – Artificial Intelligence, April 7, 2006
- [4] R.Abbas, “Back propagation Neural Network Prototype for off line signature verification”, thesis Submitted to RMIT, 2003
- [5] B. Majhi, Y. Reddy, D. Babu, “Novel Features for Off-line Signature Verification”, International Journal of Computers, Communications & Control Vol.I (2006), No. 1, pp. 17-24.
- [6] Hifzan Ahmed, Shailja Shukla, “Global Features based Static Signature Verification system Using DTW”, International Journal of Systems , Algorithms & Applications, vol 2, Issue 4, pp. 13-17, April 2012.
- [7] Jayadevan R., Satish R. Kolhe, Pradeep M. Patil, “Dynamic Time Warping Based Static Hand Printed Signature Verification”, Journal of Pattern Recognition Research 1 (2009) 52-65.
- [8] J.Edson, R.Justino, F.Bortolozzi and R. Sabourin, “Off-line signature verification using HMM for Random, Simple and Skilled Forgeries”, 2001.
- [9] P. Deng, H. Yuan Mark Liao & H. Tyan, “Wavelet Based Off-line Signature Recognition System”, Proceedings 5th Conference on Optical Character Recognition and Document Analysis, 1996, Beijing, China.
- [10] M.A. Ismail, Samia Gad, “Off-line Arabic Signature Recognition and Verification”, 2000.
- [11] H. Lv, W. Wang, C. Wang, and Q. Zhou, —Off-line Chinese signature verification based on support vector machines, PRL 2005, vol. 26, no. 15, pp. 2390–2399
- [12] Emre Ozgunduz, Tulin Senturk and M. Elif Karslıgil “Offline Signature verification and Recognition by Support Vector Machine”, EUSIPCO, 2005.
- [13] B.Schafer and S.Viriri - An Off-Line Signature Verification System□, 2009, (ICSIPA- 2009), pp.95-100.
- [14] S. Armand, M. Blumenstein - Off-line Signature Verification based on the Modified Direction Feature□ ICPR-2006, pp.509-512
- [15] H. Baltzakis, N. Papamarkos, “A new signature verification technique based on a two-stage neural network classifier”, Engineering Applications of Artificial Intelligence ,2001
- [16] L. Basavaraj and R. D Sudhaker Samuel, “Offline-line Signature Verification and Recognition: An Approach Based on Four Speed Stroke Angle”, International Journal of Recent Trends in Engineering, Vol 2, No. 3, November 2009

Throughput of Wireless Multi-Mesh Networks: An Experimental Study

P Ramachandran

Department of Electronic Systems Engineering, IISc, Bangalore, India

Abstract

To overcome the capacity and interference problem of Wireless Mesh Network (WMN), we explore the possibility of increasing the coverage area of WMN by running multiple WMNs in parallel and interconnecting them. Theoretical achievable capacity from [3] to every node in a random static wireless ad hoc network with ideal routing is estimated as $O(1/\sqrt{n} \log n)$, where n is the total number of nodes in the network. Therefore, with increasing number of nodes in a network, throughput capacity becomes unacceptably low. In this work we report our throughput measurements that show throughput in a WMN for different path length is almost the same, with nodes across two WMNs of the same path length. We propose to interconnect the networks by using multiple wireless adapters in gateway node configured with the SSID of the networks in operation. To achieve our goal we exploited the DSR protocol feature of assigning locally unique interface indices to its adapters.

Keywords :MR-LQSR, ETX, PktPair, RTT, ETX, WCETT, ARQ and MCL

1. Introduction

IEEE 802.11 standard provides infrastructure-less operating mode called as ad hoc mode. Absence of infrastructure and self-configuration capability makes ad hoc networks suitable for low-cost applications, but results in wireless medium instability and low connectivity. Hence WMN is proposed to increase the ad hoc connectivity because WMN extends the coverage area of communication by using multi-hop communications. WMN is a communication network made up of radio nodes organized in a mesh topology, wherein each node in the network may act as a router, regardless of whether it is connected to another network or not. Nodes allow continuous connections and reconfigurations around the broken or blocked links/paths by hopping from node to another node until data in the form of packets/frames reach the destination from the source node. Mesh Routers/Clients and Mesh Gateways are the components of WMN. Mesh clients are often laptops, cell phones, desktops and other wireless devices. WMN is a special type of wireless ad hoc network where each user node operates not only as host but also a router. Traffic is forwarded to and from internet connected gateways in a multi-hop fashion. WMN nodes usually do not have strict power constraint, because it is assumed that all the nodes are almost stationary, but this need not be so. Networking infrastructure is decentralized and simplified because each node needs only to transmit as far as the next node. Each node is connected to several other nodes with redundant routes and if one drops out of the network, its neighbors find another route unlike WLAN access points, which can relay messages on behalf of others. WMNs are dynamically self-organizing and self-configuring, with the nodes in the network, thus increasing range, stability and the available bandwidth. The remainder of this paper is organized as section-2 presents the existing technology and motivation to carry out this work, section-3 describes the methodology of the work, section-4 presents the results and observations, and finally section-5 concludes our work and future directions.

2. BACKGROUND

Off-the-shelf IEEE 802.11-based wireless interfaces has made easy and inexpensive to setup WMNs with mobile and PDA devices and be used as a private network. The performance of the WMN is based on the routing protocol and routing algorithm that is used. Hence research is active in the field of routing protocols and routing metrics to improve the WMN performance. Most of the routing protocol is evaluated based on simulation. One more issue on which performance of WMN improve is by using multiple interfaces in a node instead of a single interface. But limitation with using multiple interfaces in a node are several like, in conventional network for each physical network interface used, should be assigned with different IP addresses, but a node should have a single unique address irrespective of number of interfaces being used to communicate in the network. Therefore a suitable protocol with mechanism for communication between nodes equipped with single and multiple interfaces or mixture of single, multiple interfaces nodes. Routing metric worth should be used, which is directly responsible for the throughput performance. Board crosses talk, radiation leakage and an adequate distance required to separate multiple antennas in a node are some of the issues with use of multiple interfaces, hence using multiple interfaces in a node without taking proper measure would yield less performance in WMN.

i) MR-LQSR Protocol

Protocols for multi-hop routing in ad-hoc and WMNs proposed are DSDV, OLSR, TORA, and AODV DSR etc. Protocols are mainly of two types i.e. on-demand/link state routing protocol better for mobile nodes and table-driven routing protocols for static nodes. Link Quality Source Routing (LQSR) is a source routed link state routing protocol which supports link quality metrics. LQSR implements all basic Dynamic Source Routing (DSR) protocol [5] functionality including route request, route reply, route maintenance and feature of using one IP address as nodes home address for all communication while in the ad-hoc network, in-turn each node independently assigns locally unique interface index to each of its network interfaces. MR-LQSR is a combination of LQSR protocol with metric called WCETT. From [6] MR-LQSR has following four components.

- Neighbor Discover
- Link Weight Assignment
- Link weight information propagation
- Path finding

The main difference with DSR and LQSR is DSR always tries to route through shortest path, whereas MR-LQSR uses WCETT to assign the weights to links and does not follow shortest path. Shortest path routing performs worse many times. Since MR-LQSR is used in layer 2.5 architecture which does not require to modify the protocol of layer above, uses 48-bit virtual Ethernet address in its headers including source route, source reply and route error packets instead of 32-bit IP address. Mesh Connectivity Layer (MCL) from [7] which operates as layer 2.5 is a driver which generates LQSR packet by inserting an additional LQSR header into Ethernet packets received from the network layer as illustrated in fig.1+

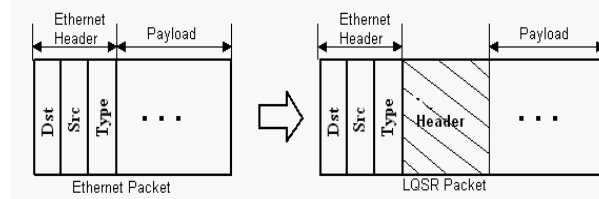


Fig.1 Ethernet Packet from IP layer , LQSR Packets generated by MCL

ii) Routing Metrics

Various routing metrics for operation in WMN is proposed and evolved from Hop Count (Hop) to Per-hop Round Trip Time (RTT), Per-hop Packet Pair Delay (PktPair), Expected Transmission Count (ETX) and Weighted Cumulative Expected Transmission Time (WCETT) with different intuitions in the way of improving network performance. We have implemented ETX, PktPair and WCETT on our testbed and observed the throughput performance.

Expected Transmission Count (ETX)

ETX is the expected number of MAC layer transmission that is needed for successfully delivering a packet through a wireless link. This metric is good in judging paths [8] by assigning large weights for long and lossy paths. ETX is derived as packet loss rate in both the forward and reverse direction denoted by p_f and p_r respectively and then computes the expected number of retransmission required to deliver the packet successfully to the destination as the IEEE 802.11 MAC retransmits a packet whose transmission is not successful. The equation 1 below illustrates the computation of ETX.

$$ETX = \frac{1}{(1 - p_f)(1 - p_r)} \dots\dots\dots 1$$

The equation also implies that ETX metric is bi-directional, that is the metric from node x to node y is same as metric from node y to node x. The weight of a path is defined as the summation of the ETX's of all links along the path. ETX does well in homogeneous single-radio, but does not perform well in environments with different data rates.

Per-hop Packet Pair Delay (PktPair)

PktPair metric concept was thought off to correct the problem of distortion of RTT measurement due to queuing delays. To calculate this metric, a node sends two probe packets back-to-back to each neighbor every second. First probe packet is small and second one is large. The neighbor calculates the delay between receipt of first and the second packets and reports this delay back to the sending node. The sender maintains an exponentially weighted moving average of these delays for each of its neighbors. The objective of Pktpair routing algorithms is to minimize the sum of these delays, if due to high loss

rate second probe packet requires retransmission by 802.11 ARQ then delay measured by the neighbor increases. The disadvantage of this metric is overheads is even greater than RTT and not completely immune to self-interference.

Expected Transmission Time (ETT)

From [4] ETT of a link k is defined as expected MAC layer duration required for a successful transmission of a packet at link k . The weight of a path p is simply the summation of the ETTs of all the links on the path. This routing metric improves the WMN performance by considering the differences in link transmission rates. The relationship between the ETT of a link k and ETX can be expressed as shown in equation 2.

$$ETT_k = ETX_k \frac{s}{b_k} \text{-----2}$$

Where b_k is the transmission rate of link k and s is the packet size. The drawback of ETT is that it still does not capture the inter-flow and intra-flow interference in the network completely. i.e. ETT may choose a path that only uses single channel, even though a path available with more diversified channels with less interference or higher throughput.

Weighted Cumulative Expected Transmission Time (WCETT)

WCETT metric was proposed to reduce the intra-flow interference, means to reduce the number of nodes operating on same channel on the path p , that is used to transmit the packets. Thus obtain high throughput in a multi-radio, multi-hop WMN. This metric does not consider the effect of inter-flow interference. One of goal of MR-LQSR protocol design is path weight should increase as more number of links are added to an existing path and that is fulfilled by this metric by adding/increasing the ETT as the links are added. It is as well as end-to-end delay experienced by a packet travelling along the path. Thus, for a path of n hops

$$WCETT = (1 - \beta) * \sum_{i=1}^n ETT_i + \beta * \max_{1 \leq j \leq k} X_j \text{---3}$$

In equation 3 β is a tunable parameter subject to $0 \leq \beta \leq 1$ and X_j is the maximum number of times the channel j appears along the path p , which captures the intra-flow interference, because WCETT metric assigns lower weights to the paths that have more diversified channel assignments on their links.

We can interpret the equation 3 in two parts. First term is the sum all transmission times of all hops in the network, which reflects the total resource consumption along this path. The second term reflects the set of hops that will have most impact in the throughput of this path. The weighted average can be viewed as an attempt to balance the two terms. WCETT selects links based upon their loss rate and bandwidth, without regard to channel diversity if $\beta = 0$ is set. It can also be observed that WCETT is only metric that selects links based on both loss rate and bandwidth and considers channel diverse paths unlike ETX.

3. Methodology

Since it is found suitable that the combination of LQSR protocol, WCETT metric for a multi-hop, multi-interface WMN along with MCL which creates an ad-hoc routing framework is used in our experimental setup



Fig.2(a) Topology of the WMN

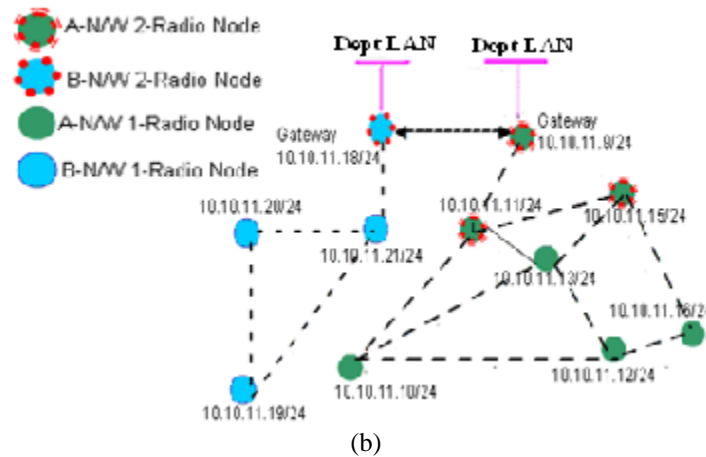


Fig.2(b) Schematic view of the testbed.

Fig. 2(a) shows a 10-node WMN testbed setup, located on the second floor of ED building with nodes placed in the offices, conference rooms and labs. Unlike wireless-friendly cubicle environments, the building has rooms with floor-to-ceiling walls and solid wooden doors. All the nodes were placed in fixed locations and never moved during testing. Node density was kept fairly high to enable variety of multi-hop path. Our testbed spans 37 meters (120 feet approx) in length and 15.5 meters (50 feet) in width. Desktop PCs used in the testbed are 1.87 GHz Intel Core Duo processors with 2 GB memory with XP SP2 OS. All the experiments were conducted on IPv4 using statically assigned addresses. Combination of single and two radio nodes is used in our testbed, i.e. 4 nodes with two radios and 6 with single radio, with an intent to test the behavior of the network with the combination of single and two radio nodes. Each node is equipped with combination of two 5 GHz and 2.4 GHz operating band wireless adapters or with any one adopter such as D-Link DWL-520+ of IEEE 802.11b, Netgear WG-311 v3, D-Link DWA-510 of IEEE 802.11g and Proxim Orinoco gold, ZyXEL AG-225H v2 of dual band that can operate on IEEE 802.11a& IEEE 802.11g standards. Our testbed comprises of two networks (groups of nodes) i.e. nodes are grouped into *N/W-A* colored with green and *N/W-B* colored with blue. Consider fig. 2(a) nodes with just circle either green or blue color is with single interface and nodes with circle either green or blue with dots outside the circle is nodes with two interfaces. SSIDs for wireless adapters belonging to nodes of *N/W-A* is configured as *MyMesh* for first adaptor and *MyMesh9* for second adaptor and for nodes having single adapter, SSID configured is *MyMesh*. In *N/W-B* network all nodes are equipped with single wireless adapter, configured with SSID *MyMesh3*, only gateway node of *N/W-B* is installed with two radios one configured as *MyMesh3*, second adapter configured as *MyMesh9*. It can be observed that adopter with SSID *MyMesh9* is present in both the gateway nodes of *N/W-A* and *A/W-B* which is responsible to bridge two networks here.

The static IP address for the nodes is assigned as given below

N/W-A - Starting from 10.10.11.9 to 10.10.11.16

N/W-B - Starting from 10.10.11.18 to 10.10.11.21

This IP address for a node is used to identify a node in the network, irrespective of the number of hardware adapters used as part of the mesh network. Also following static address was assigned for the MAC of Virtual adapters of the nodes for better monitoring while testing.

N/W-A - Starting from 74-99-99-99-AA-00 to 74-99-99-99-AA-06

N/W-B - Starting from 74-77-77-77-AA-00 to 74-77-77-77-AA-03

Fig.2 (b) illustrates the connectivity between the nodes of two networks. Since the nodes are combination of single and two radios, nodes in the testbed is so arranged, such that any node of one network can communicate with any node of other network.

Except configuring to ad hoc mode and fixing the frequency band & channel number, default configuration for the radios is used. In particular, all the cards perform auto rate selection and have RTS/CTS disabled. It was ensured that there were no other 802.11a/b/g users during the experiments.

4. Results

The software tools used in the testbed for measurement of throughputs between nodes with path lengths of one, two, three and more hops were *Iperf*, *Microsoft Network Monitor*. *Ping* to check the connectivity and *GNU-Plot* to plot the obtained results.

Single-Radio Experiment

Firstly the experiments with single radio on a best one hop path length with IEEE 802.11g and IEEE 802.11a was conducted. Both the standards are of specification 54 Mbps data rate fig.3 shows a plot which illustrates the behavior of the adopters. Procedure of the experiment is, a three minute tcp transfer was carried out between selected nodes first between a pair of nodes with IEEE 802.11g adopters then with a pair of nodes with IEEE 802.11a adopters.

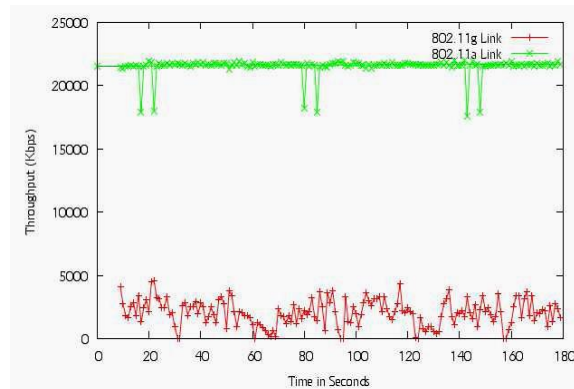


Fig.3 Comparison of throughputs between 802.11a link and 802.11g link

It is observed that 802.11a link has offered a maximum throughput approx. 21 Mbps and transferred 314 MB of data whereas 802.11g link has given only 4.5 Mbps approx. as maximum throughput and had transferred only 44.8MB of data. Though both the standards are of same data rate, 802.11g tends to be slower link compared to 802.11a link.

Impact of Band and Channel Assignment

An assumption while designing the MR-LQSR routing protocol is, if multiple radios used in a node then they should be configured to non-interfering channels. Though it is done we can observe that performance is poor in the first set of experiment. Table 1 shows that data obtained from the experiment.

	Receiver (NR Lab) Orinoco ZyXEL	Sender-1 (Average Throughput) Adapter tuned to ch 64	Sender-2 (Average Throughput) Adapter tuned to ch 36
Individually	Two 802.11a	21514 Kbps	12275 Kbps
Simultaneously		6206 Kbps	7970 Kbps
Drop in Throughput		71%	35%

Table1. Comparison of throughput between nodes with 802.11a interfaces

i) First Set of Experiment

Procedure of the experiment is three nodes all with IEEE 802.11a adopters are used. As shown in fig.2 (a) first node is placed in conference room and second in NR lab and third in e-class room. All rooms are adjacent to each other. First (Sender-1) and third (Sender -2) node is used always to send packets and second node which is in the middle at NR lab is used always to receive the packets from the other two nodes. Both the sender receiver pairs of adopters in the nodes are configured to non-interfering channels as shown in table 1.

Firstly tcp traffic was transferred for two minutes from first node only and received by NR lab and it was noted that 21514 Kbps was received. Secondly same experiment was done with third node with first node made idle and traffic received at NR lab node and noted that 12275 Kbps of average throughput received. Finally from both first node and third node tcp traffic was transferred for two minutes simultaneously and packets received at NR lab node. Now from table 1, it can be observed that at the first sender the average throughput is only 6206 Kbps and from second sender it was 7970 Kbps wherein the drop in throughput are 71% and 35% respectively compared to the throughputs with experiments when conducted individually.

ii) Second set of experiment

Here sender-2, i.e. node 3 is now equipped with 802.11g adopter instead of 802.11a, also receiver adopter at node in NR lab changed to 802.11g and configured to channel 10 as shown in Table 2

Again same set of previous experiments was carried out and results are noted as shown in table 2. It is observed that drop in throughput is reduced significantly to 10% and 6% respectively.

	Receiver (NR Lab) ZyXEL D-Link	Sender-1 (Average Throughput) Adapter tuned to ch 36	Sender-2 (Average Throughput) Adapter tuned to Ch 10
Individually	802.11a 802.11g	12345 Kbps	4698 Kbps
Simultaneously		10990 Kbps	4387 Kbps
Drop in Throughput		10%	6%

Table 2. Comparison of throughput between nodes with 802.11a and 802.11g a interfaces

Above two sets of experiments illustrates that though we use multiple interfaces with non-interfering channels, even then they interfere and performance is very poor. This drawback is overcome in the second set of experiment by using multiple interfaces but of different bands operating in 2.4 GHz and 5 GHz respectively in a node.

Experiment with Single/Two Radio with WCETT, ETX and PktPair Metrics

Test on WCETT, ETX and PktPair a shortest path routing was conducted to judge which metrics could be suitable for wireless multi-mesh network. Procedure of the experiment is, firstly tcp traffic transfer for 180 seconds for a path length of 3 hops with all the four nodes equipped with single 802.11g adopter was conducted. Secondly all the nodes are equipped with 2 interfaces one with 802.11a and another 802.11g was used and same experiment was repeated. Results are tabulated in table 3.

From this experiment it can be observed from table 3 that WCETT metric even in single radio scenario does well getting 20% and 65% more throughput compared to ETX and PktPair metrics respectively. This is because WCETT metric considers not only loss rate but also link bandwidth while assigning weight to the links. Due to this WCETT sometimes may select longer paths than ETX, even then results in better throughput. Nodes with two radios, no-doubt WCETT metric along with LQSR meant for multi-radio scenario does better than single radio performance getting 140% and 540% throughput more than ETX and PktPair metric in two radio scenario. Fig 4 shows the behavior of WCETT metric with ETX and PktPair both in single radio and two radio scenario graphically.

	Single Radio Experiment Median Throughput	Percentage Increase	Two Radio Experiment Median Throughput	Percentage Increase
WCETT	1240 Kbps	20% increase than ETX, 65% increase than Pkt Pair	2523 Kbps	140% increase than ETX, 540% increase than PktPair
ETX	992 Kbps		1031 Kbps	
Pkt Pair	434 Kbps		394 Kbps	

Table 3 Throughput with metrics WCETT, ETX and PktPair on Single/Two Radio nodes

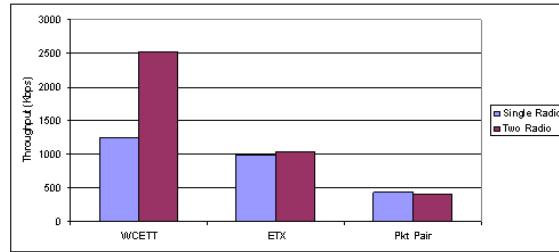


Fig. 4 Comparison of median TCP throughput with WCETT, ETX and PktPair on Single/Two radio nodes

Fig. 5 & 6, illustrates the behavior of metrics ETX and WCETT with single radio and two radio node on path length of one, two and three hops.

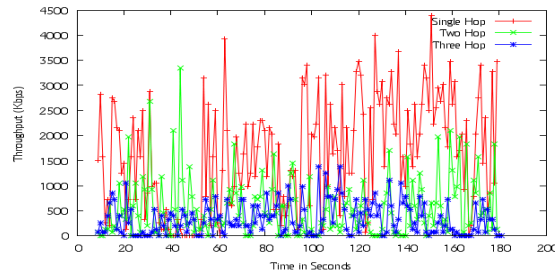


Fig. 5(a) ETX Single radio throughput comparison for single, two and three hop length

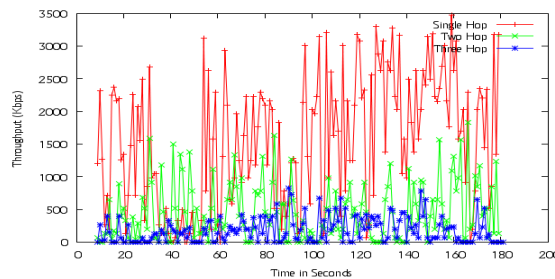


Fig. 5(b) ETX two radio throughput comparison for single, two and three hop length

From fig. 5(a) and 5(b) it can be observed that single hop throughput is almost the same, whereas the two hop path performance has reduced and the three hop performance also has no significant increase in performance. This is because ETX tries to route packets through 802.11g links which is longer range slower link even though higher throughput paths are available. Hence ETX uses the second interface in sub-optimal manner.

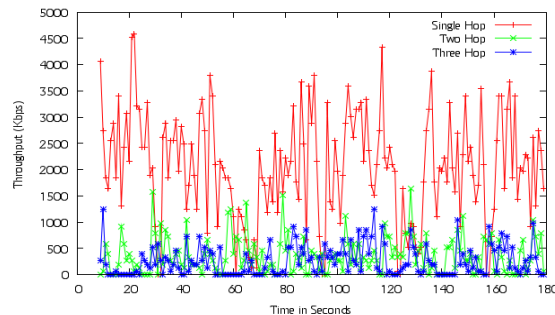


Fig.6(a) WCETT single radio throughput comparison for single, two and three hop length

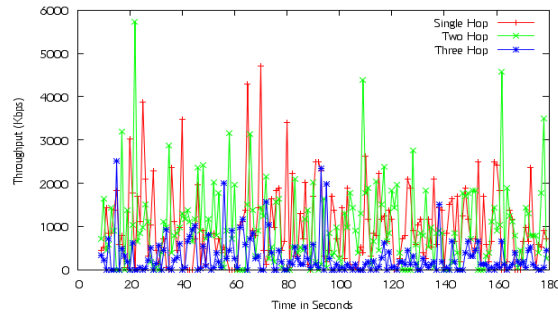


Fig. 6(b) WCETT two radio throughput comparison for single, two and three hop length

From fig 5(a) and fig. 6(a) when compared the throughputs are almost same. i.e. in single radio ETX does well but in multi-radio scenario ETX performance is worse but WCETT metric, from fig. 6(b) the two hop path length performance is almost double when compared to single radio performance. This is because WCETT uses always 802.11a link and uses 802.11g link only when it is beneficial to it and WCETT uses the second interface as an additional resource given unlike ETX using it in sub-optimal manner. Comparing fig. 6(a) and 6(b) three hop length performances has improved with two radio node compared to single radio. Fig.7 shows performance improvement in percentage compared to single radio performance with WCETT metric for various paths.

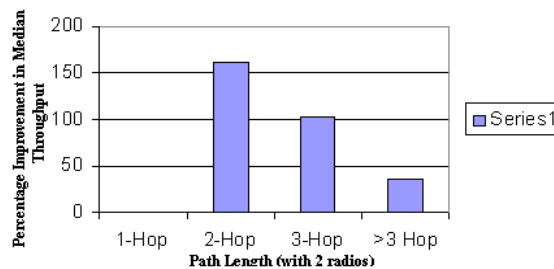


Fig. 7 Improvement in median throughput of two radio nodes over single radio for various path lengths with WCETT as the metric.

Single hop length performance improvement is not considered because of no channel diversity. Path length greater than 3 hop, has only 30% improvement in performance, this is because on longer paths TCP performs poorer because of the following reason.

- Increase in round trip time
- Higher probability of packet loss due to channel errors
- Contention between hops that are on the same channel.

Impact of Channel diversity (β)

WCETT metric is the weighted average of following two quantities

- Sum of ETTs of all hops along the path with a weight of $(1 - \beta)$
- Sum of ETTs on the bottleneck channel, with a weight of β

Experiment with path length of two, three and more hops were conducted by transferring TCP traffic for 180 seconds with the value of $\beta = 0, 0.1, 0.5$ and 0.9 set and readings are as noted in table 4 to measure the impact of channel diversity.

	2-Hop	3-Hop	>3-Hop
$\beta = 0$	66 Kbps	66 Kbps	43 Kbps
$\beta = 0.1$	1016 Kbps	262 Kbps	83 Kbps
$\beta = 0.5$	2032 Kbps	983 Kbps	671 Kbps
$\beta = 0.9$	852 Kbps	328 Kbps	272 Kbps

Table 4 Comparison of median TCP throughput for various pathlengths at various β values

Fig.8 shows β has an impact on throughput of connections of a specific path length. It is very clear that performance at $\beta = 0.5$ is better for all path lengths. At $\beta = 0$ the performance is poor for all path lengths. The reason could be links used by the metric at $\beta = 0$ may be 802.11g link which yields lower throughput as seen in previous experiment and for paths longer than 3 hops the channel diversity does not provide significant benefit.

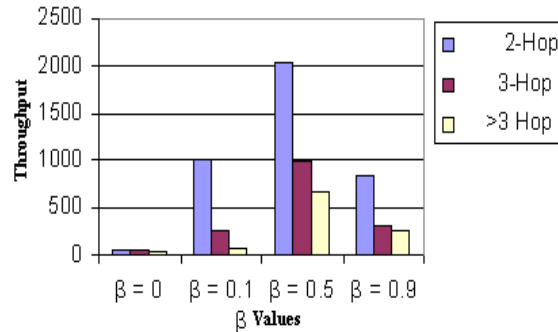


Fig. 8 GraphComparison of median TCP throughput for various pathlengths at various β values

Parallel WMN

From previous experiments it is observed that in case of using multiple interfaces then if same band interfaces are used then lot of interferences occur to extent that throughput drops to approximately 70%. This is because from [1] it is seen that activating multiple radios in a node lead to degradation in performance due any of the following reason.

- Board Crosstalk
- Radiation leakage
- Inadequate distance separation between several antennas.

[1] Shows that by taking appropriate measure like shielding of wireless cards to reduce radiation leakage, custom made platform to cancel crosstalk and adequate distance of 1 meter between the antennas, the performance can be improved to as much as 100%. [2] has shown that throughput increases as we use more number of interfaces, but limits to 5. Using more than five interfaces in a node leads to degradation of performance.

Impact of Throughput performance on parallel networks

In fig. 2(b), two mesh networks are set to operate in parallel i.e. *N/W-A* and *N/W-B*. The testbed consists predominantly single radio nodes, with a few two radio nodes used. To test transfer flow behavior between two networks, three minute TCP traffic transfer was conducted with path length of single, two, three hop lengths and also same experiment on a single WMN for comparison was done. Results are as tabulated in Table 5.

Fig.9 shows the behavior of throughput performance between nodes in a single network and across two networks. It is observed that both throughputs are almost same and closely follows except a small difference

Path Length	Median Throughput Between nodes in Single Network	Media Throughput Between nodes in Two Network	Difference in Throughput
Two-hop	2032 Kbps	2228 Kbps	196 Kbps
Three-hop	583 Kbps	712 Kbps	129 Kbps

Table 5 Comparison of throughputs between nodes in a single network nodes and nodes across two networks

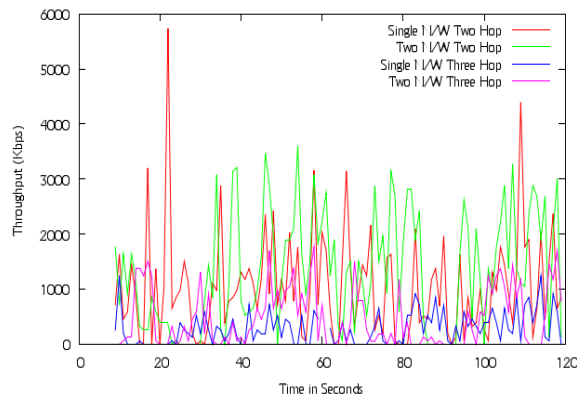


Fig. 9 Comparison of throughput between nodes in single network and nodes across network for a path length of single, two and three hops

5 Conclusions

Routing protocol that can operate with multi-radio concept like LQSR and efficient metric that utilizes the multi-radio resources beneficially like WCETT routing, also routing metric should consider both inter-flow and intra-flow interferences while routing the packets. Here WCETT does not consider inter-flow interference and hence can transmit packets to the congested route also, otherwise WCETT is the best suited metric for atmosphere like multi-hop, multi-interface and multi-mesh wireless network. As per [2] if maximum of 4 physical network interfaces can be used in a node with the measures taken to shield the network interfaces and by using custom made box to avoid crosstalk and adequate separation between antennas, then with multiple radios of different bands in a node can perform best without interference and is possible to set up multiple, say 4 WMNs that can operate in parallel, such that we can extend the coverage area of Mesh network, thus enhancing the capacity of WMN.

References

- [1] Joshua Robinson, Konstantina Papagiannaki, Christophe Diot, Xingang Guo and Lakshman Krishnamurthy. "Experimenting with a Multi-Radio Mesh Networking Testbed," in 1st workshop on Wireless Network Measurements WinMee, Trento Italy, 2005.
- [2] Chi Moon Oh, Hwa jong Kim, Goo Yeon Lee and Choong Kyo Jeong, "A Study on the Optimal Number of interface in Wireless Mesh Network" International Journal of Future Generation Communication and Networking, IJFGCN Vol. 1, No. 1 pp 59-66, Dec 2008.
- [3] Yn Zhang, Jijun Kuo and Honglin Hu. *WIRELESS MESH NETWORKING*, Boca Raton, New York: Auerbach Publications 2007.
- [4] Yaling Yang, Jun Wang and Robin Kravets "Designing Routing Metrics for Mesh Networks," IEEE Workshop on Wireless Mesh Networks (WiMesh), Santa Clara, CA, 2005.
- [5] David B. Johnson, David A. Maltz, and Josh Broch, "DSR: The Dynamic Source Routing Protocol for Multi-hop Wireless Ad-hoc Networking" in *Ad Hoc Networking*, 1/e. Charles E. Perkins, Addison-Wesley, 2001, pp. 139-172.
- [6] Richard Draves, Jitendra Padye and Brian Zill. "Routing in Multi-Radio, Multi-Hop Wireless Mesh Networks," *Mobicom*, 2004, pp 114-128.
- [7] Richard Draves, Jitendra Padye and Brian Zill. "Comparison of Routing Metrics for Static Multi-Hop Wireless Networks," *SIGCOMM'04*, 2004, pp 133-144.
- [8] Douglas S J De Couto, Daniel Aguayo, Jhon Bicket and Robert Morris, "A High-throughput Path Metric for Multi-hop Wireless Routing." *Journal of Wireless Networks*, Vol. 11, Issue 4, pp 419-434, Jul 2005.

A Study on the Satisfaction with the Use of Leisure Food and Beverage Information System – Taking Traditional Farms for Example

Hung-Teng Chang¹, Pin-Chang Chen², Han-Chen Huang^{3,*}, Hui-Min Huang⁴

^{1,2,4}Department of Information Management, Yu Da University, Miaoli County, 36143, Taiwan, R.O.C.

^{3,*}corresponding author Department of Leisure Management, Yu Da University, Miaoli County, 36143, Taiwan, R.O.C.

Abstract:

The application of food and beverage information system to traditional farms has become a current trend. In addition to providing visitors with different featured itineraries and services, it also helps develop the so-called featured farms. However, the existing studies on F&B information system of farms mainly focused on the establishment of system, and seldom discussed the satisfaction with use of system. Therefore, this study took the farms where a complete leisure F&B information system was established and those where such a system was not established as the examples, and used a questionnaire survey to analyze customers' and operators' satisfaction. In addition, this study used independent sample t-test to compare the difference between customers' and operators' satisfaction with meal reservation, management of table condition, meal management, GPS parking navigation and F&B management, in order to understand the actual difference between customers' and operators' satisfaction with the use of F&B information system.

Keywords: Customer satisfaction, Traditional farm industry, e-leisure farm, F&B information system.

1. Introduction

The development of technology has made “informationalization” no longer the symbol of industrial progress, but an indispensable survival tool which effectively introduces information system into industries to enhance competitiveness. In recent years, the progress in internationalization has changed or transformed many industries, and the original agricultural mechanism has failed to conform to the trend of times. To sustainably operate agriculture, many original systems and concepts all have to be changed to respond to the changes in the era of diversity. Therefore, traditional farms combine pastoral landscape, natural ecology and environmental resources with rural culture and farm life to provide citizens with the best travel destination of leisure and tourism. Owing to the development of information technology, a variety of websites of leisure farms which provide abundant tourist and F&B information have been set up. However, the existing studies seldom mentioned the satisfaction with the use of leisure F&B system. Consequently, this study took the traditional farms where leisure F&B information system was established as the examples, and used a questionnaire survey to analyze customers' and operators' satisfaction with the use of such a system. It is hoped that the analysis on the satisfaction of customers and operators can provide all the citizens in Taiwan with abundant information on leisure and tourist farms, as well as improve the tourist effect of traditional farms.

2. Literature Review

The application of NFC (Near Field Communication) technology to restaurants enables customers to replace membership card and credit card with a NFC cellular phone. The use of NFC technology not only increases the convenience of reservation and ordering, but also reduces restaurants' cost of service personnel. It enables customers to enjoy a refreshing dining environment and to pay the bill in a rapid and convenient manner without worrying about unauthorized use of credit card or waiting for the change after paying a bill [1, 2]. There is a difference in the need for application of internet channels between male and female customers. In addition, there are also significant differences in promotion activities, information provision, brief guidance and exchange of views between them. The study found that male customers put emphasis on the introduction to shopping and information, while female customers put emphasis on the introduction to promotion activities and information [3]. Age, level of education, residence, occupation, etc. also have an effect on them. In the future, operators may cooperate with tourist websites and other relevant websites to reduce the expense of internet advertisement and to effectively increase the number of visitors of hotel websites. In terms of the application of internet, operators should also enhance the interaction with consumers to maintain the long-term operation of websites [4-5]. The “provision of website” has a significant effect and positive explanatory power on “occupancy rate,” “operating income” and “average value output of guest rooms.” “Website functions” does not have a significant effect and positive explanatory power on four indicators of operating performance. “Online reservation” has a significant effect and positive explanatory power on “occupancy rate.”

“Online transaction” has a significant effect and positive explanatory power on “average output value of employees.” Therefore, the use of online website functions can significantly improve operating performance [6]. After the use of information technology, the average score of F&B department of international tourist hotels in the aspects of technology, organization, management and environment was higher than the theoretical average, and the difference was significant. Moreover, the difficulties in the use of information technology encountered by F&B department of international tourist hotels can be divided into four dimensions, technology, organization, management and environment. The application of information technology is significantly and positively correlated with all of them. The fact showed that the use of information technology by F&B department not only reduces difficulties, but also conforms to the developmental trend of enterprises [7-9]. Under the intense competition among numerous operators, consumers’ demand for convenience and instantaneity has increased day by day. The reason why consumers have meals in F&B industry is not only to feed themselves, but also to meet their needs for higher quality and services. As a result, the “production-oriented” F&B industry has been gradually transformed into “consumer-oriented” service industry. To reduce cost and improve service quality, how to combine modern business philosophy with various information technologies to enhance the efficiency and competitiveness of F&B service industry operation has become an issue which cannot be ignored. After the integration with information technology, the prototype of management information system can be established. This system includes four major sub-systems: menu design system, purchasing and inventory management system, ordering and food preparation system and point-of-sale information and financial information system.

The introduction of information technology creates new orders and new working approaches and for the evolution of operating procedures [11, 10]. The addition of internet marketing into leisure farms creates developmental potential. Information technology makes it possible to provide customers with services which better meet their needs. The display of characteristics of leisure farms on internet platforms enables customers to design and browse relevant information in advance via internet at home. It provides customers with instantaneous information, meets their needs and creates competitive advantages. Internet marketing is one of the effective approaches to achieve the aforesaid objectives, follow the trend of technological era and improve the effectiveness of leisure agriculture [12]. Nai-Wen Kuo [13] found that the study subject mainly chose high-cost marketing strategies and interpersonal relationship marketing, and was not good at using internet marketing tools. However, the review on other studies showed that hotel operators good at using internet marketing mainly applied it to the meal marketing of F&B department, and the effectiveness was usually positive. However, the past studies on the use of internet technology were mainly quantitative studies on satisfaction which failed to reflect the predicaments generally faced in internet marketing of organizational transformation as the introduction of information system. The studies on the introduction of information system mainly focus on the introduction of ERP (Enterprise Resource Planning), and it seems that internet marketing is not regarded as the establishment of information system. Therefore, operators should change organizational pattern, re-define working procedures and improve employees’ ability and ambition to use web2.0 internet marketing tools, in order to successfully use web2.0 internet tools to develop great internet marketing strategies and to further establish a good customer relationship with consumers. Based on the above, the introduction of leisure F&B system into traditional farms has been a popular trend which cannot be delayed. The use of information design in F&B system makes it easy to expand the functions in the future and significantly increase the system flexibility. In addition to reducing customers’ time required in learning, the integrated operating interface better improves the overall operating efficiency and saves the operating cost in the competitive leisure F&B market. Therefore, this study used a quantitative questionnaire survey to investigate the satisfaction with the use of leisure F&B information system in five dimensions, “meal reservation,” “management of table condition,” “meal management,” “GPS parking navigation” and “F&B management” as the reference for the future studies concerning F&B system. It is hoped that this study can help activate the development of leisure farms in Taiwan and achieve the objective of improving the effectiveness of overall tourism.

3. Methodology

3.1. Research Procedures

Based on the aforementioned research motivations, research objectives and questions, the research procedures of this study are shown in Figure 1. After the research themes were confirmed, this study collected relevant reference and data. Upon the confirmation of the research scope and the compilation of questionnaire, this study invited three experts to participate in the compilation and amendment of the questionnaire to confirm the items of the formal questionnaire. In the end, the results and data obtained from this study were analyzed and discussed. This study conducted a questionnaire survey on the satisfaction with the use of F&B information system. This study used simple random sampling to distribute 340 questionnaires. The research subjects were mainly the adults over the age of 20. 300 questionnaires were distributed to customers (150 of them were distributed to the customers consuming at farms where F&B information system was used, while 150 of them were distributed to those consuming at farms where F&B information system was not used), and 40

questionnaires were distributed to operators (20 of the questionnaires were distributed to the operators using F&B information system, while 20 of them were distributed to those who did not use it) to conduct the formal questionnaire survey.

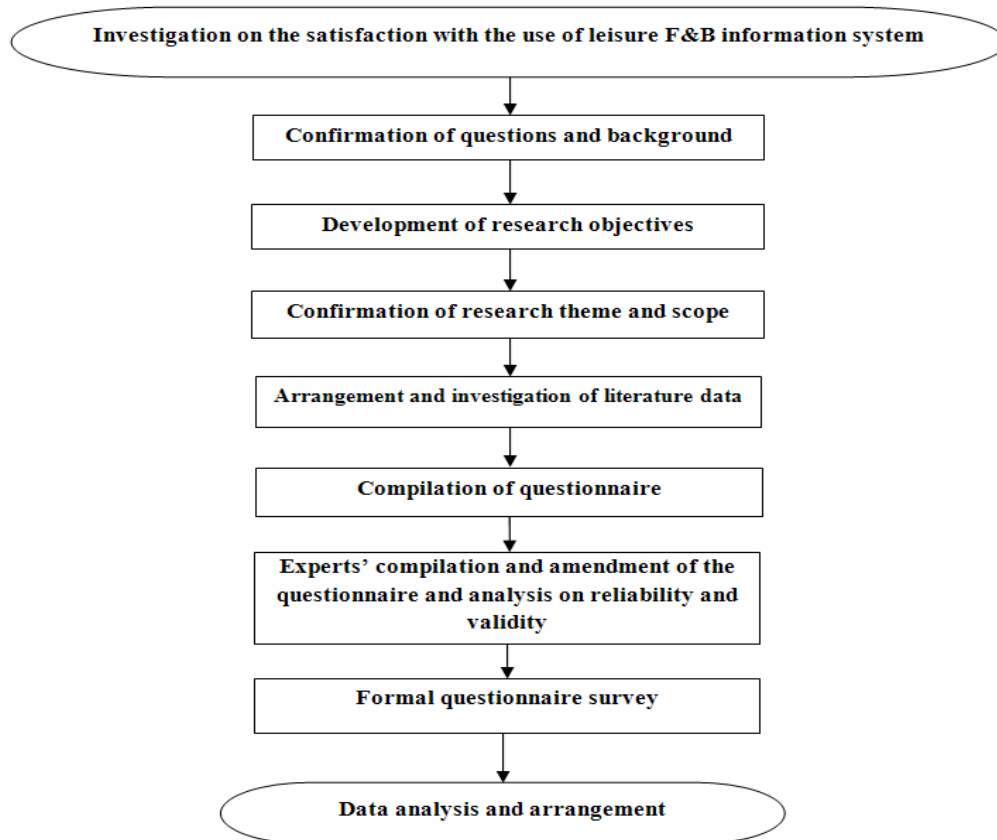


Figure 1. Research Procedures

3.2. Research Framework

The main purpose of this study is to investigate customers' and operators' satisfaction with the use of F&B information system, as well as to compare whether there is any significant difference in customers' and operators' satisfaction with the use of F&B information system. The research framework is shown in Figure 2.

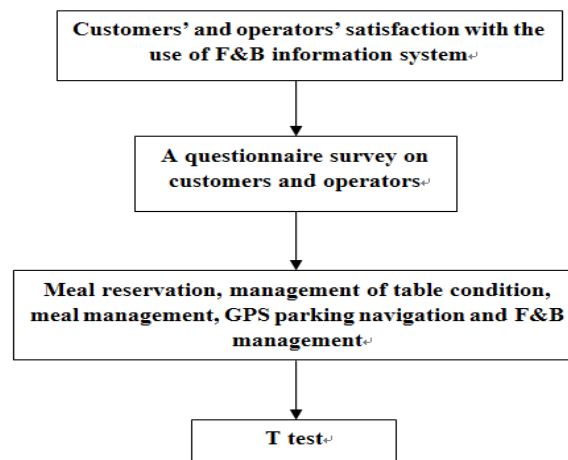


Figure 2. Research Framework

3.3. Research Tools

This study mainly selected the websites “where embedded technology is applied to the integration and development of leisure F&B information system module” as designed by National Science Council project as the samples, and used the “questionnaire on the satisfaction with the use of leisure F&B information system” as the research tool. The questionnaire mainly includes five parts of the website contents, “meal reservation,” “management of table condition,” “meal management,” “GPS parking navigation” and “F&B management”. This study tested the internal consistency of the pre-test samples. The results of the analysis on the reliability of various subscales are shown in Table 1. The correlation coefficient matrices of various subscales are shown in Table 2.

Table 1. Reliability of Various Subscales on the Satisfaction with the Use of F&B Information System

	Subscale on meal reservation	Subscale on management of table condition	Subscale on meal management	Subscale on GPS parking navigation	Subscale on F&B management
Cronbach's α	.819	.813	.721	.697	.839

Table 2. Correlation Coefficient Matrices of Various Subscales on the Satisfaction with the Use of F&B Information System

	Subscale on meal reservation	Subscale on management of table condition	Subscale on meal management	Subscale on GPS parking navigation	Subscale on F&B management
Subscale on meal reservation	1				
Subscale on management of table condition	.697**	1			
Subscale on meal management	.734**	.596**	1		
Subscale on GPS parking navigation	.424**	.543**	.560**	1	
Subscale on cost control	.627**	.532**	.691**	.475**	1

**p<.001

3.4. Data Processing

The results and data collected from all the scales in this study were arranged, converted, analyzed and input in computer. Upon the confirmation of accuracy via computer, this study used SPSS 12.0 statistical software to perform statistical analysis on the data. This study used customers and operators as the independent variables, and used meal reservation, management of table condition, meal management, GPS parking navigation and F&B management as dependent variables to perform a t test, in order to test the differences in various indicators between two groups of customers.

4. System Results

4.1. Customers' opinions on meal reservation of F&B information system

Table 3. Mean, standard deviation and t-test results of the subscale on meal reservation

Subscale	Item	Customers	M	SD	t
Meal reservation	1	Used the system	3.55	.671	3.405**
		Never used the system	3.31	.543	
	2	Used the system	3.59	.614	2.805
		Never used the system	3.40	.579	
	3	Used the system	3.41	.761	3.425
		Never used the system	3.11	.756	
	4	Used the system	3.60	.645	4.126**
		Never used the system	3.25	.827	

**p<0.01

4.2. Customers' opinions on the management of table condition of F&B information system

Table 4. Mean, standard deviation and t-test results of the subscale on management of table condition

Subscale	Item	Customer	M	SD	t
Management of table condition	5	Used the system	3.49	.673	4.723**
		Never used the system	2.78	.743	
	6	Used the system	3.91	1.074	.576**
		Never used the system	2.85	.925	
	7	Used the system	3.44	.815	.075
		Never used the system	3.43	.718	
	8	Used the system	3.21	.952	.810
		Never used the system	3.13	.900	

**p<0.01

4.3. Customers' opinions on meal management of F&B information system

Table 5. Mean, standard deviation and t-test results of the subscale on meal management

Subscale	Item	Customers	M	SD	t
Meal management	9	Used the system	3.19	.986	3.431
		Never used the system	2.81	.932	
	10	Used the system	3.82	.869	2.166*
		Never used the system	3.12	.723	
	11	Used the system	2.89	1.027	-.360
		Never used the system	2.93	.891	
	12	Used the system	2.97	1.042	1.893
		Never used the system	2.75	.969	

*p<0.05

4.4. Customers' opinions on GPS parking navigation of F&B information system

Table 6. Mean, standard deviation and t-test results of the subscale on GPS parking navigation

Subscale	Item	Customers	M	SD	t
GPS parking navigation	13	Used the system	2.58	1.082	2.677
		Never used the system	2.25	1.031	
	14	Used the system	3.67	.858	-.299*
		Never used the system	2.30	.673	
	15	Used the system	3.04	.955	3.696
		Never used the system	2.63	.951	
	16	Used the system	3.42	1.046	-2.075*
		Never used the system	2.25	.835	

*p<0.05

4.5. Operators' opinions on F&B management of F&B information system

Table 7. Mean, standard deviation and t-test results of the subscale on F&B management

Subscale	Item	Operators	M	SD	t
F&B management	17	Used the system	3.43	1.064	-1.167*
		Never used the system	2.56	.908	
	18	Used the system	3.41	.716	3.637
		Never used the system	3.10	.775	
	19	Used the system	3.37	.798	4.070*
		Never used the system	2.98	.847	
	20	Used the system	3.19	.922	4.218
		Never used the system	2.73	.939	

*p<0.05

5. Conclusion

5.1. Meal reservation:

The mean of the satisfaction with meal reservation of customers using the system was 3.5375, which was higher than that of those who did not use the system (3.2675). In addition, the t-test also showed a significant difference, suggesting that the use of F&B information system can reduce customers' time spent on waiting. Moreover, customers can fully utilize their time in the weekends to schedule for meals to prevent their appetite and the overall service quality from being affected by over-crowdedness.

5.2. Management of table condition:

In terms of the dimension of management of table condition, the mean of the satisfaction of customers using the system was 3.5125, which was higher than that of those who did not use the system (3.0475). The t-test also showed a significant difference, suggesting that the use of F&B information system enables customers to become satisfied with the arrangement of dining seats and choose the location and landscape they prefer to dine at, which significantly improve their expectation towards dining. Moreover, the use of F&B information system also speeds up the payment process, and saves customers' valuable time.

5.3. Meal management:

In terms of the dimension of meal management, the mean of the satisfaction of customers using the system was 3.2175. Although it was higher than that of those who did not use the system (2.9025), the mean of some of the items was not high. The findings showed that the customers who used the system and those who did not use the system were dissatisfied with meal management. However, the t-test showed a significant difference, suggesting that the customers using F&B information system could obtain more promotion/discount information early and learn of such information prior to departure. Compared with the customers who did not use the system, they were more satisfied with the meal management.

5.4. GPS parking navigation:

The mean of satisfaction with the GPS parking navigation of the customers using the system was 3.1775, which was higher than that of those who did not use the system (2.3575). The t-test also showed a significant difference, suggesting that the use of F&B information system enables visitors to rapidly find the location of the farms via online navigation and save their time. Moreover, the provision of online navigation service enables visitors to plan their route in detail and find the nearby scenic spot for resting. Furthermore, the use of embedded parking information of F&B information system also enabled customers to know the number of cars and location of parking lot to facilitate their arrangement of schedule.

5.5. F&B management:

The mean of satisfaction with F&B management of operators using the system was 3.35, which was higher than that of those who did not use the system (2.8425). The t-test also showed a significant difference, suggesting that the operators using the system could significantly reduce the operating cost. In addition, they could better control manpower deployment to prevent the provision of inadequate services. Moreover, they can also understand customers' needs through the F&B information system to fully grasp the taste of customers, as well as the overall F&B management process. To operators, F&B information system can speed up the transformation of traditional farms into leisure/tourist farms. In addition to improving the marketing value and status of traditional farms in tourist market, it can also effectively increase the service quality of tourist/leisure industry. Moreover, operators' income also increases with the introduction of information system, and consumers' expenses in tourist industry increase accordingly. To regional development, the introduction of F&B information system into traditional farms can help overcome the predicament of emigration in various places in Taiwan. In addition to increasing local working opportunities, it also improves the environmental health and living functions of the neighborhoods. Furthermore, the use of the system can also enhance the competitiveness of local tourist industry, increase regional tax income and exposure, and activate regional development, which even turns a general township into a tourist township. Besides, it can also increase the income of farmers, improve the development of B&B and preserve natural ecology and cultural landscape resources to sustainably operate regional tourist resources. To consumers, the introduction of F&B information system enables them to immediately experience the beauty of landscape in leisure farms and the local delicacy to further achieve the objective of development of tourist industry. Consumers may even use online interactive platform to design their schedules more efficiently and better understand tourist schedule without spoiling their trip. Based on the above, the introduction of F&B information system has a significant benefit on operators, regional development and consumers. The characteristics and quality of leisure/tourist industry can be improved as long as operators can be familiar with the procedures of tourist management and basic knowledge of relevant tourist industries and understand the procedures of F&B management

and relevant basic F&B knowledge. It is hoped that the development of leisure farms can be activated to achieve the objective of improving the effectiveness of the overall tourist industry..

References

- [1] Lisa H. Nishii, David P. Lepak, Benjamin Schneider. Employee Attribution of the “WHY” of HR Practices: Their Effects on Employee Attitudes and Behaviors and Customers Satisfaction. *Personnel Psychology*, 61(3), 503-545, 2008.
- [1] Bruce Cooil, Timothy L. Keiningham, Lerzan Aksoy, Michael Hsu. A Longitudinal Analysis of Customer Satisfaction and Share of Wallet: Investigating the Moderating Effect of Customer Characteristics. *Journal of Marketing*, 71(1), 67-83, 2007.
- [2] Xueming Luo, Christian Homburg. Neglected Outcomes of Customer Satisfaction. *Journal of Marketing*, 71(2), 133-149, 2007.
- [3] J.R. Winsten, C.D. Kerchner, A. Richardson, A. Lichau, J.M. Hyman. Trends in the Northeast Dairy Industry: Large-Scale Modern Confinement Feeding and Management-Intensive Grazing. *Journal of Dairy Science*, 93(4), 1759-1769, 2010.
- [4] Elisabeth Johann. Traditional Forest Management under the Influence Of Science And Industry: The Story of the Alpine Cultural Landscapes. *Forest Ecology and Management*, 249, 54-62, 2007.
- [5] McElwee Gerard, Bosworth Gary. Exploring the Strategic Skills of Farmers across a Typology of Farm Diversification Approaches. *Journal of Farm Management*, 13(12), 819-838, 2010.
- [6] Carla Barbieria, Edward Mahoney. Why is Diversification an Attractive Farm Adjustment Strategy? Insights from Texas Farmers and Ranchers. *Journal of Rural Studies*, 25(1), 58-66, 2009.
- [7] Ricardo Jardim-Goncalves, Antonio Grilo. Putting the Building and Construction Industry in the Single European Information Space. *Automation in Construction*, 19(4), 388-397, 2010.
- [8] Zhaohua Deng , Yaobin Lu, Kwok Kee Wei, Jinlong Zhang. Understanding Customer Satisfaction and Loyalty: An Empirical Study of Mobile Instant Messages in China. *International Journal of Information Management*, 30(4), 289-300, 2010.
- [9] Chih-Yao Lo, Yu-Teng Chang, Chun-Liang Chou. The Analysis of Satisfaction and Future Business Impact for Hospitality Industry in Taiwan. *Journal of Convergence Information Technology*, 6(10), 268-276, 2011.
- [10] Jianfeng Li, Yan Lin, Feng Jin. A Supply Chain Simulation Model with Customer’s Satisfaction. *International Journal of Advancements in Computing Technology*, 4(10), 125-132, 2012.
- [11] Han-Chen Huang, Guan-Ya Shen. Applying the Fuzzy Analytic Hierarchy Process to the Analysis of Leisure Business Service Failure Weights. *International Journal of Advancements in Computing Technology*, 4(22), 813- 822, 2012.
- [12] Nai-Wen Kuo. A Holistic Customer Experience Design on the Internet. *Advances in Information Sciences and Service Sciences*, 3(1), 110-117, 2011.

On Presence of Interaction In An Unbalanced Two-Way Random Model

¹F.C. Eze, ²P.E. Chigbu

¹Department of Statistics, Nnamdi Azikiwe University, Awka, Anambra State, Nigeria
²Department of Statistics, University of Nigeria, Nsukka, Nigeria

Abstract

In an unbalanced two-way random model, there is no obvious denominator for testing for the main effects as a result of the presence of inter-action. The interaction was removed from the model/data resulting to a reduced model devoid of interaction. The data were transformed by dividing the entries of each cell of the data by the inverse of the square root of the standard error to remove the interaction.

Keywords: Expected mean squares, fractional degrees of freedom, reduced model.

1. Introduction

The presence of interaction in two-way analysis of variance could be a serious problem when testing for the main effects. Chow[3] emphasized that testing the treatment effects for the two-way ANOVA model with interaction, the interaction effect has to be tested first, otherwise the result for testing the treatment cannot be interpreted in a statistical meaningful manner. In ANOVA, a large F -value provides evidence against the null hypothesis. However, the interaction test should be examined first. The reason for this is that, there is little point in testing the null hypothesis H_A or H_B if H_{AB} : no interaction effect is rejected, since the difference between any two levels of a main effect also includes an average interaction effect Cabrera and McDougall[1] argued. Moore et al [5] argued that, there are three hypotheses in a two-way ANOVA, with an F -test for each. We can test for significance of the main effect A, the main effects of B and AB interaction. It is generally a good practice to examine the test interaction first, since the presence of a strong interaction may influence the interpretation of the main effects. Muller and Fetterman [6] agreed that model reduction in the presence of non significant interaction may be attractive for unbalanced or incomplete design.

2. Methodology

Given the model

$$y_{ijk} = \mu + \alpha_i + \beta_j + \lambda_{ij} + e_{ijk} \begin{cases} i = 1, 2, \dots, a \\ j = 1, 2, \dots, b \\ k = 1, 2, \dots, n_{ij} \end{cases} \quad (1)$$

Where

y_{ijk} is the kth observation in ijth cell,

μ is the overall mean effect,

λ_{ij} is the effect of the interaction between factor A and factor B,

e_{ijk} is a random error components,

n_{ij} is the number of observation per cell; and

using the Brute-Force Method, the expected mean squares (EMS) of the parameters of Equation (1) can be shown to be

$$\begin{aligned} EMS_A &= \sigma_e^2 + k_\alpha \sigma_\alpha^2 + k_1 \sigma_\lambda^2 \\ EMS_B &= \sigma_e^2 + k_\beta \sigma_\beta^2 + k_2 \sigma_\lambda^2 \\ EMS_\lambda &= \sigma_e^2 + k_3 \sigma_\lambda^2 \\ EMS_e &= \sigma_e^2 \end{aligned}$$

where

$$k_\alpha = \frac{N - N^{-1} \sum_i N_i^2}{a - 1} \quad (2)$$

$$k_1 = \frac{(\sum_i N_i^{-1} \sum_j n_{ij}^2 - N^{-1} \sum_{ij} n_{ij}^2)}{a-1} \quad (3)$$

$$k_\beta = \frac{N - N^{-1} \sum_j N_j^2}{b-1} \quad (4)$$

$$k_2 = \frac{(\sum_j N_j^{-1} \sum_i n_{ij}^2 - N^{-1} \sum_{ij} n_{ij}^2)}{b-1} \quad (5)$$

$$k_3 = (N - \sum_i N_i^{-1} \sum_j n_{ij}^2 - \sum_j N_j^{-1} \sum_i n_{ij}^2 - N^{-1} \sum_{ij} n_{ij}^2 + 2 \sum_{ij} n_{ij}^3 N_i^{-1} N_j^{-1}) / (a-1)(b-1) \quad (6)$$

where

$$\sigma_\alpha^2 = E(\bar{y}_{i..} - \bar{y}_{...})^2 = \frac{\sum_i (\bar{y}_{i..} - \bar{y}_{...})^2}{n}$$

$$\sigma_\beta^2 = E(\bar{y}_{.j.} - \bar{y}_{...})^2 = \frac{\sum_j (\bar{y}_{.j.} - \bar{y}_{...})^2}{n}$$

$$\sigma_\lambda^2 = E(\bar{y}_{ij.} - \bar{y}_{i..} - \bar{y}_{.j.} + \bar{y}_{...})^2 = \frac{\sum_{ij} (\bar{y}_{ij.} - \bar{y}_{i..} - \bar{y}_{.j.} + \bar{y}_{...})^2}{n}$$

$$\sigma_e^2 = E(y_{ijk} - \bar{y}_{ij.})^2 = \frac{\sum_{ijk} (y_{ijk} - \bar{y}_{ij.})^2}{n}$$

k_1, k_2 and k_3 are the coefficient of the variance components of the interaction for factor A, factor B and the interaction between factor A and factor B respectively.

The expected mean squares (EMS) of Equation (1) are presented in the ANOVA Table shown in Table 1.

S.V	d.f	SS	MS	EMS
Factor A	a-1	SS_α	MS_α	$\sigma_e^2 + k_\alpha \sigma_\alpha^2 + k_1 \sigma_\lambda^2$
Factor B	b-1	SS_β	MS_β	$\sigma_e^2 + k_\beta \sigma_\beta^2 + k_2 \sigma_\lambda^2$
AxB	(a-1)(b-1)	SS_λ	MS_λ	$\sigma_e^2 + k_3 \sigma_\lambda^2$
Error	N-pq	SS_e	MS_e	σ_e^2
Total	N-1	SS_T		

Table 1: ANOVA Table for Unbalanced data.

From the expected mean squares in Table 1, we can see that the appropriate statistic for testing the no interaction hypothesis $H_0 : \sigma_\lambda^2 = 0$ is

$$F_c = \frac{MS_\lambda}{MS_e}$$

This is because, under H_0 both numerator and denominator of F_c have expectation σ_e^2 .

The case is different when testing for $H_0 : \sigma_\alpha^2 = 0$ because the numerator expectation is $\sigma_e^2 + k_1 \sigma_\lambda^2$ and no other

expectation in Table 1 that is $\sigma_e^2 + k_1\sigma_\lambda^2$ under H_0 .

The case is also the same when testing for $H_0 : \sigma_\beta^2 = 0$

The cause of the above problem is the presence of interaction and when the interaction is removed from the model, the ANOVA Table 1 reduces to the ANOVA Table shown in Table 2.

S.V	d.f	SS	MS	EMS
Factor A	a-1	SS_α	MS_α	$\sigma_e^2 + k_\alpha\sigma_\alpha^2 + k_1\sigma_\lambda^2$
Factor B	b-1	SS_β	MS_β	$\sigma_e^2 + k_\beta\sigma_\beta^2 + k_2\sigma_\lambda^2$
Error	N-a-b+1	SS_e	MS_e	σ_e^2
Total	N-1	SS_T		

Table 2: Reduced ANOVA Table for Unbalanced data.

From the ANOVA Table 2, it is obvious that the common denominator for testing for the main effects is MS_e .

3 Method of Removing the Interaction

Now to remove the interaction from the model we proceed as follows:

The least square estimate for the interaction is:

$$\lambda_{ij} = \bar{y}_{ij} - \bar{y}_{i..} - \bar{y}_{.j.} + \bar{y}_{...}$$

$\bar{y}_{ij}, \bar{y}_{i..}, \bar{y}_{.j.}, \bar{y}_{...}$ are the cell means, row means for factor A, column means for factor B and the overall means respectively for the full model.

Removing the interaction from Equation (1) we have

$$y_{ijk}^* = y_{ijk} - \bar{y}_{ij} + \bar{y}_{i..} + \bar{y}_{.j.} - \bar{y}_{...} \quad (7)$$

$$= \mu + \alpha_i + \beta_j + z_{ijk}$$

Dividing Equation (7) by k and simplifying we have

$$y_{ij.}^* = \bar{y}_{i..} + \bar{y}_{.j.} - \bar{y}_{...}$$

Similarly

$$y_{i..}^* = \bar{y}_{i..}$$

and

$$y_{...}^* = \bar{y}_{...}$$

z_{ijk} is the error associated with y_{ijk}^* for the reduced model while $\bar{y}_{ij.}^*, \bar{y}_{i..}^*$ and $\bar{y}_{...}^*$ are the cell means, row means for factor A and the overall means for the reduced model.

It then follows that

$$\begin{aligned} \bar{y}_{i..}^* - \bar{y}_{...}^* &= \bar{y}_{i..} - \bar{y}_{...} \\ \bar{y}_{.j.}^* - \bar{y}_{...}^* &= \bar{y}_{.j.} - \bar{y}_{...} \end{aligned}$$

Now

$$z_{ijk} = e_{ijk} - \bar{e}_{ij.} + \bar{e}_{i..} + \bar{e}_{.j.} - \bar{e}_{...}$$

To transform and normalize the data, we divide the original data by the inverse of the standard error. To do this we need the $\text{var}(z_{ijk})$.

From Equation (1) n_{ij} is the number of observations per cell. It then follows that

$$\begin{aligned}\sum_j n_{ij} &= N_{i.} \\ \sum_i n_{ij} &= N_{.j} \\ \sum_{ij} n_{ij} &= N_{..}\end{aligned}$$

It can be shown that

$$\begin{aligned}E(\bar{e}_{i..}) &= \frac{\sigma_e^2}{N_{i.}} \\ E(\bar{e}_{.j.}) &= \frac{\sigma_e^2}{N_{.j}} \\ E(\bar{e}_{ij.}) &= \frac{\sigma_e^2}{n_{ij}} \\ E(\bar{e}_{...}) &= \frac{\sigma_e^2}{N_{..}}\end{aligned}$$

Therefore

$$\begin{aligned}\text{Variance of } z_{ijk} &= \left(\sigma_e^2 - \frac{\sigma_e^2}{n_{ij}} + \frac{\sigma_e^2}{N_{i.}} + \frac{\sigma_e^2}{N_{.j}} + \frac{2n_{ij}\sigma_e^2}{N_{i.}N_{.j}} - \frac{3\sigma_e^2}{N_{..}} \right) \\ &= \sigma_e^2 \left(1 - \frac{1}{n_{ij}} + \frac{1}{N_{i.}} + \frac{1}{N_{.j}} + \frac{2n_{ij}}{N_{i.}N_{.j}} - \frac{3}{N_{..}} \right)\end{aligned}$$

Therefore

$$E(MS_z) = k_{ij} E(MS_e) = k_{ij} \sigma_e^2$$

Where

$$k_{ij} = \left(1 - \frac{1}{n_{ij}} + \frac{1}{N_{i.}} + \frac{1}{N_{.j}} + \frac{2n_{ij}}{N_{i.}N_{.j}} - \frac{3}{N_{..}} \right) \quad (8)$$

Therefore

$$SS_z = \sum_{ijk} \frac{1}{\sqrt{k_{ij}}} (y_{ijk} - \bar{y}_{ij.})^2 = \sum (w_{ijk} - \bar{w}_{ij.})^2$$

Where

$$w_{ijk} = \frac{y_{ijk}}{\sqrt{k_{ij}}}$$

w_{ijk} is now the transformed data.

4 Illustrative Example

The data below correspond to an experiment in which four different methods for growing crops were tested on four different types of fields (same soil but different light exposure). The yield was measured after the harvest. Because the 3rd method was not tested on the 4th type of field (because of a lack of seeds), and the 2nd method on the 4th type of

field (because of a hail storm), the experiment is a typical example of an unbalanced ANOVA.

	Type of field			
Method	1	2	3	4
1	20, 7	39, 17	34, 13	13, 5
2	35, 52	30, 28	58, 73	64
3	62, 44	82, 81	69, 84	-

Table 3: Source: Kovach Computing Services [4]

The model is the same as in Equation (1), where

y_{ijk} the yield after harvest.

μ is a constant.

α_i is the mean effects of the method representing factor A.

β_j is the mean effects of the type of field representing factor B.

λ_{ij} is the interaction between the method and type of field.

e_{ijk} is the error associated with y_{ijk} .

The sums of squares for the unbalanced data which are analogous to balanced designs are:

$$SS_A = \sum_i N_i (\bar{y}_{i..} - \bar{y}_{...})^2 \quad (9)$$

$$SS_B = \sum_j N_j (\bar{y}_{.j.} - \bar{y}_{...})^2 \quad (10)$$

$$SS_{\lambda} = \sum_{ij} n_{ij} (\bar{y}_{ij.} - \bar{y}_{i..} - \bar{y}_{.j.} + \bar{y}_{...})^2 \quad (11)$$

$$SS_e = \sum_{ijk} (y_{ijk} - \bar{y}_{ij.})^2 \quad (12)$$

Using Equations (9), (10), (11) and (12), the sums of squares divided by their respective degrees of freedom for factor A, factor B, the interaction between factor A and factor B and the error term are respectively:-

$MS_A = 4749.22$, $MS_B = 641.21$, $MS_{\lambda} = 458.7$ and $MS_e = 123$.

Testing for the main effects will need a special F -test because of the unbalanced nature of the design. However, if interaction is non significant or absent, the common denominator for testing for the main effects is the mean square error.

Testing for the interaction we have:

$$F = \frac{MS_{\lambda}}{MS_e} = \frac{458.7}{123} = 3.73$$

From $F_{6,9}^{0.05}$ we have 3.37 and since $3.73 > 3.37$, this shows the presence of interaction in the data, hence the need for appropriate transformation of data.

Using equation 8 the transformed data are shown in Table 4.

	Type of field			
Method	1	2	3	4
1	17.2, 6.02	33.5, 14.6	29.2, 11.2	9.1, 3.5
2	30.5, 45.2	26.1, 24.4	50.5, 63.5	41.6
3	55.2, 39.2	73, 72.1	61.4, 74.8	-

Table 4: Transformed unbalanced data

Having transformed the data, the new sums of squares for the main effects and error are:

$$SS_A = \sum_i N_i (\bar{y}_{i..} - \bar{y}_{...})^2 \quad (13)$$

$$SS_B = \sum_j N_j (\bar{y}_{.j} - \bar{y}_{...})^2 \quad (14)$$

$$SS_e = \sum_{ijk} (y_{ijk} - \bar{y}_{ij.})^2 \quad (15)$$

The sums of squares and the corresponding mean sum of squares for the main effects and the error terms has been calculated using Equations (13), (14) and (15) and presented in the ANOVA Table 5

S.V	d.f	SS	MS	F-ratio
Method	2	7705.35	3852.68	69.54
Type of field	3	2066.43	688.81	12.43
Error	15	831.01	92.33	
Total	20	28602.79		

Table 5: ANOVA Table

From $F_{2,15}^{0.05} = 3:68$ and $F_{3,15}^{0.05} = 3:29$, the main effects are significant.

5 Summary and Conclusion

We have shown that in an unbalanced two-way random model, there are no obvious denominator for testing for the main effects which is as a result of the presence of interactions.

When interaction is present in an unbalanced two-way random model, we need to construct an appropriate F -test for the main effects. To avoid such situation, the interaction from the data/model should be removed to have a valid result when testing for the main effects.

References

- [1] [Cabrera and McDougall 2002] Cabrera, J. and McDougall, A. (2002). Statistical Consulting. Springer.
- [2] [Castrup 2010] Castrup, H. (2010). A Welch-Satterthwaite relation for correlated errors. Integrated sciences crop Bakers eld CA 93306.
- [3] [2003] Chow, S.C. (2003) Encyclopedia of Biopharmaceutical Statistics. p 1027. Informa Health Care.
- [4] [2011] Kovach Computing Services (2011). "How can I use XLSTAT to run a two-way unbalanced ANOVA with interaction." Anglesey, Wales.
- [5] [2004] Moore, D.S., McCablee, G., Duckworth, W., and Sclove, S. (2004). Practice of business Statistics, part iv pp 15-17. Palgrave Macmillan.
- [6] [Muller and Fetterman 2002] Muller, K., and Bethel, F. (2002). Regression and Analysis of Variance. An integrated approach using SAS P.381. SAS publishing.

Wi-Max Physical Layer Simulator Using Different Modulation Schemes

Vikas Kumar¹, Sukhjit Singh²

¹M.Tech (Student), ECE Section, GTBKIET Chhapiawali, Malout

²Assistant Professor, ECE Section, GTBKIET Chhapiawali, Malout
Punjab Technical University, Jalandher, India.

Abstract

Wi-MAX is a wireless technology which offers high data rate transmission in broadband. The Worldwide interoperability for microwave access (Wi-MAX) based on IEEE 802.16, has been one of the most important technologies in communication networks providing voice, data and video services with different type of QoS (Quality of Service) during last few years. In this paper, the architecture of the Wi-MAX physical layer simulator is presented. The main blocks are implemented with the aid of the Matlab Simulink and the bit error rate (BER) curves are presented with varying SNR under different digital modulations in AWGN channel.

Keywords – Wi-MAX, Physical layer, QoS, OFDM

1. Introduction

Wi-MAX (Worldwide Interoperability for Microwave Access) is based on the IEEE802.16 standard for Metropolitan Area Networks (MAN). Its goal is to deliver wireless broadband access to customers using base stations with coverage distances in the order of miles. Originally, the standard considered only fixed and nomadic links (802.16-2004) that could be used for “last mile” connectivity providing an alternate to T1 and DSL wired lines or as a back-haul for cellular or Wi-Fi networks. In order to address mobile subscribers, Wi-MAX was expanded to include portable devices (802.16e) such as personal digital assistants (PDAs), laptops, or phones. Requirements for mobility support include provisions for roaming, also inter-cell handoff and incorporating more flexibility into the standard to sustain multiple users demanding various types of services[1] [2]. In mobile Wi-Max, the system’s resources are dynamically allocated to deliver high data rates seamlessly to terminals traveling at vehicular speeds. The frequencies allocated for Wi-Max span the 2-66 GHz range. The exact frequency of operation for any given system is dependent on the propagation conditions that are encountered during its use. The frequencies higher than 10 GHz are practical only for fixed line-of-sight (LoS) type services. Non-line of sight (NLoS) communications perform better when the frequencies of operation are kept under 10 GHz. The frequencies below 6 GHz have better propagation properties and are better suited for mobile communications because they most likely guarantee service to all the niches of the coverage area[3] [4]. Wi-Max is a part of the evolution from voice-only wireless communications systems to ones that provide additional services like web browsing, streaming media, gaming, instant messaging, and other content. Being able to deliver a wide variety of services also requires a delivery system that is flexible and can efficiently allocate system resources. The 802.16 standard offers adjustable data rate to and from each user while maintaining the required quality of service (QoS). Certain applications require higher error resilience and latency requirements that directly factor into the QoS. Real-time services, for example, have strict latency tolerances.

The system resources are allocated and scheduled dynamically by the base station on a frame by frame basis to keep up with the need of the users in the environment. To approach the theoretical capacity of the system, Wi-Max uses a combination of adaptive modulation schemes and coding ranging from rate QPSK to 5/6 rate 64QAM. The amount of error correction applied to each transmission is adjustable and can be changed depending on the required QoS and based on the reliability of the link between each user and the base station. The higher modulation constellations offer a larger throughput per frequency-time slot but not all users receive adequate signal levels to reliably decode all modulation types. Users that are close to the base station that exhibit good propagation and interference characteristics are assigned with higher modulation constellations to minimize the use of system resources. While users that are in less favourable areas use the lower order modulations for communications to ensure data is received and decoded correctly at the expense of additional frequency/time slots for the same amount of throughput. Assigning modulations based on the link conditions increases the overall capacity of the system. The use of variable or adaptive modulations to increase capacity is a trend also observed in other recently developed mobile phone and data standards like WCDMA[5] [6]. Rest of this paper is organized as follows: Section II gives a brief overview about different Wi-Max standards. In Section III detailed study about the Wi-Max physical layer is presented. Section IV shows our simulation results. Finally conclusion and future work are presented in section V.

2. IEEE 802.16

IEEE 802.16 is a series of Wireless Broad band standards authored by the Institute of Electrical and Electronics Engineers (IEEE). The IEEE Standards Board in established a working group in 1999 to develop standards for broadband Wireless Metropolitan Area Networks. The Forum promotes and certifies compatibility and interoperability of products based on the IEEE 802.16 standards.

IEEE 802.16a

The second version of Wi-Max standard 802.16a was an amendment of 802.16 standards and has the capability to broadcast point-to-multi point in the frequency range 2 to 11 GHz. It was established in January 2003 and assigned both licensed and unlicensed frequency bands. Unlicensed bands cover maximum distance from 31 to 50 miles. It improves the Quality of Service (QoS) features with supporting protocols for instance Ethernet, ATM or IP.

IEEE 802.16b

IEEE 802.16b extension clarifies broadband wireless access metropolitan network functions and capabilities of the radio-air interface. License-exempt BWA metropolitan networks support multimedia services. It also increases the spectrum of 5 and 6 GHz frequency bands and provides quality of service which ensures priority transmission for real time voice and video.

IEEE 802.16c

The third version of Wi-Max standard 802.16c was also an amendment of 802.16 standards which mostly dealt with frequency ranging 10 to 66 GHz. This standard addressed various issues, for instance, performance evaluation, testing and detailed system profiling. The system profile is developed to specify the mandatory features to ensure interoperability and the optional features that differentiate products by pricing and functionality.

IEEE 802.16d

In September 2003, a revision project known as 802.16d began which aimed to align with a particular view of European Telecommunications Standards Institute (ETSI) Hiper-MAN. This project was deduced in 2004 with the release of 802.16d-2004 including all previous versions' amendments. This standard supports mandatory and optional elements along with TDD and FDD technologies. Theoretically, its effective data rate is 70 Mbps but in reality, the performance is near about 40 Mbps. This standard improves the Quality of Service (QoS) by supporting very large Service Data Units (SDU) and multiple polling schemes.

IEEE 802.16e

802.16e was an amendment of 802.16d standard which finished in 2005 and known as 802.16e-2005. Its main aim is mobility including large range of coverage. Sometimes it is called mobile Wi-Max. This standard is a technical updates of fixed Wi-Max which has robust support of mobile broadband. Mobile Wi-Max was built on Orthogonal Frequency Division Multiple Access (OFDMA). It mentioned that, both standards (802.16d-2004 and 802.16e-2005) support the 256-FFT size. The OFDMA system divides signals into sub-channels to enlarge resistance to multipath interference. For instance, if a 30MHz channel is divided into 1000 sub-channels, each user would concede some sub-channels which are based on distance.

3. Wi-Max PHYSICAL LAYER

Physical layer is the most important layer. The role of the physical layer is to encode the binary digits that represent MAC frames into signal and transmit and receive these signals across the communication media. The Wi-Max physical layer is based on OFDM which is used to enable high speed data, video and multimedia used by a variety of commercial application. Now we discuss about the Wi-Max physical layer.

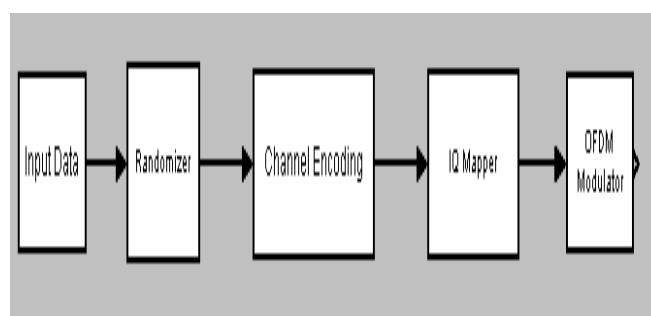


Fig.1 Physical Layer (Transmitter Side)

Randomizer

Randomization is the first process carried out in the physical layer after the data packet is received from the higher layers. The randomization process is used to minimize the possibility of transmissions of non-modulated subcarriers.

Channel Encoding

The encoding process consists of a concatenation of an outer Reed-Solomon (RS) code and an inner convolutional code (CC) as a FEC scheme. That means that first data passes in block format through the RS encoder, and then, it goes across the convolutional encoder. The last part of the encoder is a process of interleaving to avoid long error bursts. Now we consider various blocks of channel encoder in detail.

RS Encoder

A Reed-Solomon code is specified as RS (n, k, t) with l-bit symbols. This means that the encoder takes k data symbols of l bits each and adds 2t parity symbols to construct an n-symbol codeword. Thus, n, k and t can be defined as:

- n: number of bytes after encoding,
- k: number of data bytes before encoding,
- t: number of data bytes that can be corrected.

The error correction ability of any RS code is determined by (n - k), the measure of redundancy in the block. If the location of the erroneous symbols is not known in advance, then a Reed-Solomon code can correct up to t symbols, where t can be expressed as $t = (n - k)/2$.

Convolutional encoder

After the RS encoding process, the data bits are further encoded by a binary convolutional encoder, which has a native rate of 1/2 and a constraint length of 7. A convolutional code is a type of FEC code that is specified by CC (m, n, k), in which each m-bit information symbol to be encoded is transformed into an n-bit symbol, where m/n is the code rate ($n > m$) and the transformation is a function of the last k information symbols, where k is the constraint length of the code [7].

Puncturing Process

Puncturing is the process of systematically deleting bits from the output stream of a low-rate encoder in order to reduce the amount of data to be transmitted, thus forming a high-rate code.

Interleaver

Interleaving does not change the state of the bits but it works on the position of bits. Interleaving is done by spreading the coded symbols in time before transmission. The incoming data into the interleaver is randomized in two permutations. First permutation ensures that adjacent bits are mapped onto non-adjacent subcarriers. The second permutation maps the adjacent coded bits onto less or more significant bits of constellation thus avoiding long runs of less reliable bits. The block interleaver interleaves all encoded data bits with a block size corresponding to the number of coded bits per OFDM symbol. The number of coded bits depends on the modulation technique used in the Physical layer. Wi-Max 802.16e supports 4 modulation techniques and is adaptive in the selection of a particular technique based on the channel conditions and data rate.

IQ Mapper

Once the signal has been coded, it enters the modulation block. All wireless communication systems use a modulation scheme to map coded bits to a form that can be effectively transmitted over the communication channel. Thus, the bits are mapped to a subcarrier amplitude and phase, which is represented by a complex in-phase and quadrature-phase (IQ) vector. QPSK, 16QAM and 64QAM modulations are supported by the system.

There are three important types of digital modulation which are used as follows:

- Binary Phase Shift Keying (BPSK)
- Quadrature Phase Shift Keying (QPSK)
- Quadrature Amplitude Modulation (QAM)
- Binary Phase Shift Keying (BPSK): The BPSK is a binary level digital modulation scheme of phase variation which has two theoretical phase angle i.e. +90 and -90. This gives high immunity against the interference and noise and a robust modulation which gives improved BER performance.
- Quadrature Phase Shift Keying (QPSK): If there are 4 phases that consists of 0, 90, -90 and 180 then the M-ary PSK is termed as Quadrature Phase Shift keying (QPSK). It uses more symbols as compared to BPSK. In QPSK, the number of bits used per symbol is two-bit of modulation symbols.
- Quadrature Amplitude Modulation: Quadrature Amplitude Modulation (QAM) uses different kind of phases which are 16, 32, 64, and 256. Each single state is defined as a specific phase and amplitude. This proves the detection of symbols and generation is much more complex than amplitude device or a simple phase. In QAM, two sinusoidal carriers are transmitted that change their amplitude depending on the digital sequence; these carriers are out of phase to each other by 90. QPSK and QAM-4 are referred as the same modulation which is consider as the complex

symbols of data. The most efficient modulation of 802.16 is 64-QAM, in which 6 bits modulation symbol are transmitted. The IQ plot for a modulation scheme shows the transmitted vector for all data word combinations. The use of variable or adaptive modulations to increase capacity is a trend also observed in other recently developed mobile phone and data standards like WCDMA [8], [9]. The constellation mapped data are assigned to all allocated data subcarriers of the OFDM symbol in order of increasing frequency offset index.

IFFT

This block implements the OFDM modulation. The IQ mapped data are sent to IFFT for time domain mapping. Mapping to time domain needs the application of Inverse Fast Fourier Transform (IFFT). In our case we have incorporated the MATLAB 'IFFT' function to do so.

Cyclic Prefix Insertion

Cyclic prefix [10] must be added after the IFFT operation to combat the effect of multipath. Four different duration of cyclic prefix are available in the standard. Being G the ratio of CP time to OFDM symbol time, this ratio can be equal to 1/32, 1/16, 1/8 and 1/4.

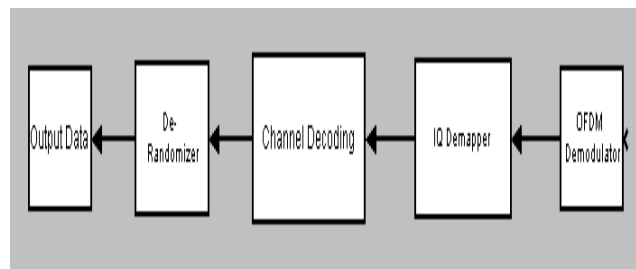


Fig.2 Physical Layer (Receiving side)

Channel: The channel that we used is pure AWGN .This is a noise channel. This channel effects on the transmitted signals when signals passes through the channel. It adds white Gaussian noise to the input signal. After adding Gaussian noise data is then passed to the receiver.

Receiver: The complementary blocks are implemented in the receiver. The CP is removed, sub-carriers are demodulated via the FFT transform, and then sub-carrier de-mapping is performed. After that Channel decoding process is performed with the help of de-interleaver, convolution decoder and RS decoder. Data is then de randomized and in last we get final data.

4. Model Simulation Results

The Model for the Wi-Max is built from the standard documents [11, 12]. The performance of the Wi-Max-PHY layer was tested and evaluated at different noise levels. We performed our simulation in Matlab Simulink version 7.4. We have preferred the Matlab because it is adequate for the simulation of different signal processing methods used in wireless networks [13].The simulation result based on the adaptive modulation technique for BER calculation was observed in this section. The adaptive modulation techniques used in the Wi-Max are QPSK, 16-QAM and 64-QAM respectively. Various BER vs. SNR plots are presented for all these modulation techniques.

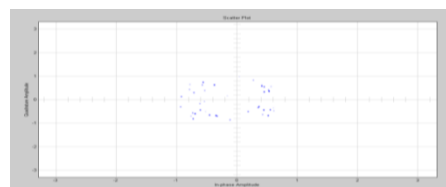


Fig.3 QPSK Modulation Scatter Plot at SNR=10

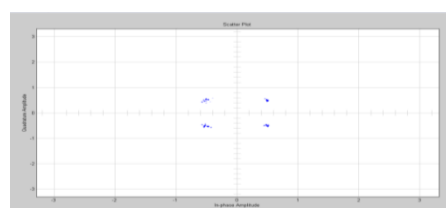


Fig.4 QPSK Modulation Scatter Plot at SNR= 15

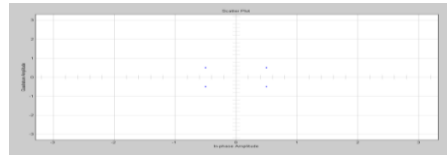


Fig.5 QPSK Modulation Scatter Plot at SNR=20

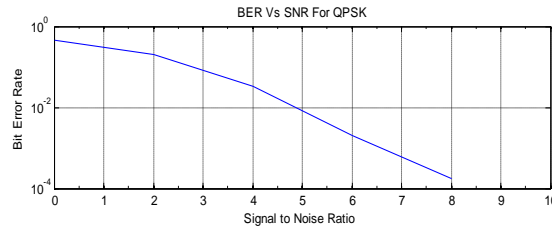


Fig.6 BER Vs SNR Plot for QPSK

Fig. 3, 4 and 5 shows the constellation points of the receiving data at different SNR using QPSK at coding rate 1/2 in pure AWGN. It is clear from fig. 3, 4 and 5 that increasing the value of SNR decreases the spread of constellation points. Our results show that at SNR value 20 constellation points of receiving data match with the constellation points of sending data. Fig. 6 shows the BER Vs SNR plot for QPSK in pure AWGN. Our result shows that increasing the value of Signal to Noise Ratio (SNR) decreases Bit Error Rate (BER) and at SNR value 9 it is zero



Fig.7 16-QAM Modulation Scatter Plot at SNR=10

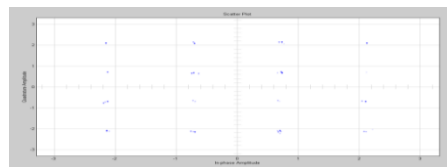


Fig.8 16-QAM Modulation Scatter Plot at SNR=20

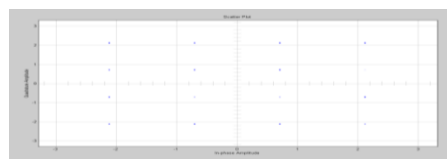


Fig.9 16-QAM Modulation Scatter Plot at SNR=30

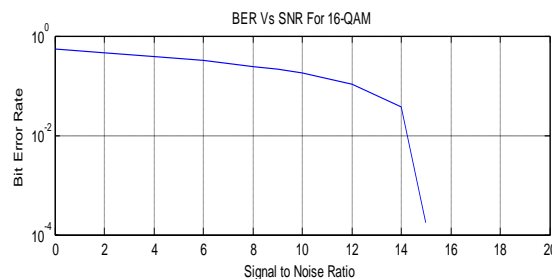


Fig.10 BER Vs SNR Plot for 16-QAM

Fig. 7, 8 and 9 shows the constellation points of the receiving data at different SNR using 16-QAM at coding rate 1/2 in pure AWGN. It can be observed from the Figs. 7, 8 and 9 that spread reduction is taking place with the increasing values of Signal to noise ratio. Our results show that at SNR value 30 constellation points of receiving data match with the constellation points of sending data. Fig. 10 shows the BER Vs SNR plot for 16-QAM in pure AWGN. Our result shows that increasing the value of Signal to Noise ratio (SNR) decreases Bit Error Rate (BER) and at SNR value 15 it is zero.

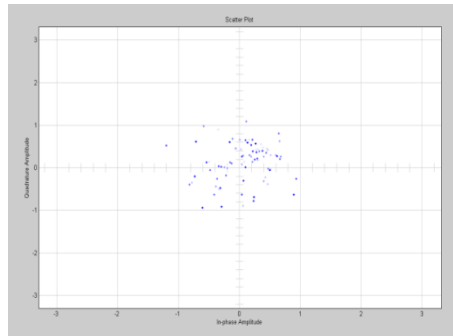


Fig.11 64-QAM Modulation Scatter Plot at SNR=15

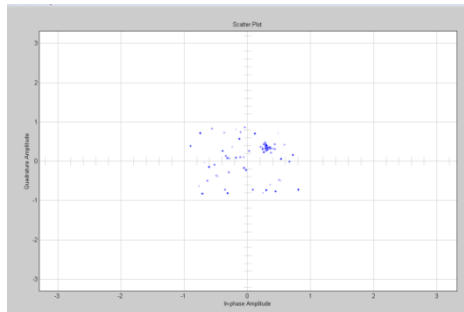


Fig.12 64-QAM Modulation Scatter Plot at SNR=25

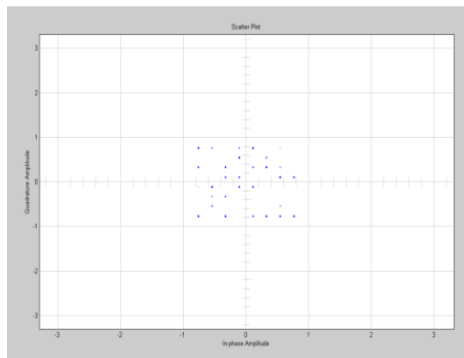


Fig.13 64-QAM Modulation Scatter Plot at SNR=40

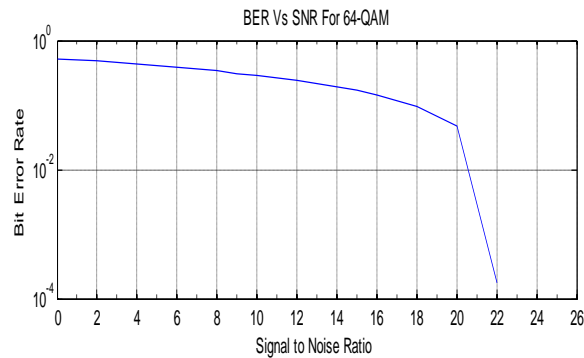


Fig.14 BER Vs SNR Plot for 64-QAM

Fig. 11, 12 and 13 shows the constellation points of the receiving data at different SNR using 64-QAM at coding rate 1/2 in pure AWGN. It is clear from fig. 11, 12 and 13 that increasing the value of SNR decreases the spread of constellation points. Our results show that at SNR value 40 constellation points of receiving data match with the constellation points of sending data. Fig. 14 shows the BER Vs SNR plot for 64-QAM in pure AWGN. Our result shows that increasing the value of Signal to Noise Ratio (SNR) decreases Bit Error Rate (BER) and at SNR value 23 it is zero.

Fig. 15 Compares the Bit Error Rate (BER) for all three modulation schemes implemented in our physical layer modal of Wi-Max.

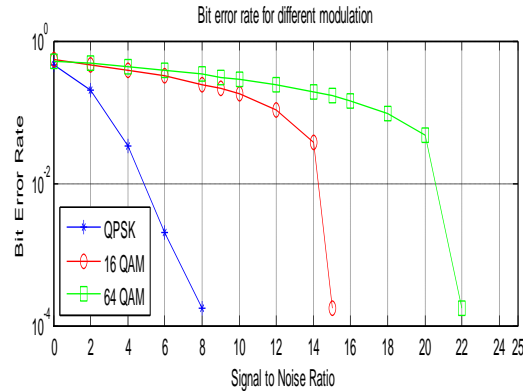


Fig.15 Bit Error rate (BER) for different modulations techniques.

5. CONCLUSIONS

The main objective of this paper is to implement the Wi-Max physical layer using MATLAB in order to evaluate the physical layer performance. The performance of the Wi-Max-PHY layer based on the IEEE 802.16e standard was evaluated and assessed at different modulation schemes and noise levels. Scatter plots are generated to validate the model in terms of general trends in reception quality as we perturb different parameters. A key performance measure of a wireless communication system is the BER. The BER curves are used to compare the performance of different modulation techniques. Thus we can conclude, lower modulation and coding scheme provides better performance with less SNR. As a result of the comparative study, it was found that: when channel conditions are poor, energy efficient schemes such as QPSK were used and as the channel quality improves, 16-QAM or 64-QAM was used.

References

- [1] F. Ohrtman, "Wi-Max Handbook: Building 802.16 Wireless Networks," McGraw-Hill, 2008.
- [2] J.G. Andrews, A. G hosh, R. Muhamed, "Fundamentals of Wi-Max: Understanding Broadband Wireless Networking," Prentice Hall Communications AND Engineering Technologies Series, 2007.
- [3] S.Ahsonand M. Ilyas, "Wi-Max: Standards and Security," CRC Press, (Taylor and Francis Group), 2008.
- [4] L. Nuaymi, "Wi-Max: Technology for Broadband Wireless Access," John Wiley & Sons, 2007
- [5] Y. Xiao, "Wi-Max-Mobile Fi: Advanced research and technology," Auerbach publications, 2008.
- [6] R.B. Marks, K. Stanwood, D. Chang, et al., "IEEE Standard for Local and Metropolitan Area Networks, Part 16: Air Interface for Fixed Broadband Wireless Access Systems," October, 2004.
- [7] Nuaymi Loutfi 2007, WI-Max Technology for Broadband Wireless Access, Wiley, London
- [8] Y. Xiao, "Wi-Max-Mobile Fi: Advanced research and technology," Auerbach publications, 2008.
- [9] R.B. Marks, K. Stanwood, D. Chang, et al., "IEEE Standard for Local and Metropolitan Area Networks, Part 16: Air Interface for Fixed Broadband Wireless Access Systems," October, 2004.
- [10] Pedro Neves, Joao Monteiro, Thomas M. Bohnert, "Quality of Service Differentiation Support in Wi-Max Networks."2008
- [11] ETSI TS 102177 Version 1.3. 1, February 2006,"Broadband Radio Access Networks (BRAN); Hiper MAN; Physical (PHY) Layer"
- [12] IEEE 802.16-2006:"IEEE Standard for Local and Metropolitan Area Networks-Part 16: Air Interface for Fixed Broadband Wireless Access Systems"
- [13] J. C. Ikuno, M. Wrulich, M. Rupp, System level simulation of LTE networks, 2010 IEEE First Vehicular Technology Conference: VTCS2010, Taipei, Taiwan, 16-19May, 2010.

Reliability of Thermal Stresses in Bars When Stress Follows Half-Logistic Distribution

P.Hari Prasad¹, T.S.Uma Maheswari²

¹, Department of Mathematics, Kakatiya University – 506009. A.P. India,

Abstract

This paper deals with the reliability of Thermal stresses in simple bars whose body may be expand or contract due to some increase or decrease in the temperature of the body when stress follows the Half-logistic distribution. For such thermal stresses in simple bars we are particularly interested in investigating the reliability by using the Half-logistic distribution function. It is also compared the results between the reliability of thermal stresses in bars if the ends of the bars are fixed to rigid supports and if the supports yield by an amount equal to Δ . It is observed that the reliability is depending on the coefficient of linear expansion α . This coefficient of linear expansion is different for each material.

Keywords: Thermal stresses, Temperature, Reliability, Coefficient of linear expansion, Simple bars, Half-logistic distribution, Hazard Rate.

1. Introduction:

Whenever there is some increase or decrease in the temperature of a body, it causes the body to expand or contract. A little consideration will show that if the body is allowed to expand or contract freely, with the rise or fall of the temperature, no stresses are induced in the body. But if the deformation of the body is prevented, some stresses are induced in the body. Such stresses are called thermal stresses or temperature stresses. The corresponding strains are called the thermal strains or temperature strains. In probability theory and statistics, the half-logistic distribution is a continuous probability distribution. The distribution of the absolute value of a random variable following the logistic distribution. Reliability is used for developing the equipment manufacturing and delivery to the user. A reliable system is one which operates according to our expectations. Reliability of a system is the probability that a system perform its intended purpose for a given period of time under stated environment conditions. In some cases system failures occur due to certain type of stresses acting on them. These types of system are called stress dependent models of reliability. These models nowadays studied in many branches of science such as Engineering, Medicine, and Pharmaceutical Industries etc [1]. In assessing system reliability it is first necessary to define and categorize different modes of system failures. It is difficult to define failure in unambiguous forms. However a system's performance can deteriorate gradually over time and sometimes there is only a fine line between systems success and system failure. Once the system function and failure modes are explicitly stated reliability can be precisely quantified by probability statements.

2. Statistical Methodology:

The probability of failure as a function of time can be defined by

$$F(t) = P(T \leq t), \quad t \geq 0 \quad (1.1)$$

Where T is a random variable denoting the failure time. **Reliability** function is defined as the probability of success for the intended time t

$$R(t) = 1 - F(t) = P(T > t) \quad (1.2)$$

The Hazard function $h(t)$ is defined as the limit of the failure rate as the interval approaches zero. Thus the hazard function is the instantaneous failure rates is defined as

$$z(t) = \frac{f(t)}{R(t)} = \frac{f(t)}{1 - F(t)} \quad \text{where } f(t) = \frac{dF(t)}{dt} \quad (1.3)$$

2.1. Stress Dependent Hazard Models: Basically, the reliability of an item is defined under stated operating and environmental conditions. This implies that any change in these conditions can effect. The failure rate of almost all components is stress dependent. A component can be influenced by more than one kind of stress. For such cases, a power function model of the form [2]

$$h(t) = z(t)\sigma_1^a \sigma_2^b \quad (1.4)$$

where a, b are positive constants, σ_1 and σ_2 are stress ratios for two different kinds of stresses, and $z(t)$ is the failure rate at rated stress conditions.

3. Thermal Stresses In Simple Bars:

The thermal stresses or strains bar may be found out as discussed below:

The thermal stresses or strains may be found out first by finding out amount of deformation due change in temperature, and then by finding out thermal strain due to the deformation. The thermal stress may now be found out from the thermal strain as usual. Now consider a body subjected to an increase in temperature [3].

Let l = original length of the body,
 θ = increase of temperature and
 α = coefficient of linear expansion
 E = modulus of elasticity (young's modulus)

We know that the increase in length due to increase of temperature

$$\delta l = l \cdot \alpha \cdot \theta, \quad (1.5)$$

If the ends of the bar are fixed to rigid supports, so that its expansion is prevented, then compressive strain induced in the bar.

$$\varepsilon = \frac{\delta l}{l} = l \cdot \alpha \cdot \frac{\theta}{l} = \alpha \cdot \theta \quad (1.6)$$

Stress $\sigma = \varepsilon \cdot E = \alpha \cdot E \cdot \theta \quad (1.7)$

If the supports yield by an amount equal to Δ , then the actual expansion that has taken place,

$$\delta l = l \cdot \alpha \cdot \theta - \Delta \quad (1.8)$$

And strain, $\varepsilon = \frac{\delta l}{l} = \frac{l \cdot \alpha \cdot \theta - \Delta}{l} = \left(\alpha \theta - \frac{\Delta}{l} \right) \quad (1.9)$

Stress, $\sigma = \varepsilon \cdot E = \left(\alpha \theta - \frac{\Delta}{l} \right) E$

3.1. The value of a coefficient of linear expansion of materials in day use is given below in table:

S.NO	MATERIAL	COEFICIENT OF LINEAR EXPANSION/ ^o C(α)
1	STEEL	11.5×10^{-6} to 13×10^{-6}
2	WROGHT IRON, CAST IRON	11×10^{-6} to 12×10^{-6}
3	ALUMINIUM	23×10^{-6} to 24×10^{-6}
4	COPPER, BRASS, BRONZE	17×10^{-6} to 18×10^{-6}

3.2. When Stress Follows half -logistic Distribution:

A continuous Random variable X having the probability density function

$$f(x) = \frac{2e^{-x}}{(1+e^{-x})^2}, \quad x \geq 0 \quad (1.10)$$

is said to have Half Logistic Distribution.

Then $F(t) = \frac{2}{1+e^{-t}} - 1$

Hazard Rate is $Z(t) = \frac{f(t)}{1-F(t)} = \frac{1}{1+e^{-t}} \quad (1.11)$

3.2.1. When σ = stress in the bar if the ends of the bar are fixed to rigid supports:

Stress in the bar $\sigma = \alpha \cdot \theta \cdot E \quad (1.12)$

Therefore Reliability of the bar $R(t) = \exp \left[- \int_0^t h(t) dt \right] = \exp \left[- \int_0^t (z(t) \times \sigma) dt \right]$

$$= \exp \left[- \int_0^t \frac{1}{1+e^{-t}} \times \alpha \cdot \theta \cdot E dt \right] = \exp \left[- \alpha \cdot \theta \cdot E \times \int_0^t \frac{e^t}{1+e^t} dt \right] \quad (1.13)$$

$$\text{Put } e^t + 1 = s$$

$$e^t dt = ds$$

$$= \exp \left[-\alpha \cdot \theta \cdot t \int_0^t \frac{ds}{s} \right] = \exp \left[-\alpha \cdot \theta \cdot E \times [\log(s)]_2^1 \right] = \exp \left[-\alpha \cdot \theta \cdot E \times (\log(e^t + 1) - \log(2)) \right]$$

$$= \exp \left[-\alpha \cdot \theta \cdot E \times \left(\log \left(\frac{e^t + 1}{2} \right) \right) \right] = \exp \left[-\alpha \cdot \theta \cdot E \times \left(\log \left(\frac{e^t + 1}{2} \right) \right) \right] = \exp \left[\alpha \cdot \theta \cdot E \times \left(\log \left(\frac{2}{e^t + 1} \right) \right) \right]$$

$$= \exp \log \left(2 / (e^t + 1) \right)^{\alpha \cdot \theta \cdot E} = (2 / (e^t + 1))^{\alpha \cdot \theta \cdot E}$$

3.2.2. When σ =stress in the bar if the supports yield by an amount equal to Δ :

Stress in the bar $\sigma = (\alpha\theta - \frac{\Delta}{l})E$ (1.14)

Therefore Reliability of the bar $R(t) = \exp \left[- \int_0^t h(t) dt \right] = \exp \left[- \int_0^t (z(t) \times \sigma) dt \right]$

$$= \exp \left[- \int_0^t \frac{1}{1+e^{-t}} \times (\alpha \cdot \theta - \frac{\Delta}{l}) E dt \right] = \exp \left[- (\alpha \cdot \theta - \frac{\Delta}{l}) E \times \int_0^t \frac{e^t}{1+e^t} dt \right]$$

$$\text{Put } e^t + 1 = s$$

$$e^t dt = ds$$

$$= \exp \left[- (\alpha \cdot \theta - \frac{\Delta}{l}) E \int_0^t \frac{ds}{s} \right] = \exp \left[- (\alpha \cdot \theta - \frac{\Delta}{l}) E \times [\log(s)]_2^1 \right]$$

$$= \exp \left[- (\alpha \cdot \theta - \frac{\Delta}{l}) E \times (\log(e^t + 1) - \log(2)) \right] = \exp \left[- (\alpha \cdot \theta - \frac{\Delta}{l}) E \times \left(\log \left(\frac{e^t + 1}{2} \right) \right) \right]$$

$$= \exp \left[- (\alpha \cdot \theta - \frac{\Delta}{l}) E \times \left(\log \left(\frac{e^t + 1}{2} \right) \right) \right] = \exp \left[(\alpha \cdot \theta - \frac{\Delta}{l}) E \times \left(\log \left(\frac{2}{e^t + 1} \right) \right) \right]$$

$$= \exp \left[(\log \left(2 / (e^t + 1) \right)) \right]^{\alpha \cdot \theta - \frac{\Delta}{l} E}$$

$$= (2 / (e^t + 1))^{\alpha \cdot \theta - \frac{\Delta}{l} E} \tag{1.15}$$

3.3. Reliability computations for simple bars when σ =Stress in the rod if the ends do not yield:

Table-1[Aluminium alloy]

when $\alpha=24 \times 10^{-6}$				
t	θ	E	σ	R(t)
0.01	20	80000	38.4	0.824910818
0.02	20	80000	38.4	0.679824931
0.03	20	80000	38.4	0.559719318
0.04	20	80000	38.4	0.460390845
0.05	20	80000	38.4	0.378326103
0.06	20	80000	38.4	0.310591291
0.07	20	80000	38.4	0.25473915
0.08	20	80000	38.4	0.2087304
0.09	20	80000	38.4	0.170867499
0.1	20	80000	38.4	0.139738842

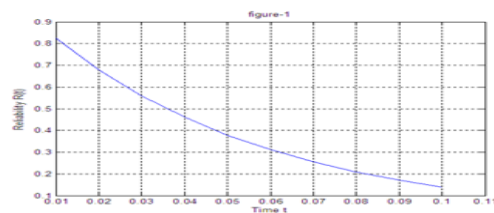
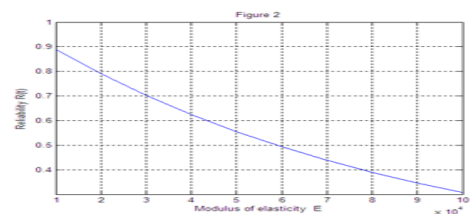


Table-2[Steel]

when t=0.1				
α	θ	E	σ	R(t)
11.5×10^{-6}	20	10000	2.3	0.888808211
11.5×10^{-6}	20	20000	4.6	0.789980035
11.5×10^{-6}	20	30000	6.9	0.702140741
11.5×10^{-6}	20	40000	9.2	0.624068456
11.5×10^{-6}	20	50000	11.5	0.554677168
11.5×10^{-6}	20	60000	13.8	0.493061621
11.5×10^{-6}	20	70000	16.1	0.438183888
11.5×10^{-6}	20	80000	18.4	0.389461438
11.5×10^{-6}	20	90000	20.7	0.346156524
11.5×10^{-6}	20	100000	23	0.30766676



3.4. Reliability Computations For Simple Bars When σ =Stress In The Rod If The Ends Yield By An Amount Equal

Table-4 [Iron]

when $\alpha=12 \times 10^{-6}$, $l=6000$, $\Delta=1$				
t	θ	E	σ	R(t)
0.01	40	200000	62.7	0.730311775
0.015	40	200000	62.7	0.623745142
0.020	40	200000	62.7	0.532519934
0.025	40	200000	62.7	0.454458668
0.030	40	200000	62.7	0.387688349
0.035	40	200000	62.7	0.330598561
0.040	40	200000	62.7	0.281805218
0.045	40	200000	62.7	0.240119251
0.050	40	200000	62.7	0.20451955
0.055	40	200000	62.7	0.174129596

Table-5 [Iron]

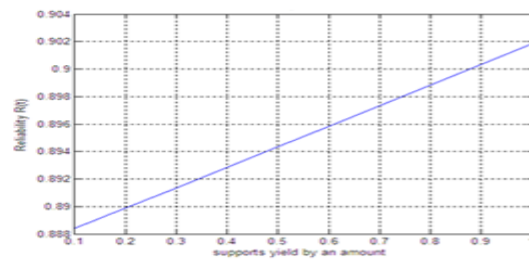
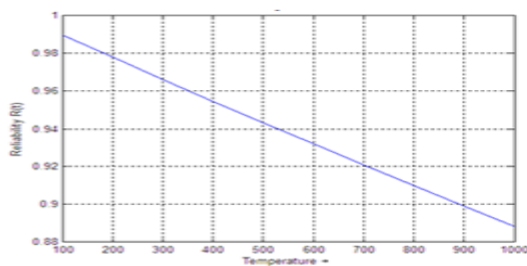
when $t=0.001$, $\Delta=1$, $l=6000$				
α	θ	E	σ	R(t)
12×10^{-6}	100	200000	207	0.901652692
12×10^{-6}	200	200000	447	0.799670209
12×10^{-6}	300	200000	687	0.709222574
12×10^{-6}	400	200000	927	0.629005125
12×10^{-6}	500	200000	1170	0.557024391
12×10^{-6}	600	200000	1410	0.494021495
12×10^{-6}	700	200000	1650	0.438144616
12×10^{-6}	800	200000	1890	0.388587756
12×10^{-6}	900	200000	2130	0.344636083
12×10^{-6}	1000	200000	2370	0.305655616

Table-6 [Iron]

when $t = 0.001$, $\alpha=12 \times 10^{-6}$, $l=6000$				
Δ	θ	E	σ	R(t)
1	100	200000	207	0.901652692
0.9	100	200000	210	0.900300889
0.8	100	200000	213	0.898951113
0.7	100	200000	217	0.897154559
0.6	100	200000	220	0.8958095
0.5	100	200000	223	0.894466458
0.4	100	200000	227	0.892678866
0.3	100	200000	230	0.891340517
0.2	100	200000	233	0.890004175
0.1	100	200000	237	0.888225502

Table-7 [Copper]

when $t=0.1$, $\Delta=1$, $l=6000$, $\alpha=17 \times 10^{-6}$				
l	θ	E	σ	R(t)
10000	40	200000	116	0.559087106
20000	40	200000	126	0.531753633
30000	40	200000	129	0.523817209
40000	40	200000	131	0.518592176
50000	40	200000	132	0.515999237
60000	40	200000	133	0.513419262
70000	40	200000	133	0.513419262
80000	40	200000	134	0.510852187
90000	40	200000	134	0.510852187
100000	40	200000	134	0.510852187



4. Conclusions:

Reliability of the Thermal stresses or strains are found out first by finding out amount of deformation due to change in temperature, and then by finding out thermal strain due to the deformation. Reliability computations are obtained for simple bars when stress (σ) in the Rod i) if the ends do not yield and ii) if the ends yield by an equal to amount Δ for various Materials. When the temperature increases Reliability decreases. Also when the amount Δ is increases, Reliability increases. It is also compared the results between the reliability of thermal stresses in bars if the ends of the bars are fixed to rigid supports and if the supports yield by an amount equal to Δ . It is observed that the reliability is depending on the coefficient of linear expansion α . This coefficient of linear expansion is different for each material. Also the Reliability is depending on Time in this paper.

References:

- [1]. Kapur, K.C and L.R.Lamberson (1977): Reliability in Engineering Design, Jhon Wiley and Sons, In., NewYork
- [2]. T.S.Uma Maheswari (1991): Studies on some Stress-Strength reliability models, Ph.D.Thesis, Kakatiya University, Warangal.
- [3]. Abu-Bakr Iris (2007): Reliability Analysis of Simply Supported Steel Beams
- [4]. Australian Journal of Basic and Applied Sciences, 1(1): 20-29, 2007, INSInet Publication
- [5]. R.S. KHURMI, Strength of Materials [Mechanical of Solids], S. Chand Publications
- [6]. Lorenzo Bardella (2008): Reliability of First Order Shear Deformation Models for Sandwich Beams, Journal of Mechanics of Materials and Structures, Vol. 3, No.7, 2008

A Multihop Dynamic Channel Assignment Scheme For Cellular Network

Mr. Chetan D. Jadhav¹, Prof. A. S. Joshi²

¹Sipna College of Engineering & Technology, Badnera Road, Amravati, M.S.444701, India.

²Asst. Professor, Sipna College of Engineering & Technology, Badnera Road, Amravati, M.S.444701, India.

Abstract

A multihop Dynamic Channel Assignment Scheme is proposed here for Multihop Cellular network. The proposed scheme splits the cell into microcell and macrocell to accept and complete the call as single hop, two hops, or three hops call. The radio resources are assigned to each call based on the interference information in the surrounding cells, stored in Interference Information Table at MSC. Two different channel searching algorithms, namely, Sequential Channel searching and packing based Channel searching are proposed and studied here. Such schemes with channel re-assignment procedure to further enhance the system performance, is also investigated. The MDCA scheme for significant improvement of system capacity and call blocking probability is simulated and studied. Further the situation of Hot-Spot is also studied for avoiding call blocking.

Index Terms — Multihop Cellular Network, Channel Assignment, Mobile Ad-Hoc Networks, Clusters.

1. Introduction

Traditional 2G Cellular networks are expanding exponentially and has almost 4 billion of subscriber till now [1]. Essentially we have a limited resource transmission spectrum that must be shared by several users. Each cell is allocated a portion of the total frequency spectrum. As users move into a given cell, they are then permitted to utilize the channel allocated to that cell. As users move into a given cell, they are then permitted to utilize the channel allocated to that cell [2]. The virtue of the cellular system is that different cells can use the same channel given that the cells are separated by a minimum distance according to the system propagation characteristics; otherwise, intercellular or co channel interference occurs. Such channel allocation technology is a matured technology and quite successful also, beside a drawback of call blocking and inability to handle different spatial traffic demands. In such situations, Mobile Adhoc Networks (MANETs) are appropriate choice, but they also have their own demerits. TCNs have mature technology support for reliable performance. However, building and expanding their necessary infrastructure is costly. MANETs, on the other hand, are simple to deploy and easily expandable. Nevertheless, many of their implementation issues are still in the research phase. By taking into account the advantages and drawbacks of TCNs and MANETs, researchers notice that a combination of them is the logical solution to the next generation mobile networks. In 1996, Adachi and Nakagawa raised the concept of cellular ad-hoc united communication system [3]. Subsequently, many similar proposals were reported, such as multihop cellular network (MCN) [4]. MCN-type systems are expected to bring considerable amount of benefits. However, with the limited bandwidth for cellular communications, channel assignment becomes even more challenging in MCN-type systems [5]. An ad hoc GSM (A-GSM) protocol is proposed for using the cellular frequency band for relay stations (RSs) to relay traffic [6]. However, the study did not clearly address how the resources are allocated to the BS and RSs. Recently; clustered MCN (CMCN) has been proposed and studied using a fixed channel assignment (FCA) scheme [7]. It uses cellular frequency band for traffic relaying. Results show that CMCN with FCA can improve the system capacity [8]. However, FCA is not able to cope with temporal changes in the traffic patterns and thus may result in deficiency. Moreover, it is not easy to obtain the optimum channel assignment for uplink and downlink under FCA, which is used to achieve the lowest call blocking probability. Therefore, dynamic channel assignment (DCA) is more desirable [9]. In this paper, we propose a Multihop Dynamic Channel Assignment scheme that is based on Interference Information Table [10] stored at MSC for each cell. Two different channel searching algorithms, namely, Sequential Channel searching and packing based Channel searching are proposed and studied here. Such schemes with channel re-assignment procedure to further enhance the system performance, is also investigated. The MDCA scheme for significant improvement of system capacity and call blocking probability is simulated and studied. Further the situation of Hot-Spot is also studied for avoiding call blocking.

2. Clustered Multihop Cellular Network

The basic idea behind the CMCN is to divide the cell into hierarchical overlaid system of microcell and macrocell [11] by integrating MANET clustering in to the TCN [12]. BS in TCNs covers the entire macrocell with a radius r_M . The transmission ranges of traffic and control channels are the same and equal to r_M for both the BSs and MSs. In CMCN, a macrocell is divided into seven microcells with a radius of r_m . Each virtual microcell can be divided into two regions: inner half

and outer half. The inner half is near the central microcell. The transmission range of the traffic channels in CMCN for both the BSs and MSs is equal to r_m . The transmission range of the control channels for the BSs and MSs is equal to r_M so that the BS can communicate with all the MSs within its macrocell area for control information exchange.

3. Proposed MDCA Scheme

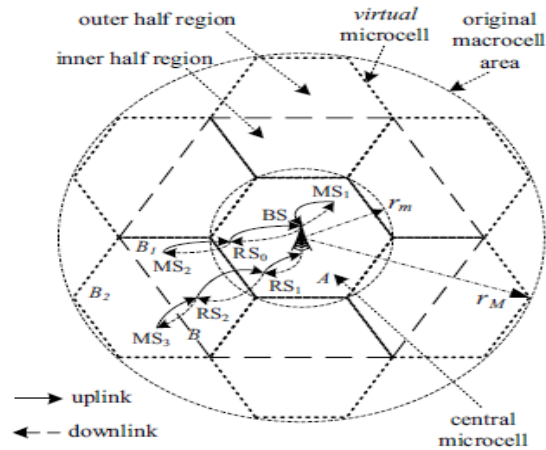


Fig. 1. Channel Assignment in CMCN

Figure 1 shows typical channel assignment scheme used in CMCN. The scheme assigns radio resources to a particular call in a cell depending on the following type of classification of call initiated.

3.1 One Hop Call

The one hop call refers to call originated from MSs in a central micro cell A in figure 1. It requires one uplink channel and one down link channel free in microcell A. The call is accepted if microcell has at least one free uplink channel and one free downlink channel, otherwise, call is blocked.

3.2 Two hop call

Two hop calls refers to call originated from MSs in the inner half region of a virtual microcell, such as MS2 in region B1 of microcell B in Fig. 1. The BS is able to find another MS, RS0, in the central microcell acting as a RS. For uplink transmission, a two-hop call requires one uplink channel from the microcell B, for the transmission from MS2 to RS0, and one uplink channel from the central microcell A, for the transmission from RS0 to the BS. For downlink transmission, a two-hop call requires two downlink channels from the central microcell A, for the transmission from the BS to RS0, and from RS0 to MS2, respectively. A two-hop call is accepted if all the following conditions are met: (i) there is at least one free uplink channel in microcell B; (ii) there is at least one free uplink channel in the central microcell A; and (iii) there are at least two free downlink channels in the central microcell A. Otherwise, the call is blocked.

3.3 Three Hop Call

Three-hop calls refer to calls originated from MSs in the outer half region of a virtual microcell, such as MS3 in region B2 of microcell B in Fig. 1. The BS is responsible for finding two other MSs, RS1 and RS2, to be the RSs for the call; RS1 is in the central microcell A and RS2 is in the region B1. For uplink transmission, a three-hop call requires two uplink channels from microcell B and one uplink channel from the central microcell A. The three uplink channels are used for the transmission from MS3 to RS2, from RS2 to RS1 and RS1 to the BS, respectively. For downlink transmission, a three-hop call requires two downlink channels from central microcell A and one downlink channel from microcell B. A three-hop call is accepted if all the following conditions are met: (i) there is at least one free uplink channel in the central microcell A; (ii) there at least two free uplink channels in the microcell B; (iii) there are at least two free downlink channels in the central microcell A; and (iv) there is at least one free downlink channel in microcell B. Otherwise, it is blocked.

As it is clear, the channel assignment scheme is unbalanced in a sense that, no. Of uplink and downlink channel channels assigned to a call are unequal. This is something different from a TCN, where same no. of uplink and downlink channels is allotted to every call [9].

3.4 Interference Information Table

Cell	Channel				
	1	2	3	...	N
0	L	L	2L	...	L
1		2L	U ₂₂	...	U ₃₃
2	L	L	2L	...	2L
3	L	U ₁₁	2L	...	L
...
12		U ₁₁	U ₁₁	...	L
...
48	U ₂₂	L	U ₃₃	...	

Table 1. Interference Information Table

The proposed MDCA scheme works on the information provided by the Interference Information Table (IIT) [10]. Two global IITs are stored in mobile switching centre (MSC) for uplink and downlink channels. Every BS is able to access to the global IITs. Denote the set of interfering cells of any microcell A as I(A). The information of I(A) is stored in the Interference Constraint Table (ICT). Different reuse factor N_r values will have different I(A) for a given microcell A and we can implement MDCA with any N_r by changing the interfering cells information in the ICT. Table I shows the uplink IIT for the CMCN shown in Fig. 2, which includes the shared N system uplink channels in each cell. The downlink IIT is similar and hence not illustrated here. The content of an IIT is described as follows.

- 1) Used Channels: a letter 'U_{11/22/33}' in the (microcell A, channel j) box signifies that channel j is a used channel in microcell A. The subscript indicates which hop the channel is used for; 'U₁₁', 'U₂₂', 'U₃₃' refer to the first-hop channel, the second-hop channel and the third-hop channel, respectively.
- 2) Locked Channels: a letter 'L' in (microcell A, channel j) box signifies that microcell A is not allowed to use channel j due to one cell in I(A) is using channel j. Similarly, 'nL' in (microcell A, channel j) box indicates n cells in I(A) are using channel j.
- 3) Free Channels: an empty (microcell A, channel j) box signifies that channel j is a free channel for microcell A.

3. Channel Searching Strategies

1) Sequential Channel Searching (SCS): When a new call arrives, the SCS strategy is to always search for a channel from the lower to higher-numbered channel for the first-hop uplink transmission in the central microcell. Once a free channel is found, it is assigned to the first-hop link. Otherwise, the call is blocked. The SCS strategy works in the same way to find the uplink channels for second- or third-hop links for this call if it is a multihop call. The channel searching procedure is similar for downlink channel assignment as well.

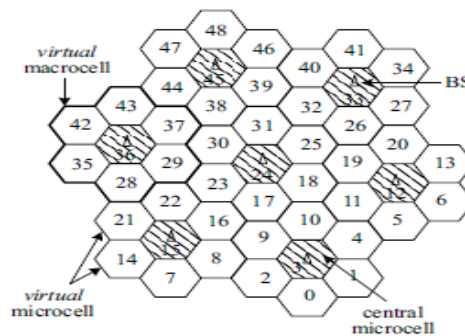


Figure 2. Simulated 49 Cell Network

2) Packing-Based Channel Searching (PCS): The PCS strategy is to assign microcell A a free channel j which is locked in the largest number of cells in I(A). The motivation behind PCS is to attempt to minimize the effect on the channel availability in those interfering cells. We use $F(A, j)$ to denote the number of cells in I(A) which are locked for channel j by cells not in I(A). Interestingly, $F(A, j)$ is equal to the number of cells in I(A) with a label 'L' in channel j's column in the IIT. Then the cost for assigning a free channel j in microcell A is defined as,

$$E(A, j) = I(A) - F(A, j) \text{ -----(1)}$$

If there is more than one such channel, the lower-numbered channel is selected. For example, Table II shows a call in cell 15 requesting a first-hop channel. Channels 1, 2 and 3 are the three free channels in cell 15. Refer to Fig. 2, $I(15) = 2, 7, 8, 9, 13, 14, 16, 17, 20, 21, 22, 23, 27, 28, 29, 34, 47, 48$ with $N_r = 7$. Since most of the cells in $I(15)$ are locked for channel 2, it is suitable to assign channel 2 as the first-hop channel in cell 15 because $F(15, 2) = 15$ is largest among the $F(15, j)$ values for $j = 1, 2$ and 3. The best case solution is when $E(A, j) = 0$. However, it might not be always feasible to find such a solution. The proposed PCS strategy attempts to minimize the cost of assigning a channel to a cell that makes $E(A, j)$ as small as possible. Thus, it results in a sub-optimal solution.

4. Channel Updating

1) Channel Assignment: when the BS assigns the channel j in the microcell A to a call, (i) it will inform the MSC to insert a letter 'U11/22/33' with the corresponding subscript in the (microcell A , channel j) entry box of the IIT; and (ii) it will also inform the MSC to update the entry boxes for $(I(A), \text{channel } j)$ by increasing the number of 'L'.

2) Channel Release: when the BS releases the channel j in the microcell A , (i) it will inform the MSC to empty the entry box for (microcell A , channel j); and (ii) it will also inform the MSC to update the entry boxes for $(I(A), \text{channel } j)$ by reducing the number of 'L'.

5. Channel Re-Assignment

When a call using channel i as a k th-hop channel in microcell A is completed, that channel i is released. The MSC will search for a channel j , which is currently used as the k th-hop channel of an ongoing call in microcell A . If $E(A, i)$ is less than $E(A, j)$, the MSC will reassign channel i to that ongoing call in microcell A and release channel j . CR is only executed for channels of the same type (uplink /downlink) in the same microcell. Thus, CR is expected to improve the channel availability to new calls. Mathematically, the motivation behind CR can be expressed as a reduction in the cost value:

$$\begin{aligned} \Delta E(A, i \rightarrow j) &= E(A, i) - E(A, j) \\ &= F(A, j) - F(A, i) < 0 \end{aligned} \text{ ----- (2)}$$

6. Simulation Results

6.1 Simulation Model

The simulated network is shown in Fig. 2, and the wraparound technique is used to avoid the boundary effect. The number of system channels is $N=70$ (70 uplink channels and 70 downlink channels). We use $N_r=7$ as illustration, hence a channel used in cell A cannot be reused in the first and the second tier of interfering cells of A , i.e. two-cell buffering. Two traffic models are studied: uniform traffic model generates calls which are uniformly distributed according to a Poisson process with a call arrival rate λ per macrocell area, while hot-spot traffic model only generates higher call arrival rate in particular microcells. Call durations are exponentially distributed with a mean of $1/\mu$. The offered traffic to a macrocell is given by $\rho = \lambda/\mu$. Each simulation runs until 100 million calls are processed. The 95% confidence intervals are within $\pm 10\%$ of the average values shown. For the FCA in TCNs, the results are obtained from Erlang B formula with $N/7$ channels per macrocell.

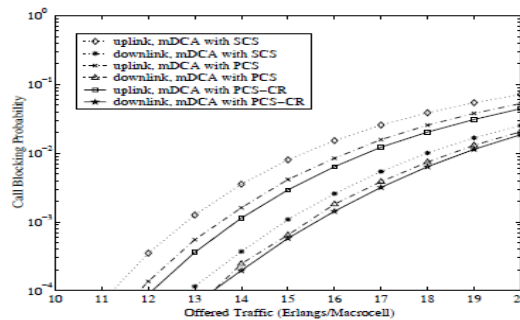


Fig. 3. Asymmetric capacity for uplink/downlink for CMCN using MDCA.

6.2 Simulation With Uniform Traffic

Fig. 3 shows both the uplink and downlink call blocking probability, i.e. $P_{b,U}$ and $P_{b,D}$. Notice that the $P_{b,U}$ is always higher than the $P_{b,D}$ due to the asymmetric nature of multihop transmission in CMCN that downlink transmission takes more channels from the central microcell than uplink transmission. The channels used in the central microcells can be reused in the other central microcells with minimum reuse distance without having to be concerned about the co-channel interference constraint, because two-cell buffering is already in place. The system capacity based on $P_{b,U} = 1\%$ for MDCA with SCS and PCS are 15.3 and 16.3 Erlangs, respectively. With PCS-CR (channel reassignment), the capacity of MDCA is increased by 0.4 Erlangs. Fig. 4 shows the average call blocking probabilities for FCA and DCA-WI for TCNs [10], AFCA for CMCN [9], MDCA with SCS, PCS and PCS-CR. DCA-WI, known as DCA with interference information, is a distributed network-based DCA scheme for TCNs. Under DCA-WI, each BS maintains an interference information table and assigns channels according to the information provided by the table. Only the $P_{b,U}$ for MDCA is shown because uplink transmission has lower capacity. At $P_{b,U} = 1\%$, the system capacity for the FCA and DCAWI are 4.5 Erlangs and 7.56 Erlangs, respectively. AFCA with optimum channel combinations, (NU,c=22, NU,v=8) and (ND,c=40, ND,v=5), can support 9.3 Erlangs. The MDCA with SCS, PCS, and PCS-CR can support 15.3 Erlangs, 16.3 Erlangs and 16.7 Erlangs, respectively. As compared to DCAWI and AFCA, the improvements of MDCA with PCS-CR are 120.9% and 79.6%, respectively.

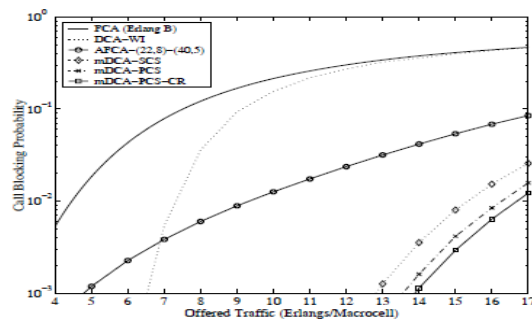


Fig. 4. Capacity comparison with $N=70$.

6.3 Simulation results with Hot-Spot

As in [14], we adopted the same methodology to simulate the hot-spot scenarios. Two scenarios are studied. From Fig. 2, microcell 24 is chosen for the isolated one hot-spot model and microcells 2, 9, 17, 24, 31, 39, 46 are chosen to form the expressway model. First, each of the seven macro cells is initially loaded with a fixed nominal amount of traffic, which would cause 1% blocking if the conventional FCA were used. Next, we increase the traffic load in hot-spot microcells until the call blocking in any microcell reaches 1%. Then we can obtain the capacity values for the hot-spot microcell areas. With $N = 70$, each of the seven macro cells will be initially loaded at 4.46 Erlangs. For the isolated one hot-spot model, FCA, AFCA and MDCA supports about 0.6 Erlangs, 9 Erlangs and 38 Erlangs per microcell, respectively. For the expressway model, FCA, AFCA and MDCA supports about 0.6 Erlangs, 1 Erlangs and 6 Erlangs per microcell, respectively. It can be seen that MDCA has a huge capacity to alleviate the blocking in hot-spot cells. Significant capacity improvements of MDCA have been observed with a larger N , e.g. $N = 210$, with uniform and hot spot traffic. Due to limited space, the results are not shown here.

7. Conclusion

The feasibility of applying DCA scheme for MCN-type systems is investigated. A multihop DCA (MDCA) scheme with two channel searching strategies is simulated for clustered MCN (CMCN). A channel reassignment procedure is investigated. Results show that MDCA can improve the system capacity greatly as compared to FCA and DCA-WI for TCNs and AFCA for CMCN. Furthermore, MDCA can efficiently handle the hot-spot traffic.

References

- [1] The Portio Research Limited, Worldwide Mobile Market Forecasts 2006- 2011, Market Study, UK, 2006.
- [2] E. Perkins, Ad Hoc Networking. Boston MA: Addison-Wesley, 2001.
- [3] T. Adachi and M. Nakagawa, "A study on channel usage in cellular Adhoc united communication system for operational robots," IEICE Trans. Commun., vol. E81-B, pp. 1500-1507, July 1998.
- [4] Y.-D. Lin and Y.-C. Hsu, "Multihop cellular: a new architecture for wireless communications," in Proc. IEEE INFOCOM'00, vol. 3, pp. 1273-1282, Tel Aviv, Israel, Mar. 2000.
- [5] H. Wu, C. Qiao, S. De, and O. Tonguz, "Integrated cellular and ad hoc relaying systems: iCAR," IEEE J. Select. Areas Commun., vol. 19, pp. 2105-2115, Oct. 2001.
- [6] H. Wu, S. De, C. Qiao, E. Yanmaz, and O. Tonguz, "Managed mobility: a novel concept in integrated wireless systems," in Proc. IEEE MASS'04, pp. 537-539, Fort Lauderdale, FL, Oct. 2004.

- [7] H. Luo, R. Ramjee, P. Sinha, L. E. Li, and S. Lu, "UCAN: a unified cellular and ad-hoc network architecture," in Proc. ACM MOBICOM'03, pp. 353-367, San Diego, CA, Sept. 2003.
- [8] G. N. Aggelou and R. Tafazolli, "On the relaying capacity of next generation GSM cellular networks," IEEE Personal Commun., vol. 8, pp. 40-47, Feb. 2001.
- [9] J. Li and P. H. J. Chong, "A fixed channel assignment scheme for multihop cellular network," in Proc. IEEE GLOBECOM'06, vol. WLC 20-6, pp. 1-5, San Francisco, CA, Nov. 2006.
- [10] P. H. J. Chong and C. Leung, "A network-based dynamic channel assignment scheme for TDMA cellular systems," International J. Wireless Inform. Networks, vol. 8, pp. 155-165, July 2001.
- [11] S. S. Rappaport and L.-R. Hu, "Microcellular communication systems with hierarchical macrocell overlays: traffic performance models and analysis," Proc. IEEE, vol. 82, pp. 1383-1397, Sept. 1994.
- [12] J. Y. Yu and P. H. J. Chong, "A survey of clustering schemes for mobile ad hoc networks," IEEE Commun. Survey & Tutorials, vol. 7, pp. 32-48, First Quarter, 2005.
- [13] S. W. Herber, Algorithms and Complexity. Prentice-Hall, 1986.
C.-L. I and P.-H. Chao, "Local packing: distributed dynamic channel allocation at cellular base station," in Proc. IEEE GLOBECOM'93, vol. 1, pp. 293-301, Houston, TX, Nov. 1993.

Calculation of Stress And Deflection In Double Layer Microcantilever For Biosensor Application

^{1,2}Lia Aprilia, ¹Ratno Nuryadi, ²Djoko Hartanto

¹Center for Material Technology, Agency for the Assessment and Application of Technology, BPPT Building II, 22 floor. M.H. Thamrin 8 street, Jakarta 10340, Indonesia

²Departement of Electrical Engineering, Faculty of Engineering, University of Indonesia, Depok 16424, Indonesia

Abstract

In microcantilever-based biosensor, a sensitive layer plays an important role as a place for the establishment of functional layer for detecting molecules target. When a sensitive layer is coated on the microcantilever surface, a surface stress change is induced as a consequence of adsorbate-surface interaction, resulting in a deflection of the microcantilever. However, the microcantilever with the sensitive layer of gold (Au) or 3-Aminopropyltriethoxysilane (aminosilane) which are commonly used in biosensor, has not been reported. In this paper, we study a dependence of the microcantilever deflection on the gold / aminosilane layers thickness in static mode operation. From a derivation of Stoney equation, it is found that the influence of material properties on the deflection of double layer microcantilever from the film stress and radius of curvature. Such relationship is important because the microcantilever deflection directly influences the sensor sensitivity. Our results indicate that the material and the thickness of sensitive layer should be considered to obtain a high sensitivity of microcantilever sensor.

Keywords: Microcantilever, double layer, deflection, stress, sensitive layer, thickness.

1. Introduction

Microcantilever-based sensors have attracted considerable interest for recognition of target analytes because of their fast, compact read-out, and high sensitivity [1-2]. Such sensor has been investigated in the fields of environment, medicine, chemistry, physics, and biology. In previous research, we have developed the microcantilever-based sensor for environmental monitoring, especially for humidity detection [3]. However, to act as biosensor, there are two important requirements for the microcantilever. First, the functional layer (usually antibody) must be coated on the microcantilever surface for detecting targeted object (antigen). Second, a sensitive layer (gold or 3-Aminopropyltriethoxysilane/aminosilane) is needed to provide a surface for attaching functional molecules. When the sensor operates in a static mode, the sensitivity is mainly determined by the microcantilever deflection, where, the deflection of the microcantilever depends on thickness coating of the sensitive layer [4]. The microcantilever with the sensitive layer (double layer structure) can be seen in Fig. 1.

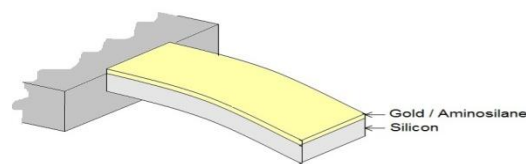


Figure 1. Double layer microcantilever

It is important to be noted that the sensitive layer coating on the microcantilever surface can induce a surface stress change as consequence of adsorbate-surface interaction. The surface stress can be obtained from the measurement of the curvature change by applying Stoney equation, which provides a linear relationship between surface stress change and the curvature change [5]. Stoney conducted the experiment of how glass substrates bent due to metal deposited on the surface [6]. However, the model does not contain any parameters related to coating film as shown in Fig. 1. Recently, Yoshikawa reported an analytical model for static deflection and optimization of a mechanical cantilever coated with a solid receptor film [7]. The model provides accurate values which are a good agreement with finite element analysis. However, to our knowledge, the microcantilever with the sensitive layer of gold (Au) or aminosilane which are commonly used, has not been reported. The gold is usually used as sensitive layer due to have a good corrosion resistance and biocompatible [8]. On the other hand, aminosilane is also widely used for the sensitive one because it is biocompatible and getting a covalent bind to immobilization layer [9]. In this paper, we investigate the dependence of the microcantilever deflection on the sensitive layer (gold and aminosilane) thickness in static mode operation. Such characteristic is important to be found because the microcantilever deflection directly influences the

sensor sensitivity. Both gold and aminosilane have large differences in their Young's moduli properties, therefore, the influence of material properties to sensitivity of double layer microcantilever via the film stress and radius of curvature is an interesting to be studied.

2. Analytical Model For Stress And Deflection

The stoney equation, shown in equation (1), is commonly used for relating substrate curvature to film stress. From the equation, the deflection (Δz) induced by surface stress (σ) can be estimated. Here, ν is Poisson's ratio, E is Young's moduli, l and t are respectively the length and thickness of microcantilever. It is noted that this equation does not contain any parameters relating with a coating film inducing the surface stress.

$$\Delta z = \frac{3(1-\nu)l^2}{Et^2} \sigma \quad (1)$$

In this section, the stoney equation is derived for suitable analytical model of static deflection a microcantilever sensor coated with sensitive layer. When the sensitive layer is coated on the microcantilever surface, stress (σ) is set up in the top and bottom of each layer, as shown in Fig. 2(a). As a result, the composite will bend in response to these stresses. Here, we define the numbers of 1 and 2 in Fig. 2(b) as a substrate layer (first layer) and a coating film or sensitive layer (second layer), respectively.

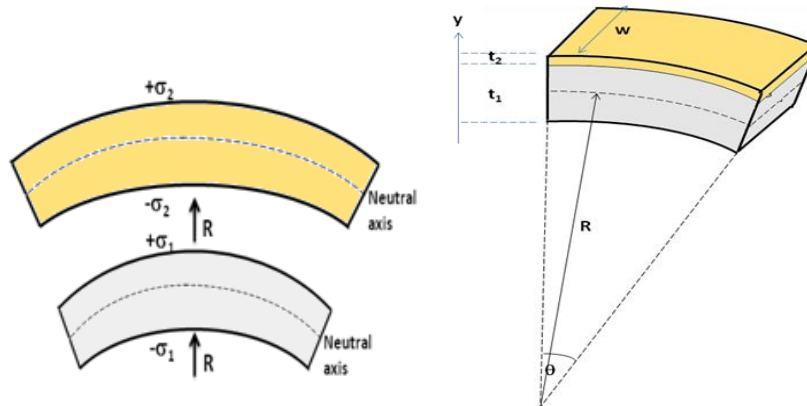


Figure 2. (a) Stress in each layer, (b) Radius of curvature

The radius of curvature, R , can be calculated from the mechanical equilibrium condition, where both force and moment must be in balance, as described in equation (2). It is noted that the radius of the curvature can be shown in Fig. 2(b).

$$\frac{E_1 w t_1^3}{12R} + \frac{E_2 w t_2^3}{12R} + F_1 \frac{t_1}{2} + F_2 \left(t_1 + \frac{t_2}{2} \right) = 0 \quad (2)$$

Here, F_i is internal force distributed throughout the i -th layer. Since $F_2 = -F_1$ in the case of equilibrium, and $F_1 = -\frac{E_1 E_2 t_1 t_2 w}{(E_1 t_1 + E_2 t_2)} \left(\epsilon_{21} + \frac{(t_1 + t_2)}{2R} \right)$, the radius of curvature can be described as,

$$R = \frac{(E_1 w t_1^3 + E_2 w t_2^3)(E_1 t_1 + E_2 t_2) + 3(t_1 + t_2)^2 E_1 E_2 t_1 t_2 w}{12(E_1 t_1 + E_2 t_2) - 6(t_1 + t_2) E_1 E_2 t_1 t_2 w \epsilon_{21}} \quad (3)$$

The joined two layers also generate strain in each layer. The strain which exists in the composite, ϵ_{21} , is the difference of total strain in the bottom of second layer, ϵ_2 , and total strain in the top of first layer, ϵ_1 , as described below,

$$\epsilon_{21} = \epsilon_2 - \epsilon_1 \quad (4)$$

The radius of curvature is needed to calculate sensitive layer stress as a function of position within the layer, $\sigma(y)$. Noted that the stress in each layer varies and may change sign over its entire thickness. The stress in any layer, $\sigma_i(y)$ consists of stress due to internal force and stress due to bending stress. The stress in the sensitive layer is shown in equation (5) [10],

$$\sigma_2(y) = \frac{F_2}{w t_2} + \frac{E_2}{2R} \left(y - \frac{t_2}{2} \right) \quad (5)$$

Here, y is position in i -th layer measured from bottom of the i -th layer (see Fig. 2(b)). The stress in first layer (substrate) is determined by similar formula of equation (5). For two-dimensional nature of the stress and bending problem, E_i is replaced by $E_i/(1 - \nu_i)$, which includes the Poisson ratio, ν_i , of any material. For the microcantilever with the assumption of the deflection $\Delta z = l^2/2R$, Δz is described in the equation below [7],

$$\Delta z = \frac{3l^2(t_2 - t_1)}{(A+4)t_2^2 + (A^{-1}+A)t_1^2 + 6t_2t_1} \epsilon_2 \quad (6)$$

where $A = [E_2 w_2 t_2 (1 - \nu_1)] / [E_1 w_1 t_1 (1 - \nu_2)]$, t_1 is thickness of microcantilever, t_2 is film thickness, and ϵ_2 is a strain of a coating film, shown as

$$\epsilon_2 = \frac{\sigma_2 (1 - \nu_2)}{E_2} \quad (7)$$

3. Result and Discussion

First, we investigated the dependence of the curvature radius on thickness of the coating film (sensitive layer) for gold and aminosilane using the equation (3). The simulation was run by using MATLAB Programming with detail parameters listed in Table 1.

Table 1. The parameters used in the calculation

No.	Parameters	Value
1	Thickness of Microcantilever, t	3 [μm]
2	Length of Microcantilever, l	100 [μm]
3	Width of Microcantilever, w	50 [μm]
5	Silicon Young's moduli, E_1	190 [GPa]
6	Silicon Poisson Ratio, ν_1	0.27
8	Gold Young's moduli, E_2	79 [GPa]
9	Gold Poisson Ratio, ν_2	0.44
10	Aminosilane Young's moduli, E_3	5 [GPa]
11	Aminosilane Poisson Ratio, ν_3	0.31
12	Surface stress	0.1 [N/m]

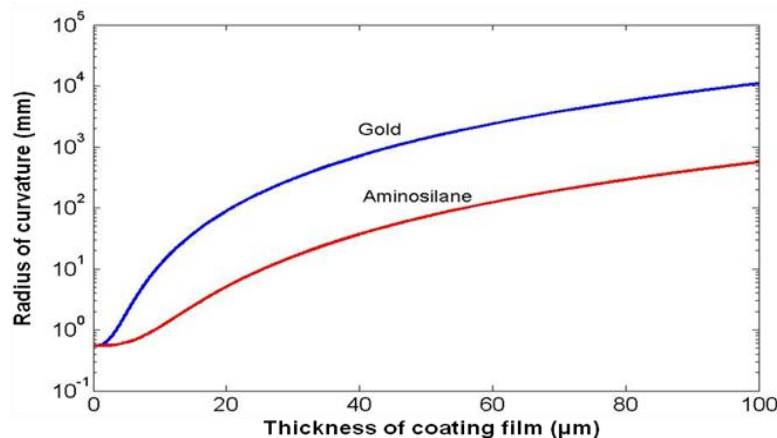


Figure 3. Dependence of curvature radius on the thickness of coating film for gold and aminosilane

Figure 3 shows the calculated radius of the curvature as a function of the various thickness of gold and aminosilane coating film. It can be seen in equation (3) that the radius of curvature is influenced by Young's moduli, thickness of each layer, and strain at the interface of double layers. As results, the higher Young's moduli of gold generates the higher radius of curvature on gold layer than aminosilane layer as shown in the figure. The radius of curvature increases exponentially with the increasing thickness of coating film for both gold and aminosilane layer. Previously, Olsen and Ettenberg reported the stress distribution in the multilayer structures [10], where they found that the layer thickness influenced the radius of curvature. Our result agrees with their result.

Next, the stress distribution in position y in the sensitive layer, $\sigma_2(y)$ was calculated using equation (5). Since strain is induced by adsorption analytes on the sensitive layer, we can assume that the strain is not generated in the microcantilever during this process ($\epsilon_1 = 0$). Therefore, the strain which exists in the composite (ϵ_{21}) is only the strain in the second layer or sensitive layer (ϵ_2), defined as equation (7). Figure 4 shows the stress distribution for both sensitive layers as a function of position y within the layer. Here, the thickness of the sensitive layers is fixed to be 6 nm. As results, for both gold and aminosilane, the stress distribution throughout the coating films increases with the increasing its position from the bottom. The change sign on thickness reflects the tension ($+\sigma$) and compression ($-\sigma$). The maximum tension and maximum compression for both sensitive layers are about 20000 N/m^2 and -20000 N/m^2 , respectively. On the position of a half thickness of sensitive layer (3 nm), the stress distribution for gold and aminosilane layers is 1187 N/m^2 and 94 N/m^2 , respectively. Such stress distribution on this position is only determined by stress due to internal force, where the internal force is influenced by the strain at the interface of two layers. Since the strain is determined by Young's moduli of a material, the higher Young's moduli of gold layer produces the higher stress distribution than that of the aminosilane layer. The stress on the top surface layer for gold and aminosilane is 21000 N/m^2 and 19900 N/m^2 , respectively, whereas the stress on the bottom of gold and aminosilane layers is -19000 N/m^2 and -20000 N/m^2 , respectively.

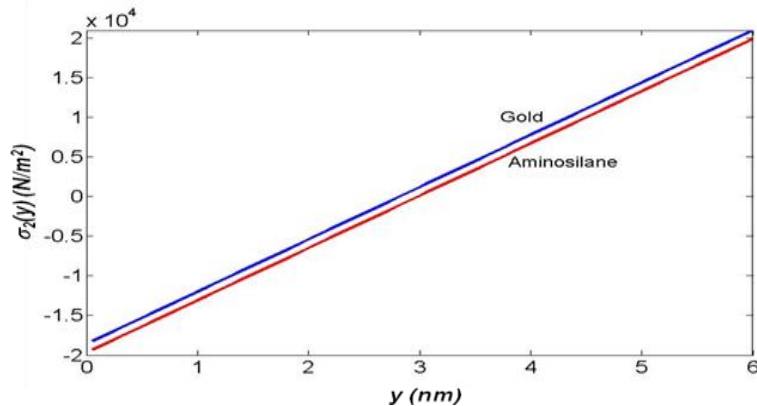


Figure 4. Stress on the film $\sigma_2(y)$, where the position y is measured from the bottom of coating film

Next, we calculated the total stress of the coating film as a function of its thickness, as shown in Fig. 5. The calculated stress is a total of the stress distribution on all positions of thickness layer. In this calculation, it is assumed that all values of the stress are positive. We can see that, for both the sensitive layers, the stress increases with increasing the thickness the stress until a certain value and then decreases thereafter. The maximum stresses of $1.249 \times 10^{10} \text{ N/m}^2$ and $1.728 \times 10^9 \text{ N/m}^2$ are obtained at the thickness of 2900 nm and 7800 nm for gold and aminosilane, respectively. This result agrees with Fig. 4, where the stress of higher Young's moduli (gold) generates the higher stress than one (aminosilane). It indicates that the peak of maximum stress is reduced in lower Young's moduli.

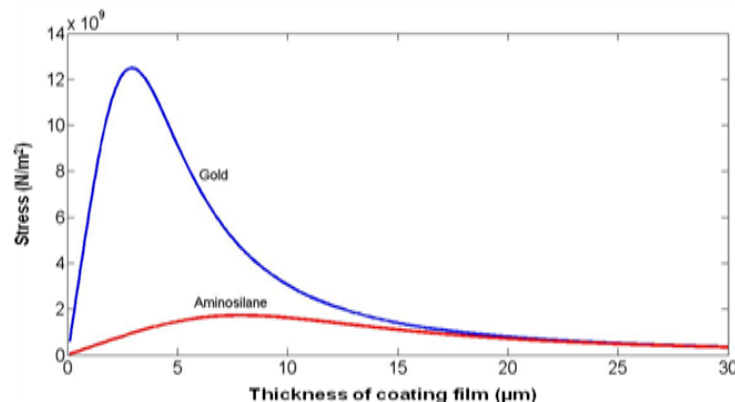


Figure 5. Relationship of the stress and the thickness of coating film

Figure 6 shows the simulation result of the microcantilever deflection as a function of sensitive layer thickness for both gold and aminosilane. The deflection increases with increasing the thickness until a certain value and then the value decreases. For microcantilever with aminosilane layer, the maximum deflection of $141.8 \mu\text{m}$ is reached at the layer thickness of 7300 nm, while for gold layer, the maximum deflection of $111 \mu\text{m}$ is obtained at the layer thickness of 2600 nm.

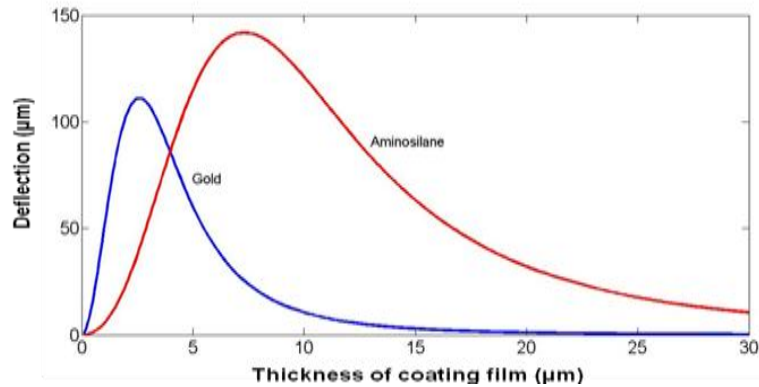


Figure 6. Dependence of the sensor sensitivity on the thickness of coating film for gold and aminosilane

By comparing Fig. 5 and Fig. 6, we can see that the maximum deflection is reached at the thickness of coating film which generates a maximum stress. However, the material with the lower Young's moduli does not always induce the higher deflection value. At the lower thickness, it is possible to obtain the higher deflection value on a material with the higher Young's moduli. These results indicate that the material properties and the thickness of sensitive layer should be considered to obtain a high sensitivity of microcantilever sensor. Therefore, the radius of curvature, strain, and stress distribution are important parameters to study a deflection mechanism of the microcantilever sensor.

4. Conclusion

We have investigated the influence of the material properties and the thickness on deflection of double layer microcantilever via the film stress and the radius of curvature. The film stress distribution is calculated as a function of a position within the film. On the position of a half thickness of sensitive layer (3 nm for layer thickness of 6 nm), the stress distribution for gold and aminosilane layers is 1187 N/m² and 94 N/m², respectively. The stress on the top surface layer for gold and aminosilane is 21000 N/m² and 19900 N/m², whereas the stress on the bottom of gold and aminosilane layers is -19000 N/m² and -20000 N/m², respectively. From the relationship between stress and microcantilever deflection, it is found that, for gold layer, the maximum stress of 1.249×10^{10} N/m² is reached at the thickness of 2500~2900 nm, resulting in the maximum deflection of 111 μm. For aminosilane layer, the maximum stress of 1.728×10^9 N/m² is obtained at the thickness of 7300~7800 nm and the maximum deflection of 141.8 μm is found. These result indicate that stress induces the maximum deflection of the microcantilever and influences the sensor sensitivity.

5. Acknowledgement

We would like to thank Indonesia State Ministry of Research and Technology for funding the research project.

References

- [1] R. Raiteri, M. Grattarola, H. Butt, and P. Skladal, "Micromechanical cantilever-based biosensor," *Sens. Actuators B.*, vol. 79, 2001, pp. 115-126.
- [2] S. K. Vashist, "A review of microcantilevers for sensing applications," *J. Nanotechnol.*, vol. 3, 2007, pp. 1-15.
- [3] R. Nuryadi, A. Djajadi, R. Adiel, L. Aprilia, and N. Aisah, "Resonance frequency change in microcantilever-based sensor due to humidity variation," *Mater. Sci. Forum*, vol. 737, 2013, pp. 176-187.
- [4] R. Nuryadi, W. Rianti, and L. Aprilia, "The Effect of variuos immobilization layer materials to microcantilever sensor sensitivity," *Proceeding of International Conference on Physics 2012*, Yogyakarta, 18-19 September 2012.
- [5] M. Ohring, *The Materials Science of Thin Films*. Boston, NJ: Academic Press, 1991, pp. 403-423.
- [6] G. G. Stoney, "The tension of metallic films deposited by electrolysis," *Proc. R. Soc. Lond.*, vol. 82, no. 553, 1909, pp. 172-175.
- [7] G. Yoshikawa, "Mechanical analysis and optimization of a microcantilever sensor coated with a solid receptor film," *Appl. Phys. Lett.*, vol. 98, 2011, pp. 173502-1_173502-3.
- [8] A. H. Schmid, S.E. Stanca, M.S. Thakur, K. R. Thampia, and C. R. Suri, "Site-directed antibody immobilization on gold substrate for surface plasmon resonance sensors," *Sens. Actuators B.*, vol. 113, 2006, pp. 297-303.
- [9] D. Maraldo, and R. Mutharasan, "Optimization of antibody immobilization for sensing using piezoelectrically excited-millimeter-sized cantilever (PEMC) sensors," *Sens. Actuators B.*, vol. 123, 2007, pp. 474-479.
- [10] G. H. Olsen and M. Ettenberg, "Calculated stresses in multilayered heteroepitaxial structures," *Appl. Phys. Lett.*, vol. 48, no. 6, 1977, pp. 2543 - 2547.

Fatigue Failure Analysis of Small Wooden Wind Turbine Blade

Maldhure S. S.¹, Dr. kharde Y.R.²

¹(Dept. of mechanical engineering, Pravara Rural Engineering Collage, Loni, Pune University, India)

²(Principal Sai baba Engineering Collage, pune University, India)

Abstract:

Advances in engineering technology in recent years have brought demands for reliable wind turbine blade which can operate at different climatic condition and speeds. When failures occur they are expensive, not only in terms of the cost of replacement or repair, but also the costs associated with the down-time of the system of which they are part. Reliability is thus a critical economic factor and for designers to produce wind turbine blade with a high reliability they need to be able to accurately predict the stresses experienced by the different load condition. A wooden 1.5m wind turbine blade was tested by means of a mechanically operated test rig for fatigue failure. The rig uses a crank eccentric mechanism by variable load for each load cycle. The stress distribution in fatigue critical areas of the blade during testing was found to be similar to the expected stress distribution under normal operational condition

Keywords: Wind turbine, blade, bending stresses, analysis, wood, fatigue.

1. Introduction

Wind power is a source of non-polluting, renewable energy. Using wind as an energy source is not a new technology as the first reliable source of the existence of windmills dates back to 644 A.D. and some have claimed to have found remains of windmills 3000 years old. From that time windmills were used to mill grain and later pump water. In the early 1900s, wind was first used to generate electricity. Today, wind turbines (WT) can generate megawatts of power and have rotor diameters that are on the order of 100 meters in diameter. Modern WT, like the one shown in Figure are nearly all horizontal-axis WT (HAWT) and have three rotor blades. The blades of modern WT are manufactured borrowing technology from the boat building industry, are made of both glass and wood composites, and have an airfoil shape adapted from aeronautical engineering. The blades have the ability to pitch in the rotor hub to maintain the optimal angle of attach given the conditions as well as to pitch far enough to stop the rotor in extreme conditions. Some turbines also have internal brakes to stop the rotor. Wind power is one of the fastest growing energy technologies in the world. Wind power has been the second largest source of new power generation in the country for the past two years second only to natural gas, but wind still only currently makes 1% of the country's total electric generation capacity . However, the wind resource is vast and relatively untapped in the United States and theoretically could supply all of the nation's energy. Wind as a sole power source is of course a hypothetical possibility, but the federal government has made a goal for 20% of the country's power to be supplied by wind . However, for this goal to become a reality, WT technology must be improved. The Department of Energy's Wind Energy Program works with the WT industry and research labs, like Sandia National Laboratories (SNL) and the National Renewable Energy Laboratory's (NREL) National Wind Technology Center (NWTC), to improve wind energy technology.

1.1 Wind turbine blades:

Following fig. 1.1 shows different types of failure of wind turbine blade. Wind turbine blade is only 7% still my main emphasis on wind turbine blade because of the following reason.

- 1) Cost of wind turbine blade is almost 30% cost of wind turbine. For composite blade.
- 2) Failure of wind turbine blade means total turbine failure for long period of time. Because replacement of blade takes long period of time.
- 3) Also replacement cost of wind turbine blade is too high. And it may be performed by skilled technical person with highly skilled crane operator.
- 4) Maintaining the inventory of wind turbine blade required huge capital.
- 5) Sudden failure or failure of wind turbine blade in running condition hamper the total wind turbine set ultimately 90% loss of total wind turbine cost.
- 6) Lastly if failure occur at the time when person working with near by it may loss of life to human being.
- 7) Table no. 1 shows the wind potential available in different states of INDIA.

Table no 1 : Wind power potential in INDIA [1]

Sr. no.	State	Gross potential (MW)	Technical potential (MW)
1	Andhra Pradesh	8275	1920
2	Gujarat	9675	1780
3	Karnataka	6620	1180
4	Kerala	875	605
5	Madhya Pradesh	5500	845
6	Maharashtra	3650	3040
7	Orissa	1700	780
8	Rajasthan	5400	910
9	Tamilnadu	3050	1880
10	West Bengal	450	450
	Total	45 195	13 390

In this work fatigue failure of small wooden wind turbine blade by bending strength is found out with the help of crank eccentric bending fatigue failure test rig. A wind turbine blade of 1500 mm length and angle of attack 12 degree for maximum wind speed 25 m/s and rated output for 5 Kw. The long-term goal is to develop general approaches and generic models for each possible failure modes, so that the material properties can be fully utilized and the structural design can be optimized. The new design methods will enable the wind turbine industry to improve their design details and their choice of materials.



Fig 1.1 Different types of failure of wind turbine due to failure of blade

2. Materials and Methods

2.1 Mechanical properties

Table 1 shows the mechanical properties of material used for the experimental investigation of fatigue failure analysis of . all wood wind turbine blade.

Table no 2. Mechanical properties of material [2]

Name of material (Botanical name)	Poisson ratio	Yield stress(Mpa)	Ultimate tensile stress (Mpa)	% Elongation	Modulus of elasticity (Mpa)	Density (Kg/m ³)
Pine (Pinus strobes)	0.328	11500	40	4.01	11500	470
Teak wood (Tectona grandis)	0.341	10830	95	3.88	9400	630
Spruce (picea glauca)	0.372	9800	88	3.50	8500	400

2.2 Material manufacturing

Material is purchase from 1) Gil timber mart, bazarpeth, sangamner. 2) Krushna saw mill, Opposite to bus stand, sangamner. 3) Electronic switches K-11, Ambad MIDC , nasik. 4) Composite mart, 161, 3-pancham ellipse, vishvantwadi, airport road, pune.

Blade manufacturer Vitthal Date , Near navale fabrication, ghulewadi, sangamner.

2.3 Testing facilities

Crank eccentric type fatigue test rig with strain gauges and Load cell is use to measure the applied load.



Fig. 2.1 Test rig used for rotating bending fatigue. And test specimen of wood wind turbine blade.

2.4 Testing condition

Normal operating temperature condition at the time of testing is 35⁰ C .

3. Result and Discussion

Wind turbine blade fatigue testing involves the automated cyclic loading of blades typically at resonant frequency and under closed-loop control, as a means of exciting the blade and achieving the desired strain rate. Cyclic loads are applied to blades at resonant frequency for flap-wise (20 Hz) evaluations. This constant-amplitude fatigue testing can be used to validate blade models, characterize design durability, confirm load profiles and track early failures, cracks and changes in properties. Because of practical limitations, laboratories cannot test a blade with such a large number of design-load cycles in a time period that is reasonable. The advantage of laboratory testing is that the load-amplitude may be increased to accelerate the level of damage per load cycle by as much as two orders of magnitude over the design condition in order to achieve the same total damage in a fraction of the time. The difficulty comes in knowing the properties of the structure well enough to predict where the high damage will occur.

Blade sample	Stress (N/mm ²)	Load (N)	No. of cycle
Pine sample 1	43	399	4.578x10 ⁴
Pine sample 2	42	395	4.547x10 ⁴
Teak sample 1	35	330	1.447x10 ⁶
Teak sample 2	34	324	1.486x10 ⁶
Spruce sample 1	24	268	3.635x10 ⁶
Spruce sample 2	22	239	4.005x10 ⁶

Table no.2 Test result of bending fatigue test

Table no 2 shows the test result of pine wood, teak wood which is commonly available in India. And spruce wood are tested for the different types of load at that time stress is calculated when blade is damage.

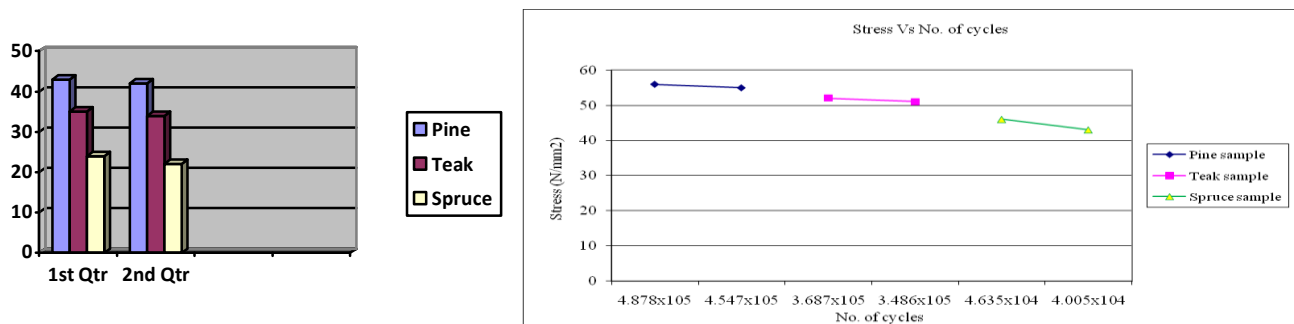


Fig 3.1 Fatigue life of different sample and stress level at that time.

From fig. 3.1 it identified that Teak wood sustain high stress with respect to number of cycle at the time of fatigue life of blade in comparison with the Pine wood and spruce wood also teak wood is very good solution for small types of blade.

4. Conclusions

A 1.2 m wooden wind turbine blade has been successfully tested and it is generally observed that failure of wind turbine blade is 7% as that of total component available in wind turbine generator (WTG). But in actual practice when the WTG blade is fail at running condition total WTG system is collapse and approximate 90% cost of WTG is going to be waste. So it is necessary to search a alternative material for WTG. In the present work 1.2 m wood wind turbine blade has been tested for fatigue test. Following are the advantages of Teak wood, Pine wood, Spruce wood which has been successfully test in this study.

- Easily availability of material.
- Cost of material is low.
- Non pollutant to environment.
- Weight is low.
- High strength for small WTG blade.

Limitation.

- It is difficult to form a aerodynamic shape of blade.
- High length knot free wood is difficult to search.
- Cost of making a blade is equal to cost of material.

Still it is concluded that for the use of micro and mini size wind turbine blade wood is the best material for wind turbine blade.

- 1) Approximate cost of wood wind turbine blade (each) is Rs 1000/- for a 5 years of reliability and for 15 years of reliability Rs 3000/- while it compare to composite material each blade is to be 12000 Rs/- for 15 years of reliability. It means cost shaving in blade material and down time cost due to failure of blade is to be avoided.
- 2) Fatigue life is also considerable for 5 years of life of wind turbine.

References

- [1] Government of India ministry of New and Renewable Energy.
- [2] www.matwed.com (Material property data).
- [3] Chia Chen Ciang. Structural health monitoring for a wind turbine system : a review of damage detection methods. IOP publishing, pages 1-20, 2008.
- [4] John F. Mandell. New Fatigue Data for Wind Turbine Blade Materials, Journal of Solar Energy Engineering,, Vol. 125 to 513, November 2003
- [5] Jayantha A. Epaarachehi, Accelerated full scale fatigue testing of a small composite wind turbine blade using a mechanically operated test rig,SIF 2004 Structural integrity and fracture, 2008.
- [6] Leon Mishnaevsky Jr, Small wind turbine with timber blade for developing countries material choice, development, installation and experiences. Science direct renewable energy 36,2011
- [7] Dayton A. Griffin,Alternative Composite Materials for Megawatt-Scale Wind Turbine Blades: Design Considerations and Recommended Testing, Global Energy Concepts, Vol. 125, November 2003,pp 515-521 (Journal of Solar Energy Engineering)
- [8] R. P. L. Nijssen, Alternative Fatigue Lifetime Prediction Formulations for Variable-Amplitude Loading, Delft University of Technology, Vol. 124, November 2002, pp 396-403. (Journal of Solar Energy Engineering)

Dependency Analysis of Other Service Sectors On ICT

¹Narinder Singh Rana, ²Dr. S N Panda

¹Research Scholar, Punjab Technical University, Jalandhar, Punjab, India

²Professor, RIMT-Regional Institute Of Mgt & Tech., Mandi Gobindgarh, Punjab, India

Abstract

The use of the computational and communication devices has been increasing at an exponential rate for the last couple of decades. Today, along with the Information Technology (IT) and IT enabled Services (ITeS), all other sectors such as financial institutions, manufacturing and retail, transportation and logistic services, tourism, pharmaceuticals, education, public governance etc are highly dependent on ICT (Information and Communication Technology) infrastructure and resultantly the economic growth and stability of a country are highly dependent on the secure and continuous availability of the ICT resources. A miscreant or an adversary today just needs to target this subtle and neophyte backbone of the neo economy and bring more disaster to the country than any weapon can. It has been observed in past that the breakdown in the ICT infrastructure has caused a ripple effect in the economy and created an environment of instability. In this paper, the authors have studied the impact of the ICT sector on other sectors of the economy and the society as a whole.

1. Introduction

The last three decades can very well be termed as the computer age, as in this tenure we have seen the sapling called ‘Personal Computer’ growing into a tree called the Internet. It is paradoxical to understand whether the growth of ICT sector has influenced other sectors to expand and depend on it or, the growth in other sectors and their need for communication propelled the ICT sector. But eventually the effect has been that today all the sectors of economy are heavily dependent on ICT sector. In this paper, the authors have used the data from the sectoral e-Business watch study conducted on different sectors of the European economy by various organizations in contract with the European Commission, Enterprise & Industry Directorate General to study and assess the impact of ICT on European enterprise and industries in general and the economy as a whole. The analysis is primarily based on the e-business watch surveys and Eurostat data. According to the latest data available from the Eurostat, Fig 1.1 shows, in percentage, the value added in the GDP and personnel employed by the ICT sector in various European countries. The graph exhibits that the ICT sector had a significant contribution of average 4.2 % in the GDP of the European countries in 2008 and employed average of 2.4% of the total personnel employed in the member countries. This impact of the ICT sector is only a fraction of contribution that the ICT is making to the growth of the industries and overall economic development of the countries.

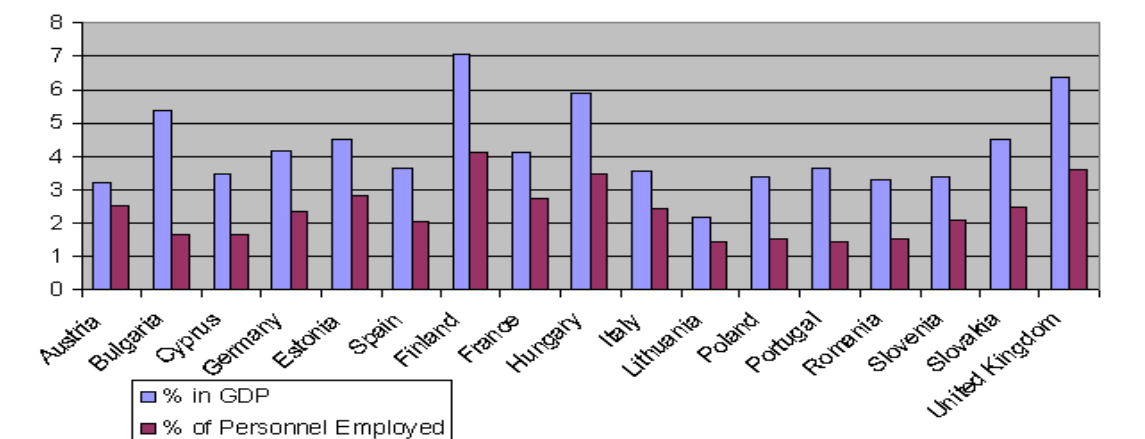


Fig 1.1 Percentage of Value added by ICT sector on GDP

In the following sections, the assessment of the impact and use of ICT technologies in other prominent sectors will be studied. A common framework and methodology is used to assess the preparedness, implementation, efficiency and value addition done by the ICT in conducting e-business in other sectors. Following parameters have been used to assess the preparedness of the businesses to embrace and successfully implement e-business. Firstly, penetration level of the internet in the sector (as it is primary pre-requisite to implementation of ICT), secondly the use of network technologies like intranet, extranet, remote access to data etc, and lastly the security and authentication in place to protect the business from the perpetrators. Further the contribution of ICT as the driver of process and product efficiency and/or innovation is used to establish the impact ICT has on that particular sector. Also, some of the business application and innovation brought about by use of ICT in various sector are briefly discussed with the help of a business case study.

2. Financial Institutions

If we have to select one sector that has been revolutionized by use of ICT, it would certainly be Banking, Insurance and other financial institutions sector. The last couple of decades have seen fundamental changes in the quality and content of these sectors worldwide. Automatic Teller Machines, Real Time Gross Settlement, Electronic Fund Transfer, Electronic Data Interchange, Mobile Banking, Online Bills Payments etc have become common terms and represent the novel instrument to carry out financial transactions. According to the latest data from Eurostat, the financial services sector generates more than 20% in value added revenues and employs more than three million people in EU-25. The Financial Institutions(FI) are quite advanced when it comes to the general ICT uptake indicators like Internet access, intranet, extranet and remote access of data. Almost all (99%) of the Financial Institutions in EU-25 had internet access and almost 80% of these (weighted by employment) had broadband connection. The survey also shows that 9 out of 10 companies either had Local Area Network(LAN) or Wireless Local Area Network (WLAN) based intranet, almost half of the financial institution, 5 out of 10, were also found to have extranet connection with some customers. The uptake for the remote data access in the FI has been slow at 37%, primarily because of the security concerns and nature of data. In term of the security measures and authentication procedures the financial institution are forthright as antivirus software and firewall were implemented by 9 out of 10 organizations. As many as 87% of banks have reported that they take periodic backups to recover data in case of catastrophic failure or security breach. One technology that still has scope of further inclusion in financial institution is the secure server technology as currently only 8 out of 10 banks are using it, especially the small and medium banks have further scope of improvement in implementation of secure servers as they are considered vital for secure transactions. Also in authentication techniques PIN codes and encryption are used by 68% and 61% organization respectively but digital signature are being used only by about 38% FIs. Almost 90% of Large (250+ employees) and Medium (50-249 employees) banks and 77% of Small (10-49 employees) banks have reported to have website which is used for e-Marketing and e-Banking interaction with the customers. Due to the cost effective nature of e-Marketing it is being used as the most commonly used tool for marketing and advertisement. It has been observed that the small banks which have effectively used websites for marketing purposes have shown a significant improvement in turnover and profit as compared to the banks that do not have a website.

Another important factor which shows the ICT uptake in the banking industry is that 8 in 10 banks have reported that they regularly interact with public authorities through Internet. The interaction activities include gathering information, e-tendering and e-filling which are rather common in most industries. During the further analysis of the impact of ICT investment on increased labor productivity, innovation, market structure and sector value chain, it has been observed that ICT investment has a positive effect of the total productivity of the financial institutions but ICT capital has to be appropriately supported with the complementary organizational changes and highly skilled human capital. To analyze the Impact of ICT on innovation is proxied by the number of Initial Public Offerings (IPO) because the new entrepreneurial venture can be facilitated to ICT as it does not require old capital as is evident from the Internet only banks such as Egg Bank and SkandiaBanken.

3. Retailing

Another significant sector of the European economy is the retail sector which, according to the Eurostat data, generates more than 20% in value added revenues and employs about 16.74 million people in around 3.73 million firms out of which 3.5 million firms are micro firms employing 1-9 people. The retail sector comprise of three processes of trade, between wholesaler and retailer, internal operations and, interaction between retailer and the end user of the product. The retail sector has a high ICT uptake as indicated by factors such as Internet access, intranet, extranet and remote access of data. A 95% of the firms weighted by employment are connected to the Internet, the percentage is slightly lower as compared to other sectors as a large number of family run retail stores operate even without a computer. Although the penetration rate of Internet is 100% and 99% in large and medium sized organizations respectively. Almost half of these organizations (53%) had a broadband internet access. The survey also shows that 66% companies weighted by employment are connected using either a Local Area Network(LAN) or Wireless Local Area Network (WLAN) based intranet. The uptake for the remote data access in the retailing is about 45% In the survey, about 60% of the firms said that they were budgeting the same amount for ICT in the next financial year, 35% said that they are actually planning to increase the ICT budget for next year and only 3% planned to decrease it. The most important aspect of the retail management that is effected by ICT is the Supply Chain Management (SCM) which is divided into the upstream supply chain from the manufacturer or the wholesaler to the retailer i.e. e-procurement, the internal supply chain from the ware house to the stores and movement of the products within the store i.e. e-operations and lastly the e-marketing and e-sales which constitute the downstream supply chain from the retail firm to the customer. In 2007, almost 60% of large retailers said that they either process or exchange data electronically, as an industry average, retailer accounting for 55% of total employment said that they order at least some goods online and 50% said that they received at least some invoices electronically, soon all B2B exchanges of invoices is going to be electronic, especially for the organizations which do business regularly. In EU-7 about 31% of firms have been conducting most or good amount of internal processes electronically. Bar-coding is another advanced electronic mechanism that is being used by firms representing 59% of employment, in their in-house operations. Latest technology such as RFID is also being increasingly used by the retailer in Europe. The use of ICT in the downstream SCM, i.e., from the retailer to the customer has also been increasing continuously as in 2007 retail firms representing 69% of employment had website which is used to sell products,

facilitate access to product catalogue or provide after sale service. As in case of financial institutions, ICT has a positive effect on the productivity in the retail sectors, but it has to be appropriately, complemented with the organizational changes and skilled human capital. ICT implementation has also been found to positively effect the product and process innovation in the retail sector as 21% of retails firms, representing 32% of total employment, made some kind of product innovation in 2006/07 out of which 70 % of these innovations were enabled by ICT. It has also enabled large number of process innovations as 45% of firms had introduced such innovation enabled by ICT. According to almost half of firms weighted by employment also believe that ICT usage also has a considerable effect on the competition and market structure in Europe.

4. Transportation And Logistics Industry

The Transport and Logistics Industry (TLI), which covers the rail and road transport (both freight and passenger), warehousing and storage, cargo handling and other support activities, has a contribution of 7% in the GDP of the European Union and employs about 5% of the total people employed in EU-27. The TLI sector has been growing consistently at rate of 2.5% since last one decade, mainly due to the economic decisions and agile manufacturing which requires just in time delivery of raw material, and on demand supply of products, but it has also led to more congestion, accidents, noise and air pollution and dependence on fossil fuels, so the efficiency gained by ICT implementation in this sector would also mean environmentally sustainable, economic growth. The road transport, because of its capacity to move goods any where in the continent with low cost, has the highest share of 44% in movement of goods followed by short sea shipping which accounts for movement of another 41% goods and railways and inland shipping accounts for 10% and 4% respectively. Whereas in case of transportation of people, road transport accounts for 85% followed by railways and airways at 6% and 5% respectively. The transportation sector alone is responsible for 28% of CO₂ emission out of which road transport alone account for 85% of total emission by transport sector. This has a huge effect on the air quality, noise pollution and other environmental hazards. Other important consideration, especially in road transport is road safety. According to an estimate, around 40,000 people die and other 1.2 million are injured in road accidents in Europe every year, so a better use of ICT can be undertaken to bring these figures down. ICT also plays an important role in the logistics industries in form of efficient identification technologies such as bar codes and RFID, communication technologies such as E-mail, Value added services and electronic data interchange and data acquisitions methodologies such as scanning and warehouse management systems. The TLI has a high ICT uptake which is evident as 97% of the firms with 10 or more employees are connected to Internet. All (100%) medium and large industries are connected to the internet and 50% of them have a broadband connection which is considered a prerequisite to the successful implementation of e-business. The internal network such as LAN or WLAN has been implemented by 50% and 22% companies respectively. In the SeBW survey the firms have agreed that ICT implementation has a positive effect on the productivity, turnover and profitability of the organization, so almost all firms (97%) said that they will increase or keep the same budget for ICT investment as that of the previous year.

The security technologies such as Public Key Cryptography (PKI), digital signatures and RFID are also heavily being used in the transportation sector as around 31% of the firms that were interviewed said that they have been occasionally or frequently using the digital signatures. The RFID, although in its inception stage, has a tremendous potential to contribute to efficiency and security, and add a new dimension to the quality of service provided for transportation of people and goods. The RFID technology is being used by firms accounting for 13% of employment in the TLI sector but in future, as the technology would mature and become more affordable, its use would grow tremendously. In the internal management of TLI sector e-Procurement, Customer Relationship Management(CRM), Enterprise Resource Planning(ERP) are also being used by 21%, 17% and 44% respectively by firms weighted by employment. In the logistic sector 92% firms said that they had implemented some ICT applications to comply with request from the customers who wanted to use these applications to better manage and track their consignments. As with other sectors studied above, ICT has been found to have a positive affect on the productivity of the firms but only if it is complemented with appropriate changes in the organizational processes and human skills, it implies that the investment in ICT has to be complemented with the investment in human resource training and skill development. In case of innovations also ICT has a huge impact on the development and implementation of innovative business products and processes, as about 57% of all companies that had introduced new product in last one year said that it was directly related to ICT and around 66% of innovative process introduced in last one year were enabled and implemented by ICT. This figure is even more important for large (250+ employees) firms as 90% of the product and process innovation in these firms have been observed to be driven or/and enabled by ICT.

5. Tourism Industry

Tourism industry is another important and fast growing sector in the European economy which employs around 8.1 million people in 1.4 million tourism related firms. The analysis of the tourism sector has been done on basis of 2006 survey of e-business watch with data primarily from EU-10 countries which represent almost 80% of European population and thus the representation of the EU. The tourism sector includes the subsectors of accommodation, gastronomy, travel and tour operators and aviation sector. The globalization and new tourist destinations have enabled better contribution of ICT in this sector in form of readily available information, comparison and purchase of tourism

products online. The tourism sector is inline with the average internet connectivity index of all the sectors in the EU with 90% of the firms representing 93% of employment were connected to the internet, out of which almost 80% firms are connected through a broadband connection. A total of 53% employees in tourism industry have been found to be using the internet regularly which is significantly higher than the all sector average of 43%, but the adoption of remote access to data is only around 13% primarily because most of the firms are micro firms, but the remote access is available to employees of 71% large firms. The adoption of LANs is also quite high in tourism industry as 63% small firms, 73% medium firms and 92% of large firms use them. The tourism sector is also a heavy user of contemporary technologies such as Voice-over-IP and Virtual Private Network as 16% of the firms have reported to be using them. The preceding analysis ensures that the necessary infrastructure of uptake of ICT is available in the tourism sector. According to the e-business watch survey, ICT expenditure corresponds to around 7% of the total cost of the company. Out of all firms that were surveyed 66% said that they would keep the ICT budget for the next year at the level of current year whereas 24% firms said that they would increase the ICT budget while only 8% would decrease it. The use of open source technologies such as Linux operating system, Mozilla browser etc and security technologies such as secure server technology and firewalls are also being adopted in the tourism sector in EU as around 34% of the firms have reported use of open source technologies and 17% firms have reported the use of secure server technologies such as Secure Socket Layer(SSL) and Transport Layer Security(TLS) in their firms in case of large firm the uptake of these technologies is much higher as 77% of them have reported to be using them. The firewalls are being used by 64% of firms which represent 81% of employment of the sector. The ERP software, accounting software and document management software is also being used by 15% , 67% and 13% of the firms weighted by employment. E-invoicing is also being used by a considerable number of firms representing 20% of employment as 24 % firms send or receive e-invoice. The ICT infrastructure is also being recognized as a major driver for the e-marketing and e-sales and it is true even for tourism sector as 49% of firms weighted by employment take orders online out of which 32% firms have reported to receive more than 25% of their total orders online, whereas 28% firms weighted by employment uses e-marketing and e-selling. As with other sectors, tourism sector also has been found to enable product and process innovation by using ICT infrastructure and technologies as in the survey 32% firms weighted by employment said that they have introduced an innovative product in last one year, out of which 53% firms said that the innovations were related to or enabled by ICT. Similarly 35% firms weighted by employment said that they had made some process innovation in last one year out of which 76% firms said that their innovation was directly related or enabled by ICT.

6. Hospital Sector

The last sector analyzed by the authors is the acute care hospital sector which serves the in-patients who stay at least over night for medical treatment and not the out-patients who are treated ambulatory. The term used in this study is e-health instead of e-business as the patients in the hospital are not treated as customers and commercialization of health care activities is considered against the medical ethos. According to the survey of e-business watch in 2005 there were 13,000 hospitals in EU and employed around 2.5 million people. The total health expenditure in percentage of GDP is between 6% (Slovak Republic) to 12 % (Switzerland) and the acute care hospitals have as average share of 35% in the total health care expenditure. The hospital sectors has been found to have very good ICT infrastructure in term of internet penetration and technologies used as 98% of hospitals representing almost 100% of employment have internet connectivity and a majority of them, 85% weighted by employment, have broadband connection. Also 34% of hospitals have said that they provide remote access of data to its employees or other authorized medical practitioners who require such data. Hospitals also has the requisite LAN and WLAN in place as 96% and 32% firms weighted by employment have reported to have them, VPN is also being used by around 63% of the firms which represent 71% of the employment. Also 57% of hospitals have said that they employee ICT practitioners and 39% said that they provide regular training to their employees. The hospitals reported that they had sent 8% of their total budget on ICT infrastructure during last year and 58% firms said that they are going to keep their ICT spending at the same level for next 12 months, while 34% said that they would increase ICT spending whereas only 8% plan to decrease it. Hospitals are also heavy user of open source technologies as 58% of the hospitals surveyed have reported to be using them. The security technologies are also being used by most of the hospitals in EU. The hospitals store, process and distribute a huge amount of very personal data related to its patients and have to face a dilemma, as on one hand they need to make this data easily available, to ensure proper treatment to the patients and on the other hand they need to protect this data from unauthorized access. In the survey 47% of the hospitals which represent 63% of employment have reported to be using secure server technology, 40% of hospitals weighted by employment are using digital signatures and more than 90% of hospitals are using firewalls to protect their networks and data from unauthorized access or manipulation of data. The hospitals are also using the ICT in internal and external process integration as hospitals representing 75% of employment have Intranet in the hospitals, more then 90% hospitals using computerized accounting system and contemporary technologies such as ERP, and electronic medical record management software are being used by 33% and 69% of firms weighted by employment respectively. E-invoices are also used by 58% of hospitals for sending document to public and private insurance firms. 67% of firms also said that they purchase online from their suppliers. As with all other sectors in the study ICT has been found to have a huge impact on innovation in hospitals as well as out of 30% of hospitals who made a product or service innovation in last 12 months, 55% said that their innovation was directly related or enabled by ICT, similarly out of 44%

of hospitals that said that they made some process innovation in last 12 months, 77% said that the innovation was enabled or related to ICT.

References:

- [1] ICT and e-Business Impact in the banking Industry”, A Sectoral e-Business Watch, Ramboll Managment
- [2] Information and Communication Technology (ICT) in Banking Operations in Nigeria - An Evaluation of Recent Experiences”, UNPAN, Akinlolu Agboola
- [3] Deutsche Bank Research Deutsche Bank Research”, E-economics, Vol. 63, July 31, 2007
- [4] Implications of Web 2.0 for Financial Institutions: Be a Driver, Not a Passenger”, Deutsche Bank Research, Stefan Heng, Thomas Meyer, Antje Stobbe,
- [5] The ICT environment, financial sector and economic growth: a cross-country analysis”, Journal of Economic Studies, Farkhanda Shamim
- [6] ICT, E-BUSINESS and SMEs”, OECD, Graham Vickery, Ken Sakai
- [7] ICT and e-Business Impact in the Retail Industry”, A Sectoral e-Business Watch, empirica GmbH
- [8] The Effects of ICT and E-business on EU Trade: a Retail Industry Perspective”, Journal of Collaboration and the Knowledge Economy, Maria Woerndl,
- [9] Impact of ICT on Indian Business Sectors”, Dr Atanu Ghosh, Gargi Banerjee, IIT Bombay
- [10] ICT and e-Business Impact in the Transport & Logistics Industry”, A Sectoral e-Business Watch, Consultrans S.A.
- [11] ICT and e-Business Impact in the Tourism Industry, ICT adoption and e-business activity in 2006”, Salzburg Research
- [12] Study on Critical Dependencies of Energy, Finance and Transport Infrastructures on ICT Infrastructure”, European Commission DG Justice, Freedom and Security, Dr. Stephan Gottwald
- [13] ICT Innovation and Sustainability of Transport Sector”, European Journal of Transport and Infrastructure Research , William R. Black, Marina van Geehuizen,
- [14] Perception On Information And Communication Technology Perspectives In Logistics: A Study Of Transportation And Warehouses Sectors In Singapore”, Journal Of Enterprise Information Management, Shaligram Pokharel,
- [15] ICT And E-Business Impact In Hospital Activities, ICT Adoption And E-Business Activity In 2006”, Empirica GmbH
- [16] Productive Innovations In Hospitals: An Empirical Research On The Relation Between Technology And Productivity In The Dutch Hospital Industry”, Journal Of Health Economics, Jos L. T. Blank, Bart L. Van Hulst
- [17] Electronic Business in the ICT Services Sector”, The European e-Business W@tch, Montpellier Brussels

Computer-Aided Design of Concrete Mixes

¹D.O. Onwuka, ²C.E. Okere, ³O.M. Ibearugbulem, ⁴S.U. Onwuka
^{1,2,3,4}Civil Engineering, Federal University of Technology, Owerri, Nigeria

Abstract

The determination of mix components and their proportions is referred to as mix design. Traditional methods of designing concrete mixes are based on laid down rules, design standards and codes of practice. These methods are arbitrary and require several trial mixes. Consequently, it is not possible to select at once, the exact mix proportions required to produce concrete of specified or desired property. Thus this work focuses on the development of computer programmes (code in VISUAL BASIC Language) based on simplex and modified regression theories for the designing of concrete mixes. The computer programs can predict all possible combinations of concrete mix proportions if given a desired compressive strength of concrete. Conversely, they can predict the compressive strength of concrete if the mix proportion is specified as well as the optimum value (for the case of the Scheffe's based program). The programs developed are user friendly, easy and inexpensive to use and yield quick and accurate results. The results obtained from the programs agreed with the experimental results and with each other.

Keywords: computer programs; computer-aided design; concrete mixes; compressive strength; simplex method; modified regression method; visual basic language.

1. Introduction

Concrete is an inevitable material in construction industry. It is the backbone of infrastructural development of every country. It is made by mixing cement, water, fine and coarse aggregates and sometimes admixtures in their right proportions to obtain the specified property. The proportions of these constituent materials control the properties of concrete. Majid [1] stated that the compressive strength of hardened concrete is the most convenient property to measure among many properties of concrete. Two main objectives of hardened concrete tests are control of quality and compliance with specifications [2]. Concrete cube strength test is one of the major tests carried out on concrete before it can be used effectively. In addition, concrete grades are usually specified in standard construction work. Various methods have been developed in order to achieve the desired property of concrete cube strength. However, the methods require trial mixes [3]. In this work, statistical theories by Scheffe [4] and Osadebe [5] and experimental results were used to develop model programs for designing of concrete mixes. For example, if the concrete strength is specified as input, the computer prints out all mix proportions that match the concrete strength. On the other hand, if the concrete mix proportion is specified as input, the computer prints out the compressive strength obtainable from that concrete mix proportion.

2. Numerical Analysis

The model programs are based on numerical functions derived from simplex and modified regression statistical theories.

2.1 Simplex Function

The simplex theory of statistics by Scheffe [4] and some experimental results were used for the derivation of the simplex function on which the model programs are based. In his work, Scheffe considered experiment with mixtures in which the desired property depends on the proportions of the constituent materials present as atoms of the mixture. He assumed that $n+1$ mixture components acting as atoms will interact within n -dimensional space, provided the sum of all the proportions of the constituent components, X_i , is equal to unity. That is

$$\sum X_i = 1 \quad (1)$$

and

$$X_i \geq 0 \quad (2)$$

For normal concrete, the components are four in number and so it was analysed using a three dimensional factor space (i.e. a tetrahedron).

In the simplex theory, the response function (i.e. property of the mixture sought) with the following equation

$$Y = b_0 + \sum b_i X_i + \sum b_{ij} X_i X_j \quad (3)$$

where b_i and b_{ij} are constants

X_i and X_{ij} are pseudo components

For a four-component mixture, i and j which represent points on the 3-dimensional space is given as follows

$$0 \leq i \leq j \leq 4 \quad (4)$$

The application of the Scheffe's equation (i.e. Eqn 3) to a four –component mixture, normal concrete yielded the following simplex function derived by Okere et. al. [6].

$$Y = 26.22X_1 + 30.22X_2 + 24X_3 + 27.55X_4 + 2.68X_1X_2 - 2.68X_1X_3 + 20.46X_1X_4 + 16X_2X_3$$

$$- 25.78X_2X_4 + 0.9X_3X_4 \quad (5)$$

where Y is the response (concrete cube strength).

X₁, X₂, X₃ and X₄ are the pseudo components which represent the proportion of the ith component in the mixture.

In order to satisfy the condition given by Eqn (1), normal mixes such as 1:2:4 and 1:3:6 must be transformed using Eqn (6).

$$[Z] = [A] [X] \quad (6)$$

where [Z] = matrix of actual component proportions

[X] = matrix of pseudo components proportions

[A] = matrix of coefficients

Generally, the final simplex function for the response of a four- pseudo component mixture, is given by Eqn (7)

$$Y = \sum \alpha_i X_i + \sum \alpha_{ij} X_i X_j \quad (7)$$

where $1 \leq i \leq j \leq 4$

Y is the response

α_i = coefficient corresponding to the response to pure component i

α_{ij} = coefficient corresponding to the response of binary mixture of components i and j.

2.2 Modified Regression Function

The second model program is based on a modified regression function derived from modified regression theory of statistics by Osadebe [5] and some experimental results. In his work, Osadebe [5] assumed the following continuous response function which is differentiable with respect to its predictors, Z_i

$$F(Z) = \sum F''(Z^{(0)}) * (Z_i - Z^{(0)})/m! \quad (8)$$

where

Z_i = fractional portions or predictors

=ratio of the actual proportions components to the quantity of concrete, S

$0 \leq m \leq \infty$

m = degree of the response function

Using Taylor's series, the response function was expanded up to the second order in the neighbourhood of a chosen point, Z⁽⁰⁾ = Z₁⁽⁰⁾, Z₂⁽⁰⁾, Z₃⁽⁰⁾, Z₄⁽⁰⁾, Z₅⁽⁰⁾ to obtain the Eqn (9)

$$F(z) = F(z^{(0)}) + \sum [\partial F(z^{(0)}) / \partial z_i] (z_i - z_i^{(0)}) + 1/2! \sum \sum [\partial^2 F(z^{(0)}) / \partial z_i \partial z_j] (z_i - z_i^{(0)}) (z_j - z_j^{(0)}) + 1/2! \sum \sum [\partial^2 F(z^{(0)}) / \partial z_i^2] (z_i - z_i^{(0)})^2 + \dots \quad (9)$$

where $1 \leq i \leq 4$, $1 \leq i \leq 4$, $1 \leq j \leq 4$, and $1 \leq i \leq 4$ respectively.

This function was used to derive the following modified regression function, F(z) for the response of a normal concrete, which is a four-component mixture [7].

$$Y = -394790933.1Z_1 - 220057975.6Z_2 - 4093499.945Z_3 + 1283.021096Z_4 + 1204352313Z_1Z_2 + 318501118.4Z_1Z_3 + 395949693.6Z_1Z_4 + 284162641.2Z_2Z_3 + 219194875.1Z_2Z_4 + 4214942.072Z_3Z_4 \quad (10)$$

where Y is the response symbol (concrete cube strength).

Z₁, Z₂, Z₃ and Z₄ are the fractional portion i.e. the ratio of the actual portions, S_i to the quantity of concrete, S.

At nth observation point, the response Y⁽ⁿ⁾ corresponding with the predictor Z_i⁽ⁿ⁾, is given by Eqn (11).

$$Y^{(n)} = \sum \alpha_i Z_i^{(n)} + \sum \alpha_{ij} Z_i^{(n)} Z_j^{(n)} \quad (11)$$

where $1 \leq i \leq j \leq 4$ and n = 1,2,3, 10

In general, Eqn (11) is given as follows:

$$[Y^{(n)}] = [Z_i^{(n)}] \{ \alpha \} \quad (12)$$

where [Y⁽ⁿ⁾] = matrix of response function

[Z_i⁽ⁿ⁾] = matrix of predictors

{α} = matrix of coefficients of the regression

3. Model Programs

Two distinct computer programs were developed in VISUAL BASIC Language and presented in Appendices 2 and 3. The first model program based on the simplex function is given in Appendix 2 while the second model program based on modified regression function is given in Appendix 3. For both programs, the concrete compressive strength can be obtained by inputting into the computer the mix proportions of the concrete components. On the other hand, the input of mix proportions of the constituent concrete materials into the computer gives the compressive strength as output

The outputs of the model programs based on the simplex functions and modified regression models are given below
Part 1: Output of model programs for computation of concrete mix ratios corresponding to desired concrete cube strength.

The executed program segment shown in Table 1 used desired concrete cube strength of 28N/mm²

TABLE 1. SIMPLEX MODEL OUTPUT

STRENGTH	WATER	CEMENT	SAND	GRANITE
27.932	0.536	1	2.145	4.58
27.983	0.535	1	2.15	4.6
28.033	0.535	1	2.155	4.62
28.083	0.534	1	2.16	4.64
27.961	0.461	1	2.895	5.605
27.933	0.526	1	2.245	4.73
28	0.525	1	2.25	4.75
28.066	0.525	1	2.255	4.77
27.913	0.586	1	1.645	3.725
27.938	0.514	1	2.365	5.36
27.978	0.513	1	2.37	5.38
28.019	0.513	1	2.375	5.4
28.058	0.512	1	2.38	5.42
28.097	0.512	1	2.385	5.44
27.907	0.489	1	2.61	5.315
27.957	0.488	1	2.62	5.33
28.008	0.487	1	2.63	5.345
28.06	0.486	1	2.64	5.36
27.903	0.504	1	2.46	5.215
27.959	0.503	1	2.47	5.23
28.015	0.502	1	2.48	5.245
28.072	0.501	1	2.49	5.26
28.061	0.522	1	2.285	4.935
MAXIMUM CUBE STRENGTH OF CONCRETE PREDICTABLE BY THIS MODEL IS				
31.71N/mm ²				
THE CORRESPONDING MIXTURE RATIO IS AS FOLLOWS:				
WATER	CEMENT	SAND	GRANITE	
0.4845	1	2.655	5.845	

The executed program segment shown in Table 2 used desired concrete cube strength of 21.7N/mm².

TABLE 2. MODIFIED REGRESSION MODEL OUTPUT

STRENGTH	WATER	CEMENT	SAND	GRANITE
21.764	0.484	1	2.69	7.889
21.778	0.437	1	3.115	6.341
21.768	0.48	1	2.742	7.598
21.779	0.439	1	3.128	6.22
21.768	0.488	1	2.642	7.663
21.78	0.451	1	3.018	6.389
21.768	0.451	1	2.977	6.359
21.762	0.478	1	2.721	7.138
21.768	0.488	1	2.635	7.332
21.779	0.444	1	3.047	5.873

21.765	0.469	1	2.797	6.451
21.776	0.454	1	2.968	5.813
21.773	0.478	1	2.75	6.513
21.77	0.501	1	2.514	7.209
21.764	0.476	1	2.77	6.326
21.775	0.486	1	2.64	6.65
21.77	0.457	1	2.944	5.68
21.762	0.447	1	3.025	5.38
21.773	0.47	1	2.82	6.04
21.78	0.494	1	2.597	6.732
21.761	0.45	1	2.987	5.357
21.776	0.451	1	2.983	5.219
21.761	0.471	1	2.805	5.635
21.78	0.46	1	2.895	5.232
21.772	0.461	1	2.869	5.202
21.773	0.487	1	2.62	5.933
21.766	0.513	1	2.397	6.649
21.776	0.513	1	2.397	6.605
21.766	0.466	1	2.844	5.233
21.774	0.512	1	2.409	6.507
21.772	0.465	1	2.838	5.158
21.766	0.502	1	2.505	6.135
21.778	0.468	1	2.808	5.115
21.778	0.505	1	2.475	6.121
21.76	0.496	1	2.559	5.787

Part 2: A computer model output for the computation of concrete cube strength corresponding to a specified mix ratio. Tables 3 and 4 show the simplex model output and modified regression model output respectively for specified mix ratios.

TABLE 3. SIMPLEX MODEL OUTPUT

STRENGTH	WATER	CEMENT	SAND	GRANITE
27.57367	0.55	1	2	4

TABLE 4. MODIFIED REGRESSION MODEL OUTPUT

STRENGTH	WATER	CEMENT	SAND	GRANITE
28.89249609	0.525	1	2.25	5

4. Discussion Of Results

Each program is in two parts. The computer print-out shows all possible mix ratios for the desired concrete cube strength. The computer model programs can also predict the concrete cube strength if the mix ratios are given. The simplex model program can also predict the maximum concrete cube strength which in the above case is 31.71N/mm². The computer results were obtained within seconds.

4.1 Comparison With Existing Codes And Implications

Mathematical modelling for optimisation of concrete mix design is quite different from the conventional method of concrete mix design and as such codes from both methods cannot be effectively compared numerically.

However, the following comments can be made. Concrete mix design is still very much a problem of trial and error and any calculation based on design data are really only a means of providing at best a starting point so that the first test can be conducted. Simon et. al.,[8] stated that the general approach to concrete mixture proportioning can be described by the following steps:

- (1) Identifying a starting set of mixture proportions
- (2) Performing one or more trial batches, starting with the mixture identified in step (1) above, and adjusting the proportions in subsequent trial batches until all criteria are satisfied.

Various methods are available. These include American Concrete Institute (ACI) mix design method, the British Method of mix design, DOE method, USBR method, to mention but a few. All these methods basically follow the same approach stated above. Apparently, time and energy used in order to get the appropriate mix proportions may be enormous. The method applied may not be cost effective. This shows that the various mix design methods have limitations. To minimize some of these limitations, an optimisation procedure has been proposed. A process that seeks for a maximum or minimum value for a function of several variables while at the same time satisfying a number of other imposed requirements is called an optimisation process [1]. As the cost of materials increases, optimising concrete mixture proportions for cost becomes more desirable. Furthermore, as the number of constituent materials increases, the problem of identifying optimal mixtures becomes increasingly complex [8]. With the model equations and the corresponding computer programs developed, several analyses are possible. For instance, a user could determine which mixture proportions would yield one or more desired properties. The mixture proportion that has the highest or most desired property is the optimum mixture. A user also could optimise any property subject to constraints (specified requirements) on other properties. Simultaneous optimisation to meet several constraints is also possible. For example one could determine the lowest cost mixture with strength greater than a specified value. These are some of the advantages of computer –aided optimisation of concrete mixture design. In addition, the computer output results are obtained instantaneously. The user needs only to specify the strength of concrete desired and almost immediately, the computer provides all the possible mix ratios that can yield the desired concrete cube strength. The model computer program can also produce the concrete cube strength if mix proportions are given. The simplex model program is able to predict the maximum concrete cube strength. With these computer model programs, the arbitrary choice of constituent mix and the use of trial mix have been reduced. The effort used in traditional system of design mixes is also reduced. In addition, the use of these models will make concrete production less expensive.

5. Conclusion

It is worthy of note here that concrete cube strength has been characterised by equations (models) which were formulated in previous works [6-7]. The strength is expressed as an algebraic function of factors (individual component proportions) such as water-cement ratio, cement content and aggregate content. Without the programs developed, the models cannot be used effectively. An attempt to use the models without the computer programs will be a waste of precious time. Two computer programs, each in two parts, for optimisation of concrete cube strength were developed i.e. simplex model and modified regression model. The programs were written in visual basic language. With the models, the user needs only to specify the concrete cube strength and almost immediately the computer provides all the possible mix ratios that can yield the desired cube strength. The model can also produce the concrete cube strength if the mix ratios are given as well as the optimum cube strength. With these models, the arbitrary choice of constituent mix and the use of trial mix have been reduced. The effort used in traditional system of design mixes is also reduced. In addition, the use of these models will make concrete production less expensive.

References

- [1] Majid, K.I., (1974). Optimum Design of Structures. London: Butterworth & Co. Ltd.
- [2] Neville, A.M.,(1996). Properties of concrete, England: Longman.
- [3] Teychenne, D.C., Franklin, R.E., and Erntrouy, H.C., (1975). Design of Normal Concrete Mixes. A Publication of Building Research Establishment, Transport and Road Research Laboratory and Cement and Concrete Association.
- [4] Scheffe, H., (1958). Experiments with Mixtures. Royal Statistical Society Journal, vol. 20, pp. 344-360.
- [5] Osadebe, N.N., (2003). Generalised mathematical modelling of compressive strength of normal concrete as a multi-variant function of the properties of its constituent components. A paper delivered at college of Engineering, University of Nigeria, Nsukka. unpublished.
- [6] Okere, C.E., Onwuka, D.O., Onwuka, S.U. and Arimanwa, J.I., (2013). Simplex-based concrete mix design. IOSR Journal of Mechanical and Civil Engineering, vol. 5 No. 2, pp. 46-55.
- [7] Onwuka, D.O., Okere, C.E., Arimanwa, J.I. and Onwuka, S.U., (2011). Prediction of concrete mix ratios using modified regression theory. Computational Methods in Civil Engineering, vol. 2 No. 1, pp. 95-107.
- [8] Simon, M.J., Langergren, E.S., Snyder, K.A., (1997). Concrete mixture optimisation using statistical mixture design methods. Proceeding of PCI/FHWA International symposium on high performance concrete, New Orleans, pp. 230-244.

APPENDIX 1

List of some of the Arrays and Variables used in the programme.

Arrays

A = matrix whose elements are obtained from arbitrary mix proportions prescribed.

B = inverse of matrix A

z = fractional portions or predictors

α = coefficients of regression.

Variables

Z = matrix of actual components

X = matrix of pseudo components

Desired concrete cube strength

Mix ratios.

APPENDIX 2

```
Private Sub ENDMNU_Click()
```

```
End
```

```
End Sub
```

```
Private Sub STARTMNU_Click()
```

```
Dim oExcel As Object
```

```
Dim oBook As Object
```

```
Dim oSheet1 As Object
```

```
Dim oSheet2 As Object
```

```
'Start a new workbook in Excel
```

```
Set oExcel = CreateObject("Excel.Application")
```

```
Set oBook = oExcel.Workbooks.Add
```

```
Rem ONE COMPONENT
```

```
Cls
```

```
ReDim X(4)
```

SCEFHE'S SIMPLEX MODEL FOR COMPRESSIVE STRENGTH

```
Print " THE PROGRAM WAS WRITTEN BY"
```

```
Print: Print
```

```
Print " DR. DAVIES ONWUKA"
```

```
Print:
```

```
WWWWW = InputBox("CLICK OK. TO CONTINUE"): Cls
```

CIVIL ENGINEERING DEPARTMENT, FUTO

```
ReDim MIX(300, 4), STRGTH(300, 1), MIXX(1, 4)
```

```
Dim NP As Variant
```

```
KK = 0: MM = 1: CT = 0: OPSTRENGTH = 0: OPT1 = 0: OPT = 0: KKK = 0
```

```
ReDim X(10), A(4, 4), Z(4), N(15), M(15), B(4, 4), XX(4), ZZ(4): QQ = 1
```

```
XX(1) = 0: XX(2) = 0: XX(3) = 0: XX(4) = 0
```

```
Cls
```

```
E1 = 1: E2 = 2: E3 = 3: E4 = 4: J1 = 1: J2 = 0: J3 = 0: J4 = 0: TT = 1
```

```
5 QQ = InputBox("WHAT DO YOU WANT TO DO? TO CALCULATE MIX RATIOS GIVEN DESIRED  
STRENGTH OR CALCULATING STRENGTH GIVEN MIX RATIO?", "IF THE STRENGTH IS KNOWN TYPE 1  
ELSE TYPE 0", "TYPE 1 OR 0 and CLICK OK")
```

```
If QQ <> 1 And QQ <> 0 Then EE = InputBox("No Way! You must ENTER 1 or 0", , "CLICK OK and do so"): GoTo  
5
```

```
If QQ = 0 Then GoTo 900
```

```
Rem *** CONVERSION MATRIX ***
```

```
A(1, 1) = 0.55: A(1, 2) = 0.5: A(1, 3) = 0.45: A(1, 4) = 0.6
```

```
A(2, 1) = 1: A(2, 2) = 1: A(2, 3) = 1: A(2, 4) = 1
```

```
A(3, 1) = 2: A(3, 2) = 2.5: A(3, 3) = 3: A(3, 4) = 1.5
```

```
A(4, 1) = 4: A(4, 2) = 6: A(4, 3) = 5.5: A(4, 4) = 3.5
```

```
YY = InputBox("WHAT IS THE DESIRED STRENGTH?"): YY = YY * 1
```

```
Q = -4
```

```
10 X(1) = 1: X(2) = 0: X(3) = 0: X(4) = 0: Q = Q + 1: GoTo 2000:
```

```
11 X(1) = 0: X(2) = 1: X(3) = 0: X(4) = 0: Q = Q + 1: GoTo 2000:
```

```
12 X(1) = 0: X(2) = 0: X(3) = 1: X(4) = 0: Q = Q + 1: GoTo 2000:
```

```
13 X(1) = 0: X(2) = 0: X(3) = 0: X(4) = 1: Q = Q + 1: GoTo 2000:
```

Rem TWO COMPONENTS

14 E = 1: R = 1: F = R: Y1 = 1: Y2 = 0: Y3 = 0: Y4 = 0: T = 1: U = 1: V = 1: Q = 1: QQ = 1

X(1) = 0: X(2) = 0: X(3) = 0: X(4) = 0

20 Y1 = Y1 - 0.01: Y2 = Y2 + 0.01

If F + 1 > 4 Then GoTo 30

25 X(E) = Y1: X(F + 1) = Y2

If T = 100 Then T = 1: GoTo 30

T = T + 1

GoTo 2000

28 GoTo 20

30 If U = 3 Then U = 1: GoTo 40

X(1) = 0: X(2) = 0: X(3) = 0: X(4) = 0

U = U + 1: F = F + 1: Y1 = 1: Y2 = 0: GoTo 20

40 If V = 3 Then GoTo 50

V = V + 1: E = E + 1: F = R + 1: R = F: Y1 = 1: Y2 = 0

X(1) = 0: X(2) = 0: X(3) = 0: X(4) = 0: GoTo 20

50 Rem THREE COMPONENTS

Rem FIRST ROUND

Q = Q + 1: X(1) = 0: X(2) = 0: X(3) = 0: X(4) = 0

E = 1: R = 1: F = R: Y1 = 0.89: Y2 = 0.01: Y3 = 0.1: Y4 = 0: T = 1

60 Rem

70 X(E) = Y1: X(F + 1) = Y2: X(F + 2) = Y3

If T = 99 Then GoTo 80

T = T + 1:

GoTo 2000

75 Y1 = Y1 - 0.01: Y2 = Y2 + 0.01: GoTo 70

80 Rem SECOND ROUND

Q = Q + 1: X(1) = 0: X(2) = 0: X(3) = 0: X(4) = 0

E = 1: R = 1: F = R: Y1 = 0.89: Y2 = 0.1: Y3 = 0.01: Y4 = 0: T = 1

90 X(E) = Y1: X(F + 1) = Y2: X(F + 2) = Y3: X(F + 3) = Y4

Rem

If T = 99 Then GoTo 120

T = T + 1

GoTo 2000

115 Y1 = Y1 - 0.01: Y3 = Y3 + 0.01: GoTo 90

120 Rem THIRD ROUND

Q = Q + 1: X(1) = 0: X(2) = 0: X(3) = 0: X(4) = 0

E = 1: R = 1: F = R: Y1 = 0.89: Y2 = 0.01: Y3 = 0: Y4 = 0.1: T = 1

130 X(E) = Y1: X(F + 1) = Y2: X(F + 2) = Y3: X(F + 3) = Y4

If T = 99 Then GoTo 160

T = T + 1

GoTo 2000

155 Y1 = Y1 - 0.01: Y2 = Y2 + 0.01: GoTo 130

160 Rem FOURTH ROUND

Q = Q + 1: X(1) = 0: X(2) = 0: X(3) = 0: X(4) = 0

E = 1: R = 1: F = R: Y1 = 0.89: Y2 = 0.1: Y3 = 0: Y4 = 0.01: T = 1

170 X(E) = Y1: X(F + 1) = Y2: X(F + 2) = Y3: X(F + 3) = Y4

If T = 99 Then GoTo 200

T = T + 1

GoTo 2000

195 Y1 = Y1 - 0.01: Y4 = Y4 + 0.01: GoTo 170

200 Rem FIFTH ROUND

Q = Q + 1: X(1) = 0: X(2) = 0: X(3) = 0: X(4) = 0

E = 1: R = 1: F = R: Y1 = 0.89: Y2 = 0: Y3 = 0.01: Y4 = 0.1: T = 1
 210 X(E) = Y1: X(F + 1) = Y2: X(F + 2) = Y3: X(F + 3) = Y4

If T = 99 Then GoTo 240
 T = T + 1
 GoTo 2000

235 Y1 = Y1 - 0.01: Y3 = Y3 + 0.01: GoTo 210

Rem SIXTH ROUND
 Q = Q + 1: X(1) = 0: X(2) = 0: X(3) = 0: X(4) = 0
 E = 1: R = 1: F = R: Y1 = 0.89: Y2 = 0: Y3 = 0.1: Y4 = 0.01: T = 1
 240 X(E) = Y1: X(F + 1) = Y2: X(F + 2) = Y3: X(F + 3) = Y4

If T = 99 Then GoTo 270
 T = T + 1
 GoTo 2000

265 Y1 = Y1 - 0.01: Y4 = Y4 + 0.01: GoTo 240

270 Rem FOUR COMPONENTS

Rem FIRST ROUND
 ' Print " THIS IS OWUS"
 Q = Q + 1: X(1) = 0: X(2) = 0: X(3) = 0: X(4) = 0
 E = 1: R = 1: F = R: Y1 = 0.79: Y2 = 0.01: Y3 = 0.1: Y4 = 0.1: T = 1
 280 X(E) = Y1: X(F + 1) = Y2: X(F + 2) = Y3: X(F + 3) = Y4

290 Y1 = Y1 - 0.01: Y2 = Y2 + 0.01
 If T = 79 Then GoTo 300
 T = T + 1
 GoTo 2000

295 GoTo 280

300 Rem SECOND ROUND
 Q = Q + 1: X(1) = 0: X(2) = 0: X(3) = 0: X(4) = 0
 E = 1: R = 1: F = R: Y1 = 0.79: Y2 = 0.1: Y3 = 0.01: Y4 = 0.1: T = 1
 310 X(E) = Y1: X(F + 1) = Y2: X(F + 2) = Y3: X(F + 3) = Y4

320 Y1 = Y1 - 0.01: Y3 = Y3 + 0.01
 If T = 79 Then GoTo 330
 T = T + 1
 GoTo 2000

325 GoTo 310

330 Rem THIRD ROUND
 Q = Q + 1: X(1) = 0: X(2) = 0: X(3) = 0: X(4) = 0
 E = 1: R = 1: F = R: Y1 = 0.79: Y2 = 0.1: Y3 = 0.1: Y4 = 0.01: T = 1
 340 X(E) = Y1: X(F + 1) = Y2: X(F + 2) = Y3: X(F + 3) = Y4

350 Y1 = Y1 - 0.01: Y4 = Y4 + 0.01
 If T = 79 Then GoTo 360
 T = T + 1
 GoTo 2000

355 GoTo 340

360 Rem FOURTH ROUND
 Q = Q + 1: X(1) = 0: X(2) = 0: X(3) = 0: X(4) = 0
 E = 1: R = 1: F = R: Y1 = 0.69: Y2 = 0.2: Y3 = 0.01: Y4 = 0.1: T = 1
 370 X(E) = Y1: X(F + 1) = Y2: X(F + 2) = Y3: X(F + 3) = Y4

380 Y1 = Y1 - 0.01: Y3 = Y3 + 0.01
 If T = 69 Then GoTo 390
 T = T + 1
 GoTo 2000

385 GoTo 370

390 Rem FIFTH ROUND
 Q = Q + 1: X(1) = 0: X(2) = 0: X(3) = 0: X(4) = 0
 E = 1: R = 1: F = R: Y1 = 0.69: Y2 = 0.2: Y3 = 0.1: Y4 = 0.01: T = 1
 400 X(E) = Y1: X(F + 1) = Y2: X(F + 2) = Y3: X(F + 3) = Y4

410 Y1 = Y1 - 0.01: Y4 = Y4 + 0.01
 If T = 69 Then GoTo 420

T = T + 1
GoTo 2000
415 GoTo 410

420 Rem SIXTH ROUND
Q = Q + 1: X(1) = 0: X(2) = 0: X(3) = 0: X(4) = 0
E = 1: R = 1: F = R: Y1 = 0.59: Y2 = 0.3: Y3 = 0.01: Y4 = 0.1: T = 1
430 X(E) = Y1: X(F + 1) = Y2: X(F + 2) = Y3: X(F + 3) = Y4
440 Y1 = Y1 - 0.01: Y3 = Y3 + 0.01
If T = 59 Then GoTo 450
T = T + 1
GoTo 2000
445 GoTo 430

450 Rem SEVENTH ROUND
Q = Q + 1: X(1) = 0: X(2) = 0: X(3) = 0: X(4) = 0
E = 1: R = 1: F = R: Y1 = 0.59: Y2 = 0.3: Y3 = 0.1: Y4 = 0.01: T = 1
460 X(E) = Y1: X(F + 1) = Y2: X(F + 2) = Y3: X(F + 3) = Y4
470 Y1 = Y1 - 0.01: Y4 = Y4 + 0.01
If T = 59 Then GoTo 480
T = T + 1
GoTo 2000
475 GoTo 460

480 Rem EIGHTH ROUND
Q = Q + 1: X(1) = 0: X(2) = 0: X(3) = 0: X(4) = 0
E = 1: R = 1: F = R: Y1 = 0.49: Y2 = 0.4: Y3 = 0.01: Y4 = 0.1: T = 1
490 X(E) = Y1: X(F + 1) = Y2: X(F + 2) = Y3: X(F + 3) = Y4
500 Y1 = Y1 - 0.01: Y3 = Y3 + 0.01
If T = 49 Then GoTo 510
T = T + 1
GoTo 2000
505 GoTo 490

510 Rem NINETH ROUND
Q = Q + 1: X(1) = 0: X(2) = 0: X(3) = 0: X(4) = 0
E = 1: R = 1: F = R: Y1 = 0.49: Y2 = 0.4: Y3 = 0.1: Y4 = 0.01: T = 1
520 X(E) = Y1: X(F + 1) = Y2: X(F + 2) = Y3: X(F + 3) = Y4
530 Y1 = Y1 - 0.01: Y4 = Y4 + 0.01
If T = 49 Then GoTo 540
T = T + 1
GoTo 2000
535 GoTo 520

540 Rem TENTH ROUND
Q = Q + 1: X(1) = 0: X(2) = 0: X(3) = 0: X(4) = 0
E = 1: R = 1: F = R: Y1 = 0.39: Y2 = 0.5: Y3 = 0.01: Y4 = 0.1: T = 1
550 X(E) = Y1: X(F + 1) = Y2: X(F + 2) = Y3: X(F + 3) = Y4
560 Y1 = Y1 - 0.01: Y3 = Y3 + 0.01
If T = 39 Then GoTo 570
T = T + 1
GoTo 2000
565 GoTo 550

570 Rem TENTH ROUND
Q = Q + 1: X(1) = 0: X(2) = 0: X(3) = 0: X(4) = 0
E = 1: R = 1: F = R: Y1 = 0.39: Y2 = 0.5: Y3 = 0.1: Y4 = 0.01: T = 1
580 X(E) = Y1: X(F + 1) = Y2: X(F + 2) = Y3: X(F + 3) = Y4
590 Y1 = Y1 - 0.01: Y4 = Y4 + 0.01
If T = 39 Then GoTo 600
T = T + 1
GoTo 2000
595 GoTo 580

600 Rem ELEVENTH ROUND

```

Q = Q + 1: X(1) = 0: X(2) = 0: X(3) = 0: X(4) = 0
E = 1: R = 1: F = R: Y1 = 0.29: Y2 = 0.6: Y3 = 0.01: Y4 = 0.1: T = 1
610 X(E) = Y1: X(F + 1) = Y2: X(F + 2) = Y3: X(F + 3) = Y4
620 Y1 = Y1 - 0.01: Y3 = Y3 + 0.01
    If T = 29 Then GoTo 630
    T = T + 1
    GoTo 2000
625 GoTo 610

630 Rem TWELVETH ROUND
Q = Q + 1: X(1) = 0: X(2) = 0: X(3) = 0: X(4) = 0
E = 1: R = 1: F = R: Y1 = 0.29: Y2 = 0.6: Y3 = 0.1: Y4 = 0.01: T = 1
640 X(E) = Y1: X(F + 1) = Y2: X(F + 2) = Y3: X(F + 3) = Y4
650 Y1 = Y1 - 0.01: Y4 = Y4 + 0.01
    If T = 29 Then GoTo 660
    T = T + 1
    GoTo 2000
655 GoTo 640

660 Rem THIRTEENTH ROUND
Q = Q + 1: X(1) = 0: X(2) = 0: X(3) = 0: X(4) = 0
E = 1: R = 1: F = R: Y1 = 0.19: Y2 = 0.7: Y3 = 0.01: Y4 = 0.1: T = 1
670 X(E) = Y1: X(F + 1) = Y2: X(F + 2) = Y3: X(F + 3) = Y4
680 Y1 = Y1 - 0.01: Y3 = Y3 + 0.01
    'GoTo 2000
    If T = 19 Then GoTo 690
    T = T + 1
    GoTo 2000
685 GoTo 670

690 Rem FOURTEENTH ROUND
Q = Q + 1: X(1) = 0: X(2) = 0: X(3) = 0: X(4) = 0
E = 1: R = 1: F = R: Y1 = 0.19: Y2 = 0.7: Y3 = 0.1: Y4 = 0.01: T = 1
700 X(E) = Y1: X(F + 1) = Y2: X(F + 2) = Y3: X(F + 3) = Y4
710 Y1 = Y1 - 0.01: Y4 = Y4 + 0.01
    'GoTo 2000
    If T = 19 Then GoTo 720
    T = T + 1
    GoTo 2000
715 GoTo 700

720 Rem THREE COMPONENTS CONTIUES
Rem SEVENTH ROUND
Q = Q + 1: X(1) = 0: X(2) = 0: X(3) = 0: X(4) = 0
E = 1: R = 1: F = R: Y1 = 0: Y2 = 0.89: Y3 = 0.01: Y4 = 0.1: T = 1
750 X(E) = Y1: X(F + 1) = Y2: X(F + 2) = Y3: X(F + 3) = Y4
    If T = 99 Then GoTo 760
    T = T + 1
    GoTo 2000
755 Y2 = Y2 - 0.01: Y3 = Y3 + 0.01: GoTo 750

760 Rem EIGHTH ROUND
Q = Q + 1: X(1) = 0: X(2) = 0: X(3) = 0: X(4) = 0: P = 1
E = 1: R = 1: F = R: Y1 = 0: Y2 = 0.89: Y3 = 0.1: Y4 = 0.01: T = 1
790 X(E) = Y1: X(F + 1) = Y2: X(F + 2) = Y3: X(F + 3) = Y4
    If T = 99 Then GoTo 800
    T = T + 1
    GoTo 2000
795 Y2 = Y2 - 0.01: Y4 = Y4 + 0.01: GoTo 790
800
2000 Rem PRINTING OF RESULTS
' Y = 26.22 * X(1) + 30.22 * X(2) + 24 * X(3) + 27.55 * X(4) + 2.68 * X(1) * X(2)
' Y = Y - 2.68 * X(1) * X(3) - 20.46 * X(1) * X(4) + 16 * X(2) * X(3) - 25.78 * X(2) * X(4) + 0.9 * X(3) * X(4)

```

$$Y = 26.22 * X(1) + 30.22 * X(2) + 24 * X(3) + 27.55 * X(4) + 2.68 * X(1) * X(2) - 2.68 * X(1) * X(3) - 20.46 * X(1) * X(4) + 16 * X(2) * X(3) - 25.78 * X(2) * X(4) + 0.9 * X(3) * X(4)$$

If Y > OPSTRENGTH Then For I = 1 To 4: ZZ(I) = 0: Next I

$$\text{If } Y > \text{OPSTRENGTH Then } YOP = 26.22 * X(1) + 30.22 * X(2) + 24 * X(3) + 27.55 * X(4) + 2.68 * X(1) * X(2) - 2.68 * X(1) * X(3) - 20.46 * X(1) * X(4) + 16 * X(2) * X(3) - 25.78 * X(2) * X(4) + 0.9 * X(3) * X(4)$$

If Y > OPSTRENGTH Then OPSTRENGTH = Y: For I = 1 To 4: For J = 1 To 4: ZZ(I) = ZZ(I) + A(I, J) * X(J): Next J: Next I

If Y > YY - 0.1 And Y < YY + 0.1 Then GoTo 810 Else GoTo 830

810 NP = NP + 1

CT = CT + 1

For I = 1 To 4: Z(I) = 0: Next I

For I = 1 To 4

For J = 1 To 4

Z(I) = Z(I) + A(I, J) * X(J)

Next J

Next I

If Z(2) > 1.01 Or Z(2) < 0.9998 Then GoTo 830

If Z(1) < 0 Or Z(2) < 0 Or Z(3) < 0 Or Z(4) < 0 Then GoTo 830

' If QQQ = 15 Then QQQQ = InputBox("PRESS OK TO CONTINUE", , , 5500, 6000): QQQ = 1: Cls

QQQ = QQQ + 1

STRGTH(NP, 1) = Format(Y, "0.00#")

MIX(NP, 1) = Format(Z(1), "0.00#")

MIX(NP, 2) = Format(Z(2), "0.00#")

MIX(NP, 3) = Format(Z(3), "0.00#")

MIX(NP, 4) = Format(Z(4), "0.00#")

' Print " STRENGTH = N"; Format(Y, "0.00"),

' Print " WATER "; Format(Z(1), "0.00#");

' Print " CEMENT "; Format(Z(2), "#");

' Print " SAND "; Format(Z(3), "0.00#");

' Print " GRANITE "; Format(Z(4), "0.00#")

830 If Q = -3 Then GoTo 11

If Q = -2 Then GoTo 12

If Q = -1 Then GoTo 13

If Q = 0 Then GoTo 14

If Q = 1 Then GoTo 28

If Q = 2 Then GoTo 75

If Q = 3 Then GoTo 115

If Q = 4 Then GoTo 155

If Q = 5 Then GoTo 195

If Q = 6 Then GoTo 235

If Q = 7 Then GoTo 265

If Q = 8 Then GoTo 295

If Q = 9 Then GoTo 325

If Q = 10 Then GoTo 355

If Q = 11 Then GoTo 385

If Q = 12 Then GoTo 415

If Q = 13 Then GoTo 445

If Q = 14 Then GoTo 475

If Q = 15 Then GoTo 505

If Q = 16 Then GoTo 535

If Q = 17 Then GoTo 565

If Q = 18 Then GoTo 595

If Q = 19 Then GoTo 625

If Q = 20 Then GoTo 655

If Q = 21 Then GoTo 685

If Q = 22 Then GoTo 715

If Q = 23 Then GoTo 755

If PP = 7 Then GoTo 2100

PP = PP + 1

If Q = 24 Then GoTo 795

2100 'Add headers to the worksheet on row 1

Set oSheet1 = oBook.Worksheets(1)

Set oSheet2 = oBook.Worksheets(2)

'oSheet.Range("A3").Resize(1, NN + 1).Value = MF

oSheet1.Range("A2").Resize(NP + 1, 2).Value = STRGTH

'oSheet.Range("A1").Resize(NP + 1, 2).Value = YYY

oSheet1.Range("C2:F2").Resize(NP + 1, 5).Value = MIX

' oSheet.Range("C2").Resize(NP + 1, 2).Value = CM

' oSheet.Range("D2").Resize(NP + 1, 2).Value = LT

' oSheet.Range("E2").Resize(NP + 1, 2).Value = GT

oSheet1.Range("B1:G1").Value = Array("STRENGHT", " ", "WATER", "CEMENT", "SAND", "GRANITE")

' If CT = 0 Then oSheet.Range("J2").Resize(2).Value = "**** SORRY THE COMPRESSIVE STRENGTH IS OUTSIDE THE FACTOR SPACE ****"

oSheet1.Range("J3").Resize(2).Value = "MAXIMUM CUBE STRENGTH OF CONCRETE PREDICTABLE BY THIS MODEL IS"

oSheet1.Range("J4").Resize(2).Value = Format(OPSTRENGTH, "0.##")

oSheet1.Range("J5").Resize(2).Value = "THE CORRESPONDING MIXTURE RATIO IS AS FOLLOWS:"

oSheet1.Range("I7:L7").Resize(1, 5).Value = ZZ

oSheet1.Range("J6:M6").Value = Array("WATER", "CEMENT", "SAND", "GRANITE")

'oSheet.Range("B2:I2").Value = Array("MF1", "MF2", "MF3", "MF4", "MF5", "MF6", "MF7", "MF8")

'Save the Workbook and Quit Excel

oBook.SaveAs "C:\Book1.xls"

oExcel.Quit

' QQQQ = InputBox("PRESS OK TO CONTINUE", , , 5500, 6000)

' Print: Print

' If CT = 0 Then Print " **** SORRY THE STRENGTH IS OUTSIDE THE FACTOR SPACE ****"

' Print: Print

' Print " MAXIMUM CUBE STRENGTH OF CONCRETE PREDICTABLE BY THIS MODEL IS "

' Print " N"; Format(OPSTRENGTH, "0.00"); Print

"Print Format(YOP, "0.00#"); Print

' Print " THE CORRESPONDING MIXTURE RATIO IS AS FOLLOWS:"

' Print " WATER ="; Format(ZZ(1), "0.00#"); " CEMENT ="; Format(ZZ(2), "0.00#");

' Print " SAND ="; Format(ZZ(3), "0.00#"); " GRANITE ="; Format(ZZ(4), "0.00#")

GoTo 22222

900

Cls

Y = 0

For I = 1 To 5: X(I) = 0: Next I

Rem **** RESPONSE AT THE CHOSEN 10 POINTS ON THE FACTOR SPACE FOR THE MODEL ****

GoTo 3010

3010 Rem **** CONVERSION MATRIX ****

B(1, 1) = 10000: B(1, 2) = -7500: B(1, 3) = 1000: B(1, 4) = -1.58595E-13

B(2, 1) = 1440: B(2, 2) = -1081.285714: B(2, 3) = 142.8571429: B(2, 4) = 0.857142857

B(3, 1) = -4300: B(3, 2) = 3224.857143: B(3, 3) = -428.5714286: B(3, 4) = -0.571428571

B(4, 1) = -7140: B(4, 2) = 5357.428571: B(4, 3) = -714.2857143: B(4, 4) = -0.285714286

Rem **** ACTUAL MIXTURE COMPONENTS ****

Z(1) = InputBox("ENTER THE VALUE OF WATER")

Z(2) = InputBox("ENTER THE VALUE OF CEMENT")

Z(3) = InputBox("ENTER THE VALUE OF SAND")

Z(4) = InputBox("ENTER THE VALUE OF GRANITE")

Rem **** PSEUDO MIXTURE COMPONENTS ****

For I = 1 To 4

For J = 1 To 4

X(I) = X(I) + B(I, J) * Z(J)

Next J

Next I

Rem *** CALCULATING THE STRENGTH (RESPONSE) ****

YM = 26.22 * X(1) + 30.22 * X(2) + 24 * X(3) + 27.55 * X(4) + 2.68 * X(1) * X(2) - 2.68 * X(1) * X(3) - 20.46 * X(1) * X(4) + 16 * X(2) * X(3) - 25.78 * X(2) * X(4) + 0.9 * X(3) * X(4)

'Add headers to the worksheet on row 1

Set oSheet1 = oBook.Worksheets(1)

Set oSheet2 = oBook.Worksheets(2)

MIXX(1, 1) = Format(Z(1), "0.00#")

MIXX(1, 2) = Format(Z(2), "0.00#")

MIXX(1, 3) = Format(Z(3), "0.00#")

MIXX(1, 4) = Format(Z(4), "0.00#")

oSheet1.Range("B2").Value = YM

oSheet1.Range("C1:F1").Resize(2, 5).Value = MIXX

oSheet1.Range("B1:G1").Value = Array("STRENGTH", " ", "WATER", "CEMENT", "SAND", "GRANITE")

oBook.SaveAs "D:\Book1.xls"

oExcel.Quit

```
' Print " STRENGTH = "; Format(Y, "0.0#");
' Print " WATER "; Format(Z(1), "0.0#");
' Print " CEMENT "; Format(Z(2), "0.0#");
' Print " SAND "; Format(Z(3), "0.0#");
' Print " GRANITE "; Format(Z(4), "0.0#")
```

22222

End Sub

APPENDIX 3

Private Sub STARTMNU_Click()

Dim oExcel As Object

Dim oBook As Object

Dim oSheet1 As Object

Dim oSheet2 As Object

'Start a new workbook in Excel

Set oExcel = CreateObject("Excel.Application")

Set oBook = oExcel.Workbooks.Add

Set oSheet1 = oBook.Worksheets(1)

Cls

Print " THE PROGRAM WAS WRITTEN BY"

Print: Print

Print " DR. DAVIS ONWUKA "

Print:

WWW = InputBox("CLICK OK. TO CONTINUE"): Cls

' CIVIL ENGINEERING DEPARTMENT, FUTO

' IT IS STRENGTH OPTIMIZATION PROGRAM BASED ON OSADEBE'S MODEL

ReDim MIX(300, 4), STRGTH(300, 1), MIXX(1, 4)

Dim NP As Variant

CT = 0: YMAX = 0: KK = 0

ReDim X(10), A(5, 5), Z(5), N(15), B(5, 5)

Rem *** COEFFICIENTS OF REGRESSION ***

A1 = -394790933.1: A2 = -220057975.6: A3 = -4093499.945: A4 = -1283.021096: A5 = 1204352313

A6 = 318501118.4: A7 = 395949693.6: A8 = 284162641.2: A9 = 219194875.1: A10 = 4214942.072

Rem *** DECISION FOR CALCULATING MIX RATIOS GIVEN DESIRED STRENGTH OR OTHER WISE

```
10 QQ = InputBox("WHAT DO YOU WANT TO DO? TO CALCULATE MIX RATIOS GIVEN DESIRED
STRENGTH OR CALCULATING STRENGTH GIVEN MIX RATIO?", " IF THE STRENGTH IS KNOWN TYPE 1
ELSE TYPE 0", "Type 1 or 0 and CLICK OK.")
```

```
    If QQ <> 1 And QQ <> 0 Then EE = InputBox("No Way! You must ENTER 1 or 0", , "CLICK OK and do so"):
GoTo 10
```

```
    If QQ = 0 Then GoTo 100
```

```
    Rem PUT IN THE VALUE OF STRENGTH DESIRED HERE
```

```
    YY = InputBox("WHAT IS THE DESIRED STRENGTH?"): YY = 1 * YY
```

```
    Rem *** Here is where the Actual Strength is calculated ***
```

```
    For Z1 = 0.04 To 0.09 Step 0.0001
```

```
    For Z2 = 0.08 To 0.16 Step 0.0001
```

```
    For Z3 = 0.2 To 0.31 Step 0.001
```

```
    Z4 = 1 - Z1 - Z2 - Z3
```

```
    Rem *** The Binary Predictors will be calculated here ***
```

```
    Z5 = Z1 * Z2: Z6 = Z1 * Z3: Z7 = Z1 * Z4
```

```
    Z8 = Z2 * Z3: Z9 = Z2 * Z4: Z10 = Z3 * Z4
```

```
    Rem CALCULATING ACTUAL STRENGTH
```

```
    YACT = A1 * Z1 + A2 * Z2 + A3 * Z3 + A4 * Z4 + A5 * Z5 + A6 * Z6
```

```
    YACT = YACT + A7 * Z7 + A8 * Z8 + A9 * Z9 + A10 * Z10
```

```
    If Z1 / Z2 >= 0.7 Then GoTo 30
```

```
    If Z1 + Z2 + Z3 + Z4 > 1 Or Z1 + Z2 + Z3 + Z4 < 1 Then GoTo 30
```

```
    If YACT > YY - 0.01 And YACT < YY + 0.01 Then NP = NP + 1: GoTo 20
```

```
    GoTo 30
```

```
20 ' If KK = 23 Then KK = 0: VV = InputBox("CLICK O.K. TO CLEAR SCREEN AND continue", "PRINT
COUNTER", , 1500, 5200): Cls
```

```
    KK = KK + 1
```

```
    STRGTH(NP, 1) = Format(YACT, "0.00#")
```

```
    MIX(NP, 1) = Format(Z1 / Z2, "0.00#")
```

```
    MIX(NP, 2) = Format(Z2 / Z2, "0.00#")
```

```
    MIX(NP, 3) = Format(Z3 / Z2, "0.00#")
```

```
    MIX(NP, 4) = Format(Z4 / Z2, "0.00#")
```

```
30
```

```
    Next Z3
```

```
    Next Z2
```

```
    Next Z1
```

```
'Add headers to the worksheet on row 1
```

```
    Set oSheet1 = oBook.Worksheets(1)
```

```
oSheet1.Range("A2").Resize(NP + 1, 2).Value = STRGTH
```

```
oSheet1.Range("C2:F2").Resize(NP + 1, 5).Value = MIX
```

```
oSheet1.Range("B1:G1").Value = Array("STRENGTH", " ", "WATER", "CEMENT", "SAND", "GRANITE")
```

```
'Save the Workbook and Quit Excel
```

```
oBook.SaveAs "C:\Book1.xls"
```

```
oExcel.Quit
```

```
70 'Print "Sorry! Desired strength is outside the range of the model"
```

```
111 GoTo 222
```

```
100 Rem *** Here is where the INPUT of the Principal Predictors will be made ***
```

```
    Cls
```

```
    Z1 = InputBox("What is Water/Cement ratio"): Z1 = Z1 * 1
```

```
    Z2 = InputBox("What is Cement value"): Z2 = Z2 * 1
```

```
    Z3 = InputBox("What is Sand value"): Z3 = Z3 * 1
```

```
    Z4 = InputBox("What is Periwinkle value"): Z4 = Z4 * 1
```

```
    TZT = Z1 + Z2 + Z3 + Z4 + Z5
```

```
    Z1 = Z1 / TZT: Z2 = Z2 / TZT: Z3 = Z3 / TZT
```

```
    Z4 = Z4 / TZT
```

```
    Rem *** The Binary Predictors will be calculated here ***
```

```
    Z5 = Z1 * Z2: Z6 = Z1 * Z3: Z7 = Z1 * Z4
```

```
    Z8 = Z2 * Z3: Z9 = Z2 * Z4: Z10 = Z3 * Z4
```

```
    Rem CALCULATING ACTUAL STRENGTH
```

```
    YACT = A1 * Z1 + A2 * Z2 + A3 * Z3 + A4 * Z4 + A5 * Z5 + A6 * Z6
```

```
    YACT = YACT + A7 * Z7 + A8 * Z8 + A9 * Z9 + A10 * Z10
```

```
'Add headers to the worksheet on row 1
```

```
Set oSheet1 = oBook.Worksheets(1)
```

```
Set oSheet2 = oBook.Worksheets(2)
MIXX(1, 1) = Format(Z1 / Z2, "0.00#")
MIXX(1, 2) = Format(Z2 / Z2, "0.00#")
MIXX(1, 3) = Format(Z3 / Z2, "0.00#")
MIXX(1, 4) = Format(Z4 / Z2, "0.00#")
oSheet1.Range("B2").Value = YACT
oSheet1.Range("C1:F1").Resize(2, 5).Value = MIXX
oSheet1.Range("B1:G1").Value = Array("STRENGTH", " ", "WATER", "CEMENT", "SAND", "GRANITE")
oBook.SaveAs "C:\Book1.xls"
oExcel.Quit
```

222

End Sub

Private Sub STOPMNU_Click()

End

End Sub

Determination through Use of ATND Method of Impact Strength of 359.0 Alloy Modified With Strontium

Jacek Pezda

Institute of Chipless Technology, ATH Bielsko-Biała, Willowa 2, 43-309 Bielsko – Biała, Poland

Abstract

The paper presents a method for determination of impact strength of the 359.0 alloy modified with strontium, based on the ATND method and regression analysis performed as early as at the stage of its preparation (melting). Method of Thermal-Voltage-Derivative Analysis (ATND in short) allows registration of voltage and temperature curves, on which one can observe a thermal and voltage effects being results of crystallization of phases and eutectic mixtures, present on the curves in form of characteristic “peaks”. Values of the temperatures and voltages, which can be read out for the characteristic points, constitute the basis for the regression analysis to obtain mathematical relationships presenting effect of changes of their values on change of impact strength of the 359.0 (AlSi9Mg) alloy. It has enabled determination of impact strength of the 359.0 alloy, using equation estimating characteristic points of the ATND method, in experimental conditions at significance level of $\alpha = 0,05$.

Keywords: silumins, modification, thermal analysis, impact strength, regression analysis.

1. Introduction

Among alloys of non-ferrous metals, aluminum alloys have found the broadest application in foundry industry. Silumins belong to the most common alloys on base of aluminum, i.e. alloys from the Al-Si system [1]. This is connected with a number of advantages – both operational and technological ones – of this group of the alloys. Silumins belong to alloys which are characterized by: low specific gravity, good thermal conductivity, good corrosion resistance, satisfactory strength parameters in normal and increased temperatures, as well as relatively low price and excellent technological properties. The most important aluminum silicon alloys are based on the aluminum-silicon system, especially the hypoeutectic alloys with composition ranging from 7 to 11 wt. % silicon. Quite a significant disadvantage from a technical point of view is their tendency to form coarse structure, which adversely affects mechanical properties of the castings. Modification is the most effective way to enable optimal structure of the castings, providing improvements in their functional properties. Quality of the modification is dependent on correct dosage of inoculant, metal temperature and time elapsing from the modification to solidification of the alloy [1-3]. Registration of crystallization processes of the alloy at stage of its preparation is directly related to implementation of theory of crystallization in control of technological processes, enabling obtainment of a suitable structure of the material, which determine its application for to a given requirements [2,4,5]. Methods employed to registration of crystallization of the alloys based on analysis of temperature change (thermal ones - ATD, DTA), electrical conductivity change (electric ones - AED) and method of thermal-voltage-derivative analysis (ATND method) enable registration of a phenomena arisen in result of solidification of the alloys [6-8]. Among materials testing, impact strength tests are the most sensitive methods to determination of strength effects connected with proper application of modification treatments of hyper- and hypo-eutectic silumins [9]. Growth of the impact strength of alloys is directly connected with change of shape of crystals of eutectic silicone resulted from the modification.

2. Methodology of the research

The ATND method consists in permanent measurement of temperature and electric voltage generated on probes during the crystallization, as well as phase transformations of solidified alloy. During the measurement are recorded generated voltage and temperature of investigated test pieces. Run of the crystallization is presented in form of a diagram generated during solidification of the alloy [6,8]. The 359.0 (AlSi9Mg) alloy is rated among hypo-eutectic silumins. It features very good cast properties and is designed for castings with complicated shapes and high strength. Investigated alloy was melted in crucible resistance furnace and refined with Rafal 1 preparation in quantity of 0,4% mass of charge. After completion of the refinement one removed oxides and slag from the metal-level, and performed treatment of modification of the alloy with strontium, using AlSr10 master alloy in quantity 0,6% mass of charge (0,06% Sr). Investigated alloy was poured into metallic mould, which was adapted to control of crystallization course with use of the ATND method.

In the Fig. 1 is presented a diagram showing course of the crystallization of refined and modified alloy, recorded during the testing, with marked characteristic points.

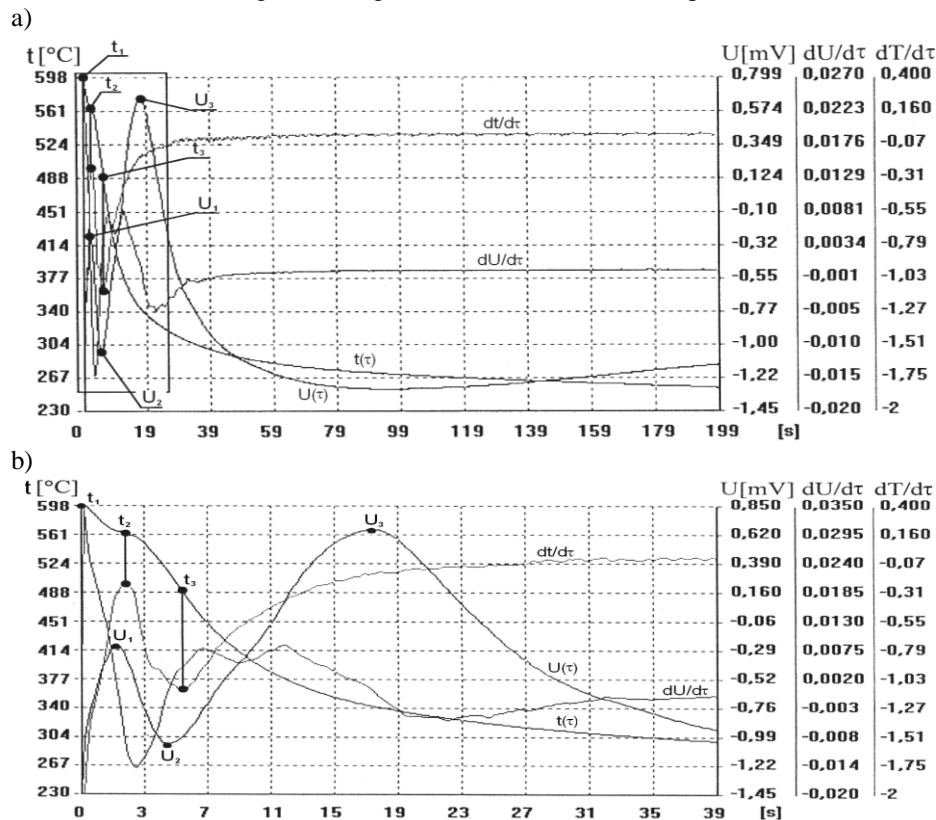


Figure 1. Crystallization curves and characteristic points of refined and modified 359.0 alloy from the ATND analysis: a) full range of crystallization process, b) extension marked area

Marked characteristic points (Fig. 1) for the ATND method are:

- a) points on thermal curve $t_1 \div t_3$,
- b) points on voltage curve $U_1 \div U_3$.

The next stage of the testing consisted in tests of impact strength of the investigated silumin. The impact test was performed with use of Charpy pendulum machine on notched-bar test pieces. After performed impact test one carried out regression analysis with use of the "Statistica" computer software developed by StatSoft, and determined correlation between change of characteristic points of the ATND method and impact strength of the investigated alloy.

3. Description of Obtained Results

Obtained values of the impact strength were contained within range from 3,4 to 14,4 J/cm². Average value of the impact strength after treatment of the refinement amounted to 4,3 J/cm², while after refinement and modification amounted to 12,9 J/cm². After input of the independent variables (temperature and voltage) and dependent variable (impact strength) one obtained the relation (1) describing effect of the input data on the impact strength of refined alloy, as well as relation (2) presenting effect of the input data on the impact strength of refined and modified alloy.

$$KCV = 4,26 - 0,01t_1 + 0,01t_3 + 0,34U_1 - 0,69U_3 \pm 0,31 \text{ [J/cm}^2\text{]} \quad (1)$$

$$R = 0,74; R^2 = 0,64$$

The relation (1) contains a free term and 4 variables which satisfy condition of significance. Remaining independent variables were neglected due to not fulfilled condition of significance.

$$KCV = -8,49 + 0,04t_3 + 3,42U_1 - 2,7U_2 \pm 0,43 \text{ [J/cm}^2\text{]} \quad (2)$$

$$R = 0,78; R^2 = 0,61$$

The relation (2) contains a free term and 3 variables satisfying condition of significance. Remaining independent variables were neglected as not fulfilling condition of significance.

In the Fig. 2 are presented exemplary values of the impact strength, observed and anticipated on base of the relation (1) and relation (2).

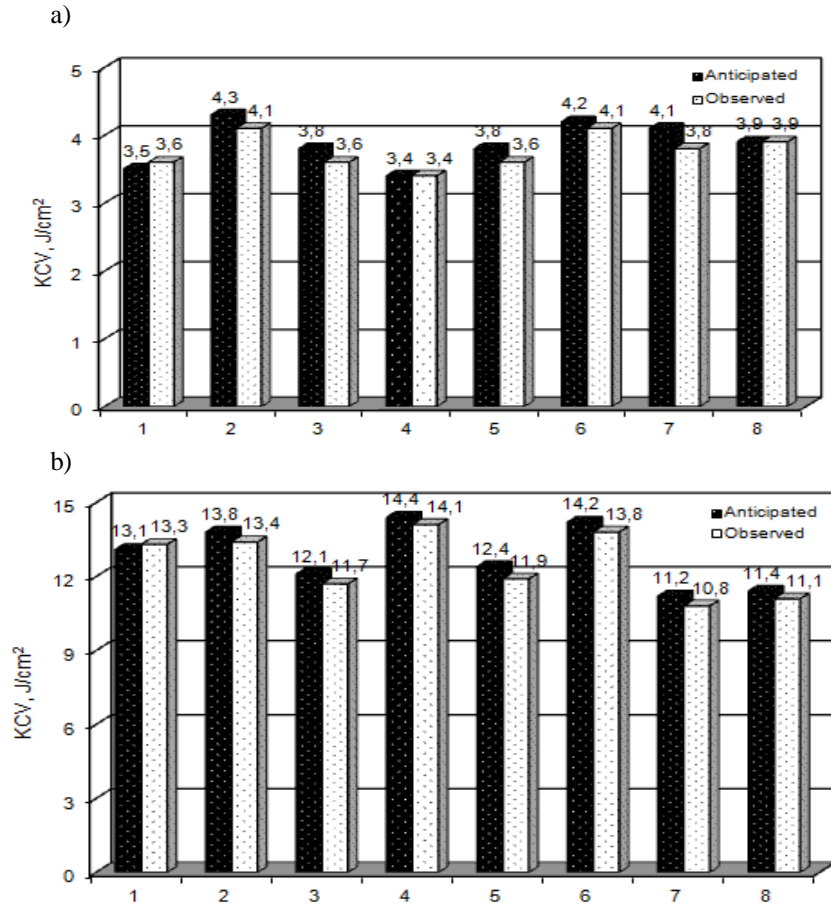


Figure 2. Exemplary values of the impact strength, observed and anticipated on base of the: a) relation (1) and b) relation (2)

Change of course of the crystallization of investigated alloy, connected with performed treatment of refinement and modification, is presented in the Fig. 3.

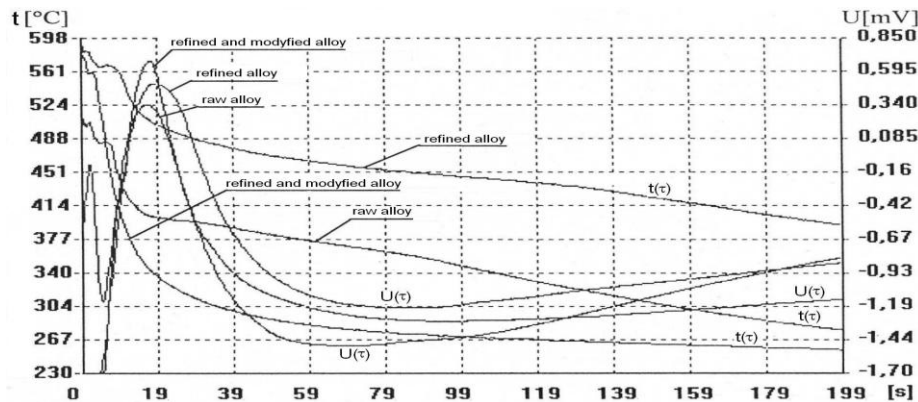


Figure 3. Representative curves from the ATND method for the 359.0 alloy

4. Conclusions

Performed tests enabled description of the KCV impact strength of refined and modified 359.0 (AlSi9Mg) alloy with equations (1) and (2), basing on characteristic points of the ATND method in experimental conditions, what enabled prompt assessment of quality of the alloy in aspect of change of its impact strength and extent of the modification (Fig. 3) as early as in stage of its preparation.

References

- [1] P. Wasilewski. Silumins – modification and its impact on structure and properties. Solidification of metals and alloys, Katowice, 1993.
- [2] S.Z Lu, A. Hellawel. Modyfication of Al-Si alloys: microstructure, thermal analysis and mechanics. IOM vol. 47, No 2, 1995.
- [3] M.M. Haque. Effects of strontium on the structure and properties of aluminium-silicon alloys. Journal of Materials Processing Technology 55: 193-198, 1995.
- [4] S.-Z. Lu, A. Hellawell. The Mechanism of Silicon Modification in Aluminum- Silicon Alloys Impurity Induced Twinning. Metalurgical Transactions A, vol. 18A: 1721-1733, 1987.
- [5] H. Fredriksson, U. Akerlid. Solidification and Crystallization Processing in Metals and Alloys, Willey 2012.
- [6] P. Wasilewski. Comparison methods research of solidification and crystallization alloys of metals. Archives of Foundry, vol. 3 Iss. 10: 323-337, 2003.
- [7] J. Pezda, M. Dudyk, T. Ciućka, P. Wasilewski. Polynomial models for mechanical properties of aluminum alloys. Solidification of Metals and Alloys. vol. 38: 131-136, 1998.
- [8] J. Pezda. Tensile strength of the AG10 alloys determination on the ATND method. Archives of Foundry, Vol. 6 Iss.18: 197-202, 2006.
- [9] Z. Poniewierski. Crystallization. structure and properties of silumins. WNT Warszawa, 1989.

BSMR: Byzantine-Resilient Secure Multicast Routing In Multi-Hop Wireless Networks

¹Vijay Bahadur Singh, ²Ashok Prasad, Mukesh Chauhan

^{1,2}Department Of Information Technology, Institute Of Technology And Management , AL-1 Sector-7 Gida , Gorakhpur

Abstract

Multi-hop wireless networks rely on node cooperation to provide unicast and multicast services. The multi-hop communication offers increased coverage for such services, but also makes them more vulnerable to insider (or Byzantine) attacks coming from compromised nodes that behave arbitrarily to disrupt the network. In this work we identify vulnerabilities of on-demand multicast routing protocols for multi-hop wireless networks and discuss the challenges encountered in designing mechanisms to defend against them. We propose BSMR, a novel secure multicast routing protocol that withstands insider attacks from colluding adversaries. Our protocol is a software-based solution and does not require additional or specialized hardware. We present simulation results which demonstrate that BSMR effectively mitigates the identified attacks.

Keywords –multi-hop destination, multicast routing, Byzantine resilient protocols. Byzantine attacks, Byzantine resiliency, Multi-hop wireless networks.

1. Introduction

Multicast routing protocols deliver data from a source to multiple destinations organized in a multicast group. Several protocols were proposed to provide multicast services for multi-hop wireless networks. These protocols rely on node cooperation and use flooding [1], gossip [2], geographical position [3], or dissemination structures such as meshes [4], [5], or trees [6], [7]. A major challenge in designing protocols for wireless networks is ensuring robustness to failures and resilience to attacks. Wireless networks provide a less robust communication than wired networks due to frequent broken links and a higher error rate. Security is also more challenging in multi-hop wireless networks because the open medium is more susceptible to outside attacks and the multi-hop communication makes services more vulnerable to insider attacks coming from compromised nodes. Although an effective mechanism against outside attacks, authentication is not sufficient to protect against insider attacks because an adversary that compromised a node also gained access to the cryptographic keys stored on it. Insider attacks are also known as Byzantine [8] attacks and protocols able to provide service in their presence are referred to as Byzantine resilient protocols.

1.1 Statement of the Problem

Previous work focused mainly on the security of unicast services. Several routing protocols [9]-[12] were proposed to cope with outsider attacks. Methods proposed to address insider threats in unicast routing include monitoring [13], multi-path routing [14] and acknowledgment-based feedback [15], [16]. The problem of secure multicast in wireless networks was less studied and only outside attacks were addressed - [17].

1.2 Significance of the Study

In this paper we study vulnerabilities of multicast routing protocols in multi-hop wireless networks and propose a new protocol that provides resilience against Byzantine attacks. We identify several aspects that make the design of attack-resilient multicast routing protocols more Challenging than their unicast counterpart, such as a more complex trust model and underlying routing Structure. and scalability. We also discuss potential attacks against such protocols.

2. Related Work

Several routing techniques like SEAD, Ariadne and MAODV protocol .Were studied and we analyzed the drawback of every routing protocol against byzantine attacks and maintaining tree structure. In AAS we analyzed the authentication of sending data with acknowledgment but in multicast protocol sending such acknowledgment cannot be done for multi-hop wireless networks. So we used MACT to send acknowledgment from receiver to sender. We implemented an on-demand multicast protocol which threats against Byzantine attacks and maintains tree structures effectively.

3. Network and System Model

3.1 Network Model

We consider multi-hop wireless network where nodes participate in the data forwarding process for other nodes. We assume that the wireless channel is symmetric. All nodes have the same transmitting power and consequently the same transmission range. The receiving range of a node is identical to its transmission range.

3.2 Multicast Routing Protocol

This protocol is to protect from external attacks against the creation and maintenance of the multicast tree and prevents unauthorized nodes to be part of the network, of a multicast group, or of a multicast tree. It allows a node that wants to join a multicast group to find a route to the multicast tree. To prevent outsiders from interfering, all route discovery messages are authenticated. Only group authenticated nodes can initiate route request. We assume a tree-based on-demand multicast protocol such as [6]. The protocol maintains bi-directional shared multicast trees connecting multicast sources and receivers. Each multicast group has a corresponding multicast tree. The multicast source is a special node, the group leader, whose role is to eliminate stale routes and coordinate group merges. Route freshness is indicated by a group sequence number updated by the group leader and broadcast periodically in the entire network. Higher group sequence numbers denote fresher routes. The main operations of the protocol are route discovery, route activation and tree maintenance. During route discovery a node discovers a path to a node that is part of the multicast tree. A requester first broadcasts a route request message that includes the latest known group sequence number. The route request message is flooded in the network using a basic flood suppression mechanism and establishes reverse routes to the source of the request. Upon receiving the route request, a node that is part of the multicast tree and has a group sequence number at least as large as the one in the route request, generates a route reply message and unicasts it on the reverse route. The route reply message includes the last known group sequence number and the number of hops to the node that originated the route reply. During route activation, the requester selects the freshest and shortest route (i.e., with the smallest number of hops to the multicast tree) from the routes returned by the route discovery operation. The requester activates that route by unicasting a multicast activation message. Three main operations ensure the tree maintenance: tree pruning, broken link repair and tree merging. Tree pruning occurs when a group member that is a leaf in the multicast tree decides to leave the group. To prune itself from the tree, the node sends a message to indicate this to its parent. The pruning message travels up the tree causing leaf nodes that are not members of the multicast group to prune themselves from the tree, until it reaches either a non-leaf node or a group member. A non-leaf group member must continue to act as a router and cannot prune itself from the multicast tree.

4. Attacks Against Multicast Routing

4.1 Adversarial Model

We consider a three-level trust model that captures the interactions between nodes in a wireless multicast setting and defines a node's privileges: the first level consists of the source, which must be continually available and assumed not to be compromised (an unavailable or untrusted source makes the multicast service useless); the second level consists of the multicast group member nodes, which are allowed to initiate requests for joining multicast groups; and the third level consists of nonmember nodes, which participate in the routing but cannot initiate group join requests. In order to cope with Byzantine attacks, even group members are not fully trusted.

4.2 Attacks in Multicast Routing and in Multihop Wireless Networks

Nodes can maliciously report that other links are broken or generate incorrect pruning messages, resulting in correct nodes being disconnected from the network or tree partitioning. In the absence of authentication, any node can pretend to be the group leader. Although many routing protocols do not describe how to select a new group leader when needed, we note that the leader election protocol can also be influenced by attackers. Attacks against data messages consist of leaves dropping, modifying, replaying, injecting data, or selectively forwarding data after being selected on a route. A special form of packet delivery disruption is a denial-of-service attack, in which the attacker overwhelms the computational, sending, or receiving capabilities of a node. In general, data source authentication, integrity, and encryption can solve the first attacks and are usually considered application specific security. Defending against selective data forwarding and denial of service cannot be done exclusively by using cryptographic mechanisms. Because external attacks can be prevented using the authentication framework described in Section 5.2, we focus on the following Byzantine attacks:

- 1. Black hole attack:** One or several adversaries forward only routing control packets, while dropping all data packets. Adversaries are placed strategically around the multicast source, equidistant on a circle with radius of 200 meters.
- 2. Wormhole attack:** Two colluding adversaries tunnel packets between each other in order to create a shortcut in the network. The adversaries use the low cost appearance of the wormhole to increase the probability of being selected on paths; once selected on a path, they attempt to disrupt data delivery by executing a black hole attack.

3. **Flood rushing attack:** One or several adversaries rush an authenticated flood through the network before the flood traveling through a legitimate route. This allows the adversaries to control many paths. Flood rushing can be used to increase the effectiveness of a black hole or wormhole attack.
4. **Selfish Nodes:** One or several adversaries want to preserve its own resources while using the services of others and consuming their resources, such misbehaving nodes participate in the route discovery and maintenance phase but refuse to forward data packets, which degrades routing performance.

5. Secure Multicast Routing Protocol

5.1 SORB Overview

Our protocol ensures that multicast data is delivered from the source to the members of the multicast group, even in the presence of Byzantine attackers, as long as the group members are reachable through non-adversarial path. Here an authentication framework is used to eliminate outside adversaries and ensure that only authorized nodes perform certain operations (only tree nodes can perform tree operations and only group nodes can connect to the corresponding multicast tree). SORB mitigates inside attacks that try to prevent a node from establishing a route to the multicast tree by flooding both route request and route reply. Tree nodes monitor the rate of receiving data packets and compare it with the transmission rate indicated by the source in the form of an MRATE message.

5.2 Node Authentication

The authentication framework prevents unauthorized nodes to be part of a multicast tree or of a multicast group. Each node authorized to join the network has a pair of public/private keys and node certificate that binds its public key to its IP address. Each node authorized to join multicast group has an additional group certificate that binds its public key and IP address to the IP address of the multicast group. Nodes in the multicast tree are authenticated using a tree token, which is periodically refreshed and disseminated by the group leader in the multicast tree with the help of pairwise shared keys established between every direct tree neighbors. Only nodes that are currently on the tree will have a valid tree token. To allow any node in the network to check that a tree node possesses a valid tree token, the group leader periodically broadcasts in the entire network a tree token authenticator. Hop count authentication is to prevent tree nodes from claiming to be at a smaller hop distance from the group leader than they actually are, we use a technique based on a hash chain. The hop count anchor is also included by the group leader in Group Hello messages, which are broadcast periodically in the entire network. This allows a tree node to prove its hop distance from the group leader to any node in the network.

5.3 Route Discovery:

SORB's route discovery allows a node that wants to join a multicast group to find a route to the multicast tree. To prevent outsiders from interfering, all route discovery messages are authenticated using the public key corresponding to the network certificate. Only group authenticated nodes can initiate route requests and the group certificate is required in each request. Tree nodes use the tree token to prove their current tree status. The requesting node broadcasts a route request (RREQ) message that includes the node identifier and its weight list, the multicast group identifier. The RREQ message is flooded in the network until it reaches a tree node. Only new requests are processed by intermediate nodes. When a tree node receives a RREQ from a requester, it initiates a response. The node broadcasts a route reply (RREP) message that includes that node identifier, the requester's identifier and weight list from the request message. The RREP message is flooded in the network until it reaches the requester.

5.4 Multicast Route Activation

The requester signs and unicasts on the selected route an multicast activation message that include its identifier, the group identifier, and the sequence number used in the RREQ phase. The MACT message also includes a one way function applied to on the tree token extracted from RREP, $f(\text{requestor}, \text{tree token})$, which will be checked by the tree node that sent the RREP message to verify that the nodes activated the route is the same as the initial requestor. An intermediate node on the route checks if the signature on MACT is valid and if MACT contains the same sequence number as the one in the original RREQ. The node then adds to its list of tree neighbors the previous node and the next node on the route as downstream and upstream neighbors, respectively, and sends MACT along the forward route. During the propagation of the MACT message, tree neighbors use their public keys to establish pairwise shared keys, which will be used to securely exchange messages between tree neighbors. The requester and the nodes that received MACT could be prevented from being grafted to the tree by an adversarial node, selected on the forward route, which drops the MACT message. To mitigate the attack, these nodes will start a WTC-Timer upon whose expiration nodes isolate a faulty link and initiate route discovery. The timer will expire after a value proportional to a node's hop distance to the tree, in the hope that the nodes closer to the tree will succeed in avoiding the adversarial node and will manage to connect to the tree. After a node becomes aware of its expected receiving data rate, it cancels its WTC-Timer.

5.5 Multicast Tree Maintenance

Routing messages exchanged by tree neighbors, such as pruning messages are authenticated using the pair wise keys shared between tree neighbors. Tree pruning occurs when a group member that is a leaf in the multicast tree decides to leave the group. A node initiates pruning from the tree by sending a message to its parent. The group leader periodically broadcasts in the entire network a signed Group Hello message that contains the current group sequence number, the tree token authenticator, and the hop count anchor (described in Section 5.2). A signed Group Hello message containing a special flag also ensures that when two disconnected trees are merging, one of the group leaders is suppressed.

5.6 Selective Data Forwarding Detection

The source periodically signs and sends in the tree an MRATE message that contains its data transmission rate. As this message propagates in the multicast tree, nodes may add their perceived transmission rate to it. Each tree node keeps a copy of the last heard MRATE packet. The information in the MRATE message allows nodes to detect if tree ancestors perform selective data forwarding attacks. Depending on whether their perceived rate is within acceptable limits of the rate in the MRATE message, nodes alternate between two states. The initial state of a node is disconnected; after it joins the multicast group and becomes aware of its expected receiving data rate, the node switches to the connected state. Upon detecting a selective data forwarding attack, the node switches back to the disconnected state. MRATE is the difference between two distances. The source periodically signs and sends in the tree a multi-cast rate (MRATE) message that contains its data transmission rate. Nodes may add their perceived transmission rate to it. The information in the MRATE message allows nodes to detect if tree ancestors perform selective data forwarding attacks. Depending on whether their perceived rate is within acceptable limits of the rate in the MRATE message, thenode forward the request to next node until it reaches the destination.

5.7 Communication Between Multicast Groups

We can communicate between different Multicast Groups and can form a Grid. To join different Multicast Groups with each other for communication, the Multicast Group Source (Group Leader) which needs to join will send a route request RREQ with a WTC-Timer to the desired Multicast Group Source. Then, the connection has been made with the Group Certificate of both Multicast Groups. Likewise, any Multicast Group can join to the Grid. If a Multicast Group source needs to leave the Grid, It should send the request to all the Grid members with which it has the connections. Once the leaving route request has reached the connected Sources, then the leaving Source has been disconnected from the network. The data can be transmitted from one source to the other provided if the sender Source knows the Group Certificate of the member nodes irrespective of whether it may in its own group or in different group. If it is in its own group, it'll follow as a Multicast Routing Protocol and sends the Data. If it is in different Group, It should communicate with all the Sources to check whether it has the destination node as using Group Certificate, Node Certificate and Tree Token function. Once if it is found with the shortest path, It'll reply to the Sender Source as a route reply RREP. If the sender Source gets RREP, it'll send the data by Selective Data Forwarding Detection method through the Group Leader (Source) which has the destination node.

Algorithm for grid based multicast group communication Multicast protocol

```
Multicast protocol
{
// consider first node as group leader
//Create the node from group leader
Authenticate every node with RREQ, grid,
grpseqno, nc, gc and send request
If this.gc & gc is in same group
{
Add node to the existing group;
}
Else
{
Join the group leader of the different group and
make as grid;
}
//sending multicast msgs to the destinations
Find the route discovery();
Choose shortest path;
WTC-Timer starts ();
Find the MRATE value;
```

```
If distance-path>data-rate
Send data to the destination;
If data-send takes time
cancel the data transmission;
choose other shortest path and send the data
Proceed until data has been send;
send MACT-msg to sender from receiver;
//leaving a group
If this.gc and gc and confirm .yes
Cancel the node from the source and make free
from n/w;
// leaving a node
If this.nc and nc, and this.gc and gc, and
confirm-yes then
Delete the node;
Maintain tree structure ();
}
```

6. Implementation

Theoretically implementation has been completed with this idea of routing protocol Which has strong defense against Byzantine attacks and joining different Multicast Groups Group Leaders and making communication between the Group Leader to any member nodes in any Multicast Groups. We completed the implementation of a Multicast protocol over a Multicast group.

7. Conclusion

In this paper we have discussed several aspects that make designing attack-resilient multicast routing protocols for multi-hop wireless networks more challenging when compared to their unicast counterpart. A more complex trust model and underlying structure for the routing protocol make solutions tailored for unicast settings not applicable for multicast protocols. In the absence of defense mechanisms, Byzantine attacks can prevent multicast protocols to achieve their design goals. We have proposed BSMR, a routing protocol which relies on novel general mechanisms to mitigate Byzantine attacks. BSMR identifies and avoids adversarial links based on a reliability metric associated with each link and capturing adversarial behavior. Our experimental results show that BSNLR's strategy is effective against strong insider attacks such as black holes and flood rushing. We believe that this strategy can also be effective against wormhole attacks and defer the experimental validation for future work.

8. Acknowledgements

The first author would like to thank R5zvan Mus5loiou-E. for fruitful "copy-room" discussions in the Early stages of this work. This work is supported by National Science Foundation Cyber Trust Award No. 0545949. The views expressed in this research are not endorsed by the National Science Foundation.

References

- [1] R. Curtmola and C. Nita-Rotaru, "BSMR: Byzantine-Resilient Secure Multicast Routing in Multi-hop Wireless Networks", *IEEE TRANSACTIONS ON MOBILE COMPUTING*, VOL. 8, NO. 4, APRIL 2009.
- [2] R. Chandra, V. Ramasubramanian, and K. Birman, "Anonymous Gossip: Improving Multicast Reliability in Mobile Ad-Hoc Networks," *Proc. 21st Int'l Conf. Distributed Computing Systems (ICDCS '01)*, 2001.
- [3] Y.-B. Ko and N.H. Vaidya, "GeoTORA: A Protocol for Geocasting in Mobile Ad Hoc Networks," *Proc. Eighth Ann. Int'l Conf. Network Protocols (ICNP '00)*, p. 240, 2000.
- [4] E.L. Madruga and J.J. Garcia-Luna-Aceves, "Scalable Multicasting. The Core-Assisted Mesh Protocol," *Mobile Networks and Applications*, vol. 6, no. 2, 2001.
- [5] S.J. Lee, W. Su, and M. Gerla, "On-Demand Multicast Routing Protocol in Multihop Wireless Mobile Networks," *Mobile Networks and Applications*, vol. 7, 2002.
- [6] E. Royer and C. Perkins, "Multicast Ad-Hoc On-Demand Distance Vector (MAODV) Routing", Internet draft, July 2000.
- [7] S. Zhu, S. Setia, S. Xu, and S. Jajodia, "GKMPAN: An Efficient Group Rekeying Scheme for Secure Multicast in Ad-Hoc Networks," *Proc. First Ann. Int'l Conf. Mobile and Ubiquitous Systems (MobiQ'04)*, pp. 42-51, 2004.
- [8] L. Lazos and R. Poovendran, "Power Proximity Based Key Management for Secure Multicast in Ad Hoc Networks," *ACM J. Wireless Networks*, 2005.

Patient Monitoring By Using Wearable Wireless Sensor Networks with Zigbee Module

¹A.Dasthagiraiah,^{M.Tech.,} ²N.Viswanadham, ³Y.P.Venkateswarlu, ⁴B.Balaobulesh
⁵D.Murali Krishna, ⁶K.Venkateswarlu,^{M.Tech.,(Ph.D.),}

¹Asst.Prof, in Mekapati Rajamohanreddy Institute Of Technology&Science,Udayagiri.

⁶Head of the Department of ECE ,MRRITS, Udayagiri,Spsr Nellore(D.t)

^{2,3,4,5}UG (B.Tech)Students in ECE Department, MRRITS,Udayagiri, Spsr Nellore(D.t).

Abstract

Patient monitoring systems are gaining their importance as the fast-growing global elderly population increases demands for caretaking. These systems use wireless technologies to transmit vital signs for medical evaluation. In a multi hop ZigBee network, the existing systems usually use broadcast or multicast schemes to increase the reliability of signals transmission; however, both the schemes lead to significantly higher network traffic and end-to-end transmission delay. Our scheme automatically selects the closest data receiver in an any cast group as a destination to reduce the transmission latency as well as the control overhead. The new protocol also shortens the latency of path recovery by initiating route recovery from the intermediate routers of the original path. On the basis of a reliable transmission scheme, we implement a ZigBee device for fall monitoring, which integrates fall detection, indoor position- ing, and ECG monitoring. When the tri axial accelerometer of the device detects a fall, the current position of the patient is transmit- ted to an emergency center through a ZigBee network. In order to clarify the situation of the fallen patient, 4-s ECG signals are also transmitted. Our transmission scheme ensures the successful transmission of these critical messages. The experimental results show that our scheme is fast and reliable. We also demonstrate that our devices can seamlessly integrate with the next generation tech- nology of wireless wide area network, worldwide interoperability for microwave access, to achieve real-time patient monitoring.

Keywords: MEMs, FLEX, Wireless Sensors.

1. Introduction

Tracking of human motion has attracted significant interest in recent years due to its wide-ranging applications such as rehabilitation, virtual reality, sports science, medical science and surveillance. In recent years, inertial and magnetic tracking have attracted much interest as they are source-free approaches unlike the audio and radar that require an emission source. The development of micro electromechanical system technology and flex sensor technology had also made such sensors lighter, smaller, and cheaper. Consequently, they are good candidates conducted in patient's home or office. This will also reduce the frequency to visit the hospital for patients undergoing physiotherapy. This technology also used in sports technology, in this field we know about the player's behaviour. In this project the MEMS sensors, Temperature, heartbeat and FLEX sensors will be introduced in to medical and sports applications. The wireless feature enables the unrestrained motion of the human body as opposed to a wired monitoring device and makes the system truly portable. This will also allow the system to be deployed in a cluttered home environment. The small form factor and lightweight feature of the sensor nodes also allow easy attachment to the limbs.

2. BLOCK DIAGRAM

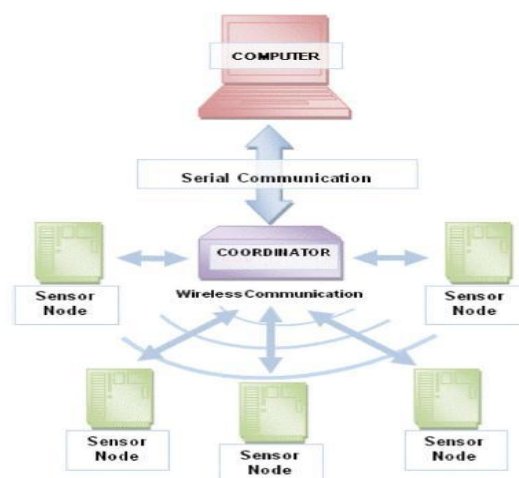


Figure 1.General configuration of the system

3. Serial Communication

Serial communication is basically the transmission or reception of data one bit at a time. Today's computers generally address data in bytes or some multiple thereof. A byte contains 8 bits. A bit is basically either a logical 1 or zero. Every character on this page is actually expressed internally as one byte. The serial port is used to convert each byte to a stream of ones and zeroes as well as to convert a stream of ones and zeroes to bytes. The serial port contains an electronic chip called a Universal Asynchronous Receiver/Transmitter (UART) that actually does the conversion. The serial port has many pins. We will discuss the transmit and receive pins first. Electrically speaking, whenever the serial port sends a logical one (1) a negative voltage is effected on the transmit pin. Whenever the serial port sends a logical zero (0) a positive voltage is affected. When no data is being sent, the serial port's transmit pin's voltage is negative (1) and is said to be in a MARK state. Note that the serial port can also be forced to keep the transmit pin at a positive voltage (0) and is said to be the SPACE or BREAK state. (The terms MARK and SPACE are also used to simply denote a negative voltage (1) or a positive voltage (0) at the transmit pin respectively). When transmitting a byte, the UART (serial port) first sends a START BIT which is a positive voltage (0), followed by the data (general 8 bits, but could be 5, 6, 7, or 8 bits) followed by one or two STOP Bits which is a negative(1) voltage.

The sequence is repeated for each byte sent. When transmitting a character there are other characteristics other than the baud rate that must be known or that must be setup. These characteristics define the entire interpretation of the data stream. The first characteristic is the length of the byte that will be transmitted. This length in general can be anywhere from 5 to 8 bits. The second characteristic is parity. The parity characteristic can be even, odd, mark, space, or none. If even parity, then the last data bit transmitted will be a logical 1 if the data transmitted had an even amount of 0 bits. If odd parity, then the last data bit transmitted will be a logical 1 if the data transmitted had an odd amount of 0 bits. If MARK parity, then the last transmitted data bit will always be a logical 1. If SPACE parity, then the last transmitted data bit will always be a logical 0. If no parity then there is no parity bit transmitted. The third characteristic is the amount of stop bits. This value in general is 1 or 2. Assume we want to send the letter 'A' over the serial port. The binary representation of the letter 'A' is 01000001. Remembering that bits are transmitted from least significant bit (LSB) to most significant bit (MSB), the bit stream transmitted would be as follows for the line characteristics 8 bits, no parity, 1 stop bit and 9600 baud. LSB (0 1 0 0 0 0 0 1) MSB. The above represents (Start Bit) (Data Bits) (Stop Bit). To calculate the actual byte transfer rate simply divide the baud rate by the number of bits that must be transferred for each byte of data. In the case of the above example, each character requires 10 bits to be transmitted for each character. As such, at 9600 baud, up to 960 bytes can be transferred in one second. The above discussion was concerned with the "electrical/logical" characteristics of the data stream. We will expand the discussion to line protocol. Serial communication can be half duplex or full duplex. Full duplex communication means that a device can receive and transmit data at the same time. Half duplex means that the device cannot send and receive at the same time. It can do them both, but not at the same time. Half duplex communication is all but out-dated except for a very small focused set of applications. Half duplex serial communication needs at a minimum two wires, signal ground and the data line. Full duplex serial communication needs at a minimum three wires, signal ground, transmit data line, and receive data line. These signals are the Carrier Detect Signal (CD), asserted by modems to signal a successful connection to another modem, Ring Indicator (RI), asserted by modems to signal the phone ringing, Data Set Ready (DSR), asserted by modems to show their presence, Clear To Send (CTS), asserted by modems if they can receive data, Data Terminal Ready (DTR), asserted by terminals to show their presence, Request To Send (RTS), asserted by terminals if they can receive data. The section RS232 Cabling describes these signals and how they are connected. The above paragraph alluded to hardware flow control. Hardware flow control is a method that two connected devices use to tell each other electronically when to send or when not to send data. A modem in general drops (logical 0) its CTS line when it can no longer receive characters. Note that hardware flow control requires the use of additional wires. The benefit to this however is crisp and reliable flow control. Another method of flow control used is known as software flow control. This method requires a simple 3 wire serial communication link, transmit data, receive data, and signal ground. If using this method, when a device can no longer receive, it will transmit a character that the two devices agreed on. This character is known as the XOFF character. This character is generally a hexadecimal 13. When a device can receive again it transmits an XON character that both devices agreed to. This character is generally a hexadecimal 11.

4. Flex Sensor

The Flex Sensor patented technology is based on resistive carbon elements. As a variable printed resistor, the Flex Sensor achieves great form-factor on a thin flexible substrate. When the substrate is bent, the sensor produces a resistance output correlated to the bend radius—the smaller the radius, the higher the resistance value. Flex sensors are sensors that change in resistance depending on the amount of bend on the sensor. They convert the change in bend to electrical resistance- the more the bend, the more the resistance value. They are usually in the form of a thin strip from 1"-5" long that vary in resistance from approximately 10 to 50 kilo ohms. They are often used in gloves to sense finger movement.

4.1. Attributes of FLEX Sensors

- Custom designed to match customer specs
- High level of reliability, consistency, repeatability

- Harsh temperature resistance
- Variety of flexible or stationary surfaces for mounting
- Infinite number of resistance possibilities and bend ratios

5. Mems

Micro-Electro-Mechanical Systems (MEMS) is a new technology that has been growing by leaps and bounds recently. MEMS are the incorporation of mechanical elements, sensors, actuators, and electronics onto a common silicon base through the use of micro fabrication technology. This technology has expanded the conventional two-dimensional design of chips; it is now possible to build three-dimensional structures into the silicon wafer. The purpose of all this is to give the ability to put an entire system onto a single chip.

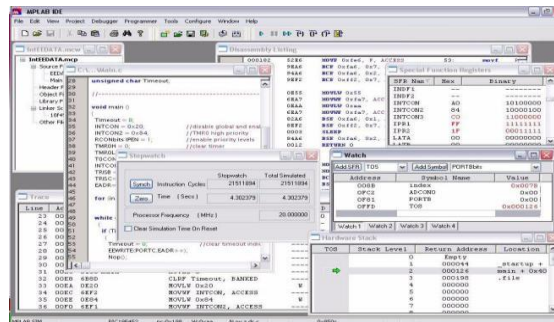
5.1 Benefits of MEMS

Because of the increase in micromachining technology, hundreds of MEMS can be made from a single 8-inch wafer of silicon. Below is an image (Figure 2.2) which shows how small MEMS are in comparison to a dime. Because an entire system can be made this small and in such quantities, prices are reduced for products which incorporate this technology. MEMS also have no moving parts, so they are much more reliable than a macro system. Because of the reduced cost and increased reliability, there is almost no limit to what MEMS can be used for.



6.

Microchip Mplab Ide



MPLAB Integrated Development Environment (IDE) is a free, integrated toolset for the development of embedded applications employing Microchip's PIC[®] and dsPIC[®] microcontrollers. MPLAB IDE runs as a 32-bit application on MS Windows[®], is easy to use and includes a host of free software components for fast application development and super-charged debugging. MPLAB IDE also serves as a single, unified graphical user interface for additional Microchip and third party software and hardware development tools. Moving between tools is a snap, and upgrading from the free software simulator to hardware debug and programming tools is done in a flash because MPLAB IDE has the same user interface for all tools. The MPLAB IDE software brings an ease of software development previously unseen in the 8/16-bit microcontroller market.

The MPLAB IDE is a Windows[®] based application that contains:

- An interface to debugging tools
- simulator
- programmer (sold separately)
- emulator (sold separately)
- in-circuit debugger (sold separately)
- A full-featured editor with colour coded context
- A multiple project manager
- Customizable data windows with direct edit of contents
- High level source code debugging

The MPLAB IDE allows you to:

- Edit your source files (either assembly or C)
- One touch assemble (or compile) and download to PIC micro emulator and simulator tools
- Debug using:
 - source files (assembly or C)
 - absolute listing file (mixed assembly and C)
 - machine code

MPLAB IDE supports multiple debugging tools in a single development paradigm, from the cost effective simulators, through low cost in-circuit debuggers, to full-featured emulators. This eliminates the learning curve when upgrading to tools with increasing flexibility and power.

7. Experimental Results

Figure shows the experimental set up of the project. The transmitter and the receiver sections are connected to PC. The MEMS sensor and the FLEX sensor are connected to the transmitter, transmits the sensed data. Receiver is connected to the COM port of the computer. It receives the data and sends to the PC via RS232 cable.

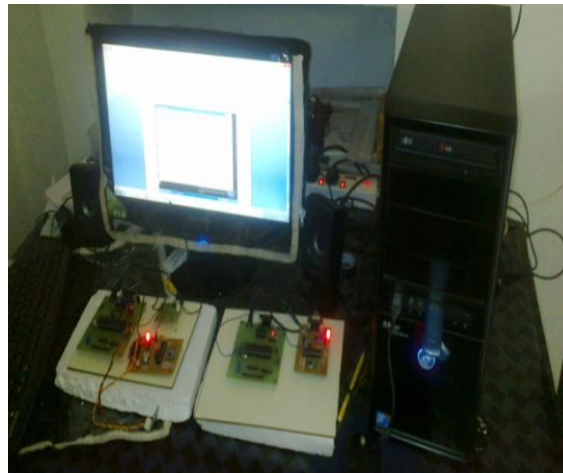


Figure 3: Experimental Set up

The MEMS sensor shown in figure 3.1 is attached to the forearm of the human as shown in figure 3.2 The FLEX sensor is attached to the fingers of the human as shown in figure 3.3 These sensors senses the movements of forearm and the fingers of the human and corresponding analog values are send to the microcontroller.

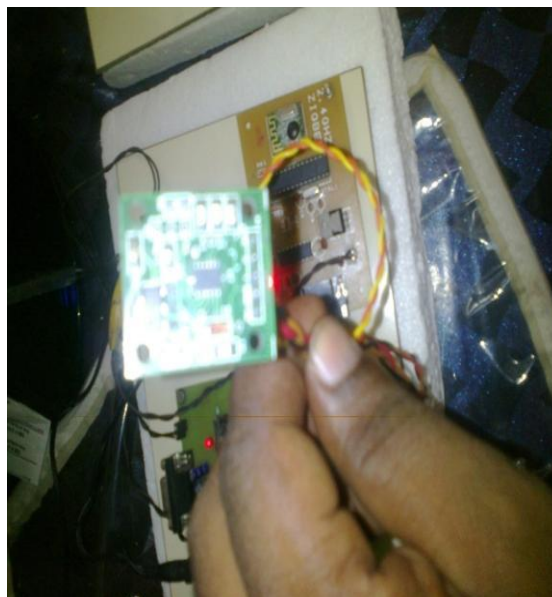


Figure 3.1: MEMS Sensor



Figure 3.2: MEMS Sensor attached to the human

The on chip ADC of the PIC microcontroller converts the analog value to Digital and sends to the RF transceiver which is then transmitted to the receiver. The receiver receives the data and sends it to the microcontroller which is then serially transmitted to the PC. The data is displayed on the PC with the help of hyper terminal.



Figure 3.3 : FLEX sensor attached to the finger of human

As the movements of forearm and fingers of human changes, the corresponding values are displayed on the PC as shown in the figure.

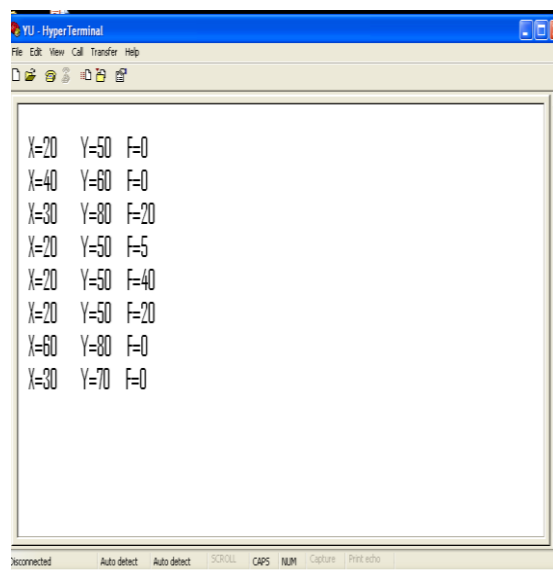


Figure 3.4: Results displayed on PC

8. Future Scope

An ambulatory and unrestrained measurement system based on a wearable wireless sensor network for tracking the human arm motion in the sagittal plane has been proposed. The wireless feature enables the unrestrained motion of the human body as opposed to a wired monitoring device and makes the system truly portable. This allows the system to be deployed in a cluttered home environment. The small form factor and lightweight feature of the sensor nodes also allow easy attachment to the limbs. As compared with other existing approaches, the new system is portable and easy to use. It allows the patients to be monitored without restraint, and rehabilitation can be carried out in a home environment instead of a specialized laboratory in the hospital. For future work, experiments conducted with stroke patients in collaboration with a hospital are being planned using the developed system. More tests can also be conducted to investigate the effect of RF interference from other patient monitoring devices and wireless systems.

REFERENCES

- [1]. H. Zhou and H. Hu, - "Human motion tracking for rehabilitation—A survey" Biomed. Signal Process. Control, vol. 3, no.1 pp.1–18, Jan. 2008.
- [2]. J.M. Zheng, K.W. Chan, and I. Gibson, -"Virtual reality" IEEE Potentials, vol. 17, no. 2, pp. 20–23, Apr. 1998.
- [3]. D. Jack, R. Boian, A. S. Merians, M. Tremaine, G. C. Burdea, S. V. Adamovich, M. Recce, and H. Poizner, "Virtual reality -enhanced stroke rehabilitation," IEEE Trans. Neural Syst. Rehabil. Eng., vol. 9, no. 3, pp. 308–318, Sep. 2001.
- [4]. D. Fitzgerald, J. Foody, D. Kelly, T. Ward, C. Markham, J. McDonald, and B. Caulfield, "Development of a wearable motion capture suit and virtual reality biofeedback system for the instruction and analysis of sports rehabilitation exercises", in Proc. 29th Annu. Int. Conf. IEEE EMBS, 2007, pp. 4870–4874.
- [5]. T. B. Moeslund, A. Hilton, and V. Krüger, "A survey of advances in vision based human motion capture and analysis," Comput. Vis. Image Underst.



A. Dasthagiraiah Was Born in Seetharamapuram, Nellore, A.P., INDIA., in 1988 and Received The B.Tech. (Hons) degree in Electronics And Communication Engineering From the JNTUA in 2009 and the M.Tech degree from the Hindustan University, Chennai, INDIA., in 2011 respectively. His research interests include Embedded Systems and Communication Theory. He Presently working as an Assistant Professor in MeRITS, Udayagiri, Since 2011.



N. Viswanadham Was Born in Tirupathi, A.P., INDIA., in 1992 and He is Studying B.Tech in Electronics And Communication Engineering, MeRITS, Udayagiri.



Y.P. Venkateswarlu Was Born in Nellore, A.P., INDIA., in 1991 and He is Studying B.Tech in Electronics And Communication Engineering, MeRITS, Udayagiri.



B. Balaobulesh was Born in Seetharamapuram, A.P., INDIA, In 1992 and he is studying B.Tech in Electronics and Communication Engineering, MeRITS, Udayagiri.



D. Murali Krishna was Born in Kadapa, A.P., INDIA, In 1992 and he is studying B.Tech in Electronics and Communication Engineering, MeRITS, Udayagiri.

Performance Analysis Of Multi Level Frequency Hopping For Cdma Systems

M.Paul Vinod Kumar¹, C.Ravi Shankar Reddy²

^{1,2}M.Tech Student, Department Of Electronics And Communication Engineering, Jntua-Anantapur,

Abstract:

Frequency hopping is performed by changing carrier frequencies while communicating. Spread spectrum techniques have become more prevalent in modern communication systems and the demand for the efficient usage of available spectrum. In this paper multi level frequency hopping is proposed for CDMA systems. The performance analysis shows that this provides better spectral efficiency and support more users at higher data rates. The results were compared against Goodman's FSK based FH-CDMA scheme at maintained constraints.

Keywords: Code division multiple access(CDMA), code modulation, frequency hopping(FH), spectral efficiency(SE), multiple access interference (MAI).

1. Introduction

Spread spectrum differs from a classical narrow-band or broadband system in that the signal energy is spread over a much wider frequency range, reducing the power spectral density of the signal and providing several advantages:

- Low Probability of Intercept, meaning that it is harder to detect the RF signals
- Higher tolerance to narrow-band noise sources, the anti-jamming property
- Reduction of sensitivity to interference from multi-path reflections
- Possibility of CDMA (Code-division multiple access) operation, where several cooperating transmitters using different frequency hopping patterns can transmit in the same frequency range without disturbing each other [9]

a) Direct-Sequence Spread Spectrum

There are two forms of spread-spectrum techniques, direct-sequence (DSSS) and frequency hopping (FHSS). Direct sequence spread spectrum involves transmitting at a much higher rate than the data-rate, and convoluting the data with a spreading code. At the receiver, the signal can be decoded by using correlation techniques, comparing the incoming signal with the spreading codes. DSSS is more complex to implement than frequency hopping, and is not suitable to low-power systems due to the high data rates involved.

b) Frequency Hopping

Frequency hopping, as implied by the name, is performed by changing carrier frequencies while communicating. In a typical system, the frequency hopping will be of the so-called slow variety, which means that several data symbols (bits) are transmitted during each hop. A rate between 50 and several hundred hops per second is practical. The lock time of the PLL when changing frequencies is 100us-200us (depending on the loop filter); while the time required reprogramming the needed registers using a 1 MHz clock is on the order of 50-60us. The time during a hop when data cannot be received or transmitted is termed the blanking interval. The dwell time is the time spent in each channel. Since spread-spectrum technology has its roots in military applications, much of the terminology refers to enemy "jammers" of varying complexity. In commercial systems, intelligent jamming is not a primary threat. Most of the time, the "jamming" signal will merely be another device trying to utilise the same frequency band for communicating. These devices will typically not be as devious as intelligent enemy jammers might be, so the security requirements can be eased a bit compared to military applications. The so-called "narrowband jammer" is probably the most representative threat seen in civilian applications. Interference from multi-path reflections is also a serious threat. These reflections can cause large frequency- and location-dependent drops in signal strength. Frequency hopping combats multi-path reflections by ensuring frequency diversity[2] [3]. In FH-CDMA, the available transmission bandwidth is divided into L carrier frequency-bands and each frequency band is used to convey one element of an L×N FH pattern, according to the address signature of the intended receiver, where L is the number of frequencies and N is the number of time slots. To apply M-ary FSK, each carrier frequency band is further subdivided into a set of M frequencies. There are totally ML frequencies, grouped into L sections (i.e., frequency-bands) of M frequencies each. The same M frequencies in each section are used to represent the M symbols in M-ary FSK, and the same jth frequency in every section is used to transmit the jth symbol, where $j \in [0; M - 1]$. By using MFSK on top of FH-CDMA, the data rate is increased because each symbol represents $\lceil \log_2 M \rceil$ data bits. In FH-CDMA scheme every frequency-band use a different frequency to represent the transmitting symbol, and the pick of the frequency in a frequency-band is controlled by a prime sequence. The prime/FH-CDMA scheme supported higher data rate than the MFSK/FH-CDMA scheme for the same number

of frequencies per frequency band, at the expense of poor performance. It was because a squared number of prime sequences (i.e., symbols) by relaxing the cross-correlation functions from zero (in MFSK) to one[5][4]. In this paper a multi level FH-CDMA system is proposed for providing frequency diversity for more users at higher data rates over fading channels. This paper is organized as follows, section II describes about the proposed multi level frequency hopping method, section III gives the probability of detection for different channels and performance evaluation.

2. MULTI LEVEL FREQUENCY HOPPING

The available transmission bandwidth is divided into M_h frequency bands with M_m carrier frequencies in each band, giving a total of $M_m M_h$ carrier frequencies. In the first (modulation) level, a number of serial data bits is grouped together and represented by a symbol. Each symbol is, in turn, represented by a modulation code of dimension $M_m \times L_m$ and weight (i.e., number of elements) w_m , where M_m is the number of frequencies, L_m is the number of time slots (i.e., code length). The number of data bits that can be represented by a symbol depends on the number of available modulation codes. If there are ϕ_m available modulation codes, each symbol can represent up to $\lfloor \log_2 \phi_m \rfloor$ data bits, where $\lfloor \cdot \rfloor$ is the floor function [6]. In the second (FH) level, each user is assigned a unique FH pattern of dimension $M_h \times L_h$ and weight (i.e., number of elements) w_h where M_h is the number of frequencies, L_h is the number of time slots (i.e., pattern length). The elements in the modulation codes and FH patterns determine the carrier frequencies of the final FH-CDMA signals. While an element of a modulation code defines the carrier frequency used in a frequency band in a given time slot, an element of the FH pattern determines which frequency band (out of M_h bands) to use. In our scheme, we can choose any families of $(M_m \times L_m, w_m, \lambda_{a,m}, \lambda_{c,m})$ modulation codes and $(M_h \times L_h, w_h, \lambda_{a,h}, \lambda_{c,h})$ FH patterns as long as $w_h \geq L_m$, where $\lambda_{a,m}$ ($\lambda_{a,h}$) and $\lambda_{c,m}$ ($\lambda_{c,h}$) denote the maximum autocorrelation side lobes and cross-correlation values of the modulation codes (FH patterns), respectively. For example the FH patterns with different prime sequences for different users is encoded shown pictorially in the figure 1

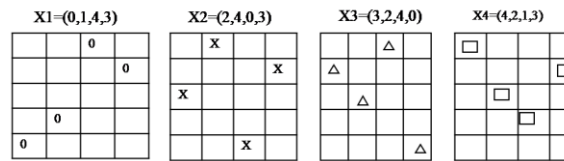


Figure 1) a) FH patterns for different users

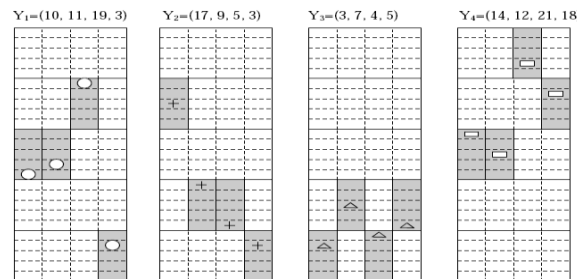


Figure 1) b) Encoded FH patterns the shaded columns in the transmitting signals; represent the frequency bands specified by the corresponding FH patterns. The decoding process is explained in the figure 2

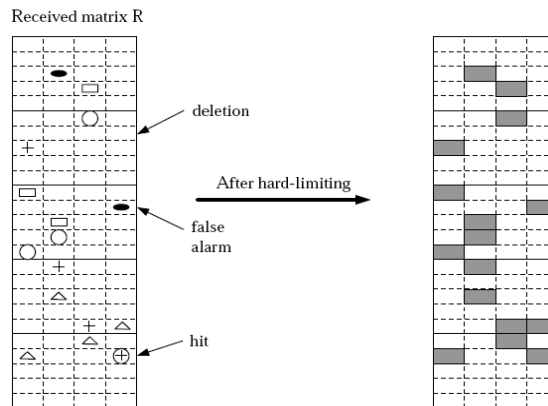


Figure 2: Decoding Process

3. Performance Analysis

In the analysis of the FH-CDMA scheme, we focus on the effects of multiple access interference (MAI) and Rayleigh fading. MAI depends on the cross-correlation functions of the FH patterns, which are related to the code length, code weight, and number of available frequencies. For the proposed FH-CDMA scheme, the cross-correlation functions of the prime sequences add extra interference and need to be considered. Overall, in the absence of fading, a decision error may occur if MAI creates additional entries representing a wrong symbol. An error may occur due to fading, which causes a frequency to be falsely detected when none has been transmitted (i.e., false alarm), or causes a received frequency to be missed (i.e. deletion). In the following analysis, we assume that the hopping frequencies are separated large enough in frequency so that the de-hopped signals at a receiver suffer from independent Rayleigh fading symbol-by-symbol. For each symbol, fading is also assumed to be frequency nonselective [8]. Assume that one-hit FH patterns of dimension $M_h \times L_h$ are used and the transmission band is divided into $M_m M_h$ frequencies, in which M_m frequencies are used to carry the modulation codes of weight w_m . Assume that there are K simultaneous users, the probability that the de-hopped signal contains n entries in an undesired

$$P(n) = \binom{w}{n} \sum_{i=0}^n (-1)^i \binom{n}{i} \left(1 - \frac{w^2}{L_h M_m M_h} + \frac{n}{w} \cdot \frac{w^2}{L_h M_h M_m} - \frac{i}{w} \frac{w^2}{L_h M_m M_h} \right)^{k-1} \quad (1)$$

Over AWGN, and Rayleigh and Rician fading channels, false alarms and deletions may introduce detection errors to the received FH-CDMA signals. A false-alarm probability, p_f , is the probability that a tone is detected in a receiver when none has actually been transmitted. A deletion probability, p_d , is the probability that a receiver missed a transmission tone.

For AWGN channel

$$P_d = 1 - Q \left(\sqrt{2 \left(\frac{E_b}{N_0} \right) \cdot \left(\frac{k_b}{w_m} \right)} \cdot \beta_0 \right) \quad (2)$$

Where Q is Marcum's Q-function and

$$\beta_0 = \sqrt{2 + \frac{\left(\frac{E_b}{N_0} \right) \cdot \left(\frac{k_b}{w_m} \right)}{2}}$$

For Rayleigh channel

$$P_d = 1 - \exp \left\{ \frac{-\beta^2}{2 + 2 \left(\frac{E_b}{N_0} \right) \cdot \left(\frac{k_b}{w_m} \right)} \right\} \quad (3)$$

For Rician channel

$$P_d = 1 - Q \left(\frac{\sqrt{2\rho \left(\frac{E_b}{N_0} \right) \cdot \left(\frac{k_b}{w_m} \right)}}{\sqrt{1 + \rho + \left(\frac{E_b}{N_0} \right) \cdot \left(\frac{k_b}{w_m} \right)}} \cdot \beta_1 \right) \quad (4)$$

Where

$$\beta_1 = \frac{\beta_0}{\sqrt{1 + \frac{\left(\frac{E_b}{N_0} \right) \cdot \left(\frac{k_b}{w_m} \right)}{(1+\rho)}}}$$

Below are the experimental results obtained when $w_m=4, M_m \times L_h=4 \times 11, M_h \times L_h=11 \times 47, \rho=12, E_b/N_0=25dB$. From the results we can conclude that the proposed method outperforms over Goldman's method for spectral efficiency about 5% achieving an error rate about 10^{-3} .

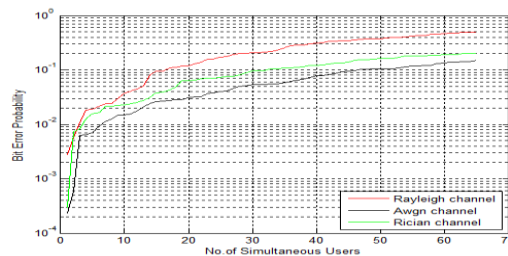


Figure 3: Performance Analysis of proposed method

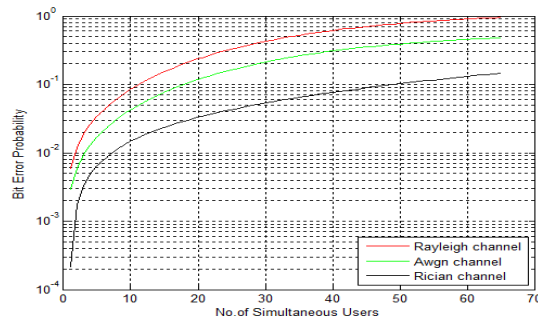


Figure 4: Performance analysis of Goldman's under different channels

4. Conclusion

In this paper, we proposed a new Multi level frequency hopping for CDMA systems. The prime/FH-CDMA and RS/FH-CDMA schemes were special cases of our scheme. The performance analyses showed that the Multi-level FH-CDMA scheme provided a trade-off between performance and data rate. The partitioned Multi-level FH-CDMA scheme increased the number of possible users and exhibited higher data rate and greater SE than Goodman's scheme. In summary, the new scheme offered more flexibility in the design of FH-CDMA systems to meet different operating requirements

5. Acknowledgement

Mr. Paul Vinod Kumar would like to thank Mr. C. Ravi Shankar Reddy, Lecturer, who had been guiding through out to complete the work successfully, and would also like to thank the HOD, ECE Department and other Professors for extending their help & support in giving technical ideas about the paper and motivating to complete the work effectively & successfully.

6. References

- [1] G.-C. Yang, S.-Y. Lin, and W.C. Kwong, "MFSK/FH-SSMA wireless systems with double-media services over fading channels," *IEEE Trans. Vehicular Tech.*, vol. 49, no. 3, pp. 900-910, May 2000.
- [2] M. Schwartz, W.R. Bennett, and S. Stein, *Communication Systems and Techniques*, McGraw-Hill, New York, 1966.
- [3] G.-C. Yang and W.C. Kwong, "Frequency-hopping codes for multimedia services in mobile telecommunications," *IEEE Trans. Vehicular Technol.*, vol. 48, no. 6, pp. 1906-1915, Nov. 1999.
- [4] G. Kaleh, "Frequency-diversity spread-spectrum communication system to counter bandlimited Gaussian interference," *IEEE Trans. Commun.*, vol. 44, pp. 886-893, July 1996.
- [5] D.J. Goodman, P.S. Henry, and V.K. Prabhu, "Frequency-hopping multilevel FSK for mobile radio," *Bell Syst. Tech. J.*, vol. 59, no. 7, pp. 1257-1275, Sept. 1980
- [6] M.-F. Lin, G.-C. Yang, C.-Y. Chang, Y.-S. Liu, and W. C. Kwong, "Frequency-hopping CDMA with Reed-Solomon code sequences in wireless communications," *IEEE Trans. Commun.*, vol. 55, no. 11, pp. 2052-2055, Nov. 2007
- [7] E. L. Titlebaum and L. H. Sibil, "Time-frequency hop signals—part II: coding based upon quadratic congruencies," *IEEE Trans. Aero. Electron. Syst.*, vol. 17, no. 4, pp. 494-500, July 1981
- [8] T. Mabuchi, R. Kohno, and H. Imai, "Multiuser detection scheme based on canceling cochannel interference for MFSK/FH-SSMA system," *IEEE J. Sel. Areas Commun.*, vol. 12, no. 4, pp. 593-604, May 1994.
- [9] Application note on "Frequency hopping systems" by Texas instruments

Gravitational Energy and Its Field

¹HARSHIT BINJU, ²DEBASISH TALUKDAR, ³SAHIL MITTAL
⁴ABHISHEK

^{1,2,3,4}UNIVERSITY OF PETROLEUM AND ENERGY STUDIES, DEHRADUN, INDIA

Abstract

Gravitation is a force which binds all of us with this Earth. After two years of research, my friends and I came to a very interesting conclusion-“Gravity force (g) of the Earth is due to its revolution on its own axis”.Reason – Since the Earth is revolving around the Sun, a force is being exerted by the Sun on the Earth. This means there has to be an energy which the Sun is providing to the Earth. We know that “energy can neither be created nor destroyed.”Hence this energy has been changing its form to another.

Our earth is utilizing this energy in two ways-

- 1) By rotating around the Sun.
- 2) And revolving on its own axis.

This energy is producing a force known as gravitational force, which is binding us.

Recently we also noted that if a body is not doing any kind of motion then it is not capable of applying any force on the bodies nearby.In simple words “a body can exert a force on another body if and only if it is in motion”.Thus a new concept of “gravitational induction” is introduced. Thus, if there is a body whose not doing any kind of motion and comes into a region of another body’s gravitational effect then it is capable of generating its own field due to gravitational induction.

Keywords: Energy, force, gravitation, gravitation induction, graviton, motion, string theory.

1. Introduction

This paper is a research work on planetary motion of the Sun and Planets; their impact on each other’s avitational forces and fields. Newton has explained the concept of gravitational force however he was unable to find the source of energy responsible for this gravitational pull. This paper attempts to understand the source of gravitation force.The theory of gravitation was first propounded by Newton. He devised in his search of reason for the apple that had fallen on his head. He said that there is force that the earth exerts on the objects and pulls them towards the Earth’s centre. With the development of superior methods the force of gravitation could be calculated at different points of the Earth. Einstein too postulated his own theory of gravitation but neither of them pointed out the exact source of this energy.

2. Explanation

Graviton particle- In physics graviton is a hypothetical particle which mediates the force of gravitation in field theory. In physics graviton is expected to be mass less since the field of gravitation is infinity. Gravitons are postulated because of the great success of intermediate particles like photons in electromagnetism; strong interactions by gluons and weak interaction by W and Z bosons.Newton’s theory of gravitation- According to Newton’s theory of gravitation ‘Gravitation force between any two bodies is inversely proportional to the square of distance between them’.

- 1) Many others theory like string theory came forward with their reasons but had limitations of their own. Such as according to string theory all the different manifestations are just one basic object known as a string.So if we take a small point which has no internal structure. A point cannot do anything but move. But, if string theory is correct then under extremely powerful microscope we would realize that the electron is nothing but a tiny loop of string.So if whole of the string theory is correct than whole of the world is made up of strings which isn’t so. All the above explanations are based on hypothesis except Newton’s. According to our theory “Earth’s gravitation is due to its revolution on its own axis”. Earth is revolving around the Sun in its elliptical orbit; the Sun is applying a force on the Earth. Since a force is being applied by the Sun on the Earth it means the Sun is also providing energy to the Earth. Now that energy is used by the Earth.

- 1) When it rotates around the Sun in its elliptical orbit.
- 2) And when it rotates on its own axis.

In the first case, as per the third law of Newton for every action there is an equal and opposite reaction. Hence when the Sun applies force on the Earth, there is bound to be force applied by the Earth on the Sun. The Earth rotates around the Sun in its elliptical orbit utilizing the energy from the Sun. Whenever energy is used force is produced. This force counters the attractive force from the Sun. Hence the Earth keeps on moving on its axis. When the Earth rotates on its axis a small force is produced by the energy of the Sun. This force is called gravity force (g). In the second case “a body can exert a force on another body if and only if they are in motion”. For example a body which is not performing any kind of motion, it will not have any kind of energy for creating its own field. In this situation, this body cannot attract any other body. In contrast, if a body does some kind of simple motion, energy will be produced. A small part of this energy will be utilized for creating gravitational field around the particle’s body. Hence we concluded that if all the objects in the space stop their motion, there will be no force of attraction between them. An important question has been raised here- how do stationary objects create an attractive force between them? For this we have introduced a new term ‘Gravitation Induction’. According to Gravitation Induction “ if any stationary body comes in the gravitational field of a moving body, then the stationary body gets induced by the field of the moving body and thus it is able to creates its own field”.

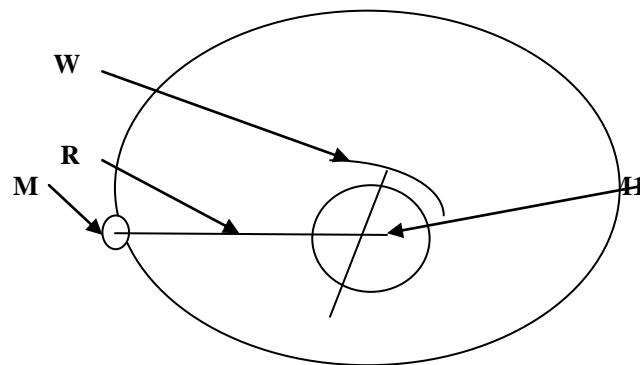


Figure (1)

In the above figure a body of mass M_1 is placed at the centre of the circular orbit of radius R . The bigger body is rotating on its own axis at an angular speed of w rad./sec. Whereas the smaller body is rotating around the bigger body and has a mass of M_2 . Mass of bodies is taken in kg. Radial distance between both the bodies is taken in meters. Whole of this system is taken in vacuum where no heat loss and no friction loss are counted. Hence, force between these two bodies will be directly proportional to the product of their masses with product of radial velocity of bigger body and linear velocity of smaller body divided by the square of distance between them.

F is directly proportional to $(M \times m \times w \times v) / R \times R$

$$F = (GB \times M \times m \times w \times v) / R \times R$$

Where GB is my constant and its value is equal to $5.829 \times (10)$ to the power (-14) .

References:

- [1] The collected papers of Albert Einstein- California Institute of Technology
- [2] Principia- Issac Newton
- [3] The complete guide to the laws of the universe

An Ultra-Low Power Physical Layer Design For Wireless Body Area Network

¹D.Venkadeshkumar , ² K.G.Parthiban

¹, Pg Student Department Of Ece Mpmj Engineering College Erode, India

², Professor&Hod Department Of Ece Mpmj Engineering College Erode, India

Objective

WBAN for health monitoring consists of multiple sensor nodes. Each node is typically capable of sensing one or more physiological signals, processing these signals storing the processed data, transmitting the data to other nodes and/or a WBAN server. The main objective is to design physical layer with lower power consumption.

Index Terms:Digital circuit design, low power, wireless body area network (WBAN), wireless communication.

Abstract

The wireless body area network (WBAN) is a wireless network used for communication among sensor nodes operating on, in or around the human body in order to monitor vital body parameters and movements. The pursuit of higher quality of life motivates people to be more concerned about their health and potential diseases. At the same time, many patients can benefit from continuous monitoring of their diagnostic procedures. All these require a convenient healthcare surveillance system to monitor people's health status anytime and anywhere. The tracking capability of such a system should also be able to provide optimal maintenance after a surgical procedure and support early detection of abnormal health conditions. This paper investigates the efficient design of the PHY layer architecture for wireless body area networks (WBAN), which targets on ultra-low power consumption with reliable quality of service (QoS). A low cost baseband transceiver specification and a data processing flow are proposed with a comparatively low-complexity control state machine. A multifunctional digital timing synchronization scheme is also proposed, which can achieve packet synchronization and data recovery. To demonstrate and to optimize the reliability of the proposed design, the dedicated bit-error-rate and power analysis is reported. VHDL code is created to describe the PHY system and SPI and is verified on a Xilinx field-programmable gate array (FPGA) platform.

1. Introduction

The pursuit of higher quality of life motivates people to be more concerned about their health and potential diseases. At the same time, many patients can benefit from Continuous monitoring of their diagnostic procedures. All these require a convenient healthcare surveillance system to monitor people's health status anytime anywhere, especially when people suffer an acute event, such as a sudden heart attack. The tracking capability of such a system should also be able to provide optimal maintenance after a surgical procedure and support early detection of abnormal health conditions. Recent advances in sensors, integrated circuits, and wireless communication are paving the way for developing miniature, lightweight, ultra-low power physiological healthcare surveillance and monitoring devices for the improvement of human lives. These devices can be integrated into wireless body area networks (WBANs) for health monitoring. A WBAN topology consists of a series of miniature invasive/non-invasive physiological sensors and is able to communicate with other sensor nodes or with a central node. The central node has higher computational capability and communicates wirelessly with a personal server and subsequently the outside world through a standard telecommunication infrastructure, such as wireless local area networks and cellular phone networks. Potential applications of WBANs include chronic disease management, medical diagnostics, home-monitoring, biometrics, and sports and fitness tracking, etc.. The power budget is quite strict for WBAN applications because the wireless device is powered by a battery. An optimized low power low data rate digital baseband IC is proposed, and its performance is analyzed in detail. The proposed baseband transceiver is configured with a frequency-shift keying (FSK) modulation/demodulation module. A specified physical layer (PHY) architecture is developed, which reduces the complexity of baseband processing but maintains satisfactory performance. To recover precisely the timing and data information from an FSK demodulator, a novel synchronization and data recovery (SDR) scheme is proposed that has comparatively low complexity. To overcome the timing drift between the transmitter and receiver, a low-complexity sampling point realignment scheme is proposed. This scheme shares the same hardware with the SDR scheme and can automatically adjust to the correct sampling point during data transmission.

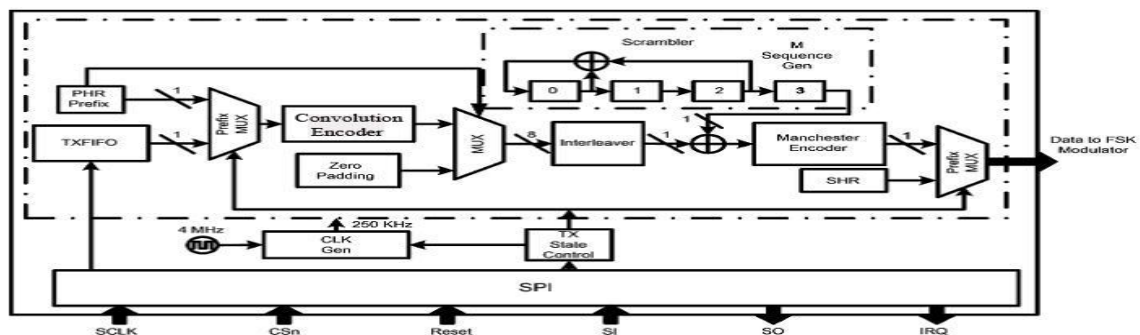
2. Existing Physical Layer Design:

The CC2420 from Texas Instruments in can cover a 20–30 m range at a power consumption of 60–70 μ W and hamming encoding technique was used. However, such operation range and power consumption are not the optimal choice for WBAN applications. The transceivers which have high data rate transmission, resulting in comparatively high power consumption.

3. Modified Technique:

Baseband Transmitter

In the transmitter block, the Physical Layer Service Data Unit (PSDU) from the MAC layer is processed in the proposed transmitter (TX) baseband processor module to generate a physical layer protocol data unit (PPDU) packet. The channel coding and signal processing are performed on the PPDU in the TX baseband processor module and the raw data rate of the TX baseband processor module output is 250 kb/s. The baseband raw data is modulated by FSK and then directly up-converted to a 2.45 GHz RF signal. In the receiver (RX) block, the received RF signal is down-converted to a 2 MHz intermediate frequency (IF) signal and then demodulated by a low power FSK demodulator. The demodulated signal is processed by the proposed RX baseband processor module. Following that, the received PSDU is fed into the MAC layer. To achieve ultra-low power consumption, a low-complexity PHY specification is proposed. The signal processing flow for TX and RX are presented. In the TX module, the baseband processor receives the PSDU from the MAC layer and constructs the PPDU. The permitted length of the PSDU within one packet should be no larger than 127 octets and this information is contained in the PHY header (PHR) in octets. Once one packet of the PSDU is generated by the MAC layer, it is fed into TXFIFO and ready for transmission. There is a Prefix MUX block controlled by the TX state control block to select the input of the encoder block. The diagram of the transmitter block of the baseband transceiver is illustrated in the following figure.



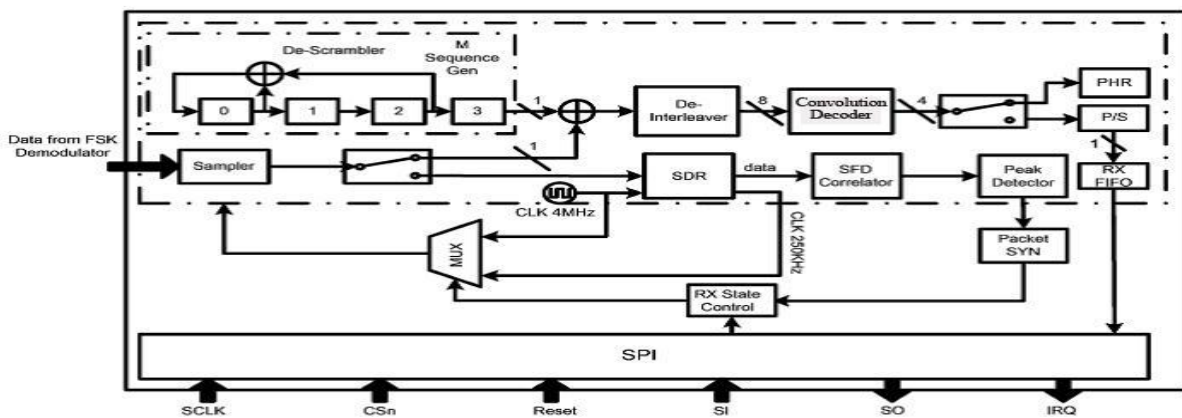
Transmitter Block

When a transmission command is sent from the MAC layer, the PHR is prefixed to the PSDU and sent into the Hamming encoder block first. The input data of the encoder block is in serial sequence with 1 bit word-length. In our design, convolution coding and interleaving techniques are used as forward error correction (FEC). For each consecutive bits of input data, the encoder block generates output data simultaneously. The output data of the convolution encoder block is fed into the matrix interleaving block to suppress the burst error. To eliminate long strings of like bits that might impair receiver synchronization and to eliminate most periodic bit patterns that could produce undesirable frequency components (including the dc component), the interleaved data payload is first fed into a scrambling block and then coded by a Manchester encoder. The scrambling block generates the scrambling code in serial sequence with 1 bit word-length. Here we use the sequence generator with as the scrambler to achieve satisfactory performance and comparatively low complexity. The output data of the interleaving block is in serial sequence with 1 bit word-length and is XOR with the generated scrambling code. The scrambled data payload is fed into the Manchester encoder. The Manchester encoder converts the bit “0” to bits “01” and converts the bit “1” to bits “10,” and thus the total number of “0” and “1” can be balanced. The output of the Manchester encoder is prefixed with the synchronization header (SHR) and is sent to the FSK modulator for transmission.

4. Baseband Receiver

In the receiver module, the received data stream is the demodulated binary signals from the FSK demodulator. A D flip-flop is used provided by the technology library to sample and to restore the analog input. If the voltage of the input signal is higher than of the D flip-flop, the output of the D flip-flop will be “1.” If the voltage of the input signal is lower than of the D flip-flop, the output of the D flip-flop will be “0.” As illustrated in Figure, the signals are first

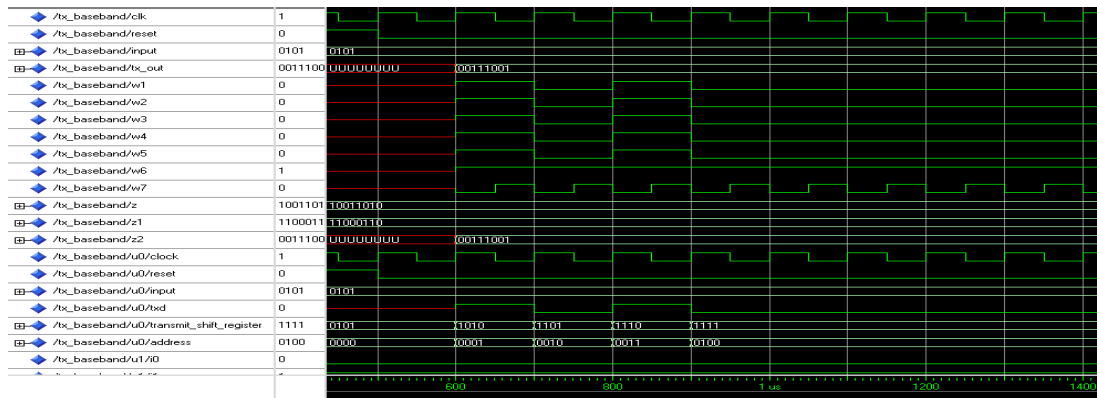
serially fed into the synchronization and data recovery (SDR) block to achieve synchronization and to recover the received data. The SDR block over-samples the incoming signal using a shift register matrix block and calculates the correlation between the incoming data and the predefined preamble sequence to achieve bit synchronization. The peak of the calculated correlation is continuously detected. Once the peak value is found, the start-of-frame delimiter (SFD) Correlate block calculates the correlations between the incoming data and the predefined SFD sequence, and the peak value is searched by the following peak detector block. Once the peak value is found, the packet synchronization is confirmed. The preamble sequence and SFD are removed and the Packet SYN block indicates to the RX State Control block that the PHR and PSDU can be received. The SDR block also generates the 250 kHz clock, and the RX State Control block selects the operation clock frequency of the RX baseband processor module which can be between 4 MHz clock and 250 kHz clock. Manchester decoding is first performed on the received PHR and PSDU data stream by detecting the first bit for every two continuous received bits. Following that, the incoming data is descrambled and the structure of the descrambling block is identical to that of the scrambling block. The output of the descrambling block has a 1-bit word-length, and XOR operations are completed with the incoming data bit by bit. Following that, the PHR and PSDU are fed into the FEC decoding block, which includes the de-interleaving block and convolution decoder block. The output of the de-interleaving block has an 1-bit word-length and is fed into the convolution decoder block. The decoder block checks whether there is any error in the incoming data and corrects the error. If the decoder block detects an error but can not correct it, the receiver will stop receiving any data and the MAC layer will request a retransmission of this packet. The PHR is decoded first and thus length information about the PSDU can be obtained by the RX state control block. The word-length of the convolution decoder block output is 2 bits, and there is a parallel to serial buffer, so that bits in the PSDU are fed into the RXFIFO in serial sequence with 1 bit word-length, and is read by the MAC layer.



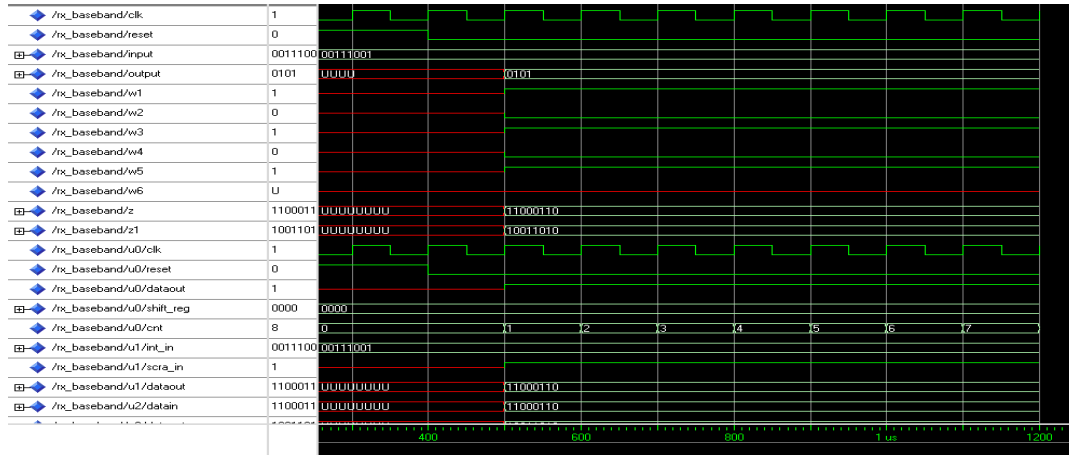
Receiver Block

5. Simulation Results:

Simulation Result Of Transmitter Baseband



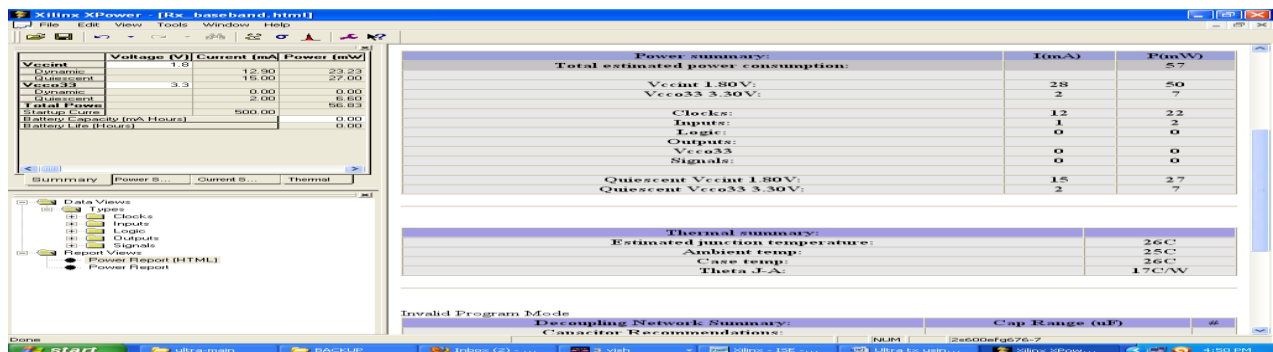
Simulation Result Of Receiver Baseband



6. Existing Technique: Power Estimation Of Existing Transmitter Block

Design:	C:\Xilinx\hamming\Tx_baseband.ncd	
Preferences:	Tx_baseband.pcf	
Part:	2s50eft256-7	
Data version:	PRELIMINARY,v1.0,07-31-02	
Power summary:	I(mA)	P(mW)
Total estimated power consumption:		76
Vccint 1.80V:	38	69
Vcco33 3.30V:	2	7
Clocks:	25	45
Inputs:	2	4
Logic:	1	2
Outputs:		
Vcco33	0	0
Signals:	0	0
Quiescent Vccint 1.80V:	10	18
Quiescent Vcco33 3.30V:	2	7

Power Estimation Of Existing Receiver Block

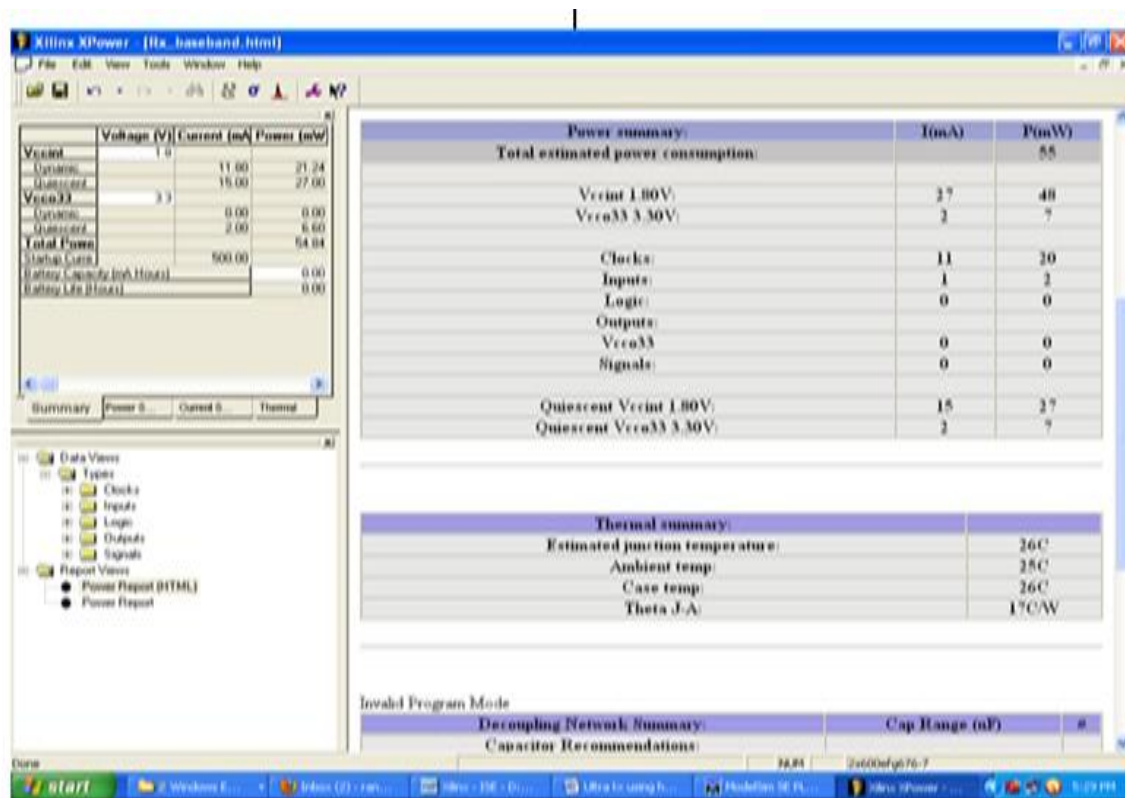


7. Modified Technique:

POWER ESTIMATION OF PROPOSED TRANSMITTER BLOCK

Design:	C:\Xilinx\convolution\Tx_baseband.ncd		
Preferences:	Tx_baseband.pcf		
Part:	2s50eft256-7		
Data version:	PRELIMINARY,v1.0,07-31-02		
power summary:		I(mA)	P(mW)
Total estimated power consumption:			62
Vccint 1.80V:		31	55
Vcco33 3.30V:		2	7
Clocks:		17	31
Inputs:		2	4
Logic:		1	2
Outputs:			
Vcco33		0	0
Signals:		0	0
Quiescent Vccint 1.80V:		10	18
Quiescent Vcco33 3.30V:		2	7

POWER ESTIMATION OF PROPOSED RECEIVER BLOCK



Power summary:		I(mA)	P(mW)
Total estimated power consumption:			
Vccint 1.80V:		27	48
Vcco33 3.30V:		2	7
Clocks:		11	20
Inputs:		1	2
Logic:		0	0
Outputs:			
Vcco33		0	0
Signals:		0	0
Quiescent Vccint 1.80V:		15	27
Quiescent Vcco33 3.30V:		2	7

Thermal summary:		
Estimated junction temperature:		26°C
Ambient temp:		25°C
Case temp:		26°C
Theta J-A:		1°C/W

POWER ANALYSIS TABLE:

Technique	Transmitter power	Receiver power
Hamming encoder (existing)	55 mW	57mW
Convolution encoder (proposed)	50mW	55mW

8. Conclusion

The efficient design of the PHY layer architecture for wireless body area networks (WBAN), which targets on ultra-low power consumption with reliable quality of service (QoS). A low cost baseband transceiver specification and a data processing flow are proposed with a comparatively low-complexity control state machine. A low power low data rate digital baseband transceiver IC is proposed, which uses low-complexity architecture to achieve satisfactory performance. The target power consumption is less. Benefiting from the novel low complexity hardware architecture design and optimized hardware implementation. Specified physical layer (PHY) architecture is developed, which reduces the complexity of baseband processing but maintains satisfactory performance. To recover precisely the timing and data information from an FSK demodulator, a novel synchronization and data recovery (SDR) scheme is proposed that has comparatively low complexity. A convolution code is a linear error-correcting code which can detect errors, and correct them; thus, reliable communication is possible between the transmitted and received bit patterns. To optimize the reliability of the proposed design, the dedicated bit-error-rate and power analysis is reported. VHDL RTL code is created to describe the PHY system and SPI and is verified on a Xilinx field-programmable gate array (FPGA) test platform.

References

- [1] Xin Liu, Yuanjin Zheng, Member, IEEE, Bin Zhao, Yisheng Wang, and Myint Wai Phyu (August 2011) "An Ultra Low Power Baseband Transceiver IC for Wireless Body Area Network in 0.18- μ m CMOS Technology" IEEE Transactions on very large scale integration systems, vol 19.no.8
- [2] Lo.B,Thiemjarus.L,King.R and Yang.G.Z, (2005) "Body sensor network—A wireless sensor platform for pervasive healthcare monitoring," in *Proc. 3rd Int. Conf. Pervasive Comput*, pp.77–80
- [3] .Ma H. H. Yu, J. Y, Chen T. W. Yu., C. Y and. Lee C. Y, , (Apr. 2008) "An OFDMA based wireless body area network using frequency pre-calibration," in *Proc. IEEE Int. Symp. VLSI Des., Autom. Test (VLSI-DAT)*,pp. 192–195.
- [4] Pansiot.J,King.R.C, McIlwraith.D.G, (Jun.2008), "ClimBSN: Climber performance monitoring with BSN," in *Proc.IEEE 5th Int. Workshop Wearable Implantable Body Sensor Netw.*, , pp. 33–36.
- [5] Schmidt.R, Nörgall.T, Morsdorf.J,Bernhard.J and Grün.T, "Body area network, a key infrastructure element for patient-centered medical applications, *Biomed. Eng.*, vol. 47, pp. 365–368, 2002.
- [6] Song S. J.,Cho. N, Kim. SS. and. Yoo H. J, (2007) "A 0.9 V 2.6mW body-coupled scalable PHY transceiver for body sensor applications," in *IEEE Int. Solid-State Circuits Conf. Dig. Tech. Papers*, ,pp. 366–367.
- [7] Wang.C.C., Huang J. M., Lee L. H. Wang., S H, and. Li C. P, (Jan. 2007) "A low-power 2.45 GHz ZigBee transceiver for wearable personal medical devices in WPAN," in *Proc. IEEE Int. Conf. Consumer Electron. (ICCE)*, , pp. 1–2.
- [8] Yang.G, (2006). *Body Sensor Networks*, , New York: Springer.
- [9] dl.acm.org/citation.cfm?id=1938079
- [10] www.freepatentsonline.com/article/KSII-Transactions-Internet-Information-Systems/294194134.html

An Elementary Review of Linkages & Gaps Among BPR, SOA & Software Reverse Engineering

1,Prasenjit Kundu, 2,Bikram Keshari Ratha, 3,Debabrata Das

¹Research Scholar, Department of Computer Science, Utkal University

²Faculty, Department of Computer Science, Utkal University

³Lecturer, Bengal School of Technology & Management

Abstract:

Research on Business Process Reengineering has started as an effort in proposing methods and techniques for organizational restructuring in order to increase organizational efficiency and effectiveness. Later on researchers and consultants started using the tools of IT as part of BPR processes and ultimately they started to develop IT based models and methodologies for BPR. One such effort is the development of Object Oriented Knowledge Based model or the OKB model of BPR which encompasses the idea of Service Oriented Architecture (SOA) and Reverse Engineering in order to implement BPR in a simple yet efficient manner. In this paper an elementary literature review has been done in order to build a linkage among the concept of BPR, SOA and Reverse Engineering as well as to identify the gaps among these from the point of view of the OKB model.

Keywords: ADRI Approach, Business Process Reengineering, Dynamic Plug in instrumentation, OKB Model, Service Oriented Architecture (SOA), Software Reverse Engineering, Software Visualization.

1. Introduction

As the name of this paper suggests, this paper is basically an elementary review of literature because the review has been done from the point of view of the OKB model of BPR. Secondly the sources of this review are mostly the free resources available on the internet through different open access database and repositories like the Google Scholar, Social Science Research Network (SSRN), Open Access Research Database (OARD), Directory of Open Access Journals (DOAJ) etc. So this review is not a complete one but an elementary one.

2. Review on BPR

The emergence of global competitiveness in developing high quality low cost products has led to the development of various approaches like CIM, JIT, lean manufacturing, concurrent engineering etc and in this way the research on BPR and enterprise modeling has been started by researchers like J.H.Manley, K.C. Hoffman, H. Rozenfeld, A.F. Rentes, W. Konig, R. P. Anjard, S. Jarzabek, W. L. Tok, S. Kim, K. Jang, K. Mertins and R. Jochem([1], [2], [3], [4], [5], [6], [7], [8]). J.H. Manley was the first person to through light on reengineering manufacturing systems and connecting BPR with enterprise modeling. Manley's thought describes the ways through which industrial engineers can assist in reengineering worn out, error prone or obsolescent real-time manufacturing systems (embedded systems) by helping computer systems and also how the communication engineers can ensure that critical information control loops, both feed forward and feedback, are complete and efficient. Manley describes two conceptual models, the Embedded Computer System (ECS) physical model and the Object Transformation Process Model (OTPM) to guide a modified process flow analysis (PFA) of existing large-scale, complex embedded systems that takes into account the process-supporting information. As per Manley this modified PFA should be called an Information Process Flow Analysis (IPFA) [1]. Using an enterprise-wide Information Systems Architecture (ISA) as a roadmap, K.C. Hoffman presents a general model of the management structure to implement a systems integration program. This Information Systems Architecture (ISA) is supported by a defined set of measures and metrics and (ISA) approach is comprehensive in covering application software and data architecture and also the computing and communications hardware infrastructure and other automation technologies that support the overall business process [2]. On the basis of these two early approaches of enterprise modeling, J. H .Manley developed his marvelous idea of a three-phase information system analysis and design methodology which can be used to continuously improve enterprise information systems as part of a six-step annual business improvement process. According to this new approach, after the senior management's strategic decisions on next year's product and/or service portfolio content, the related financial, management, engineering, and quality improvement processes are analyzed to determine their output product and/or service quality and timeliness. Next, the facilities, equipment, and personnel resources required for individual processes are inspected for either immediate or possible future improvement. Next the minimum essential information (MEI) requirements are analyzed using the Object Transformation Process Model (OTPM). Next, the individual OTPM models are linked to help identify all pertinent data sources, information destinations, and timing requirements and lastly the linked OTPM models are mapped onto an Embedded Computer System (ECS) model that defines a physical architecture for improving telecommunication paths between all humans, machines and embedded

computers that are component parts of the integrated processes. Manley thinks that this approach yields comprehensive information system logical and physical architectural models that can recursively guide high-leverage enterprise-wide improvement projects over succeeding fiscal years [3].

3. Review on Software Reverse Engineering

Software reverse engineering is defined as the process of analysing a system to identify the system's components and their interrelationships, and to create representations of the system in another form or at a higher level of abstraction [9]. Researchers believe that the interest in software reverse engineering has grown over the last twenty years due to the fact that comprehending and modifying software is at the heart of many software engineering tasks and this is also true in case of software reverse engineering. [10]. An early example of the use and application of software reverse engineering is the famous case study by E. J. Byrne. Byrne conducted an experiment to reverse engineer a program and later documented the lessons learned from the experiment as a case study. Byrne used a reverse engineering process as part of a project to develop an Ada implementation of a FORTRAN program and to upgrade the existing documentation. To achieve this project objective, first the design information was extracted from the FORTRAN source code and entered into a software development environment. Then the extracted design information was used to implement a new version of the program which was written in Ada. Byrne reported the experience gained during this study and revealed issues about recovering design information, such as, separating design details from implementation details, dealing with incomplete or erroneous information, traceability of information between implementation and recovered design, and re-engineering [11]. Erich Buss and John Henshaw mentioned Byrne's case study on reverse engineering and outlined their own initial research experiences on the application of reverse engineering technologies to large-scale legacy software systems and they realized that this application offers the opportunity to regain a measure of control and understanding of the software which can leverage the software developer's actions and knowledge, and augment the software development and maintenance processes [12]. G. Canfora, A. Cimitile & P.B. Lucarelli observe that it's difficult to define reverse engineering in rigorous terms because the field is new and rapidly evolving. They believe that traditionally reverse engineering has been viewed as a two step process and the steps are information extraction and abstraction. Information extraction deals with the analyses of subject system artifacts, primarily the source code to gather raw data whereas information abstraction deals with creation of user oriented documents and views [13]. Canfora, Cimitile & Lucarelli also support Chikofsky and Cross's definition of reverse engineering that is "the process of analyzing a subject system to identify the system's components and their interrelationships and to create representations of the system in another form or at a higher level of abstraction" ([13],[9]). Dynamic program analysis is the analysis of computer software that is performed by executing programs built from that software system on a real time basis. For dynamic program analysis to be effective, the target program must be executed with sufficient test inputs to extract and produce interesting behaviour. Dynamic program analysis helps to make a computational system reason automatically (or at least with little human assistance) about the behaviour of a program and draws conclusions that are useful to help the software developers to determine exploitability of vulnerabilities or to rapidly develop an exploit code [14]. Dynamic analysis produces output, or feeds into a subsequent analysis, that enables human understanding of the code and makes the design and testing task easy for the developers. Dynamic program analysis approach attempts to tune the application software during execution without stopping, recompiling or even rerunning the application. To achieve this objective it is necessary to use dynamic instrumentation techniques that allow the modification of the application code on the fly [15]. Program instrumentation is a general way to understand what an executing program is doing [16]. The principle of dynamic program instrumentation involves deferring program instrumentation until it is in execution and then inserts, alter and delete this instrumentation dynamically during the actual program execution. The Paradyn group at the University of Wisconsin and University of Maryland first used this approach to develop a special API that supports dynamic instrumentation and the result of their work was called DynInst API. DynInst is an API for runtime code patching that provides a C++ class library for machine independent program instrumentation during application execution. It allows attaching to an already running process or starting a new process, creating a new piece of code and finally inserting created code into the running process. The next time the instrumented program executes the modified block of code i.e. the new code is executed and the program being modified is able to continue its execution and does not require to be recompiled, re linked or restarted [16].

4. Review on SOA

Service oriented architecture can be defined as a framework to integrate business processes and supporting IT infrastructures into secure, standardized components services that can be reused and combined to address changing business activities and priorities [17]. For the last couple of years different organizations across different sectors are adopting SOA just because of its capability to ensure business process improvement and thus in this way to gain competitive advantage [18]. The reason behind strong adaptation of SOA is its link between IT and business and through SOA, services which require human interaction can be configured easily and systematically so that the whole system operates as per the operational needs. For this reason SOA reference architecture has become a clear framework for any enterprise operation [19]. According to Newcomer and Lomow, SOA should be seen as a style of design that provides guidance of creating and using business services

throughout their lifecycle as well as defines and makes provisions for the IT infrastructure that allows different applications to exchange data and participate in business processes seamlessly irrespective of the operating systems or programming languages underlying those applications. The elementary SOA ingredients are (1) Infrastructure, (2) Architecture (3) Process and (4) Governance [20]. According to Kraf-zig, Banke and Slama, SOA is based on four key abstractions: (1) Application Front Ends (2) Service (3) Service Repository and (4) Service Bus or Enterprise Service Bus (ESB). Actually the Application Frontend is the owner of the business process while the services provide business functionality which the application frontends and other services can use. A service consists of an implementation that contains business logic and data, a service contract and a service interface. The service contract specifies the functionality, usage and constraints for a client of the service and a service interface physically exposes the functionality. The service repository stores the service contracts of the individual services of an SOA and the service bus (ESB) provide the linkage between the application front ends and services. A client can either be an application front end or service. It is always an application front end that initiates a business process and receives the result. Service is a software component of unique functional meaning that typically encapsulates a high level business concept. The application frontend basically interacts with the human user and that's why it is called sometimes the client. In some cases the client can be the service itself. The client uses the interfaces to invoke the service through the ESB (enterprise Service Bus). The interface is based on the service contract and the service contract describes the service and the service fulfills the service contracts and the service contract is stored in service repository [21]. This framework can finally provide a basis for end user build front ends & applications developed according to Web 2.0 service definitions, such as mashups and the quick deployment of user oriented applications created in AJAX or similar development tool [19].

5. Review of Linkages Through The OKB Model Of BPR

Kundu, Ratha and Das's paper on Business Process Reengineering (BPR) is the cornerstone of this review paper. In their paper Kundu, Ratha and Das propose a mixed model of BPR by combining the OOM and KBM and call it the Object Oriented Knowledge Based Model or OKB Model [22]. The OKB model first identifies the business processes at the top or strategic level, middle or supervisory level and bottom or operational level and then breaks down these processes into repetitive activities. Then, the OKB model converts these repetitive activities into services as per the SOA framework. Once an enterprise wide SOA implementation blueprint gets ready, dynamic program instrumentation techniques are used to fine tune, optimize and reverse engineer the existing legacy systems across the organization [22]. Kundu, Ratha and Das's OKB model is unique in the sense that it uses the concept of SOA and dynamic program instrumentation, i.e.; it combines the principles of organizational reengineering with the tools of ICT and thus builds an effective, easy to understand and easy to implement framework for business process reengineering. The Object Oriented Knowledge Based (OKB) model has eleven steps and the steps are as follows :(Ref. Fig. 1)

- [1] Departmentation of the Organizations.
- [2] Identification of the process at three levels of management i.e. at the top or strategic level, at the middle or tactical level and at the bottom or operational level.
- [3] Classifications of the processes into a) Core Process b) Associated Process and c) Auxiliary Process.
- [4] Linking of processes or establishing the interdependency, Inter relationship and Inter connectedness among the processes.
- [5] Conduct Information Process Flow Analysis (IPFA) using the ECS and OPTM
- [6] Identify the services among the process. Step VII: Analyze the capability, usability of the existing legacy systems in the organization.
- [7] Remove the systems that are totally obsolete.
- [8] Design, Deploy New Systems using Service Oriented Architecture (SOA).
- [9] Reengineer the partly obsolete systems using dynamic program instrumentation.
- [10] Integrate the new systems with the reengineered one.

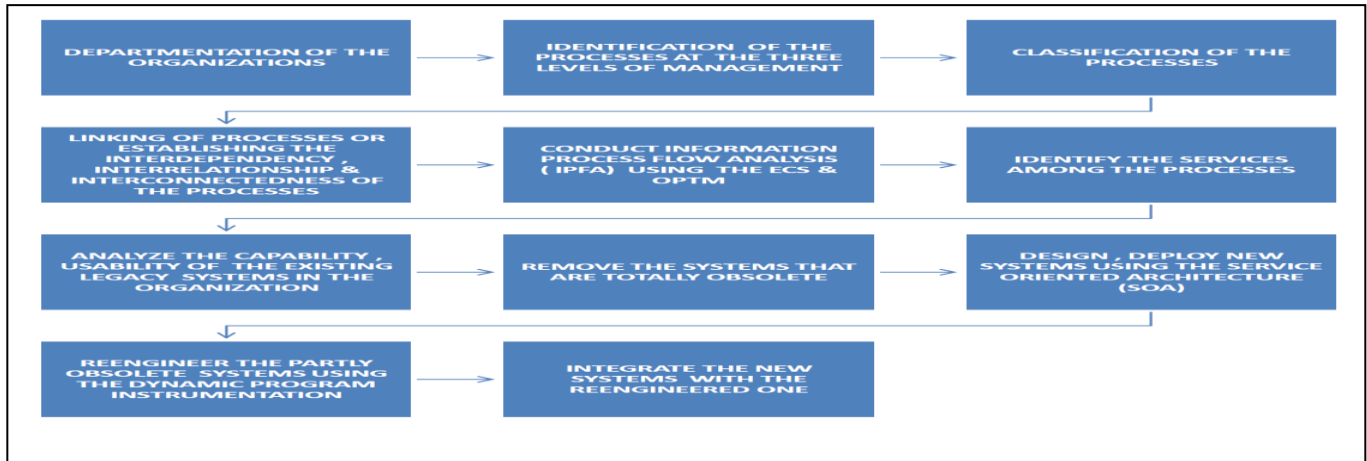


Fig. 1: The Object Oriented Knowledge Based (OKB) Model [Adopted from (Kundu, Ratha, Das, 2012)]

The last six steps of the OKB model is slightly different from their predecessors because these six steps together denote a particular process having four sequential phases Analyze , Design , Reengineer & Integrate and as per the name of these phases, the last six steps of the OKB model has been termed as ADRI approach [22]. Kundu , Ratha and Das's conceptualization of the ADRI approach is quite interesting as well as significant because this approach has been conceptualized with the single objective of combining the concept of services oriented architecture (SOA) and dynamic program analysis to produce a hybrid approach of system analysis, system design, system reengineering and system integration. The uniqueness of ADRI approach lies in the fact that it can perform all the four tasks of system analysis , system design , system reengineering and system integration in order to fulfill the ultimate objective of OKB model i.e. business process reengineering. This approach has six steps and four phases i.e. Analysis, Design, Reengineer and Integrate. All these steps are sequential in nature and these steps are needed to be performed in four phases (Ref. Fig. 2).

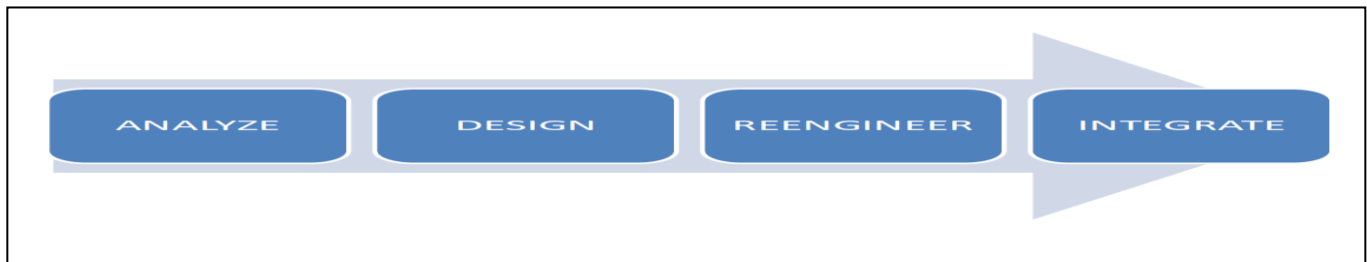


Fig. 2: The Sequential Steps of the ADRI Approach[Adopted from (Kundu, Ratha, Das, 2012)]

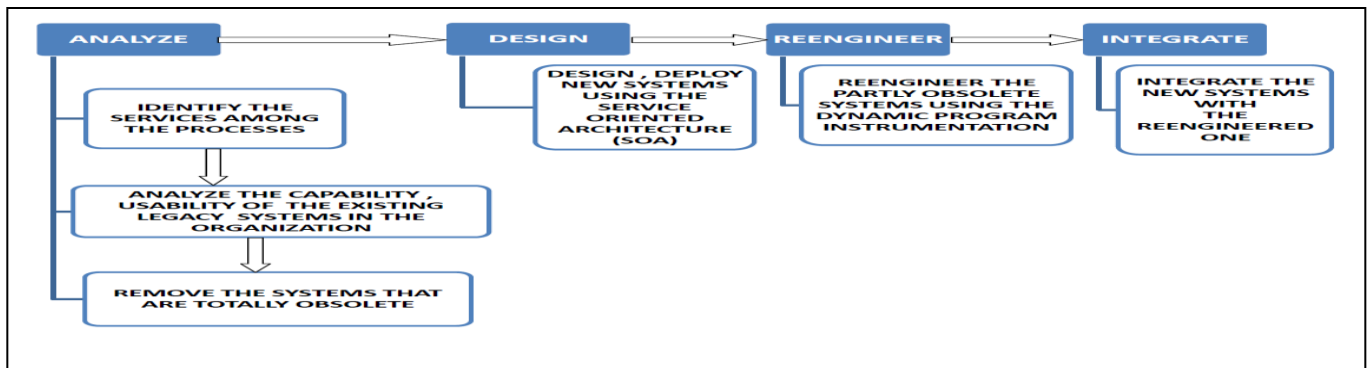


Fig. 3: Relationship between the phases and steps of ADRI approach[Adopted from (Kundu, Ratha, Das, 2012)]

The first phase is Analysis phase which has three steps and the rest of the three phases have one step each. Fig. 3 depicts the relationship between the phases and steps of ADRI approach. Kundu, Ratha and Das's work is seminal because their OKB model has far reaching significance in linking the concepts of SOA with BPR and Reverse Engineering (Ref. Fig.4).

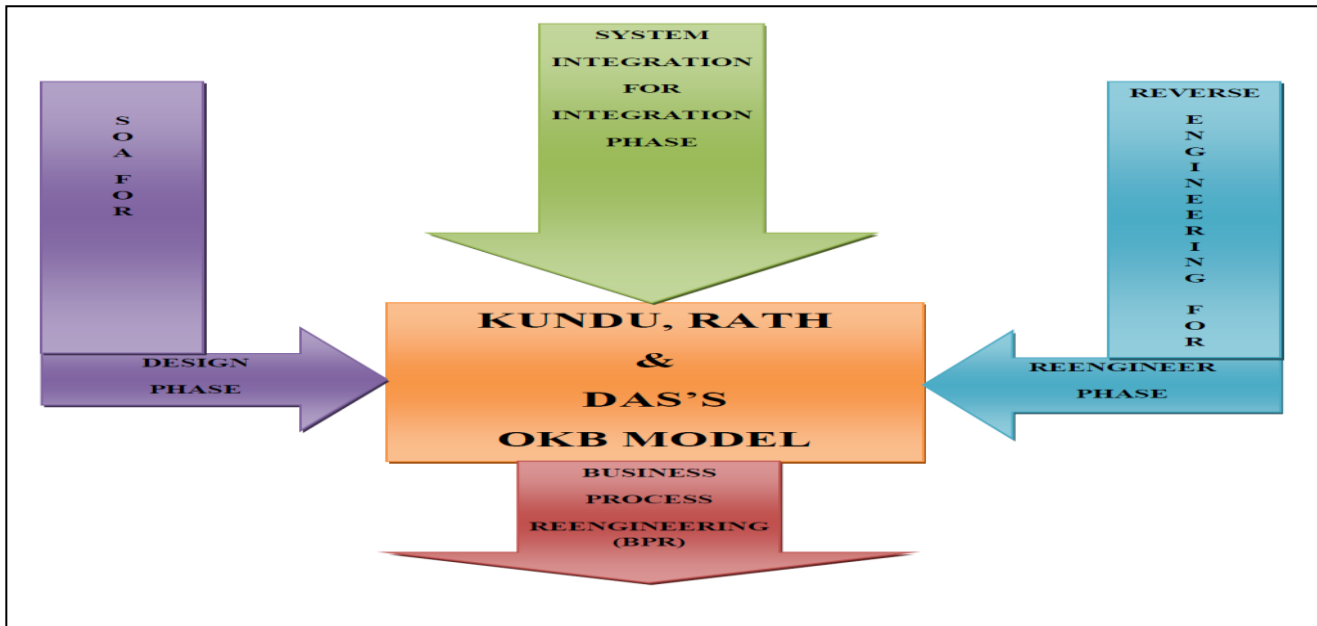


Fig. 4: The OKB Model links the concepts of SOA with BPR and Reverse Engineering

OKB model uses dynamic program instrumentation as a reverse engineering tool in the third phase of the ADRI approach i.e. the Reengineer phase. Again OKB model uses system integration tools in the fourth and final phase of the ADRI approach i.e. the Integrate phase. Also OKB model uses the concepts of SOA as a designing tool in the second phase of the ADRI approach i.e. the Design phase. So the OKB model encompasses the concepts of SOA, Reverse Engineering and System Integration through different phases of the ADRI approach (Ref. Fig.5).

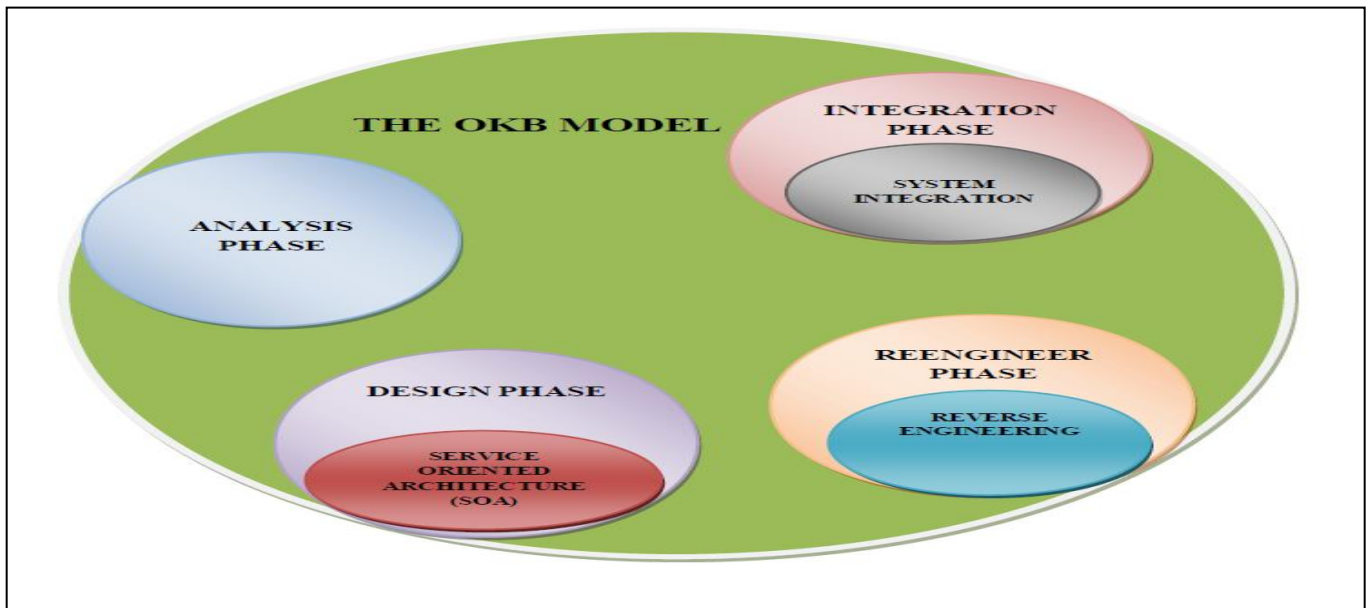


Fig. 5: The OKB Model encompasses the concepts of SOA, Reverse Engineering and System Integration through different phases of the ADRI approach

Das and Kundu developed a conceptual model for implementing a CRM model through SOA approach [22]. Based on Krafzig, Banke and Slama's definition and representation of services in the SOA (Service Oriented Architecture) approach, Das and Kundu attempted to implement a CRM process by applying the concept of SOA([23],[21]). Earlier the researchers faced difficulty in using Web Services effectively because there was no mechanism to describe the web services and that's why in response to the urgent need of describing various characteristics of a web service unambiguously WSDL was created [24]. In the literature, WSDL or Web Services Definition Language has been defined as a specification for describing the methods or data types of SOAP interface [25]. Ethan Cerami described the way of specifying services using WSDL in his book "Web Services Essentials: Distributed Applications with XML-RPC, SOAP, and UDDI & WSDL" [26]. Kundu, Das and Ratha extended the original idea of Das & Kundu's research on application of SOA in implementing a CRM process using the methods described by Ethan Cerami in his book "Web Services Essentials: Distributed Applications with XML-RPC, SOAP, and UDDI & WSDL" and thus developed WSDL specification of services for SOA based implementation of a CRM process[27]. Kundu, Das and Ratha's approach in developing WSDL specification of services for SOA based implementation of a CRM process is of utmost importance and significance because they proposed the roadmap and the WSDL codes to design services as per the SOA specifications which is the cornerstone of the design phase in the ADRI approach [22](Ref.Fig.6).

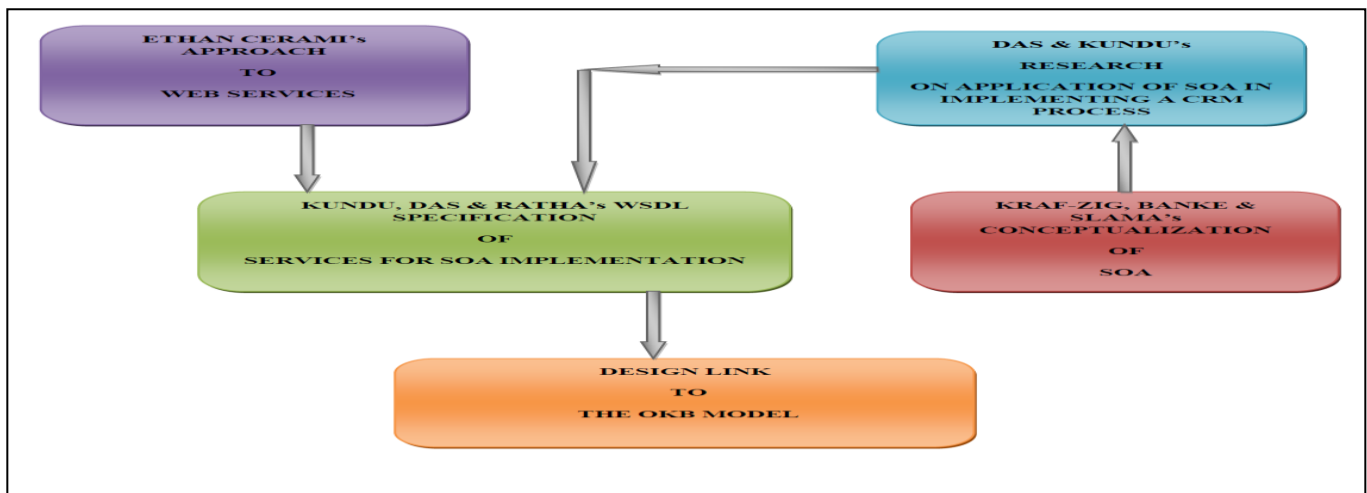


Fig. 6: Design Link to the OKB Model

In connection with the methods of software reverse engineering, Bach et al observe that dynamic program instrumentation can be implemented by performing the program instrumentation on the binary at runtime which will eliminate the need to modify or recompile the software application's source and it will also support the instrumentation of programs that dynamically generate code [28].

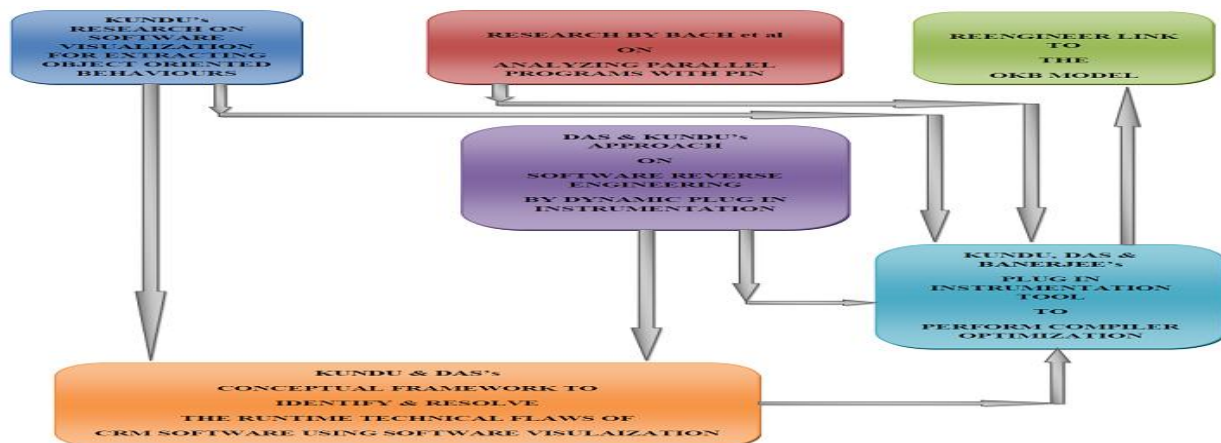


Fig. 7: Reengineer Link to the OKB Model

Based on Bach et al 's approach , Das and Kundu proposed a methodology of software reverse engineering in which an existing software can be reengineered by inserting a new module within the existing software by using dynamic plug-in instrumentation [29]. Kundu's research on software visualization for extracting object oriented behaviour shows that it is also possible to change instrumentation at any time during execution by modifying the application's binary image [30]. Based on Das and Kundu's approach on software reverse engineering by dynamic plug in instrumentation and using Kundu's software visualization approach, Kundu and Das advocated a conceptual framework to identify and resolve the runtime technical flaws of CRM software using software visualization [31]. Kundu and Das's framework serves two purposes; the primary purpose is to identify the runtime technical flaws of the CRM software and to take measures to solve the technical flaws using software visualization which can increase the level of program understanding and the secondary purpose is to use some optimization mechanisms based on death code elimination and code re-ordering approach to reduce the processing time of a CRM software package [31]. Lastly, Kundu, Das and Banerjee designed a plug in instrumentation tool based on all the previous research discussed before to perform compiler optimization and their approach has been used in the reengineer phase of the ADRI approach of the OKB Model to reengineer existing legacy CRM software ([22], [32])(Ref.Fig.7).Analysts and practitioners have developed techniques and methodologies on how to integrate legacy systems into SOA ([33]-[40]) and they believe that the process of integrating legacy systems into SOA starts with the identification of the main points of integration into the legacy mainframe. Under the OKB model, in the last phase of the ADRI approach i.e. the Integrate phase, system integration techniques have been discussed in details for proper integration of the old system with the new reengineered one.

6. Review of Gaps

As the cornerstone of this review paper is the OKB model of business process reengineering (BPR), it is quite natural that the analysis of the gaps among the BPR, SOA and reverse engineering will also involve the limitations and shortcomings of the OKB model. So, the limitations and shortcomings at different phases of the ADRI approach have been identified and also how these shortcomings can hamper the overall applicability and acceptability of the OKB model has been discussed. Kundu, Rath and Das rightly pointed out that as the OKB Model and the ADRI approach is based on the tools and techniques of SOA and reverse engineering, the inherent limitations of SOA and reverse engineering techniques will be present in this new model of business process engineering [22]. From this point of view it can be noted that as the concepts of SOA has been used in the Design phase and reverse engineering techniques have been used in the Reengineer phase of the ADRI approach, the gaps can be classified as Design level gaps and Reengineer level gaps.

6.1. Design Level Gaps

As Kundu, Das and Ratha's approach in developing WSDL specification of services for SOA based implementation of a CRM process provided the much needed roadmap and the WSDL codes to design services as per the SOA specifications which in turn is the cornerstone of the design phase in the ADRI approach [22], Kundu, Das and Ratha's observation on WSDL specification is of utmost importance. Kundu, Das and Ratha observe that the job of specifying the services through WSDL is more conceptual than technical in nature and that's why the description and specification of services through WSDL is not universal in nature and can vary according to the need of the programmer as well as per the clients' requirements [27]. Further, Cerami points out that the WSDL specification of services is the first step towards the SOA implementation of the conceptual CRM model and the actual implementation requires next level of research which is designing the WSDL Invocation Tools as per the IBM Web Services Invocation Framework (WSIF) [26]. Kundu, Rath and Das believe that though the applications of SOA have a promising future, many integration related issues are needed to be addressed while the transformation of legacy systems to SOA or migration to SOA platform [22]. Again, Caine and Hardman point out that as the legacy systems generally have proprietary data definitions; it creates the semantic discrepancy between legacy systems and other applications. [35]. Finally, the issue of standardization of SOA still remains a challenging issue and this is affecting the research in this field because in many cases the researchers find it difficult to assess the actual benefits of the SOA approach as an effective alternative to the existing legacy systems ([42], [43]).

6.2. Reengineering Level Gaps

As the application of dynamic program analysis and plug in instrumentation provide the key to the reengineer phase of the ADRI approach of the OKB model , so limitations and shortcomings of the dynamic program analysis and plug in instrumentation techniques form the basis of the reengineer level gaps. Das and Kundu believe that the dynamic program analysis and program instrumentation is still at the nascent stage and actual application in practice is an uphill task due to lack of efficient and faster program optimization techniques [29]. Kundu, Das and Banerjee point out that the working principle of the proposed plug-in Instrumentation is constrained by the limitation of execution coverage i.e. if the software program on which the proposed technique will be applied never reaches a particular point of execution, instrumentation tool at that point will not collect any data. They further observe that the application of some instrumentation techniques and tools may trigger a dramatic increase in execution time of particular software and this may limit the application of instrumentation tools to debugging contexts [32]. Researchers believe that the instrumentation technique proposed by Kundu and Das in their paper

titled “An Attempt to Analyze & Resolve the Pitfalls in CRM Software through Plug-In Instrumentation” is partially automated and fails to focus on dynamic load balancing issues ([31], [44], [45], [46]). Further, Kundu and Das point out that in their proposed instrumentation tool, security issues are another area where the proposed framework hasn’t focused. They also observe that the challenges of developing a robust instrumentation technique on Windows operating systems lie in managing the kernel/application transitions, injecting the runtime agent into the process and isolating the instrumentation from the application [31]. Finally Kundu, Rath and Das recognize that their paper titled “Revisiting BPR: A New Framework & Model For Future” does not highlight anything about the architecture of the target CPU where the optimized CRM software is needed to be executed because compiler optimization also depends on the target CPU architecture that means on the no of registers usage, type of instruction set, pipelines and number of functional units present etc [22].

7. Conclusion & Future Directions

As this review paper is basically an elementary review encompassing the concepts of Service Oriented Architecture (SOA), Software Reverse Engineering and Business Process Reengineering (BPR) and identifying the linkages and gaps among these concepts from the point of view of the OKB model of BPR, this review paper should act as a base for future scientific works involving a more comprehensive review of literature.

References

- [1] J.H. Manley. Information process flow analysis (IPFA) for reengineering manufacturing systems. *Computers & Industrial Engineering*, vol. 25, issue 1-4, pp. 275-278, September, 1993.
- [2] K.C. Hoffman. Management of enterprise-wide systems integration programs. *Journal of Systems Integration*, vol. 3, issue 3-4, pp. 201 – 224, September 1993.
- [3] J.H. Manley. Enterprise information system modeling for continuous improvement. *Computers & Industrial Engineering*, vol. 31, issue 1-2, pp. 273-276, October, 1996.
- [4] H. Rozenfeld, A.F. Rentes, W. Konig. Workflow Modeling for Advanced Manufacturing Concepts. *CIRP Annals - Manufacturing Technology*, vol. 43, issue 1, pp. 385-388, 1994.
- [5] R. P. Anjard. Re-engineering basics: one of three, new, special tools for management, quality and all other professionals. *Microelectronics Reliability*, vol. 36, issue 2, pp. 213-222. February, 1996.
- [6] S. Jarzabek, W. L. Tok. Model-based support for business re-engineering. *Information and Software Technology*, vol. 38, issue 5, pp. 355-374. May, 1996.
- [7] S. Kim, K. Jang. Designing performance analysis and IDEF0 for enterprise modeling in BPR. *International Journal of Production Economics*, vol. 76, issue 2, pp. 121-133. March 21, 2012.
- [8] K. Mertins, R. Jochem. Architectures, methods and tools for enterprise engineering. *International Journal of Production Economics*, vol. 98, issue 2, pp. 179-188. November 18, 2005.
- [9] E. J. Chikofsky and J. H. Cross II, Reverse engineering and design recovery: a taxonomy, *IEEE Software*, vol.7, issue. 1, 13–17.1990.
- [10] G.C.Harman and M.D.Penta. New frontiers of reverse engineering. FOSE’07 2007 Future of Software Engineering proceedings, pp.326-341, IEEE Computer Society, Washington DC, USA, 2007.
- [11] E.J.Byrne. Software reverse engineering: a case study. *Software: Practice and Experience*, vol.21, issue.12, pp. 1349-1364.1991.
- [12] E.Buss & J.Henshaw. Experiences in program understanding. Proceedings of the 1992 conference of the Centre for Advanced Studies on Collaborative research-Volume 1, pp. 157-189. IBM Press. November, 1992.
- [13] G.Canfora, A.Cimitile & P.B.Lucarelli. Software maintenance. *Handbook of Software Engineering and Knowledge Engineering*, 1, 91-120.2002.
- [14] R.R.Branco. Dynamic Program Analysis and Software Exploitation: From the crash to the exploit code. 2011. Retrieved on January 15, 2012, from http://www.troopers.de/wp-content/uploads/2011/04/TR11_Branco_Dynamic_program_analysis.pdf
- [15] E.Cesar, A. Morajko, T. Margalef, J. Sorribes, A. Espinosa, E. Luque. Dynamic performance tuning supported by program specification. Performance oriented application development for distributed architectures, M.Gerndt, (Ed.), IOS Press, Amsterdam, pp. 35-44.2002.
- [16] R.E.Ladner, R.Fortna, B.H. Nguyen. A Comparison of Cache Aware and Cache Oblivious Static Search Trees Using Program Instrumentation. *Experimental algorithmics: from algorithm design to robust and efficient software*, R.Fleischer, B. M. E. Moret, & E.M.Schmidt, (Eds.), Springer –Verlag, pp.78-92, Berlin, 2002.
- [17] N.Bieberstein, S.Bose, M. Fiammante, K.Jones and R.Shah, *Service Oriented Architecture Compass: Business Value, Planning and Enterprise Roadmap*, Pearson Education, Inc, Upper Saddle River, 2006.
- [18] J.P.Lawler, H.Howell- Barber, *Service Oriented Architecture: SOA Strategy, Methodology and Technology*, Auerbach Publications, 2007.
- [19] N.Bieberstein, R.G.Laird, K.Jones and T.Mitra. *Executing SOA: A practical Guide for the Service Oriented Architect*, Pearson Education, Boston, 2008.
- [20] N.M.Josuttis. *SOA in Practice: The Art of Distributed System Design*, O’Reilly Media Inc, Sebastopol, 2007.
- [21] D.Krafzig, K.Banke, D. Slama. *Enterprise SOA: Service Oriented Architecture: Best Practices*, Pearson Education, Upper Saddle River, 2005.

- [22] P.Kundu, B.K.Ratha and D.Das. Revisiting BPR: A New Framework & Model for Future, International Journal of Engineering Research and Technology, Vol. 1, Issue 8. October2012. Retrieved on January 13, 2012 from <http://ssrn.com/abstract=2169913>
- [23] D.Das, P.Kundu. Application of Service Oriented Architecture (SOA) in Implementing a CRM Process: A Conceptual Approach , Research and Higher Education in Computer Science and Information Technology, S. S. Sau and A. D. Gupta,(Eds.),SM,pp.148-152.Kolkata,2012. Retrieved on 10th April 2012 from <http://ssrn.com/abstract=2016277>
- [24] A.D.Nghiem.IT Web Services: A Roadmap for the Enterprise, Pearson Education, Inc., Upper Saddle River, 2003.
- [25] W.Iverson. Real World Web Services, O'Reilly Media, Inc., Sebastopol, 2004.
- [26] E.Cerami. Web Services Essentials: Distributed Applications with XML-RPC, SOAP, UDDI & WSDL, O'Reilly & Associates Inc., Sebastopol, 2012.
- [27] P.Kundu, D.Das, B.K.Ratha. WSDL Specification of Services for Service Oriented Architecture (SOA) Based Implementation of A CRM Process. International Journal of Scientific & Engineering Research, vol. 3, issue 10, October2012. Retrieved on January 13, 2013 from <http://ssrn.com/abstract=2159799>
- [28] M.Bach, M.Charney, R.Cohn, E.Demikhovsky, T.Devor, K.Hazelwood, A.Jaleel, C.K.Luk, G.Lyons, H.Patil, A.Tal. Analyzing Parallel Programs with Pin. 2010. Retrieved January 15, 2012, from <http://www.cs.virginia.edu/kim/docs/ieeecomputer10.pdf>
- [29] D.Das, P.Kundu. Applications of Dynamic Program Analysis in a CRM Process: A Futuristic Concept. International Journal of Scientific and Research Publications, vol.2, issue. 4, pp. 306-318. Apr.2012. Retrieved on January 13, 2013 from <http://ssrn.com/abstract=2042588>
- [30] P.Kundu. Visualization of Program for Extracting Object Oriented Behaviour & Optimization: A Futuristic Approach. Research and Higher Education in Computer Science and Information Technology, S. S. Sau and A. D. Gupta, (Eds.), SM, pp.108-112. Kolkata, 2012.
- [31] P.Kundu, D.Das. An Attempt to Analyze & Resolve the Pitfalls in CRM Software through Plug-In Instrumentation. International Journal of Scientific and Research Publications, vol. 2, Issue 5, pp. 313 – 320.May, 2012. Retrieved on January 13, 2013 from <http://ssrn.com/abstract=2051886>
- [32] P.Kundu, D.Das, A.Banerjee. Plug-In Instrumentation: A futuristic ICT approach for teaching the Runtime Behaviour of Software. U.G.C Sponsored Seminar on I.C.T in Higher Education: Opportunities & Challenges in the 21st Century Proceedings, SPS Education India Pvt. Ltd., pp. 24-27. Kolkata, 2012. Retrieved on January 13, 2013 from <http://ssrn.com/abstract=2177249>
- [33] A.Papkov. Develop a migration strategy from a legacy enterprise IT infrastructure to SOA-based enterprise architecture. 2005. Retrieved on April 13, 2012 from <http://www.ibm.com/developerworks/webservices/library/ws-migrate2soa/>
- [34] K.Channabasavaiah, E.Tuggle, Jr., K. Holley. Migrating to a service-oriented architecture. 2003. Retrieved on April 13, 2012 from <http://www.ibm.com/developerworks/webservices/library/ws-migratesoa/>
- [35] J.Caine, J. Hardman. Design strategies for legacy system involvement in SOA solutions: Understand the challenges of business transformation using SOA in legacy environments. 2007. Retrieved on April 13, 2012 from <http://www.ibm.com/developerworks/webservices/library/ws-soa-legacy/>
- [36] C.Lawrence. Adapting legacy systems for SOA: Finding new business value in older applications. 2007. Retrieved on April 13, 2012 from <http://www.ibm.com/developerworks/webservices/library/ws-soa-adaptleg/>
- [37] C. Nott. Patterns: Using Business Service Choreography in Conjunction with an Enterprise Service Bus.2004. Retrieved on April 13, 2012 from <http://www.redbooks.ibm.com/redpapers/pdfs/redp3908.pdf>
- [38] M.Keen et al. Patterns: Implementing an SOA Using an Enterprise Service Bus. 2004. Retrieved on April 13, 2012 from <http://www.redbooks.ibm.com/redbooks/pdfs/sg246346.pdf>
- [39] T. Laszewski, J. Williamson. SOA Integration in the Legacy Environment. 2008. Retrieved on April 13, 2012 from <http://www.oracle.com/technetwork/articles/laszewski-williamson-soa-legacy-082027.html>
- [40] M.A.A.Sheikh, H.A. Aboalsamh, A. Albarrak. Migration of legacy applications and services to Service-Oriented Architecture (SOA). International Conference and Workshop on Current Trends in Information Technology (CTIT) Proceedings, pp. 137 – 142, 2011.
- [41] W. Xiaofeng, S.X.K.Hu, E. Haq, H. Garton. Integrating Legacy Systems within The Service-oriented Architecture. IEEE Power Engineering Society General Meeting 2007 Proceedings, pp.1 – 7.2007.
- [42] J.Erickson and K.Siau. Web Services, Service Oriented Computing & Service Oriented Architecture. Principle Advancements in Database Management Technologies: New Applications, K.Siau and J.Erickson, Eds. Hershey, PA: Information Science Reference, pp.176-187, 2010.
- [43] P.A.Baer, Platform Independent Development of Robot Communication Software. Zugl, Kassel: Kassel University Press, 2008.
- [44] C.Xu & F.C.M.Lau, *Load Balancing In Parallel Computers: Theory & Practice*. Norwell, MA: Kluwer Academic Publishers, 1997.
- [45] R.V.Dorneles, R.L.Rizzi, A.L.Martinotto, D.Picinin Jr., P.O.A.Navaux and T.A.Diverio, —Parallel Computational Model with Dynamic Load Balancing in PC Clusters. VECPAR 2004, LNCS 3402, M. Dayde et al., Eds. Berlin Heidelberg: Springer – Verlag, pp. 468-479, 2005.
- [46] K.S.Chatrapati, J.U.Rekha and A.V.Babu, —Recursive Competitive Equilibrium Approach for Dynamic Load Balancing a Distributed System. ICDCIT 2011, LNCS 6536, R. Natarajan and A.Ojo et al., Eds. Berlin Heidelberg: Springer – Verlag, pp. 162-174, 2011.

An Appropriate F -Test for Two-Way Balanced Interactive Model

F.C. Eze¹, F.O Adimonye¹, C.P. Nnanwa² M.I. Ezeani³

¹Department of Statistics, Nnamdi-Azikiwe University, Awka, Nigeria.

² Department of Mathematics, Nnamdi-Azikiwe University, Awka, Nigeria.

³Department of Computer Science, Nnamdi-Azikiwe University, Awka, Nigeria.

Abstract

The presence of interaction in a set of data/ model in a two-way interactive model may lead to a biased result when testing for the main effects. The nuisance parameter which is the interaction was removed from the data without distorting the assumption of homogeneity condition of analysis of variance. This is done by a linear combination such that the differences between the corresponding yield row-wise as well as column-wise difference is a constant and yet the total sum of the yield remains unchanged.

Keywords: Nuisance parameter, Mixed effect model, Least squares method.

1. Introduction

A major set back in design and analysis of experiments is the presence of interaction. A two-way factor interaction may be defined as the change in response due to one factor at different levels of the factor or two independent variables interact if the effects of one of the variables differ depending on the level of the other variable. The presence of interaction may obscure the result for the test of significance for the main effects according to Moore, et al [9]. One may be tempted to vehemently maintain that we should not even test for main effects once we know that interactions are present. Presence of interaction between the two factors means both effects are not independent. In analysis of variance, a large F -value provides evidence against the null hypothesis. However, the interaction test should be examined first. The reason for this is that, there is little point in testing the null hypothesis H_A of the alternative H_B if H_{AB} : no interaction effect is rejected, since the difference between any two levels of a main effect also includes an average interaction effect Cabrera and McDougall [2] argued. Overton [12] gave a quick check for interaction using an example on two binary factors A and B as illustrated below. A simple setting in which interactions can arise is in a two-factor experiment analyzed using Analysis of Variance (ANOVA) can be shown in Table 1. Suppose we have two binary factors A and B. For example, these factors might indicate whether either of two treatments was administered to a patient, with the treatments applied either singly, or in combination.

We can then consider the average treatment response (e.g. the symptom levels following treatment) for each patient, as a function of the treatment combination that was administered Overton [10] argued.

	Factor B	
Factor A	B ₀	B ₁
A ₀	6	7
A ₁	4	5

Table 1: Two-way classification without interaction

In Table 1, there is no interaction between the two treatments. Their effects are additive. The reason for this is that the difference in mean response between those subjects receiving treatment A and those not receiving treatment A is -2 regardless of whether treatment B is administered ($4 - 6 = -2$) or not ($5 - 7 = -2$). It automatically follows that the difference in mean response between those subjects receiving treatment B and those not receiving treatment B is the same regardless of whether treatment A is administered ($7 - 6 = 5 - 4$).

	Factor B	
Factor A	B ₀	B ₁
A ₀	1	4
A ₁	7	6

Table 2: Two-way classification with interaction

In contrast, in the Table 2 there is an interaction between the treatments and hence their effects are not additive. Eze et al [3] developed a common F-test denominator for two-way interactive balanced design. In their work, they removed the interaction from the data and consequently divided the original data by the inverse of the square root of the standard error. Muhammad et al [11] argued that the effect of a medication is the sum of its drug effect placebo effect (meaning response) and their possible interaction. According to them, current interpretation of clinical trials' results assumes no interaction. Demonstrating such an interaction has been difficult due to lack of an appropriate design. However, this paper is set to resolve such problem. Park et al [13] carried out a research on the presence of interaction between direct and carry-over treatment effects by using a model in which the residual effect from a treatment depends upon the treatment applied in the succeeding period. This means a model which includes interaction between the treatment direct and residual effects. They assume that the residual effect do not persist further than one succeeding period. In the presence of higher order interaction, Kherad and Sara [7] demonstrated an exact permutation strategy applicable to fixed effect analysis of variance which can be used to test any factor. James [5] presented a paper similar to Overton [12]. In his paper, he demonstrated some common errors in interpreting interaction effects and the appropriate strategies for achieving post hoc understanding of the origin of detected interaction effects. According to him, a lack of interaction is often signified by parallel lines in a plot of cell means. Conversely, if the lines are not parallel, it signifies the presence of interaction. In ANOVA, a large F-value provides evidence against the null hypothesis. However, the interaction test should be examined first. The reason for this is that, there is little point in testing the null hypothesis H_A or H_B if H_{AB} : no interaction effect is rejected, since the difference between any two levels of a main effect also includes an average interaction. Cabrera and MacDougall [2] argued. Moore et al [9] argued that there are three hypotheses in a two-way ANOVA with an F-test for each. We can test for significance of the main effects A, the main effect B and AB interaction. It is generally a good practice to examine the test interaction first, since the presence of strong interaction may influence the interpretation of the main effects. Some statistical softwares such as XLSTAT, SPSS, Minitab etc can perform the ANOVA test but does not consider the implications of the presence of interactions.

2. Methodology

Given the model for Two-way balanced interactive model

$$y_{ijk} = \mu + \alpha_i + \beta_j + \lambda_{ij} + e_{ijk} \quad \begin{cases} i = 1, 2, \dots, p \\ j = 1, 2, \dots, q \\ k = 1, 2, \dots, r \end{cases} \quad (1)$$

where

y_{ijk} is the kth observation in the ijth cell,

μ is a constant,

α_i is the average effects of factor A,

β_j is the average effects of factor B,

λ_{ij} is the interaction effect that exists between factor A and factor B and

e_{ijk} is the error associated with y_{ijk} .

The least square estimates of the parameters can be shown to be

$$\hat{\alpha}_i = \bar{y}_{i..} - \bar{y}_{...}$$

$$\hat{\beta}_j = \bar{y}_{.j.} - \bar{y}_{...}$$

$$\hat{\lambda}_{ij} = \bar{y}_{ij.} - \bar{y}_{i..} - \bar{y}_{.j.} + \bar{y}_{...}$$

From Table 1, the least square estimates of the cell observations have been calculated and presented in Table 3.

Factor A	Factor B	
	B ₀	B ₁
A ₀	5.5 + 1.0 - 0.5 + 0.0	5.5 + 1.0 - 0.5 + 0.0
A ₁	5.5 - 1.0 - 0.5 + 0.0	5.5 - 1.0 + 0.5 + 0.0

Table 3: Least square estimates of Two-way classification without interaction

From Table 3, the interaction effects are zero.
In contrast, there are presences of interaction effects in Table 2 as shown in Table 4

Factor A	Factor B	
	B ₀	B ₁
A ₀	4.5 - 2.0 - 0.5 -1.0	4.5 - 2.0 + 0.5 +1.0
A ₁	4.5 - 2.0 - 0.5 -1.0	4.5 - 2.0 + 0.5 -1.0

Table 4: Least square estimates of Two-way classification with interaction

2.1 Expected mean squares

In this paper, Brute force method is used in deriving the expected mean squares. Brute force is a trial and error method used by application program to decode encrypted data rather than employing intellectual strategies (Bernstein [1]). Using the Brute force method the expected mean squares for Equation 1 has been derived and presented in Table 5.

S.V	d.f	SS	MS	All effects fixed	All effects random	Factor A & factor B random	Factor A & factor B fixed
Factor A	p-1	SS_{α}	MS_{α}	$qr \sum_i \frac{\alpha_i^2}{p-1} + \sigma_e^2$	$qr\sigma_{\alpha}^2 + r\sigma_{\lambda}^2 + \sigma_e^2$	$qr \sum_i \frac{\alpha_i^2}{p-1} + r\sigma_{\lambda}^2 + \sigma_e^2$	$r\sigma_{\alpha}^2 + \sigma_e^2$
Factor B	q-1	SS_{β}	MS_{β}	$pr \sum_j \frac{\beta_j^2}{q-1} + \sigma_e^2$	$pr\sigma_{\beta}^2 + r\sigma_{\lambda}^2 + \sigma_e^2$	$pr\sigma_{\beta}^2 + \sigma_e^2$	$pr \sum_j \frac{\beta_j^2}{q-1} + r\sigma_{\lambda}^2 + \sigma_e^2$
AB interaction	(p-1)(q-1)	SS_{λ}	MS_{λ}	$r \sum_{ij} \frac{\lambda_{ij}^2}{(p-1)(q-1)} + \sigma_e^2$	$r\sigma_{\lambda}^2 + \sigma_e^2$	$r\sigma_{\lambda}^2 + \sigma_e^2$	$r\sigma_{\lambda}^2 + \sigma_e^2$
Error	pq(r-1)	SS_e	MS_e	σ_e^2	σ_e^2	σ_e^2	σ_e^2
Total	pqr-1	SS_T		-	-	-	-

Table 5: Complete ANOVA Table

From Table 5, there is no obvious denominator for testing for the main effects when the model/data are fixed, random or mixed. For instance, if the data are fixed, the common denominator for testing for the main effects is MS_e . Similarly, if the data were random, the common denominator for testing for the main effects is MS_{λ} under the null hypothesis H_0 . When the data are mixed, the denominator of the F -ratio varies. The reason for this is the presence of interaction. If the interaction is removed from the data, Table 5 reduces to Table 6.

S.V	d.f	SS	MS	All effects fixed	All effects random	Factor A & factor B random	Factor A & factor B fixed
Factor A	p-1	SS_{α}	MS_{α}	$qr \sum_i \frac{\alpha_i^2}{p-1} + \sigma_e^2$	$qr\sigma_{\alpha}^2 + \sigma_e^2$	$qr \sum_i \frac{\alpha_i^2}{p-1} + \sigma_e^2$	$r\sigma_{\alpha}^2 + \sigma_e^2$
Factor B	q-1	SS_{β}	MS_{β}	$pr \sum_j \frac{\beta_j^2}{q-1} + \sigma_e^2$	$pr\sigma_{\beta}^2 + \sigma_e^2$	$pr\sigma_{\beta}^2 + \sigma_e^2$	$pr \sum_j \frac{\beta_j^2}{q-1} + \sigma_e^2$
Error	(p-1)(q-1)	SS_e	MS_e	σ_e^2	σ_e^2	σ_e^2	σ_e^2
Total	pqr-1	SS_T		-	-	-	-

Table 6: Reduced ANOVA Table

From Table 6, the common denominator for testing for the main effects is MS_e under H_0 and the model equation consequently reduces to Equation 2.

$$y_{ijk} = \mu + \alpha_i + \beta_j + e_{ijk} \begin{cases} i = 1, 2, \dots, p \\ j = 1, 2, \dots, q \\ k = 1, 2, \dots, r \end{cases} \quad (2)$$

The parameters have the same meaning as it is in Equation 1.

2.2 Method of removing the interaction

The interactions can be removed from the data/model as follows without distorting the assumptions of analysis of variance. Any linear combination such that the differences between the corresponding yield row-wise as well as column-wise differences is a constant and yet the total sum of the yield remains unchanged eliminates the interaction (Weisstein[15]). Let $x_{11}, x_{12}, \dots, x_{pq}$ be the yields or values in Two-way crossed interactive model with one observation per cell. The data format is shown in Table 7.

Factor A	Factor B				\bar{y}_i	T_i
	1	2	3	... , q		
1	y_{11}	y_{12}	y_{13}	y_{1q}	\bar{y}_1	T_1
2	y_{21}	y_{22}	y_{23}	y_{2q}	\bar{y}_2	T_2
3	y_{31}	y_{32}	y_{33}	y_{3q}	\bar{y}_3	T_3
.
.
.
p	y_{p1}	y_{p2}	y_{p3}	y_{pq}	\bar{y}_p	
T_j	$T_{.1}$	$T_{.2}$	$T_{.3}$	$T_{.q}$		$T_{..}$

Table 7: Data layout of Two-way classification with one observation per cell.

From Table 7

$$\begin{aligned} y_{12} - y_{11} &= k \Rightarrow y_{12} = k + y_{11} \\ y_{13} - y_{12} &= k \Rightarrow y_{13} = k + y_{12} = 2k + y_{11} \\ y_{21} - y_{13} &= k \Rightarrow y_{21} = k + y_{13} = 3k + y_{11} \\ y_{22} - y_{21} &= k \Rightarrow y_{22} = k + y_{21} = 4k + y_{11} \\ y_{ij} - y_{i'j'} &= k \Rightarrow y_{ij} = k + y_{i'j'} = (pq - 1)k + y_{11} \end{aligned} \quad (3)$$

$ij \neq i'j'$

3. Illustrative Example

An engineer is designing a battery for use in a device that will be subjected to some extreme variation in temperature. The only design parameter that he can select is the plate material for the battery, and he has three possible choices. The engineer decides to test all the three materials at three temperature levels- $15^{\circ}F$, $70^{\circ}F$, and $125^{\circ}F$ -as these temperature levels are consistent with the product end-use environment. Four batteries are tested at each combination of plate material and temperature; all 36 tests are run in a random. The experiment and the resulting observed battery life data are given in Table 8.

Material type	Temperature (^o F)			$T_{..k}$
	15	70	125	
1	130, 155, 74, 180	34, 40, 80, 75	20, 70, 82, 58	
2	150, 188, 159, 126	136, 122, 106, 115	25, 70, 58, 45	
3	138, 110, 168, 160	174, 120, 150, 139	96, 104, 82, 60	
				$T_{..1} = 903$
				$T_{..2} = 979$
				$T_{..3} = 959$
				$T_{..4} = 958$
				$T_{...} = 3799$

Table 8: Source: Life Data for battery design from [10] p.207

Using SPSS, the analysis of variance was performed and presented in Table 9.

Source	Type III sum of squares	df	Mean Square	F	Sig
Corrected model	59416.22	8	7427.028	11.000	0.000
Intercept	400900.028	1	400900.028	593.739	0.000
Material	10683.722	2	5341.861	7.911	0.002
Temperature	39118.722	2	19559.361	28.968	0.000
Material*Temperature	9613.778	4	2403.44	3.560	0.019
Error	18230.750	27	675.216		
Total	478547.00	36			
Corrected Total	77646.972	35			

Table 9: ANOVA Table

From the ANOVA Table 9, the main effects and the interaction are significant.

Using the expression derived from Table 7 and Equation (3), the data in Table 8 are now transformed as follows:

For the corresponding entries for y_{11} we have

$$36k - 1170 = 903 \Rightarrow k = -7.42$$

The values of k for the corresponding entries for y_{112} , y_{113} , and y_{114} are -11.56, 8.14, and -18.39 respectively.

The transformed data are shown in Table 10.

Material type	Temperature (^o F)			$T_{..k}$
	15	70	125	
1	130, 155, 74, 180	122.58, 143.44, 82.14, 161.61	115.16, 131.88, 90.28, 143.22	
2	107.74, 120.32, 98.42, 124.83	100.32, 108.76, 106.56, 106.44	92.90, 97.20, 114.7, 88.05	
3	85.48, 85.64, 122.84, 69.66	78.06, 74.08, 130.98, 51.27	70.64, 62.52, 139.12, 32.88	
				$T_{..1} = 902.88$
				$T_{..2} = 978.84$
				$T_{..3} = 959.04$
				$T_{..4} = 957.96$
				$T_{...} = 3798.72$

Table 10: Transformed data of the life Data for battery design

The ANOVA test for the transformed data is shown in Table 11

Source	Type III sum of squares	df	Mean Square	F	Sig.
Corrected model	12815.894	8	1601.987	1.870	0.1070
Intercept	400840.934	1	400840.934	467.952	0.000
Material	11534.304	2	5767.152	6.733	0.004
Temperature	1281.589	2	640.795	28.9680.748	0.48
Material*Temperature	0.000	4	0.000	0.000	1.000
Error	23127.7999	27	856.585		
Total	436784.627	36			
Corrected Total	35943.692	35			

Table 11: ANOVA Table

From Table 11, the interaction between the material and temperature is highly non-significant showing the successful removal of the interaction from the data. However, the material effects are significant while the temperature effects are non-significant. Since the interactions effects are zero, we therefore perform the ANOVA test in absence of the interaction as shown in Table 12.

Source	Type III sum of squares	df	Mean Square	F	Sig.
Corrected model	12815.894	4	3203.973	4.295	0.007
Intercept	400840.934	1	400840.934	537.278	0.000
Material	11534.304	2	5767.152	7.730	0.002
Temperature	1281.589	2	640.795	0.859	0.433
Error	23127.7999	31	746.058		
Total	436784.627	36			
Corrected Total	35943.692	35			

Table 12: Reduced ANOVA Table

The results obtained in Table 12 are the same as the result obtained in Table 11.

If we are to use the method of 3.0 we shall have the same transformed data in Table 10 and ANOVA test in Table 12.

4. Summary And Conclusion

We have successfully derived an expression that would enable us remove the interaction in our data/model. From the illustrative example given, is possible to commit an error when interaction is present in our data. For example, the temperature effects were significant when interaction is present as shown in Table 9. When the interaction effects were removed from the data, the temperature effects became non-significant.

We therefore recommend that analysis of variance test should be done when interaction is highly non-significant or zero.

References

- [1] Bernstein, D.J. (2005), "Understanding Brute Force", Department of Mathematics, Statistics and Computer Science, The University of Illinois, Chicago.
- [2] Cabrera, J., and MacDougall, A. (2002), *Statistical Consulting*. Springer.
- [3] Eze, F.C., Ehiwario, J.C., and Ogum G.E.O (2009), "Common F-test Denominator for Two-Way Interactive Balanced Design", *Natural and Applied Sciences Journal*, Vol.10 N0.2.
- [4] Hinkeman, K and Kempthorne, O (2008), *Design and Analysis of Experiments*, Vol. 1 Second Edition, Willey.
- [5] James, M.G. (2000), "Interaction Effect: Their Nature and Some Post Hoc Exploration strategies", Texas A and M University 77843-4225.
- [6] Kovach Computing Services (2011), "How Can I Use XLSTAT to Run a Two-way Unbalanced Design with Interaction", Anglesey, Wales.

- 7] KHERAD PAJOUH, Sara, RENAUD, Oliver (2010), “An Exact Permutation Method for Testing any Effect in Balanced and Unbalanced Fixed Effect ANOVA”, *Journal of Computational Statistics and Data Analysis*, Vol.54, pp. 1881-1893.
- [8] Michael, W.T. (2001), An Introduction to Statistical Inference and Data Analysis., Department of Mathematics, College of William and Mary, P.O. Box 8795, Williamsburge, VA 23187-8795.
- [9] Moore, D.S., McCablee, G, Duckworth, W., and Sclove, S. (2004), “Practice of business Statistics”, part iv pp 15-17. Palgrave Macmillan.
- [10] Montgomery, D.C. (2001), Design and analysis of experimnts, John Willey and sons.
- [11] Muhammad, M.H., Eman, A., Syed, A., and Muhammad, B.H. (2010), “Interaction between Drug and Placebo Effects: a cross-over balanced placebo design trial”, Center for Clinical Studies and Empirical Ethics, King Faisal Specialist Hospital and Research Centre, Riyadh, Saudi Arabia.
- [12] Overton, R.C. (2001), “Moderated multiple regression for interaction involving categorical variables- a Statistical control for heterogeneous variable across two groups. *Psychol. Methods*, 6(3), pp 218-233.
- [13] Park, D.K., Bose, M., Notz, W.I. and Dean, A. (2011), “Efficient Cross-over Designs in the Presence of Interactions between Direct and Carry-Over Treatment Effects”, *Journal of Statistical Planning and Inference*, 141, (2), 846-860.
- [14] Sabine, L., and Brian, S.E. (2004), A Handbook of Statistical Analyses Using SPSS, Boca Raton, London.
- [15] Weisstein, E. W. (2012), “Linear Combination”, from Mathworld-A wolfran Web Resource.<http://mathworld.wolfran.com/linearcombination.html>.

Deploying Self-Organizing-Healing Techniques for Software Development of Iterative Linear Solver.

Okon S. C.¹ and Asagba P. O.²

¹Department Of Computer Science, Akwa Ibom State University, Ikot Akpaden, Mkpata Enin L. G. A. Akwa Ibom State, Nigeria.

²Department Of Computer Science, University Of Port Harcourt, Choba, Rivers State, Nigeria.

Abstract:

Self-Organization and Self-Healing are fundamental survival/evolutionary techniques in natural complex systems. In this work we present a formal approach to the specification and design of software that can apply the technique of Self-Organization and Self-Healing to survive unforeseen circumstances. We achieved this by engineering a system that can autonomously reconfigure, reorganize its states to overcome faults/errors thus continuing normal, gracefully degrading or enhanced performance at execution time. Our specification shows how we apply structured system analysis and design methodology, neural network and descriptive model as methodologies to engineer software whose constituent parts are designed and developed as rule players as is obtainable in autonomous natural complex systems. Our prototype software is in the area of solving systems of linear equations iteratively. This work can easily be adopted for other software projects by making all modules participate in the software architecture as rule players.

Keywords: Self-Organization, Self-Healing, Software Component Capacity, Rule Player

1. Introduction

This paper presents the methodology used, the analysis and design of the proposed system. We will also present the algorithms for our software prototype, to demonstrate self-organizing-healing principles. We identify with the fact that, it is becoming increasingly important for software to have a built-in capability to adapt at runtime in varying resources, system errors and changing environmental parameters. Our research has shown that various ongoing works exist on modeling self-organizing [5, 6, 7, 14, 15, 19, 21], self-healing [25, 36] based hardware and/or information communication technology systems. We employ a combined therapy for software architecture based on both self-organizing and self-healing software systems. Finally a self-organizing and self-healing mechanism of the software framework is designed and a prototype model developed and analyzed by applying a formal systematic software architecture specification and analysis methodology in order to establish that our system has satisfied the system's time constraint requirements and improve the system's availability and reliability.

2. Methodology

There are several methodologies applicable in the analysis and design of a generic software system. We have decided to use; Structured System Analysis and Design Method (SSADM), Neural Network and Descriptive Models as our methodologies. Here we use models to represent the structure and internal dynamics of individual components, or the deterministic interactions between components. Our model provides leverage on the difficult and important problem of connecting local, autonomous behaviours of individual components to the global, emergent properties of the system. Figure 1 shows the families of models for self-organizing systems. We have used Descriptive model which has assisted us in the modularization of both mechanisms and components of the system. The transformation from a descriptive, validation and analytical model to a self-organizing application is a forward engineering process while that of self-organizing application to the models is reverse engineering process.

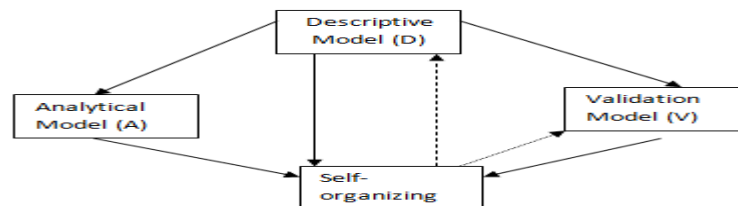


Figure 1: Families of models for self-organizing system

Under modularization, we design the components of our system in modules which are self-similar entities thus defining our software organizational structure. In order to allow modular and reusable modeling that minimizes the impact on the underlying architecture, we proposed a framework based on an organizational approach. We have adopted the Role-Interaction-Organization (RIO) model to represent organizations or systems which enables our module to acquire mechanism for dynamic role playing. We have leaned on this model since it enables formal specification. Neural network principles are used to establish the interaction between the modules.

2.1 Module Capacity

Large scale systems are expected to organize and cooperate in open environments [34]. To satisfy their needs and goals, agents in this case modules often have to collaborate. Thus a module has to be able to estimate the competences of its future partners to identify the most appropriate collaborator. We have introduced the notion of capacity to deal with this issue. The capacity allows us to represent the competences of a module or a set of modules. A capacity is a description of a know-how/service. This description contains at least a name identifying the capacity and the set of its input and output variables which may have default values. The *requires* field defines the constraints that should be verified to guarantee the expected behaviour of the capacity. Then the *ensures* field describe what properties the capacity guarantees, if requires is satisfied. Finally, we add a textual description to informally describe the behaviour of the capacity.

2.1.1 Design of Module Capacity for SOR

Figure 2 defines a modules capacity for SOR Module. This capacity definition applies for the other four modules namely; CGIM, IRM, GSIM, and JAM. Each of them derived their operational competence from the required parameter and their ranking. Table 1 shows the Ranking and Condition for choice module. The ranking is based on their convergence rate.

<p>Name : SuccesiveOverRelaxation</p> <p>Input : The number of equations and unknowns n; the entries a_{ij} of matrix A; the entries b_i of b; the entries XO_i of XO; omega; tolerance; maximum number of iterations.</p> <p>Output : The approximate solution x_1, \dots, x_n or a message that number of iterations was exceeded.</p> <p>Requires : Requires the parameter Omega</p> <p>Ensures : That the solution vector x_1, \dots, x_n is within the tolerance level TOL</p>

Figure 2: The SuccesiveOverRelaxation capacity

However, from the system point of view, we can categorize the systems capacities into three subcategories:

Atomic: The capacity is already present in one of the members of the modules. In this case, the head has to simply request the member possessing the required capacity to perform it.

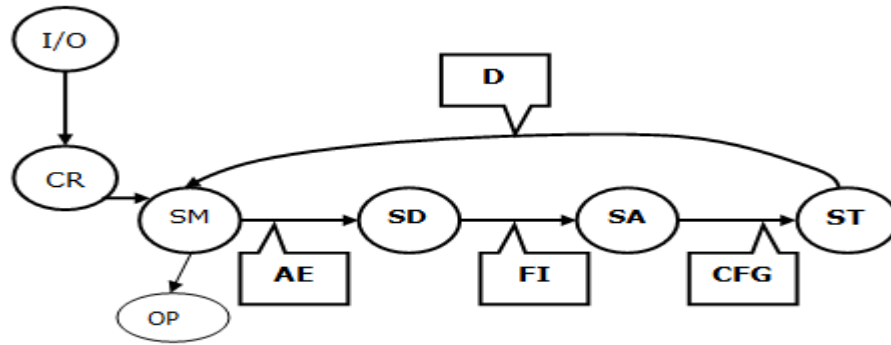
Liaised: The capacity is obtained from a subset of the member's capacities.

Emergent: The capacity is not present as an atomic capacity nor obtained as composition of them, but the capacity emerges from the interactions of the members.

The capacity is atomic for a system if one of the members provides the capacity, but it does not have any implications on how this member obtains this capacity. This taxonomy of capacity is only relative to the system point of view.

3. Analysis Of Self-Organizing-Healing System

Here we used a descriptive model to analysis the operation of a self-organizing-healing system Figure 3 shows input (I/O) being supplied to the system, then a choice (Choose Role Player) is made out of the components present to carry out execution, then the system monitors (Self Monitor) itself for indications of anomalous behavior (Anomalous Event). When such is detected, the system enters a self-diagnosis mode (Self Diagnosis), that is aimed at identifying the fault (Fault Identification) and extract as much information as possible with respect to its cause, symptoms, and impact on the system. Once these are identified, the system tries to adapt (Self Adaptation) itself by generating candidate fixes (Candidate Fix Generation), which are tested to find the best target state (Deployment). Output is published if there is no error.



Key

I/O – Input/Output	CR – Choose Role player
SM - Self Monitor	AE – Anomalous Event
SD – Self Diagnosis	FI – Fault Identification
SA – Self Adaptation	CFG– Candidate Fix Generation
ST – Self Testing	D – Deployment
	OP - Output

Figure 3: Descriptive model of Self-organizing-healing System.

4. Design

This section presents the design showing the system architecture with components interconnections.

4.1 Design of the New System

Research has shown that almost 80% of software fault is due to design flaws, while almost 20% is caused by data flaws [9]. Our solution to design flaws is to construct our software in a modular form, where each module has the capacity of solving the same problem, thus implicitly applying design diversity. Some of the techniques used here to solve systems of linear equations rearrange the matrix A (say into diagonal matrices). This rearrangement of the data sets provides for a solution to an envisaged data flaw by applying data diversity. Our software prototype is dissected into two main operational modes namely; Self-organizing mode as shown in Figure 4 and self-healing mode as shown in Figures 5, 6, 7, 8 where bio-inspired computing as applied in hardware engineering are now being projected into software reliability engineering. Self-organization refers to a property by which complex systems spontaneously generate organized structures, patterns or behaviors from random initial conditions. It is the process of macroscopic outcomes emerging from local interactions of components. In our software prototype we developed SOR, CGIM, IRM, GSIM, and JAM as modules and enable them to interact in order to achieve the system goal. Here the system receives input (the required parameter) from the input file, then autonomously chooses the module with the capacity to solve the problem. Self-healing mode enables our prototype to automatically detect, diagnose and repair localized software problems. Hence it is able to perceive that it does not operate correctly and, without human intervention, makes the necessary adjustments to restore itself to normalcy (leaning on the ranking of the modules). Our software prototype is based on five methods of solving systems of linear equations iteratively. It demonstrates self-organization and self-healing principles at run time and is highly reliable and robust.

4.2 Components of the New System

Our new system is a programmable Self-Organizing-Healing System which has answered the following questions. Can software re-arrange its parts and evolve towards better performance? Can a swarm of software agents self-organize, self-heal and collectively innovate in problem solving tasks?

Figure 4 shows an overview of Self-organized Software Modules in interaction. The system behaviour is based on the assumption that the role player has the ability and capacity to Solve Linear Equations Iteratively. As long as the implementation honors the constraints established by the capacity, the module is authorized to play the role. In our Prototype, five implementations are present. The SOR owns an implementation based on the Successive over relaxation algorithm, JAM obtains its capacity through Jacobian method, GSIM obtains its capacity from Gauss Seidel technique, CGIM obtains its capacity through conjugate gradient iterative technique while IRM obtains its capacity through iterative refinement method.

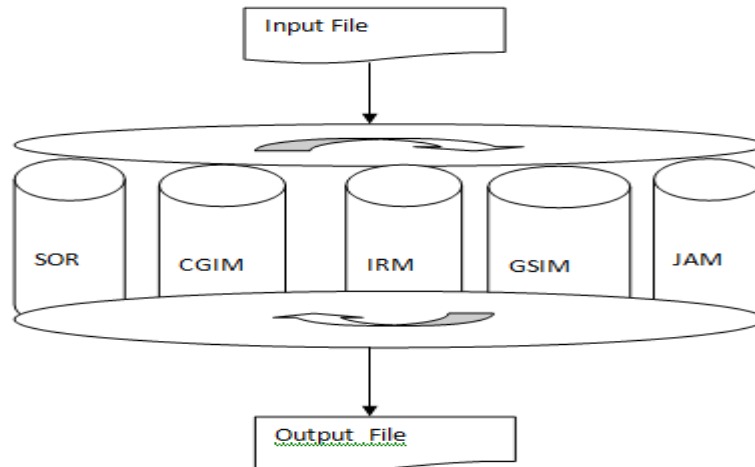


Figure 4: Overview of Self-organized Software Modules in interaction (role interaction basis).

4.3 Schematic Diagrams of the Proposed System.

Here, we will present our proposed system in pictorial forms. Figure 5 shows a descriptive model of our Self-organizing system, demonstrating a network of five modules namely; SOR, CGIM, IRM, GSI, and JAM. Figure 6 shows a neural network representation, where each module is a node at the hidden level in the network and can processes information using a connectionist approach. Like other artificial neural network our system changes its structure base on external or internal information flow through the network. In Table 1, the required parameter is shown. This is the external signal, which triggers state change. Figure 5 forms our descriptive model that enable us to illustrate the network of simple processing element (modules) that exhibit complex global behavior determined by connections between modules and certain parameters (required parameter). Our algorithms are designed to alter the strength (capability) of the connections in the network to produce the desired signal flow through the system. Our attraction in using neural network is that; given a set of systems of linear equations to be solved, our system can use a set of observations to find the solution optimally; this simply means that our system can learn in a supervised manner. Our System based on artificial neural network can self-organize by creating its own organization or representation of the information it receives. It is also capable of graceful degradation in the face of fault or partial destruction, thus retaining the system capability by reconfiguring its state were another module will render the needed services as shown in figures 7, 8, 9 and 10.

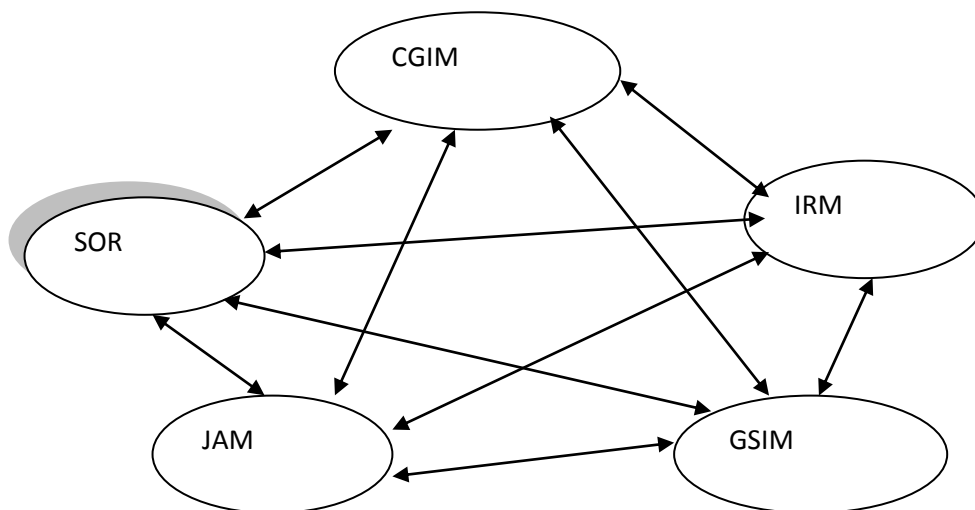
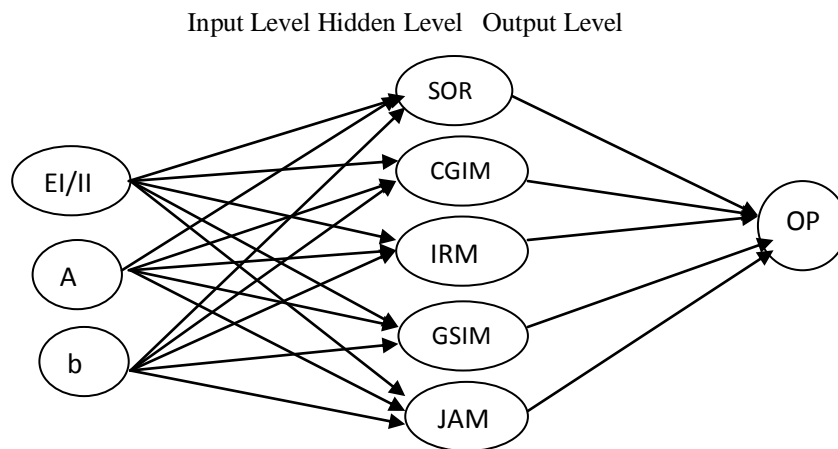


Figure 5: A descriptive model of our Self-organizing system

Table 1: Ranking and Condition for choice module

RANK	MODULE	REQUIRES PARAMETER
1	SOR	Omega
2	CGIM	Pre-condition inverse matrix
3	IRM	'A' the coefficient of X being ill-conditioned
4	GSIM	Few iterations needed
5	JAM	More iteration needed



Key:EI/II-External Input (Required Parameter)/
Internal Input (Rank), A-Matrix A, b – Vector b,
OP- Output (Mode, Scheme, Solution Vector, etc).

Figure 6: Neural Network representation of new system

Figure 7 shows self-healing mode with Recovery block Scheme were SOR was used while executing under self-organization. Figure 8 is for self-healing mode if IRM was used while executing under self-organization. The system continues to change its state/structure based on internal or external input. Consequently, the network structure continues to change until the desired result is found, being one of the benefits of using neural networks. Thus at the failure of self-organizing mode the four other modules are used as alternative modules until result is found.

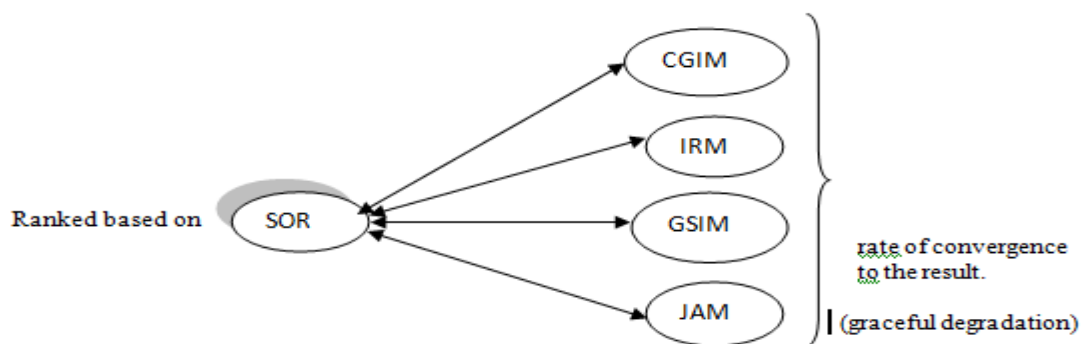


Figure 7: Recovery block as SOR fails in Self-Organization mode

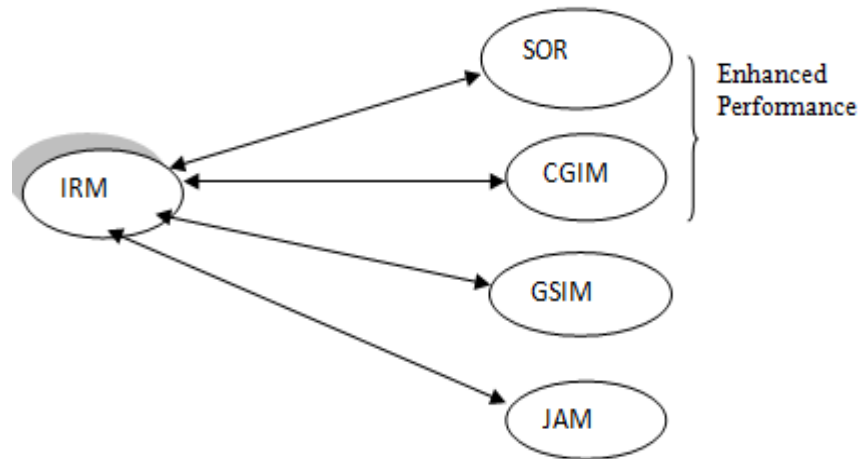
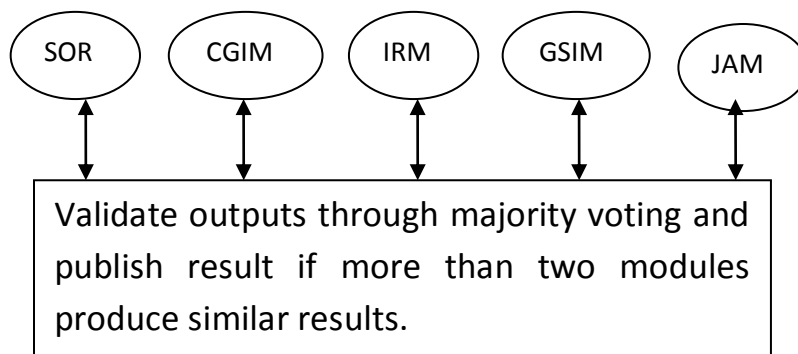


Figure 8: Recovery block as IRM fails at Self-Organization mode.

If the recovery block scheme fails to produce acceptable result, the self-healing mode enters into the N-version scheme as shown in Figure 9. Here the system carry out a majority vote on all the results from all the module, if more than two modules have the same/similar result the result is adopted and publish as the answer.



Para venture, N-version scheme of the self-healing mode fails to produce a result, the system state change to Consensus Recovery block. Here the importance of the algorithm use in testing the result for acceptability is reduced as like other algorithms it may have its own fault. The result of the N-version may not agree due to round-off errors and or hardware constraints (e.g. word length). This may lead to rejection of multiple correct results by the N-version scheme. Here some of the results submitted by the N-version are deem to be correct hence a modified recovery block is entered were a variant of the acceptance test that does not test for correctness but test whether any of the results falls within an acceptable region is used and if that happen the result is announced otherwise a system failure is announces as shown in Figure 10.

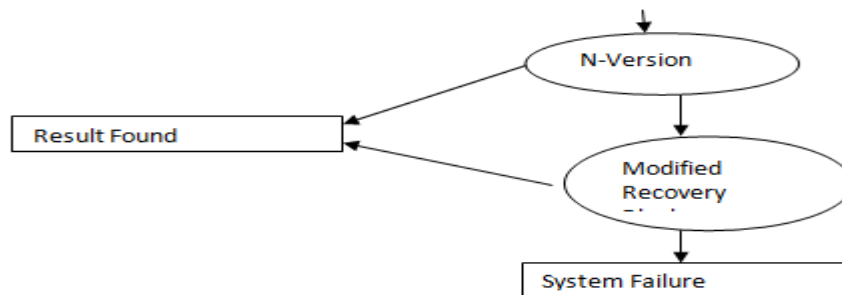
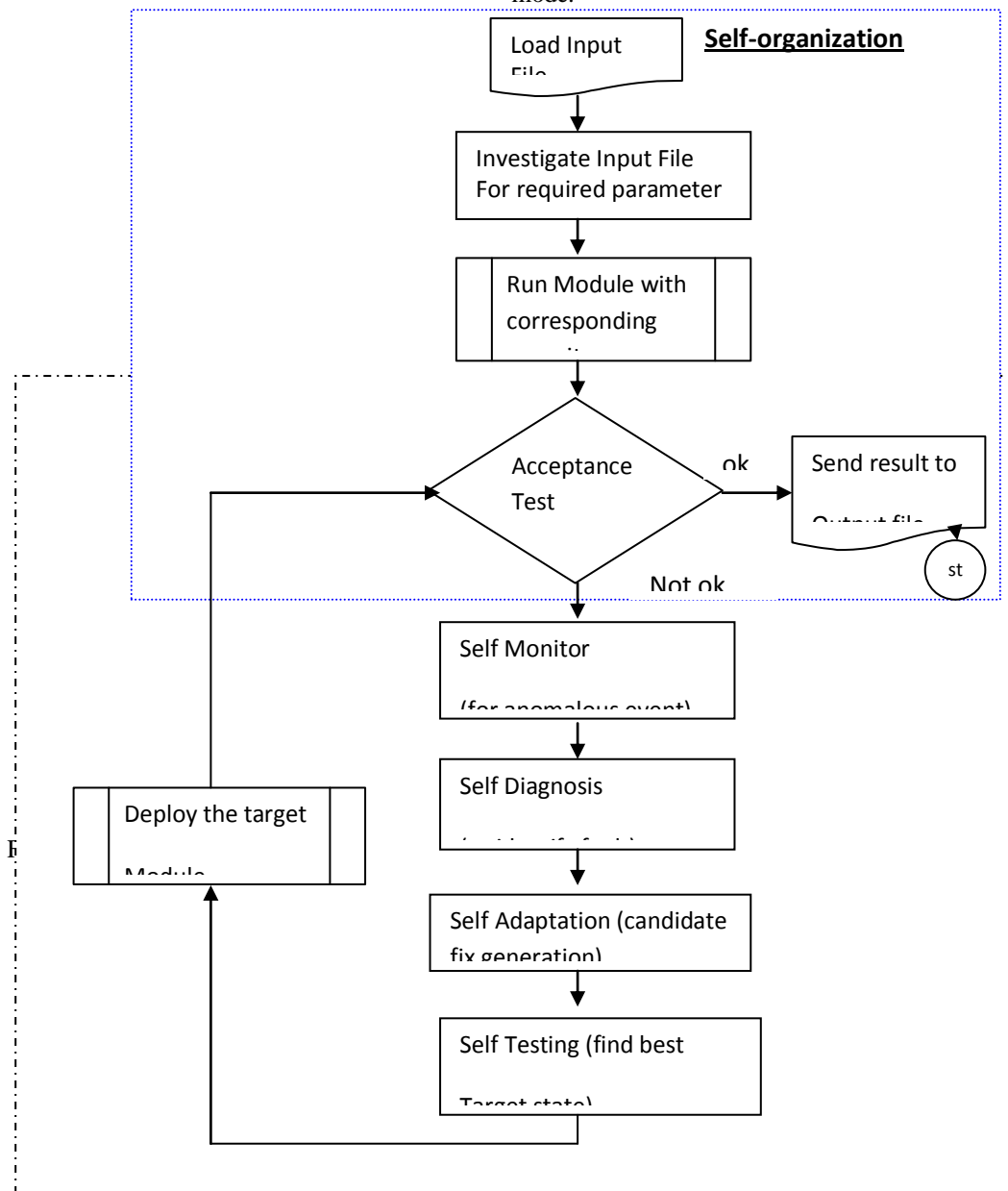


Figure 10: Consensus Recover Block

4.4 System Flowchart of the new System

The figure 11 shows the System Flowchart of the new system highlighting the self-organization and self-healing mode.



4.5 Algorithm for the Self-Organizing-Healing System

In this section we present the algorithm of the Self-organizing-healing software system. Step 1-5 falls under self-organization while step 6-11 falls under self-healing. In steps 6, 7, 8, 9 and 10 the system state is reconfigure and an appropriate scheme is loaded for execution.

1. Load Input File.
2. Search Input File for Required Parameter.
3. Execute Module with corresponding Capacity
4. Submit result for Acceptance Test
5. If result satisfies the Acceptance Test, publish the result and Stop
6. Perform Self Monitor.
7. Perform Self Diagnosis.
8. Perform Self Adaptation
9. Perform Self Test

10. Deploy Target Module.
11. Goto Step 4.

4.6 Design Specification

The System is design to receive input from an Input file, the input include the matrix A, the vector b, the initial approximations and the required parameter as shown in Figure 12. Figure 13 shows the specification of the output file.

$\begin{matrix} A_{11} & A_{12} & A_{13} & b_1 \\ A_{21} & A_{22} & A_{23} & b_2 \\ A_{31} & A_{32} & A_{33} & b_3 \\ I_1 & I_2 & I_3 & \\ R_1 & R_2 & R_3 & R_4, R_5 \end{matrix}$	$\begin{matrix} A_{11} & A_{12} & A_{13} & A_{14} & b_1 \\ A_{21} & A_{22} & A_{23} & A_{24} & b_2 \\ A_{31} & A_{32} & A_{33} & A_{34} & b_3 \\ A_{41} & A_{42} & A_{43} & A_{44} & b_4 \\ I_1 & I_2 & I_3 & I_4 & \\ \square & \square & \square & \square & \square \end{matrix}$
---	--

Figure 12: Input File Format, where A_{ij} are elements of Matrix A, b_i are elements of scalar b, I_i are initial approximations and R_i are the required parameters

Mode of Operation: _____

Scheme: _____

Module Name: _____

Solution Vector: _____

Number of Iteration: _____

Tolerance: _____

Figure 13: Output File Format.

5. Conclusion

Our paper presents self-organization and self-healing as useful techniques in engineering a safety software system. These ensure software reliability and availability of the resulting software product. Natural Complex Systems have shown resilience in terms of reliability by employing self-organization and self-healing of itself and or its components; it is therefore recommendable for Software Engineers to embrace these techniques in their attempt at developing reliable and available software systems especially in safety critical application.

References

- [1] Bar-Yam, Y. and Minai, A. A. (2006), "Complex Engineered Systems: Science Meets Technology", Springer.
- [2] Beal, J. and Bachrach, J.(2006), Infrastructure for engineered emergence on sensor/actuator networks, IEEE Intelligent System. 21 (2), pp. 10–19.
- [3] Bloch, I. (1995); Information Combination Operators for Data Fusion: A Comparative Review with classification. IEEE Transaction on Systems, Man and Cyber metrics.
- [4] Buttazzo G. C. (2005); Hard Real Time Computing System: Predictable Scheduling Algorithms and Applications. Kluwer Academic Publishers, Norwel, Ma, USA.
- [5] Camazine S., Deneubourg J., and Bonabeau (2001); Self-organization in Biological Systems, Princeton University Press.
- [6] Camazine, Deneubourg, Franks, Sneyd, Theraulaz, Bonabeau,(2003). "Self-Organization in Biological Systems", Princeton University Press. ISBN 0-691-11624-5 --ISBN 0-691-01211-3.
- [7] Christian P. (2005); Self-organization in Communication Networks: Principles and Design Paradigms, IEEE Communication Magazine.
- [8] Denney, R. (2005), "Succeeding with Use Case: Working smart to deliver Quality. Addison- Wesley Professional Publishing.
- [9] Dubey A. (2006); Towards a Verifiable Real-time, Autonomic, Fault Mitigation Framework For Large Scale Real-time System. Innovations in Systems and Software Engineering, N ashville, TN 37203, USA

- [10] Doursat, R.(2006), “The growing canvas of biological development: multiscale pattern generation on an expanding lattice of gene regulatory networks”, *InterJournal: Complex Systems* 1809.
- [11] Doursat, R. (2008), “Programmable architectures that are complex and self-organized: from morphogenesis to engineering, in 11th Int’l Conf. Simulat. Synth. Living Syst.(ALIFE XI), pp. 181–188, MIT Press.
- [12] Doursat, R. and Ulieru, M. (2008), Emergent engineering for the management of complex situations, 2nd Int’l Conf. Autom. Comput. Commun. Syst. (Autonomics).
- [13] Doursat, R. (2009), “Facilitating evolutionary innovation by developmental modularity and variability. Generative Dev. Syst. Workshop (GDS 2009), 18th Genet. Evol. Comput. Conf. (GECCO).
- [14] Doursat, R. (2010), “Morphogenetic Engineering weds Bio Self-organization into Human Designed Systems”, Complex Systems Institute, Paris Ile-de-France, CREA, Ecole Polytechnique, Paris, France.
- [15] Doursat, R., Sayama, H., and Michel, O. (2010), “Morphogenetic Engineering: Toward Programmable Complex Systems”, NECSI Studies on Complexity, Springer.
- [16] Doursat, R. (2011), “The myriads of Alife: importing complex systems and self- organization into engineering”, Proc. 3rd IEEE Symp. Artificial Life (IEEE-ALIFE), pp.xii–xix.
- [17] Emmanuel Adam and René Mandiau.(2005). A hierarchical and by role multi-agent organization: Application to the information retrieval. In ISSADS, pages 291–300, 2005.
- [18] Endy, D. (2005), “Foundations for engineering biology”, *Nature* 438, pp. 449–45.
- [19] Eric Matson and Scott A. DeLoach.(2005). Autonomous organization-based adaptive information systems. In IEEE International Conference on Knowledge Intensive Multiagent Systems (KIMAS ’05), Waltham, MA, April 2005.
- [20] Eric Matson and Scott A. DeLoach.(2005). Formal transition in agent organizations. In IEEE International Conference on Knowledge Intensive Multiagent Systems (KIMAS ’05), Waltham, MA, April 2005.
- [21] Falko D. (2007), “Self-organization in Sensor and Actor Network”, Wiley & Sons.
- [22] Ghosh, D., Sharman, R., Rao, H.R., and Upadhyaya, S. (2007), "Self-healing systems- Survey and synthesis", *Decision Support Systems*, 42(4):2164–2185,2007.
- [23] Kennedy, J. and Eberhart, R. C. (1995), “Particle swarm optimization”, Proc. IEEE International Conference on Neural Networks, pp. 1942–1948.
- [24] Mikhail P. (2008), “Advances in Applied Self-organizing Systems”, Springer.
- [25] Modafferi, S., Mussi, E., and Pernici, Barbara (2006), “A Self-Healing plug-in for Ws-BPEL engines, Middleware for Service Oriented Computing (MW4SOC)”, Workshop of the 7th International Middleware Conference Nov. 2006, Melbourne, Australia
- [26] Musa, J. D. (2005). Software reliability engineering: more reliability software faster and cheaper, 2nd Edition, AuthorHouse.
- [27] Myrna E. (2006), “Self-organizing Natural Intelligence: Issues of Knowing, Meaning, and Complexity, Springer-Verlag.
- [28] Nabuco, O., Halima, R. Ben, Didra, K., Fugini, M. G., Modafferi, S., and Mussi, E.,(2008), “Model-based QoS-enabled self-healing Web Services”, EN-FINES’08 DEXA Workshop, Turin.
- [29] Okon S. C. (2006); A Fail-safe Strategy for Scientific/Engineering Project (A Tool for Sustainable Development). *Journal of Sciences and Technology Research* Vol. 5 No. 2, pp. 6-9.
- [30] Okon S. C. (2006); Microprocessor Devices (Computer) like Man; A Self-organizing System. *Journal of Research in Physical Sciences* Vol. 2 No. 4 pp. 1-7.
- [31] Ricard V. and Jordi B. (2006), “Self-organization in Complex Ecosystems”, Princeton University Press.
- [32] atnam A., Kai G. , and Alice A. (2007); A Framework for Intelligent Sensor Validation, Sensor Fusion, and Supervisory Control of Automated Vehicles in IVHS. Intelligent System Research Group, Department of Mechanical Engineering, UC Berkeley.
- [33] Scott K. J. A. and Engstrom D. A. (2006), “The Complementary Nature”, MIT Press, Cambridge, MA.
- [34] Sebastian Rodriguez, Vincent Hilaire, and Abder Koukam(2005). Fomal specification of Holonic multi-agent system framework. In Intelligent Agents in Computing Systems, International Conference on Computational Science (3), number 3516 in LNCS, pages719–726, Atlanta, USA.
- [35] Takahashi, M. and Kamayachi, Y.(1995), “An Emprical study of a Model for Program Error Prediction,” Proc. Int. Conference on Software Engineering, Aug. pp. 330-336.
- [36] The WS-Diamond Team (2008), “Self-healing Web Services in the WS-DIAMOND project”. Proc. E-Challenges Conference, October 2008, The Hague.
- [37] Ulieru, M. and Doursat, R. (2011), “Emergent engineering: a radical paradigm shift”, *International Journal on Autonomous and Adaptive Communication System. (IJAACS)* 4(1), pp. 39–60.
- [38] Wasson, C. S. (2006), “System analysis, design and development”, John Wiley & Sons. ISBN 0471393339.

Computation of Least Cost Pipe Network –An Alternate Method

Briti Sundar Sil¹, Ajeet Kumar², Pallavi Saikia³, P. Jarken Bui⁴, Preetam Banerjee⁵

¹Asst. Prof, Department Of Civil Engineering, Tezpur University, Assam
^{2,3,4,5} Btech Student, Department Of Civil Engineering, Tezpur University, Assam

Abstract

The paper is based on the optimal design of pipe networks for the water distribution. The treated water has to be supplied to the consumers in their individual homes. This function of carrying water is accomplished through well planned distribution system with optimal design of pipes as it comprises the major investment in the system. So for economy and cutting down huge expenditures, design of water distribution networks has to be such that the cost incurred is minimal and simultaneously it meets the demands and discharges at various outlets of the network. The problem in this paper has thus been solved with a view to reduce the cost of pipe networking with the required amount discharge in the outlet, Hardy Cross Method has been used for estimating the required discharge in each outlet of the pipe network, and optimization of the system has been done to reduce the cost with the help of Microsoft-excel. The proposed optimization setup has been very close to the original value, thereby validating its use for optimization.

1. Introduction

A water distribution network is a system by which the water treated in a treatment plant is distributed to the consumers in their individual homes. Therefore the water to be supplied in the houses is carried through a system, this system for distributing water contains pipes, reservoirs, pumps, valves of different types, which are connected to each other to provide water to consumers or when expanding the existing system to larger population. It is a vital component of the urban infrastructure and requires significant investment. The process of distributing water generally consists of different phases like designing of layout for distributing system, designing of pipe network and process of operation. The problem of optimal design of water distribution networks has various aspects to be considered such as hydraulics, reliability, material availability, water quality, and infrastructure and demand patterns. The objective here is to determine the optimal diameters of pipes in a network with a predetermined layout. This includes providing the pressure and quantity of the water required at every demand node. The problem of optimizing network requires the determination of pipe sizes from a set of commercially available diameters ensuring a feasible least cost solution. Here we have considered a two – loop network supplied by gravity, with the objective of determining the minimum cost for a given layout. Here we will be dealing with the determination of the optimal diameters of pipes in a network with a predetermined layout. The cost of realizing the network is a function of the diameters. The smaller the diameter, the lower is the price. However the energy head at the consumers also decrease, therefore the problem is to minimize the cost under the constraint that the energy heads at the interior nodes are above some given lower limits. The loss of head and the discharge in every loop forming the pipe network system is determined through Hardy Cross Method where trial distribution of discharge at each node is done in such a way that continuity equation is satisfied. The algebraic sum of the pressure drops around a closed loop must be zero, i.e. there can be no discontinuity in pressure. This secures the overall mass balance in the network. For n nodes in the network, this can be written as

$$\sum_{i=0}^n Q_i = 0 \quad 1$$

Where Q_i represents the discharges into or out of the node i . The desired discharge value for the predetermined loop of the network system is then being optimized, considering the diameters of the pipes in the network as decision variables, the problems can be considered as a parameter optimization problem with dimension equal to the number of pipes in the network. Market constraints, however, dictate the use of commercially available pipe diameters. With this constraint the problem can be formulated in Microsoft Excel, where the optimization is done by Newton – Raphson Method.

2. Literature Review

As the pipe networking works involve a huge amount of money, so there have been many endeavors to optimize the pipe networks so that the cost gets lowered. Various methods of optimization have been developed, implemented and validated on many different pipe networks by many researchers so far. Most of the works of optimization have been applied on some standard water distribution networks like the Two-loop water distribution network (first presented by Alperovits and Shamir in 1977 consisting of 7 nodes, 8 pipes and two loops, fed by gravity from a reservoir with a 210m fixed head. As the scope of this work deals with the optimization of two loop pipe network presented by Alperovits and Shamir, we will be discussing the various works carried out earlier on optimization of two-loop network.

The two-loop network, shown in figure 1, was originally presented by Alperovits and Shamir (1977), followed by Goulter *et al.* (1986), Kessler and Shamir (1989), Savic and Walters (1997), and Cunha and Sousa (1999). The network has seven nodes and eight pipes with two loops, and is fed by gravity from a reservoir with a 210-m (=689 ft.) fixed head. The pipes are all 1000m (=3281 ft.) long with a Hazen-Williams coefficient C of 130. The minimum head limitation is 30m (=98.4 ft.) above ground level.

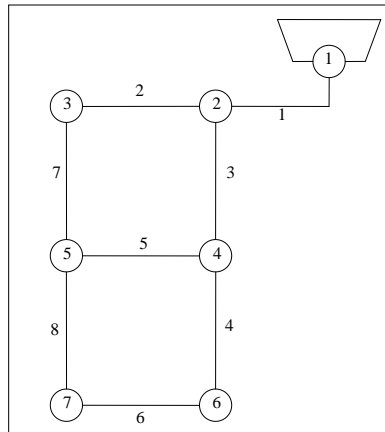


Figure 1. A Two loop network

Alperovits & Shamir (1977) methods for optimal design of looped systems which was divided into two methods. In first method they used An optimization solver at each iteration of the optimization. The solver first solves for the head loss and calculate discharges in the pipe network, then uses the solutions in some procedure to modify the design. The second method does not use a conventional network solver. The minimum cost of the proposed two loop pipe network was obtained as \$ 497,525 by Alpoerovits and Shamir. Goulter *et al.* (1986) further modified the work following LP method and the result obtained was \$435,015. Kessler and Shamir also modified the work and obtained the results as \$ 417,500. Both Goulter *et al.* and Kessler and Shamir used the LP approach and modified the work by optimizing the network by changing the pipe diameters. Cunha and Sousa (1999) used the Simulated annealing (SA) method and found the cost \$ 419,000. Savic and Walters (1997) took Genetic algorithm (GA) for optimization and obtained results of \$ 419,000 each. A genetic algorithm is a member of class of search algorithms based on artificial evolution.

3. Objective Of The Present Study

Objective of the present study is to provide a solution for optimization using Microsoft Excel solver tool. The objective here is to determine the optimal diameters of pipes in a network with a predetermined layout. This includes providing the water required at every demand node satisfying the minimum required conditions of pressure and quantity (discharge). The objective here, requires the determination of pipe sizes from a set of commercially available diameters ensuring a feasible least cost solution and that too without the involvement of such technical complexities which are present in most of the complex programs, algorithms and search mechanisms employed for optimization so far.

3.1 Methodology

In the present study, the two-loop network where flow occurs due to gravity is taken into account. It was first formulated using Linear Programming Gradient method by E. Alperovits and U. Shamir (1977). The aim of the water distribution network analysis is to find least cost pipe network by optimizing pipe diameters in such a way that the analysis fulfills water demand and required pressure head in every node. To find out the optimal values, two modules, namely hydraulic module and an optimization module are brought into consideration. Both the process has been compiled using a solver application of excel spreadsheet.

3.2 Model Formulation

The model which has been formulated to accomplish the required task is done by formulating a hydraulic module which deals with the hydraulic aspects and the optimization module which deals with the optimization aspect and then compiling both the processes using a solver application in Microsoft excel spreadsheet. Flow chart of the model is shown in figure 2.

3.3 Hydraulic module:

Analysis of pipe network

For the analysis of pipe network, the following two necessary conditions must be satisfied.

1. The algebraic sum of the pressure drops around a closed loop must be zero, i.e. there can be no discontinuity in pressure.
2. The flow entering a junction must be equal to the flow leaving the same junction; i.e. the law of continuity must be satisfied. Based upon these two basic principles, the pipe networks are generally solved by the method of successive approximation because any direct analytical solution is not possible. The analysis of a pipe network requires many equations, most of which being nonlinear, to be solved simultaneously. The important methods used for solving such problems are briefly discussed in the next section 4.1.3.

4. Hardy-Cross Method

The procedure suggested by Hardy and Cross (Garg S.K, 1977) requires that the flow in each pipe be assumed by the designer (in magnitude as well as direction) in such a way that the principle of continuity is satisfied at each junction (i.e the inflow at any junction becomes equal to the outflow at that junction). Correction to these assumed flows is then computed successively for each pipe loop in the network, until the correction is reduced to an acceptable magnitude.

If Q_a is the assumed flow and Q is the actual flow in the pipe, then the correction ΔQ is given by

$$\Delta Q = Q - Q_a \quad 2$$

$$\Rightarrow Q = Q_a + \Delta Q \quad 3$$

Now expressing the head loss (H_L) as

$$H_L = K \cdot Q^x \quad 4$$

$$\text{where, } K = \frac{L}{470 \cdot d^{4.87}} \text{ (for Hazem-William formula)}$$

L = length of pipe between two node.

x = a constant (1.852, for Hazen Williams formula ; 2, for Mannings or Darcy Weisbach formula)

the head loss in a pipe can be calculated as

$$H_L = K \cdot (Q_a + \Delta Q)^x$$

$$H_L = K \cdot [Q_a^x + x \cdot Q_a^{x-1} \cdot \Delta Q + \dots + \text{negligible terms of higher power}]$$

$$H_L = K \cdot [Q_a^x + x \cdot Q_a^{x-1} \cdot \Delta Q] \quad 5$$

Now around a closed loop, the summation of head loss must be zero.

$$\text{i.e } \sum K \cdot [Q_a^x + x \cdot Q_a^{x-1} \cdot \Delta Q] = 0$$

Since ΔQ is same for the all the pipes of the considered loop, it can be taken out of the summation.

Therefore,

$$\Delta Q = - \frac{\sum K \cdot Q_a^x}{\sum x \cdot K \cdot Q_a^{x-1}} \quad 6$$

Since ΔQ is given the same sign (or direction) in all pipes of the loop, the denominator of the above equation is taken as the absolute sum of the individual items in the summation. Hence

$$\Delta Q = - \frac{\sum K \cdot Q_a^x}{\sum |x \cdot K \cdot Q_a^{x-1}|} \quad 7$$

$$\Delta Q = - \frac{\sum H_L}{x \sum \left| \frac{H_L}{Q_a} \right|} \quad 8$$

Where H_L = head loss for the assumed flow Q_a

The numerator of the above equation is the algebraic sum of the head losses in the various pipes of the closed loop computed with the assumed flow. Since the direction and magnitude of flow in these pipes is already assumed, their respective head losses with due regard to sign (The head loss in clockwise direction may be taken as +ve and that in the anti-clockwise direction as -ve) can be easily calculated after assuming their diameters. The absolute sum of respective $K \cdot Q_a^{x-1}$

or $\frac{H_L}{Q_a}$ is then calculated. Finally the value of ΔQ is found out for each loop, and the assumed flows in each pipe are

corrected by using equation (8). Pipes common to two loops will receive both corrections with due attention to sign. After correcting the flows in the entire pipe network in the first iteration, the second correction can be applied to the already corrected flows in the previous step, and the re-corrected flows are again worked out in the entire network (consisting of one or more loops). The flows in pipes, common to two loops, should be corrected for the computed corrections of both the loops, as stated earlier. The procedure can be repeated to obtain more accurate results. The hydraulic module selects the optimal pipe sizes in the final network satisfying all constraints such as conservations of mass and energy and on the other hand pressure head and design constraints. The hydraulic constraints, for example, deal with hydraulic head at certain nodes to meet a specified minimum value. However, diameter constraints enforce the algorithms to select the trial solution within a predefined limit. A hydraulic network solver handles the implicit constraints and simultaneously evaluates the hydraulic performance of each trial solution that is a member of population of points. The hydraulic model first checks the head across each node of whether it satisfies the minimum pressure head conditions and then keeps on iterating until the minimum pressure head condition is satisfied by changing the diameter of each pipe within a given diameter range. Optimization module selects best fitted diameters from a set of diameters and minimizes the total cost of the pipe network.

4.1 Optimization Module

The optimization model involves the use of an excel solver which estimates the cost of the network and settles with the least cost satisfying all the constraints. The network cost is calculated as the sum of the pipe costs where pipe costs are expressed in terms of cost per unit length. Total network cost is computed as follows:

$$C = \sum c_k(D_k) \cdot L_k \quad 9$$

where, $c_k(D_k)$ = cost per unit length of the k^{th} pipe with diameter D_k ,
 L_k = length of the k^{th} pipe.

The optimization module keeps on checking the combination of pipe diameters satisfying the head conditions and resulting in the least cost of the network.

While using solver for the optimization the following parameters was kept as constraints:

- (i) Pressure head across each node must be at least 30m.
- (ii) The diameter of the any of the pipe must be within the range of 0.025m-0.508m.

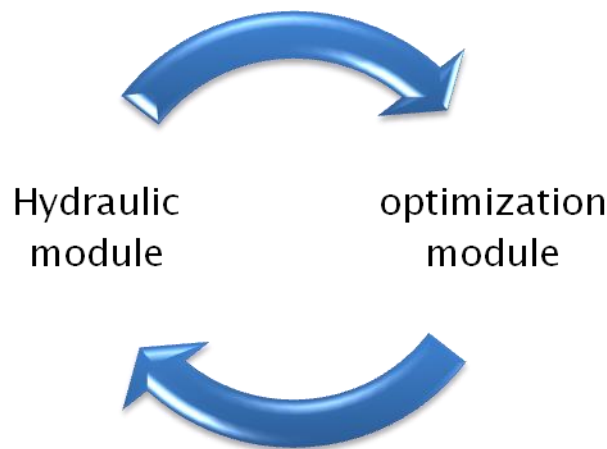


Figure 2 Flow chart of the model

5 Model Application

The application part involves the application of the two modules viz. the hydraulic module and the optimization module compiled using a solver application of excel spreadsheet onto the Two-loop pipe network proposed by Alperovits and Shamir. For finding the cost incurred, data provided in table 1 have been taken for pipe diameters available in the market and their unit costs per meter length.

Table 1 Pipe diameters and their corresponding costs

Diameter (inches)	Diameter (m)	Unit cost (per meter length)
1	0.0254	2
2	0.0508	5
3	0.0762	8
4	0.1016	11
6	0.1524	16
8	0.2032	23
10	0.254	32
12	0.3048	50
14	0.3556	60
16	0.4064	90
18	0.4572	130
20	0.508	170

Then the optimization for least cost was carried out based on the above data in Microsoft Excel and the sizes of the respective pipes and the total cost incurred was determined which was compared with some earlier works and the results are shown in table 2.

Table 2 Comparison of pipe diameters and total cost for two loop network

Pipe number	Alperovits and Shamir	Goulter Et al.	Kessler and Shamir	Present study
1	20 - 18	20 - 18	18	20
2	8 - 6	10	12 - 10	12
3	18	16	16	14
4	8 - 6	6 - 4	3 - 2	10
5	16	16 - 14	16 - 14	12
6	12 - 10	12 - 10	12 - 10	10
7	6	10 - 8	10 - 8	12
8	6 - 4	2 - 1	3 - 2	12
Cost(\$)	497,525	435,015	417,500	440,000

6. Conclusion & Discussion

Any water distribution system consists of basic three components pumps, storage tanks and distributing pipe networking. So, the process of optimization helps in reducing the cost of pipe networks by selecting and recognizing to adopt the best possible diameter to guarantee the best flow rate. The design for optimal distribution of the network is a complex task, various search methods, complex programs and algorithms have been proposed and attempted for the main concern of designing the most least cost network simultaneously satisfying the required minimum pressure head and discharge at the demand nodes. However, Microsoft Excel was used here for optimization to achieve the minimum cost but at the same time it also holds some drawbacks as it does not involve complex mechanisms for optimization as in the case of many algorithms which employ complex mechanisms for search of global optimal solution. As these methods involve complex algorithms, programs and function which require a lot of technical know-how's it becomes difficult to implement such mechanisms for optimization by everyone in many cases. So our approach was to provide with an easy method for optimization which doesn't involve such complexities. As is clear from the results embodied in this report, the cost incurred was lesser than that of Alperovits and Shamir; this is a good option for optimization if one doesn't want to go into such complexities. The total cost however could have been a bit lower as well and well near about the range of some other works on the same network. But the reasons for such fluctuations might be because of the following reasons:

1. As we have used Darcy Weisbach's formula for determination of head loss and the value of n is assumed to be 2 for turbulent flows, whereas in many cases Hazen-William Equation has also been used and the value of n is taken near about 1.85, so this might be a cause for fluctuations in the total cost.
2. Further another reason might be that we have assumed $\Delta Q \rightarrow 0$ instead of $\Delta Q = 0$.

6.1 Future Work

There have been a lot of works on the optimization of pipe networks and the results have improved over the time. There are still a lot of works which can be done on optimization of pipe networks, various algorithms can further be improved to further improve the effectiveness of optimization, make them simpler, less tedious and user friendly. Further diversification of this work can be done by devising on developing an application which optimizes the cost of pipe networks and provide a solution for least cost pipe network for an area by considering different locations of reservoir and then calculating the cost on the basis of length and diameters of the pipes required for satisfying the requirements of pressure and discharge at every node for every possible alternative and then selecting the alternative which requires the least cost.

References

- [1] Alperovits E., Shamir U., Design of optimal water distribution systems, *Water Resources Research.*, 1977, 13(6), 885–900.
- [2] Cunha, M.C. and Sousa, J., Water distribution network design optimization simulated annealing approach. *J. Water Resources Planning & Mgmt.*, 1999, 125, 215 – 224.
- [3] Goulter, I.C, B.M Lussier, and D.R. Morgan, Implications of head loss path choice in the optimization of water distribution network, *Water Resour. Res.*, 22(5), 819-822, 1986.
- [4] Garg S.K “Water Supply Engineering”, *Environmental Engineering (Vol1)*p733-735, 1977
- [5] Kessler, A. & U. Shamir, Analysis of the linear programming gradient method for optimal design of water supply networks. *Water Res. Research*, 1989, 25(7), 1469-1480.
- [6] Savic, D.A. &Walters G.A, Genetic algorithms for least-cost design of water distribution networks. *WaterRes. Planning & Management*, 1997, 123(2), 67-77.

Design of Low Power Column bypass Multiplier using FPGA

J.sudha rani¹,R.N.S.Kalpana²

Dept. of ECE¹, Assistant Professor ,CVSR College of Engineering,Andhra pradesh, India,
Assistant Professor²,Dept. of ECE,Stanley college of Engineering & Technology for women,Andhra pradesh, India,

Abstract

It is well known that multipliers consume most of the power in DSP computations. Hence, it is very important for modern DSP systems to develop low-power multipliers to reduce the power dissipation.. In this paper, we presents low power Column bypass multiplier design methodology that inserts more number of zeros in the multiplicand thereby reducing the number of switching activities as well as power consumption. The switching activity of the component used in the design depends on the input bit coefficient. This means if the input bit coefficient is zero, corresponding row or column of adders need not be activated. If multiplicand contains more zeros, higher power reduction can be achieved. To reduce the switching activity is to shut down the idle part of the circuit, which is not in operating condition. Use of look up table is an added feature to this design. Further low power adder structure reduces the switching activity. Flexibility is another critical requirement that mandates the use of programmable components like FPGAs in such devices.

Keywords: Low Power, Multiplier, Reduced Switching,Column By passing

1. Introduction

As we get closer to the limits of scaling in Complementary metal. oxide. semiconductor (CMOS) circuits, power and heat dissipation issues are becoming more and more important. In recent years, the impact of pervasive computing and the internet have accelerated this trend. The applications for these domains are typically run on battery-powered embedded systems. The resultant constraints on the energy budget require design for power as well as design for performance at all layers of system design. Thus reducing power consumption is a key design goal for portable computing and communication devices that employ increasingly sophisticated and power hungry signal processing techniques. Flexibility is another critical requirement that mandates the use of programmable components like FPGAs in such devices.The multiplication is an essential arithmetic operation for common DSP applications, such as filtering and fast Fourier Transform (FFT). To achieve high execution speed, parallel array multipliers are widely used. These multipliers tend to consume most of the power in DSP computations, and thus power-efficient multipliers are very important for the design of low-power DSP systems.This paper presents a new multiplier design in which switching activities are reduced through architecture optimization. This paper is organized as follows. In the next section we give some preliminary information, including array multiplier architectures and previous works on low power multipliers. Our multiplier design is presented in Section 3, and some experimental results on the performance of various multipliers are shown in Section 4.

2. Preliminaries

A. Parallel Multiplier

Consider the multiplication of two unsigned n-bit numbers, where $A = a_{n-1}a_{n-2} \dots a_0$ is the multiplicand and $B = b_{n-1}b_{n-2} \dots b_0$ is the multiplier. The product $P = p_{2n-1}, p_{2n-2} \dots p_0$ can be written as follows:

$$P = \sum_{i=0}^{n-1} \sum_{j=0}^{n-1} (a_i \cdot b_j) 2^{i+j} \quad (1)$$

A 4X4 unsigned multiplication example is shown in figure 1. The multiplicand A_i is added to the incoming partial product bit based on the value of the multiplier bit B_j . Each row adds the multiplicand to the incoming partial product, PP_i to generate the outgoing partial product $PP_{(i+1)}$, if $Y_i = 1$. If $Y_i = 0$, PP_i is passed vertically downward unchanged.

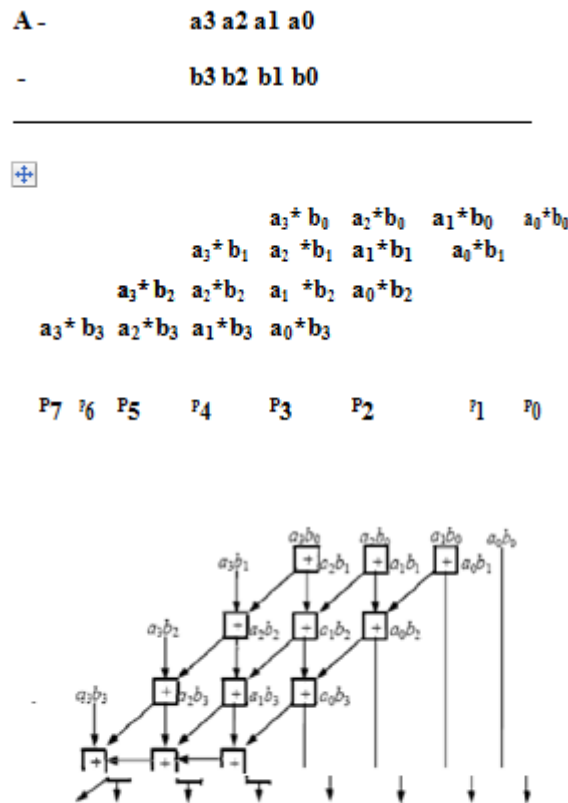


Figure 2. A 4x4 Braun multiplier.

An array implementation, known as the Braun multiplier, is shown in Figure 2. In the 4x4 Braun multiplier, the multiplier array consists of 3 rows of carry-save adders (CSAs), in which each row contains 3 full adders (FAs). Each FA has three inputs and two outputs: the sum bit and the carry bit. 3 FAs in the first CSA row that have only two valid inputs can be replaced by 3 half adders (HAs) and 3 FAs in the last row can be constructed as a 3-bit ripple-carry adder. On the other hand, the Baugh-Wooley multiplier uses the same array structure to handle 2's complement multiplication, with some of the partial products replaced by their complements. The multiplier array consists of (n-1) rows of carry-save adders (CSA), in which each row contains (n-1) full adders (FA). The last row is a ripple adder for carry propagation. In this paper, we shall propose a low power design for this multiplier.

B. Related Research

The power dissipation in CMOS circuit has several components that are usually estimated on the device parameters of the technology used. The total power in the circuit is given by the following equation,

$$P_{total} = P_{switching} + P_{shortcircuit} + P_{static} + P_{leakage} \quad (2)$$

where $P_{switching}$ is switching component of the power and it is a dominating component in these calculations. $P_{shortcircuit}$ is the power dissipated due to the fact that during the circuit operation PMOS and NMOS transistors of CMOS gate become simultaneously during the transition at the input level, static consumption is from the leakage current. For static power dissipation, the consumption is proportional to the number of the used transistors. For dynamic power dissipation, the consumption is obtained from the charging and discharging of load capacitance.

The average dynamic dissipation of a CMOS

gate is given by equation 3.

$$P_{avg} = 0.5 \times C_L \times VDD^2 \times f_p \times N \tag{3}$$

where C_L is the load capacitance, f_p is the clock frequency, VDD is the power supply voltage and N is the number of switching activity in a clock cycle.

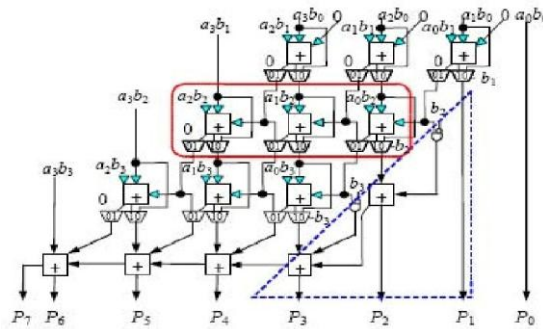


Figure 3. 4x4 Row bypassing Multiplier with reduced switching Activity

Thus, the power consumption can be reduced if one can reduce the switching activity of a given logic circuit without changing its function. An obvious method to reduce the switching activity is to shut down the idle part of the circuit, which is not in operating condition. Figure 3 shows the 4 X 4 row bypassing architecture with reduced switching. The design included $(n-1)(n-1)$ full adders, $2 \times (n-1) \times (n-1)$ multiplexers, and $3 \times (n-1) \times (n-1)$ three state gates.

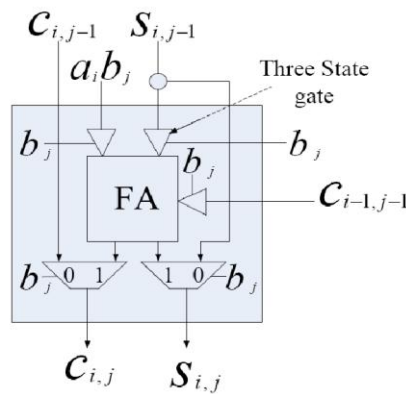


Figure 4. Row Bypassing Adder Cell (RA)

Figure 4 shows the Row Bypassing Adder Cell (RA)

When the corresponding partial product is zero, the RA disabled unnecessary transitions and bypassed the inputs to outputs. The demerit of this technique is that it needs extra correction circuitry shown in triangle. Structure of the full adder is complex as well. The Braun multiplier removes the extra correction circuitry needed. Also, number of adders is less. But, the is that it cannot stop the switching activity even if the bit coefficient is zero that ultimately results in unnecessary power dissipation.

3. The Proposed Design

The switching activity of the component used in the design depends on the input bit coefficient. This means if the input bit coefficient is zero, corresponding row or column of adders need not be activated. If multiplicand contains more zeros, higher power reduction can be achieved. Instead of bypassing rows of full adders, we propose a multiplier design in which columns of adders are bypassed. In this approach, the operations in a column can be disabled if the corresponding bit in the multiplicand is 0. There are two advantages of this approach. First, it eliminates the extra correcting circuit as shown in Figure 3. Second, the modified FA is simpler than that used in the row-bypassing multiplier, as shown in Figure 7(a). Consider the multiplication shown in Figure 5, which executes 1010×1111 . Note that, in the first and third diagonals (enclosed by dashed lines), two out of the three input bits are 0: the “carry” bit from its upper right FA, and the partial product $a_i b_j$ (note that $a_0 = a_2 = 0$). As a result, the output carry bit of the FA is 0, and the output sum bit is simply equal to the third bit, which is the “sum” output of its upper FA. Now, consider another multiplication of 1111×1000 . Since multiplicand contains no zero, all columns will get

A. Basic Idea

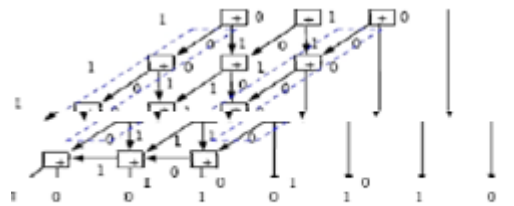


Figure 5. A column-bypassing example.

switched and consume more power. High power reduction can be achieved if the multiplicand contains more number of zeros than 1's. In this approach we propose Booth Recoding unit which will force multiplicand to have number of zeros, if it does not have a single zero. The advantage here is that if multiplicand contains more successive number of ones then booth-recoding unit converts these ones in zeros.

as Detection of Zero Unit, Booth Recoding Unit and Multiplication Unit.

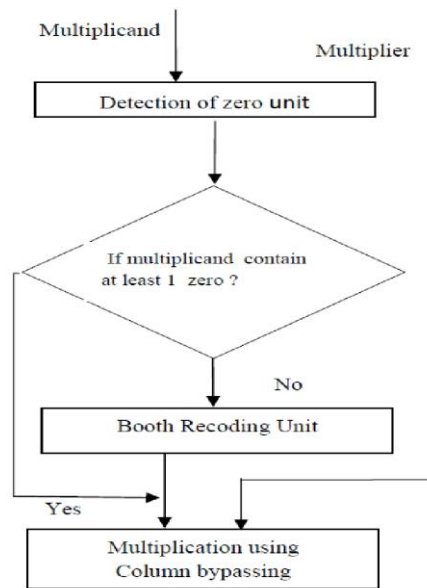


Figure 6. Proposed multiplier architecture

B. Multiplier Design

The low power multiplier can be constructed as shown in figure 7. It is organized in three units

Detection of zero unit:

This unit scan the number of zeros and their respective position in the multiplicand, so as to bypass the corresponding column. If multiplicand contain at least one zero then it will feed the column bypass multiplier and multiplication will be performed using column bypassing. If multiplicand does not contain zero, multiplicand will be given to the Booth Recoding Unit and after that multiplication will perform.

Booth Recoding Unit :

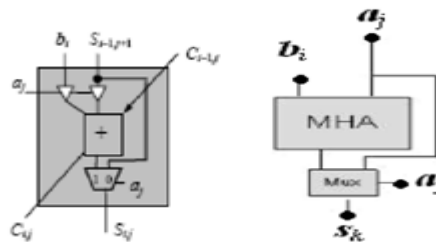
This unit chooses force the multiplicand to have greater number of zeros in case multiplicand does not have zero using Booth Table 1.

Table 1: - Booth Recoding Table

Multiplicand		Version of multiplier selected by bit i
Bit i	Bit i-1	
0	0	0 X M
0	1	+1 X M
1	0	-1 X M
1	1	0 X M

Column Bypassing Multiplier :

The column bypassing multiplier is constructed as follows. First, the modified HA cell is shown in Figure 7(b). Note that we only need two three-state gates and one multiplexor in this design. If $a_j = 0$, the HA will be disabled. For a Braun multiplier, there are only two inputs for each FA in the first row (i.e., row 0). Therefore, when $a_j = 0$, the two input of FA0,j are disabled, and thus its output carry bit will not be changed. Therefore, all three inputs of FA1,j are fixed, which prohibit its output from changing.



number of 2 TO 1 Multiplexers required to design column bypass multiplier are $(n-1)*(n-1)$.

Figure 8 shows the 4x4 low power multiplier structure. This technique will be very useful as we go for higher width of the multiplicand specially when there are successive numbers of ones. if multiplicand contain at least one zero, it does not uses the Booth recoding unit and if multiplicand is "11" then only it will use Booth recoding table shown in table 1. so we do not need sign bit circuitry.

Figure 9(a) simulation results for 32-bit array multiplier power due to the extra bypassing logic and our proposed design reduces the power dissipation.

	Voltage (V)	Current (m)	Power (m)
Quiescent		2.00	5.00
Total Pow			264.00
Startup Curr		0.00	
Battery Capacity (mA Hours)			0.00
Battery Life (Hours)			0.00

Simulation results for the array multiplier and Row Bypassing multiplier are given in figure 9,10 and for proposed multiplier is given in figure 11.

Table 2:- Synthesis results on XPower Tool

Multiplier Type(32bit)	Array Multiplier	Row Bypass	Proposed
Vendor	Xilinx	Xilinx	Xilinx
Device and Family	Spartan 3E	Spartan 3E	Spartan 3E
Estimate Delay	87.636nsec	114.677nsec	80.870nsec
Total memory usage	299.736 MB	198.008MB	181.528MB
Power Dissipation	264 mW	184.77 mW	169.57mw

Table 3: - Synthesis results on Xilinx XST

Multiplier (32x32)	Number of LUTs
Without bypassing	2015
Row Bypassing	2960
Proposed	2014

Figure 9(b) simulation results for 32-bit array multiplier

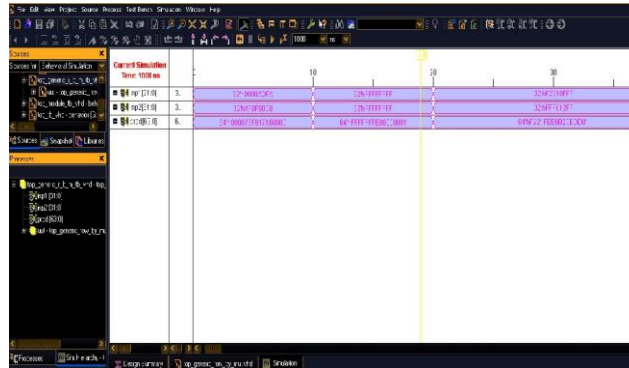
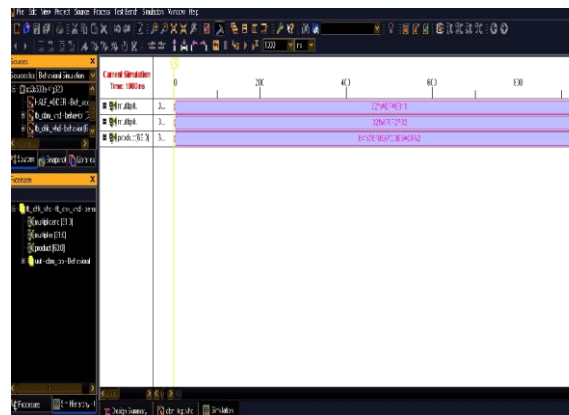


Figure 10(a) simulation results for 32-bit Row Bypassing multiplier

	Voltage [V]	Current [mA]	Power [mW]
Vccint	1.2		
Dynamic		17.60	21.12
Quiescent		26.91	32.29
Vccaux	2.5		
Dynamic		0.00	0.00
Quiescent		18.00	45.00
Vcco25	2.5		
Dynamic		32.54	81.36
Quiescent		2.00	5.00
Total Power			184.77
Startup Current [mA]		0.00	
Battery Capacity [mA Hours]			0.00
Battery Life [Hours]			0.00

Figure 10(b) simulation results for 32-bit Row Bypassing multiplier



Future scope

The project can be implemented to 64 and 128 bit column bypassing multiplier. Less switching activity can be achieved in this multiplier. Low Power consumption can be achieved. In this multiplier, a low power multiplier design column bypassing using Booth recoding is proposed. Compared with other multipliers such as row bypassing array, the results achieve higher power reduction and hardware overhead.

Figure 11(a) simulation results for 32-bit Column Bypassing multiplier

	Voltage (V)	Current (m)	Power (m)
Quiescent		2.00	5.00
Total Pow			169.57
Startup Curr		0.00	
Battery Capacity (mA Hours)			0.00
Battery Life (Hours)			0.00

Figure 11(b) simulation results for 32-bit Column Bypassing multiplier

5. Conclusions

In this paper we have presented a new methodology for designing of low power parallel multiplier with reduced switching. Method for increasing number of zeros in the multiplicand is discussed with the help of Booth Recoding Unit. Based on the modification of the half adders instead of full adders in an array multiplier, a low-power design column bypassing using Booth recoding is proposed. Compared with the row bypassing or array-multipliers, the experimental results show that our proposed low-power multiplier achieves higher power reduction with lower hardware overhead.

References

- [1] Oscar T. -C. Chen, Sandy Wang, and Yi-Wen Wu, .Minimization of Switching Activities of Partial Products for Designing Low-Power Multipliers., IEEE Transactions on VLSI Systems, June 2003 vol. 11, no. 3.
- [2] Rajendra M. Patrikar, K. Murali, Li Er Ping, .Thermal distribution calculations for block level placement in embedded systems., Microelectronics Reliability 44(2004) 129-134
- [3] Hichem Belhadj, Behrooz Zahiri, Albert Tai .Power-sensitive design techniques on FPGA devices., Proceedings of International conference on IC Taipei (2003).
- [4] A. Wu, .High performance adder cell for low power pipelined multiplier., in Proc. IEEE Int. Symp. on Circuits and Systems, May 1996 , vol. 4, pp. 57-60.
- [5] S. Hong, S. Kim, M.C. Papaefthymiou, and W.E.Stark, .Low power parallel multiplier design for DSP applications through coefficient optimization., in Proc. of Twelfth Annual IEEE Int. ASIC/SOC conf., Sep. 1999, pp. 286-290.
- [6] C. R. Baugh and B. A.Wooley, .A two's complement parallel array multiplication algorithm., IEEE Trans. Comput., Dec. 1973, vol. C-22, pp. 1045-1047.
- [7] I. S. Abu-Khater, A. Bellaouar, and M. Elmasry, Circuit techniques for CMOS low-power highperformance multipliers., IEEE J. Solid-State Circuits, Oct. 1996, vol. 31, pp. 1535-1546.
- [8] J. Ohban, V.G. Moshnyaga, and K. Inoue, .Multiplier energy reduction through bypassing of partial products., Asia-Pacific Conf. on Circuits and Systems. 2002.,vol.2, pp. 13-17.